



**HAL**  
open science

## Northwest Africa 8694, a ferroan chassignite: Bridging the gap between nakhlites and chassignites

Roger Hewins, M. Humayun, Jean-Alix J-A Barrat, B Zanda, J.-P Lorand, S Pont, N. Assayag, P. Cartigny, S Yang, V Sautter

### ► To cite this version:

Roger Hewins, M. Humayun, Jean-Alix J-A Barrat, B Zanda, J.-P Lorand, et al.. Northwest Africa 8694, a ferroan chassignite: Bridging the gap between nakhlites and chassignites. *Geochimica et Cosmochimica Acta*, 2020, 282, pp. 201-226. 10.1016/j.gca.2020.05.021 . hal-03023209

**HAL Id: hal-03023209**

**<https://hal.sorbonne-universite.fr/hal-03023209>**

Submitted on 25 Nov 2020

**HAL** is a multi-disciplinary open access archive for the deposit and dissemination of scientific research documents, whether they are published or not. The documents may come from teaching and research institutions in France or abroad, or from public or private research centers.

L'archive ouverte pluridisciplinaire **HAL**, est destinée au dépôt et à la diffusion de documents scientifiques de niveau recherche, publiés ou non, émanant des établissements d'enseignement et de recherche français ou étrangers, des laboratoires publics ou privés.

1  
2  
3  
4  
5  
6  
7  
8  
9  
10  
11  
12  
13  
14  
15  
16  
17  
18  
19  
20  
21  
22  
23  
24  
25  
26  
27  
28  
29  
30  
31  
32  
33  
34  
35  
36  
37  
38  
39  
40  
41  
42  
43

**NORTHWEST AFRICA 8694, A FERROAN CHASSIGNITE: BRIDGING THE GAP BETWEEN  
NAKHLITES AND CHASSIGNITES**

R.H. Hewins<sup>1,2</sup>, M. Humayun<sup>3</sup>, J.-A. Barrat<sup>4</sup>, B. Zanda<sup>1,5</sup>, J.-P. Lorand<sup>6</sup>, S. Pont<sup>1</sup>, N. Assayag<sup>7</sup>, P.  
Cartigny<sup>7</sup>, S. Yang<sup>3</sup> and V. Sautter<sup>1</sup>.

Corresponding author: Roger Hewins, Muséum national d'Histoire naturelle,  
[Hewins@scarletmail.rutgers.edu](mailto:Hewins@scarletmail.rutgers.edu), +33 6 16 21 29 91 & +33 1 4709 3769

<sup>1</sup>IMPMC, MNHN, Sorbonne Universités, 75005 Paris, France.

<sup>2</sup>EPS, Rutgers University, Piscataway, NJ 08854, USA.

<sup>3</sup>DEOAS & NHMFL, Florida State University, Tallahassee, FL 32310, USA.

<sup>4</sup>UBO-IUEM and CNRS UMR 6538, 29280 Plouzané, France.

<sup>5</sup>IMCCE, Observatoire de Paris, CNRS UMR 8028, 75014 Paris, France.

<sup>6</sup>LPGN, CNRS UMR 6112, Université de Nantes, BP 92208, 44322 Nantes, France.

<sup>7</sup>IPGP UMR 7154, Université Denis Diderot (Paris 7) & PRES Sorbonne Paris Cité, Paris 75005, France.

[\(hewins@rci.rutgers.edu\)](mailto:hewins@rci.rutgers.edu)

Resubmitted to *Geochimica et Cosmochimica Acta*, 12 March, 2020

44  
45  
46  
47  
48  
49  
50  
51  
52  
53  
54  
55  
56  
57  
58  
59  
60  
61  
62  
63  
64  
65  
66  
67  
68  
69  
70  
71  
72  
73  
74  
75  
76  
77  
78  
79  
80  
81  
82  
83  
84  
85  
86  
87  
88  
89  
90  
91  
92  
93  
94  
95  
96  
97

**Abstract**—The origin(s) of the chassignites and nakhlites, closely related martian olivine and augite cumulates, respectively, are much debated. Northwest Africa (NWA) 8694 is the third chassignite to be discovered and the most ferroan, containing 85% olivine (Fo<sub>54</sub>). Its O-isotope compositions ( $\delta^{18}\text{O} \sim 4.4\text{‰}$ ,  $\Delta^{17}\text{O} \sim 0.30\text{‰}$ ) are typical of other martian meteorites. It has adcumulate texture and contains cumulus chromite, poikilitic pigeonite (En<sub>56</sub>Fs<sub>37</sub>Wo<sub>7</sub>) and mesostasis (trapped interstitial liquid). The latter contains pyroxene and plagioclase (An<sub>23</sub>Ab<sub>70</sub>Or<sub>8</sub>) plus rare K-feldspar (Or<sub>74</sub>), and has a trachyandesitic to trachytic bulk composition. Melt inclusions in olivine contain a variety of phases including biotite and rare amphibole. Olivine, chromite, and pigeonite compositions are intermediate between those of the other chassignites and those of the nakhlites. Augite, which appears to mantle pigeonite, has a composition overlapping that in nakhlite NWA 998 and some other nakhlites at (En<sub>41-40</sub>Wo<sub>38-39</sub>). The augite lamellae in pigeonite 1-2  $\mu\text{m}$  in apparent width, and the survival of Ca zoning in olivine, suggest a near-surface cooling environment. The bulk-rock REE concentrations in the three chassignites do not correlate with Mg# but depend on the abundance of trapped liquid. The form of REE patterns calculated for olivine subtraction is very like those of nakhlite mesostases, but the observed concentrations of LREE in NWA 8694 trapped liquid have a very steep slope. This is explained by undersampling of baddeleyite and zirconolite that occur near olivine contacts with mesostasis. Though pyroxene is unzoned, its trace element variations indicate fractional crystallization. The range of olivine compositions in the three chassignites (Fo<sub>79-54</sub>) is too large to result from the crystallization sequential growth of olivine from a single magma undergoing fractional crystallization. The Ge/Si ratios show degassing of NWA 8694 which sets this chassignite apart from other chassignites and nakhlites, implying a unique batch of magma for its genesis. Many potential parent liquids are capable of generating the NWA 8694 olivine composition, though not its alkaline mesostasis. We calculated that Nakhla parent liquid NA01a (Stockstill et al., 2005) with 10% Nakhla core olivine added would produce both olivine crystals and alkaline daughter liquids with compositions matching those of NWA 8694. This meteorite is a chassignite cumulate containing nakhlitic mesostasis, a direct link between the chassignites and the nakhlites and the association of dunitic to trachytic compositions is reminiscent of terrestrial shield volcanoes. Chassignites and nakhlites were possibly formed when solidification fronts on chamber walls were disrupted, mainly as side eruptions of olivine-charged magmas from the deeper zones, and augite-charged fractionated magmas from nearer the summit of a volcano resembling Piton de la Fournaise on Earth.

## 1. INTRODUCTION

Martian meteorites have been a major source of information on Mars since Nakhla was first recognized as having the mineral assemblage of a planetary igneous rock (Reid and Bunch, 1975) with a young crystallization age (Gale et al., 1975). That same year Mason et al. (1975) suggested that Chassigny was a cumulate from the nakhlite parent liquid. The chassignites are the least well known of the SNC meteorites (shergottites; nakhlites and chassignites), consisting until now of only two meteorites, Chassigny (Floran et al., 1978; Johnson et al., 1991) and North West Africa (NWA) 2737 (Beck et al., 2006; Treiman et al., 2007; He et al., 2013). Chassignites share many characteristics with nakhlites, including crystallization and ejection ages (Nyquist et al., 2001), trace element abundance patterns (Mason et al., 1975; Wadhwa and Crozaz, 1995; Beck et al., 2006; Udry and Day, 2018), and volatile element abundances (McCubbin et al., 2013). Chassignites are adcumulate dunites with cumulus olivine and chromite, while nakhlites are augite cumulates. Chassignite and nakhlite textures resemble those of cumulates in Archean rocks - dunite in komatiite flows and pyroxenite in the lower parts of associated thick differentiated tholeiitic flows (Arndt et al., 1977; Friedman-Lentz et al., 1999; Treiman, 2005; Day et al., 2006). Dunites similar to chassignites have also been observed in association with shield volcanoes, as xenoliths and as cumulates beneath the basaltic lavas (Barrat and Bachèlery, 2019; Babkine et al., 1966).

A genetic relationship between chassignites and nakhlites has long been considered (Mason et al., 1975; Stolper et al., 1979; McCubbin et al., 2013). There is a sequence of textures and compositions in nakhlites reflecting cooling history that allowed them to be ordered as in a single igneous body (Mikouchi et al., 2003; Day et al., 2006), with chassignites added to the base of this sequence (e.g. McCubbin et al., 2013). However, considering subtle

98 differences in otherwise similar nakhlites and in chassignites, such as their Ar-Ar ages and augite incompatible  
99 element fractionation trends, these rocks may represent several closely related flows or shallow intrusions, possibly  
100 with different parent magmas derived from a common mantle source (Wadhwa and Crozaz, 1995; Jambon et al.,  
101 2016; Balta et al., 2017; Mikouchi et al., 2017, Cohen et al. 2017; Udry and Day, 2018). Nevertheless, the  
102 similarities of nakhlites and chassignites suggest that the most magnesian nakhlites, like NWA 998 (Treiman and  
103 Irving, 2008), could have a close physical or genetic relationship to the most evolved chassignites.

104  
105 Northwest Africa 8694 is a 55 g stone obtained in Agadir in July, 2014. It has a texture and modal composition  
106 like those of the other chassignites, but is highly ferroan (Hewins et al., 2015, 2017). The olivine composition of  
107 NWA 8694 expands the known range of Mg# (100 x atomic Mg/(Fe+Mg) ratio) in the chassignites from 77 in NWA  
108 2737 to 54 in NWA 8694, and is intermediate between those of Chassigny and nakhlites. We have therefore  
109 undertaken a petrologic and geochemical study of this key meteorite, and compare it to the most magnesian, least  
110 fractionated, most mesostasis-poor nakhlites like NWA 998 (Mikouchi et al., 2006; Treiman and Irving, 2008).  
111 Cosmic-ray exposure (CRE) ages and noble gas compositions observed for NWA 8694 ~~chassignite~~ suggest it is  
112 launch-paired with Miller Range (MIL) nakhlites (Nagao et al., 2019). Our study sheds light on the origin and  
113 evolution of chassignite parent magmas, and confirms the close relationships between chassignites and nakhlites.


## 114 115 116 2. SAMPLES AND METHODS 117

### 118 2.1. Oxygen Isotopes

119 Triplicate oxygen isotope analyses were performed at the Institut de Physique du Globe de Paris,  
120 over three distinct sessions. Analytical methods are similar to those documented in Rumble et al. (1997).  
121 Briefly, prior to analysis, samples were pre-fluorinated overnight using BrF<sub>5</sub>. Both samples and garnet  
122 standard UWG-2 (Gore Mountain mine, Adirondack Mountains, New York, see Valley et al. 1995) were  
123 then analysed using laser fluorination. Oxygen isotopic ratios (<sup>18</sup>O/<sup>16</sup>O) were normalized to UWG-2  
124 garnet with δ<sup>18</sup>O = 5.75‰ (Valley et al. 1995) and reported versus the international standard, V-SMOW  
125 (standard mean ocean water) using the conventional delta-notation, where

$$126 \delta^{1X}O = \left( \frac{{}^{1X}O/{}^{16}O_{\text{sample}}}{{}^{1X}O/{}^{16}O_{\text{standard}}} - 1 \right) \times 1000, \text{ with } \delta^{1X}O \text{ denoting either } {}^{17}O \text{ or } {}^{18}O.$$

### 127 128 2.2 Mineralogy-petrology

129  
130 Three parallel polished sections of NWA 8694 exposing a total area of ~3 cm<sup>2</sup> were died using optical  
131 microscopy, scanning electron microscopy (SEM), and electron probe microanalysis (EPMA). Two sections were  
132 subsequently split horizontally to make doubly polished, double-sided epoxy mounts. Similar analyses were made  
133 on Chassigny and NWA 2737 for comparison. Backscattered electron (BSE) maps, X-ray maps, and images of  
134 selected regions were made at MNHN using a Tescan VEGA II LSU SEM in conventional mode (mainly 15 keV  
135 and <20 nA), and minerals were characterized with an SD3 (Bruker) Energy Dispersive Spectrometer (EDS). We  
136 used a scan speed of 64 μs/pxl and a pixel size of 884 nm for cartography. Phases were identified from BSE  
137 intensity and modal abundances were calculated after scanning ~200,000,000 px<sup>2</sup> per section. Sulfide microphases  
138 were located by manual scans in the BSE mode on sections 2 and 3, and were identified with EDS. Their  
139 compositions were analyzed at 15 kV accelerating voltage by a PhiRhoZ EDS standardless procedure after careful  
140 imaging of each grain in the BSE mode at high magnification (x 2,000-x 10,000); information on the accuracy of  
141 this technique are given in Gattacceca et al. (2013). Minor-element X-ray maps of olivine crystals were also made  
142 using a Cameca SX100 electron microprobe at the Université Paris VI with a 500 nA current, after quantitative  
143 analyses because of the risk of beam damage (Goodrich et al., 2013). Quantitative analyses of all minerals except for  
144 sulfides were made by wavelength-dispersive spectrometry on the Cameca SXFive electron microprobe at the  
145 Université Paris VI, using an LaB<sub>6</sub> source, at 15 keV. The current was generally 10 nA with a focused beam but 4  
146 nA, with 6x8 μm and up to 12x15 rasters, was used for feldspathic and glassy material. The quality of the analyses  
147 was checked using San Carlos and Eagle Station olivine, and Astimex MINM25-53 albite, orthoclase, quartz,  
148 kaersutite, and biotite, as internal standards.

### 149 150 2.3. LA-ICP-MS 151

152 Laser ablation inductively coupled plasma mass spectrometry (LA-ICP-MS) analyses with an Electro  
153 Scientific Instruments New Wave™ UP193FX excimer (ArF) laser coupled to a Thermo Element XR™ sector field  
154 ICP-MS were performed at the Plasma Analytical Facility, at the NHMFL, Florida, using methods described  
155 elsewhere (Humayun et al., 2010; Yang et al., 2015; Oulton et al., 2016). A total of 78 peaks of 72 elements were  
156 monitored in low mass resolving power to correct for isobaric interferences, including from doubly charged ions  
157 (Yang et al., 2015). The ICP-MS was tuned to yield  $^{238}\text{UO}^+ / ^{238}\text{U}^+ \sim 0.3\%$ . Individual mineral grains were analysed  
158 with 25 or 50  $\mu\text{m}$  spots and 5-second laser dwell time per spot, or with 100  $\mu\text{m}$  spots and 20-second laser dwell time  
159 per spot, at 50 Hz laser repetition rate. Abundances of major elements and most lithophile elements were calibrated  
160 using the USGS glass standards BCR-2g, BHVO-2g and BIR-1g (Humayun et al., 2010; Jochum et al., 2011), with  
161 the remaining elements calibrated against NIST SRM 610, NIST SRM 1263a, and the iron meteorites Hoba and  
162 North Chile (Humayun et al., 2007; Yang et al., 2015; Oulton et al., 2016). Individual spot analyses were taken on  
163 two sections of MNHN Chassigny 2525 (Sp1 and Sp2) and on a doubly polished epoxy mount of NWA 8694. A  
164 bulk analysis of NWA 8694 was performed on the reverse side of the NWA 8694 mount with a 100  $\mu\text{m}$  spot size,  
165 rastered at 10  $\mu\text{m}/\text{s}$  with 50 Hz laser repetition rate, covering an area of 2 x 3 mm.

## 166 2.4 ICP-AES and ICP-SFMS

167  
168  
169 A 0.136 g sample of NWA 8694 was crushed using a boron carbide mortar and pestle into a homogenous  
170 fine-grained powder in clean room conditions at the Institut Universitaire Européen de la Mer (IUEM), Plouzané, at  
171 the same time as a 0.115 g sample of Chassigny. The powder was dissolved and analyzed for major and trace  
172 element concentrations by ICP-AES (inductively coupled plasma – absorption emission spectrometry), and by ICP-  
173 SFMS (inductively coupled plasma – sector field mass spectrometry) following the procedures described by Barrat  
174 et al. (2012). Based on replicate standards and samples (Barrat et al., 2012, 2014, 2016), the precision for  
175 abundances is much better than 5%. The precision for trace element ratios (e.g.,  $\text{Eu}/\text{Eu}^*$ , where  $\text{Eu}^*$  is the  
176 interpolated Eu for a smooth CI-normalized rare earth element (REE) pattern, such that  $\text{Eu}_n^* = (\text{Sm}_n \times \text{Gd}_n)^{1/2}$ ) is  
177 better than 2.5% (2 x relative standard deviation).

## 178 179 180 3. RESULTS

### 181 3.1 Oxygen isotopes

182  
183 The measured  $\delta^{18}\text{O}$ -values ranged from 4.53 to 4.17‰ with an average value of  $4.39 \pm 0.19\%$  (1 $\sigma$ ) within the  
184 range of previous measurements (e.g. Franchi et al., 1999).  $\Delta^{17}\text{O}$ -values [where  $\Delta^{17}\text{O} = \delta^{17}\text{O} ((\delta^{18}\text{O}/1000+1)^{0.5305} - 1) \times$   
185 1000] varied between 0.274 and 0.358‰, averaging  $0.303 \pm 0.048\%$  (1 $\sigma$ , n= 3, from 1 sample) values within the  
186 range of other studies (e.g.  $0.275 \pm 0.013$  using the data of Franchi et al. (1999) recalculated using the 0.5305 mass-  
187 exponent, n = 34 from 11 samples). Our measurements are shown in Fig. S1 along with the Mars Fractionation Line  
188 calculated by regression of analyses tabulated by Ali et al. (2016). Our values are typical of other martian meteorites  
189 and provide an independent validation that NWA 8694 originates from the parent body of other nakhlites and  
190 chassignites.

### 191 3.2 Petrography

192  
193  
194 The textures of the three chassignites are compared in Fig. 1. NWA 8694 is a cumulate dunite with 85% olivine  
195 grains up to 1 mm in size, with similar mineral proportions and textures to the two other chassignites now known,  
196 though clearly Chassigny has the most olivine and the least intercumulus material (Fig. 1). Full resolution BSE  
197 images are given in Fig. S2. Olivine displays irregular and planar fractures in NWA 8694, indicating shock as in  
198 Chassigny (Langenhorst and Greshake, 1999). Chromite is highly fractured; it is enclosed by and molded round  
199 olivine, and is euhedral where enclosed by pyroxene. The main interstitial (intercumulus or adcumulus) phases in  
200 NWA 8694 are poikilitic pigeonite and augite, both with very fine (~1-2  $\mu\text{m}$ ) exsolution lamellae. The augite occurs  
201 between olivine and pigeonite in many cases, swathing the olivine, and also in mesostasis patches and melt

202 inclusions. The pigeonite in some mesostasis patches encloses feldspar or maskelynite laths. Minor phases include  
203 apatite, and ilmenite and accessory phases are Fe-Ni (Cu) sulfides and Zr-rich oxides (baddeleyite and zirconolite).

204  
205 The abundances of constituent phases identified by BSE intensity were determined by counting ~250,000,000  
206 px<sup>2</sup> each for three sections, and are shown in Table 1, along with those of the other two chassignites (Floran et al.,  
207 1978; Udry and Day, 2018; Mikouchi et al., 2005; Beck et al., 2006; Trieman et al., 2007). NWA 8694 has  
208 significantly less olivine, 84.9±1.3%, than Chassigny and NWA 2737 with 90.5±1.3 and 90.7±2.4% respectively;  
209 and less chromite, 0.8±0.1 vs. 1.4±0.3 and 3.3±0.9%; but significantly more pyroxene, 10.6±1.9 vs. 3.2±2.1 and  
210 5.3±3.0, respectively. Abundances of feldspar/glass are not significantly different. Thus NWA 8694 contains more  
211 intercumulus material than the other chassignites, though these phases are heterogeneously distributed, as reflected  
212 in the different abundances in different sections of the same meteorite. The meteorite has an adcumulate texture  
213 except in small patches where abundant interstitial material gives an orthocumulate texture (Fig. 1).

214  
215 Interstices between olivine grains are largely filled by pigeonite and augite. The continuity of augite lamellae  
216 across different interstitial pigeonite areas (Fig. S3) indicates that the pigeonite is poikilitic to olivine and suggests  
217 that it is an adcumulus phase, as in Fig. 2 of Wager et al. (1960). The olivine contains partly crystalline melt  
218 inclusions, surrounded by radial fractures (Fig. 2a).

219  
220 The main phases in melt inclusions are orthopyroxene and K- or Na-bearing glasses; minor phases include  
221 apatite (identified in half of the 25 inclusions studied for sulfides), pyrrhotite, amphibole and biotite, which are  
222 significantly less abundant. The melt inclusions may be dominated by one phase (chromite, pyroxene or Al-rich  
223 glass) but many are polymineralic.

224  
225 Mesostasis occurs instead of pyroxene between some olivine grains (Fig. 2b). The pyroxene of this mesostasis  
226 (orthopyroxene, pigeonite, and augite) is partly attached to olivine walls and is partly subophitic to plagioclase laths.  
227 Feldspar is dominant in some interstitial patches, in which plagioclase is accompanied by minor K-feldspar. Other  
228 phases include apatite needles, biotite, pyrrhotite, pyrite, and ilmenite. Zirconolite and baddeleyite were identified  
229 by EDS as micron scale grains, occurring near olivine rims. They are partly enclosed inside ilmenite, or plagioclase,  
230 or associated with other interstitial minerals.

231  
232 Like the other two chassignites, NWA 8694 contains trace amounts of Fe-Ni (Cu) sulfides. Euhedral  
233 (prismatic) to spherical Ni-bearing pyrrhotite crystals (1 to 10 μm in maximum dimension) occur in most melt  
234 inclusions in olivine (Fig. 3a,b). Enclosed pyrrhotite often coexists with apatite, and less frequently with chromite,  
235 pyroxene and/or amphibole. Such inclusions were occasionally preserved in interstitial trapped melt. Sulfide in  
236 intercumulus spaces are either Ni-pyrrhotite (Po) enclosing occasional pentlandite blebs (Pn) or discrete pyrite (Py)  
237 which was also identified in 3 fractured melt inclusions (over the 25 studied). Both Fe sulfides occur as polyhedral  
238 blebs evenly distributed throughout the two polished thin sections investigated here. Intercumulus sulfides can occur  
239 side by side with olivine, pyroxenes, chromite and interstitial feldspathic glass (Fig. 3c,d). Pyrrhotite and pyrite have  
240 not been observed to coexist within a single sulfide bleb. Pyrite shows fracture networks filled with Fe  
241 oxyhydroxides (Fig. 3d), a well-known alteration product of Fe sulfides from hot desert meteorite finds (Lorand et  
242 al., 2015). Interstitial pyrrhotite was also locally altered. Other accessory phases include baddeleyite and zirconolite  
243 (Fig. 3e,f) both occurring close to olivine-mesostasis contacts.

### 244 3.3 Mineral compositions

#### 245 3.3.1 Olivine

246  
247 The olivine composition by EMP is Fo<sub>53.5±0.4</sub>Fa<sub>46.5±0.4</sub> (Table 2a, S1), with no Fe-Mg zoning and a typical  
248 martian FeO/MnO ratio of 48.3±1.6 (uncertainty is standard deviation and n = 227). Analysis of olivine (cores only)  
249 by LA-ICP-MS gives Fo<sub>54.1±0.1</sub>. Fig. 4 shows that NWA 8694 is intermediate in FeO content between olivine of the  
250 other chassignites (NWA 2737 and Chassigny), and the less equilibrated nakhlites such as NWA817 where olivine  
251 cores still preserve primary compositions (Sautter et al., 2002; Trieman et al., 2005; Udry et al., 2012; Udry and  
252 Day, 2018). Both EMP and LA-ICP-MS data are plotted for Chassigny. The olivine contains 346 ppm Ni (s.d. 5)  
253 compared to 419 ppm (Udry and Day, 2018) or 500 ppm (this work) for Chassigny, and 642 ppm for NWA 2737

254 (Udry and Day, 2018). Though the crystals are equilibrated in Fe-Mg, there is a large range of CaO concentrations  
255 in NWA 8694 olivine, 0.29 – 0.04 wt. % (Fig. 4b) in part due to the incompatible nature of Ca, but there is a weak  
256 depletion of Ca in crystal rims close to interstitial material ( $0.18 \pm 0.02$  to  $0.10 \pm 0.02$  wt% CaO). However we did not  
257 detect zoning in X-ray maps of selected olivine grains, including for slow-diffusing elements like P.

### 258 259 3.3.2 Pyroxenes

260 Chassignite pyroxene and olivine assemblages are shown in Fig. 5, with compositions given in Table 2b  
261 and S1. The dominant pyroxene in NWA 8694 is pigeonite with composition  $\text{En}_{55.8 \pm 0.9} \text{Fs}_{37.5 \pm 1.0} \text{Wo}_{6.7 \pm 1.3}$ , and  
262 FeO/MnO of  $28.7 \pm 1.9$ . The augite is  $\text{En}_{40.6 \pm 0.2} \text{Fs}_{16.1 \pm 0.6} \text{Wo}_{43.9 \pm 0.5}$ , s.d. 0.2, 0.6, 0.5, with an FeO/MnO ratio of 27.4, s.d.  
263 3.2, (neglecting strong overlap compositions). The minor orthopyroxene, particularly in melt inclusions in olivine, is  
264  $\text{En}_{59.9 \pm 0.4} \text{Fs}_{37.7 \pm 0.9} \text{Wo}_{2.4 \pm 0.8}$ , with FeO/MnO ratio of  $30.2 \pm 3.0$ , and  $\text{Al}_2\text{O}_3$  up to 4 wt. %. Though all NWA 8694  
265 pyroxenes cluster in Fig. 5, we distinguish poikilitic, mesostasis and inclusion pyroxene in Fig. S4, which shows that  
266 they differ mainly in orthopyroxene abundance. Calcium variation is partly due to overlap on host and exsolution  
267 lamellae.

268  
269 Although all chassignite parameters to date are more magnesian than those of nakhlites, Fig. 5 shows that the  
270 compositions of augite in NWA 8694 and in nakhlites overlap. The minor elements in augite as a function of Ca also  
271 show a partial overlap between chassignites and NWA 998, and cores in some other nakhlites (Udry and Day, 2018),  
272 as shown in Fig. 6. Other more fractionated nakhlites show a much wider range of minor element concentrations, off  
273 the scale of this figure for Al and Ti, and reaching much lower Cr values.

### 274 275 3.3.3 Chromite

276 The range of chromite compositions (Table 2a and S1) is  $\text{Spl}_{11-21} \text{Chr}_{57-76} \text{Usp}_{5-20} \text{Mag}_{7-12}$ . This range overlaps  
277 the compositions of chromite in the other chassignites, but it lacks the most Cr-rich compositions and is on average  
278 richer in Ti and  $\text{Fe}^{3+}$  (Fig. 7). Accessory ilmenite,  $\text{Ilm}_{96} \text{Hem}_{04}$ , present in the interstitial material is very similar in  
279 composition to ilmenite in Chassigny, except that the latter is more magnesian (Floran et al., 1978). Chromite is  
280 absent in nakhlites while ilmenite occurs primarily as lamellae in Ti-magnetite as a result of oxy-exsolution.

### 281 282 283 3.3.4 Feldspars

284 Feldspathic material occurs in the interstitial trapped material and, though featureless in BSE, it appears to  
285 be feldspar laths embraced in part by sub-ophitic pyroxene. EPM data for this (Table 3, S1) are plotted in Fig. 8  
286 Feldspar is mainly Na-rich with oligoclase composition ( $\text{An}_{22.5 \pm 5.1} \text{Ab}_{70.0 \pm 5.8} \text{Or}_{7.5 \pm 2.3}$ ) but has a range of  $\text{An}_{27-}\text{Or}_{7-}$   
287 through intermediate alkali feldspar to K-rich feldspar  $\text{An}_{1.9 \pm 1.0} \text{Ab}_{24.2 \pm 4.9} \text{Or}_{73.9 \pm 5.5}$ .

288 The interstitial feldspar composition in Chassigny (this work, Floran et al., 1978) has a similar range to  
289 NWA 8694 from plagioclase to alkali feldspar as shown in Fig. 8a, but is more calcic and less potassic. These two  
290 chassignites have similar feldspar compositions to those of the Lafayette, Nakhla and NWA 5790. Interstitial  
291 feldspar analyses for NWA 2737 shown in Fig. 8a are analbite, confirming work by Beck et al. (2006) and Treiman  
292 et al. (2007), and in Fig. 8b plot in the field of alkali glasses in melt inclusions (see below).

293  
294 Because of questions of Na loss, admittedly not usual in maskelynite but possible under the electron beam,  
295 we examine the stoichiometry of our analyses. Both Fig. 9a and 9b show half the join  $\text{NaAlSi}_3\text{O}_8$ - $\text{CaAl}_2\text{SiO}_8$  and  
296 their proximity to the line shows that NWA 8694 feldspar analyses are stoichiometric. Bulk analyses of interstitial  
297 trapped melt analyzed by LA-ICP-MS are also shown in Fig. 9, excluding analyses with major overlaps on olivine,  
298 pyroxene or apatite. They project fairly close to feldspar compositions, consistent with the high feldspar contents of  
299 the regions analyzed.

### 300 301 3.3.5 Melt Inclusion Glass

302 Two discrete Si- and Al-bearing glass phases may be observed as anhedral patches in the melt inclusions in  
303 olivine (Fig. 2c), the higher Z phase being richer in K (up to 5 wt%  $\text{K}_2\text{O}$ ) and also Ca (Table 4). Most of the Si-Al-  
304 rich glasses shown in Fig. 8b and 9 are far from feldspar composition. The low-Z glass is very varied in  
305 composition, and we separate it into several somewhat arbitrary composition groups. These are Al- (and Na-) rich,  
306 Al-poor (though K-rich glass is also Al-poor), and cation-poor, and are distinguished in Fig. 9 and 10. They are all  
307 very Si-rich (70-79 wt%  $\text{SiO}_2$ ) except for the Al-rich group some of which are close to albite in composition.

308

We also plotted melt inclusion glasses in the two other chassignites in Fig. 8b. For Chassigny both Floran et al. (1978) and Johnson et al. (1991) reported K- and Na-bearing glasses, similar to the “K-rich” glass of NWA 8694, and Johnson et al. (1991) also reported albitic glass similar to the “Al-rich” glass in NWA 8694. He et al. (2013) and Beck et al. (2006) reported Si-Al-rich alkali glass in inclusions in NWA 2737 with a wide range of Na/K ratios and low Ca.

### 3.3.6 Sulfides

Sulfide compositions are shown in Table 5. MI-enclosed pyrrhotite is  $(\text{Fe,Ni})_{0.87}\text{S}$  (monoclinic pyrrhotite). Interstitial grains show a larger compositional range from  $(\text{Fe,Ni})\text{S}$  (troilite) to  $(\text{Fe,Ni})_{0.82}\text{S}$  (smythite): their mean metal-to-sulfur ratio is centered on  $\text{Fe}_{0.9}\text{S}$  (hexagonal pyrrhotite) in both NWA 8694 and Chassigny (Floran et al., 1978; Lorand et al., 2018). (NWA 2737 contains troilite rather than pyrrhotite). Whether enclosed in olivine-hosted melt inclusions or occurring as interstitial grains, the NWA 8694 pyrrhotite compositions have the same Ni contents ( $1.2\pm 0.5$  vs.  $1.1\pm 0.5$  wt.%;  $n = 16$  and  $13$  for enclosed and interstitial grains respectively; uncertainty is standard deviation). By comparison, the compositional range of Chassigny pyrrhotite extends to higher Ni contents (2.9 wt.%; Lorand et al., 2018; Fig. 11). NWA 8694 pyrrhotite is intermediate in Ni content between Chassigny pyrrhotite and pyrrhotite of the most magnesian nakhilites (NWA 998; Nakhla;  $\text{Ni} < 0.8$  wt.%; Chevrier et al., 2011). Pyrite in NWA 8694 and Chassigny is slightly nickeliferous (0-1 wt.%;); some analyses of NWA 8694 pyrite show Ni contents up to 2.8 wt.% (Fig. 11).

### 3.3.7 Other phases

Biotite, amphibole and phosphate phases are of particular interest because of their anions and the possibility of estimating H concentrations, and because of the possible presence of  $\text{Fe}^{3+}$ . Analyses are given in Tables 2a and 4.

NWA 8694 contains Mg-rich biotite (approximately  $\text{Phlog}_{75}\text{Ann}_{25}$  with fairly low halogen content) in both melt inclusions and interstitial trapped melt. Although biotite ionic substitutions are particularly complicated (Dymek, 1983) this biotite seems to be close to stoichiometric with nominal valences, except for a deficiency of K in the interlayer site. Structural formulae calculated on an eleven anion basis, and on a seven cation basis (“Y”, with K excluded), give very similar results:  $\text{K}_{0.85}\text{Y}_{6.98}\text{O}_{11.00}$  and  $\text{K}_{0.85}\text{Y}_{7.00}\text{O}_{11.03}$ . Halide concentrations are higher in the interlayer site in the interstitial phlogopite than in the melt inclusion biotite (Fig. 12), with  $(\text{X}_{1.67}\text{F}_{0.25}\text{Cl}_{0.08})^{2-}$  versus  $(\text{X}_{1.88}\text{F}_{0.10}\text{Cl}_{0.02})^{2-}$ . Considering the errors in EMP analysis there is no justification for calculating  $\text{Fe}^{3+}$ . Ti contents are lower than in the other chassignites (Johnson et al., 1991, He et al., 2013), higher in interstitial biotite (0.2-3.8 wt%) than in melt inclusion biotite, and not correlated with any excess positive charge. The missing component X in the anion site is therefore likely to be entirely OH.

Amphibole in a melt inclusion is shown in Fig 2c. Its structural formulae derived on a 23 oxygen-equivalent basis can be written as  $(\square_{0.31}\text{Na}_{0.65}\text{K}_{0.04})_{1.00}(\text{Ca}_{1.81}\text{Na}_{0.19})_{2.00}(\text{Mg}_{2.30}\text{Fe}_{1.67}\text{Mn}_{0.04}\text{Ti}_{0.35}\text{Cr}_{0.01}\text{Al}_{0.70})_{5.07}(\text{Si}_{5.96}\text{Al}_{2.04})_{8.00}\text{O}_{22}(\text{X}_{1.58}\text{F}_{0.31}\text{Cl}_{0.11})_{2.00}$  (where the  $\square$  denotes vacant A sites). The OH content of amphibole is difficult to define from stoichiometry, and the history of other chassignite amphiboles is complex (Watson et al., 1994; McCubbin et al., 2010; Giesting et al., 2015). The amphibole in NWA 8694 may be moderately OH-rich, and it is close to pargasite in composition. The phosphate found in the interstitial melt is Cl-rich fluorapatite (Table 3)  $\text{Ca}_{4.77}\text{A}^*_{0.10}(\text{P,SiO}_4)_{3.00}(\text{F}_{0.62}\text{Cl}_{0.31}\text{X}_{0.07})_{1.0}$  using a 3 P+Si ion basis, where  $\text{A}^*$  is other cations and the missing fraction X is assumed to be OH. Baddeleyite contains significant Nb, Th and U, as indicated by their EDS spectra (no WDS analysis).

## 3.4 Whole rock and mineral geochemistry

Whole rock chemical analyses are provided in Tables 6 and 7. As accurate bulk  $\text{SiO}_2$  contents are difficult to obtain with available instrumental techniques, we used instead a modal recombination of EMP data for  $\text{SiO}_2$  in both Florida LA-ICP-MS and Plouzané ICP-AES analyses for NWA 8694 and Chassigny for  $\text{SiO}_2$  and recalculated the Florida data downwards to reflect the new analytical total of the major elements. This brought the major elements, especially Fe and Mg into agreement. Incompatible trace element concentrations remain higher in the Florida bulk composition (like those of the chassignite NWA 2737) than in the Plouzané data set (like those of Chassigny).



365  
366 LA-ICP-MS data for individual phases (olivine, pigeonite and mesostasis) in NWA 8694 and Chassigny are  
367 given in Tables 7 and S2. The trace element abundance patterns for bulk chassignites and mesostasis-rich nakhlites  
368 (Jambon et al., 2016) are closely parallel (Fig. 13). For clarity, we omit mesostasis-poor nakhlites, which have trace  
369 element abundances intermediate between those of chassignites and mesostasis-rich nakhlites (Udry and Day, 2018).  
370

371 The Rare Earth Element (REE) concentrations are shown in Fig. 14 along with bulk compositions.  
372 Intercumulus material has a heterogeneous distribution, as seen in Figure 2. Modal analysis of three polished  
373 sections showed different proportions of intercumulus material, and the apparent composition of mesostasis ranges  
374 from basaltic trachyandesite to trachyte. We therefore interpret the differences in the two bulk analyses (and in the  
375 other two chassignites) as due to different abundances of trapped liquid component.  
376

377 Augite, chromite, and apatite are too small for easy analysis by laser. We calculated an apparent bulk  
378 composition from olivine, pigeonite, and mesostasis abundances and compositions. Compared to the true bulk  
379 composition, there is a deficiency in P and REE. We calculated that the concentration of  $P_2O_5$  corresponds to 0.14%  
380 apatite. We assumed that this apatite contains all the REE unaccounted for. This gives an REE (Fig. S5) pattern for  
381 the missing phase close to that of Chassigny apatite (Wadhwa and Crozaz, 1995). Table 6. Whole rock analyses of  
382 three chassignites by atomic emission spectroscopy (AES) and sector field mass spectrometry (SFMS).

383 REE in average Chassigny olivine exhibit a V-shaped pattern enriched in both the light and the heavy REE  
384 (LREE and HREE) relative to Sm and Eu (Fig. 14a), while the average NWA 8694 olivine composition exhibits a  
385 classic olivine pattern with higher HREE than light REE. A slight uptick at La is visible. The REE patterns of  
386 pyroxenes from NWA 8694 exhibit a classic “humped” pattern of clinopyroxene with a prominent negative Eu  
387 anomaly, and heavy REE higher than bulk NWA 8694 REE abundances. Despite the different Fe/Mg ratios of the  
388 three chassignites, the REE concentrations of pigeonite show some overlap (Fig. 14a). The slope of the HREE  
389 pattern is steeper for two Chassigny pyroxene analyses than for five pigeonites in NWA 8694:  $(Gd/Lu)_{CI}$  of ~3 vs.  
390 ~1. LREE concentrations for NWA 8694 and Chassigny mesostasis have similar values to those of nakhlite bulk and  
391 mesostasis (Jambon et al., 2016), but their slope is steeper (Fig. 14c).

392 The abundance of Be correlates with that of  $Al_2O_3$  (Fig. 15),  $Na_2O$  (and other alkalis). Beryllium behaves  
393 moderately incompatibly with the lowest concentrations in olivines, then pyroxenes and the highest concentrations  
394 in mesostasis (Fig. 15). The correlation is weaker in the interstitial material where the concentrations of both Be and  
395  $Al_2O_3$  (or  $K_2O$ ) are highest, with a lower Be/Na ratio in NWA 8694 interstitial material than in Chassigny. The  
396 correlation between Be and other incompatible elements is weakened by the crystalline nature of the mesostasis.  
397 Boron exhibits a similar behavior to Be (Fig. 15). Boron abundances correlate with  $Al_2O_3$  in olivines and pyroxenes  
398 from both Chassigny and NWA 8694 with the highest concentrations in the mesostasis but the correlation is no  
399 longer evident for mesostasis analyses (Fig. 15). The tendency of incompatible element correlations to fall apart in  
400 analyses of the mesostasis does not allow us to infer that B was lost by outgassing.  
401  
402

## 403 4. DISCUSSION

### 404 4.1 Comparison of NWA 8694 to Chassignites and Nakhlites

405  
406 Ferroan chassignite NWA 8694 has the lowest olivine and chromite contents, and the highest pyroxene  
407 content of the three chassignites. Its low olivine content allows small pockets with isolated olivine grains giving a  
408 local orthocumulate texture. Phase compositions indicate a more evolved parent liquid than for the other  
409 chassignites. Mafic phases in NWA 8694 are the most fractionated among the chassignites. Its olivine has the lowest  
410 Mg and Ni contents; its chromite has the lowest Cr contents; its pyroxene the lowest Mg; and its amphibole the  
411 lowest Mg and Ti contents. Interstitial feldspar compositions are a little less calcic and more potassic than in the  
412 Chassigny (Fig. 5a), ranging from oligoclase  $An_{27}$  up to sanidine  $Or_{79}$ . Both NWA 8694 and Chassigny show  
413 sulfides enclosed inside olivine-hosted melt inclusions, and intercumulus sulfides but sulfides in NWA 8674 are  
414

415 richer in Fe than those in Chassigny. The amphibole in melt inclusions is more ferroan and richer in Cl than in the  
416 other chassignites, though F has similar concentration ranges in all three.

417  
418 Chassigny and NWA 2737 are weakly and strongly shocked, respectively (Floran et al., 1978; Johnson et  
419 al., 1991; Langenhorst and Greshake, 1999; Beck et al., 2006; Treiman et al., 2007; He et al., 2013) and fracturing in  
420 NWA 8694 olivine resembles that in Chassigny implying that it shares the same shock levels as Chassigny. The  
421 same main sulfide phases (pyrrhotite, pyrite, pentlandite) identified in the Chassigny meteorite (Floran et al., 1978;  
422 Lorand et al., 2018) were also preserved in NWA 8694. The pyrite shows planar fractures consistent with weak  
423 shock (Lorand et al., 2015). NWA 2737 also shows sulfides in similar amount as in Chassigny and NWA 8694  
424 meteorites. However, the strong shock event that liberated NWA 2737 from Mars deeply altered its igneous and  
425 hydrothermal sulfides in an assemblage of troilite and Fe-Ni metal (Lorand et al., 2012).

426  
427 NWA 8694 has some properties closer to those of nakhlites than those of the other chassignites: its olivine  
428 composition  $Fo_{54}$  (Fig. 4) approaches that of the least equilibrated nakhlites with a maximum of  $Fo_{45}$  in NWA 817  
429 (Udry and Day, 2018); its augite composition ( Fig. 5, 6, 14) overlaps with those of the most magnesian nakhlites  
430 (Friedman-Lentz et al., 1999; Treiman, 2005; Treiman and Irving, 2008; Udry and Day, 2018) and all other  
431 nakhlites have augite cores with very similar composition. Specifically, some Lafayette and NWA 998 points  
432 (Treiman and Irving, 2008; Udry and Day, 2018) coincide at  $En_{41-40}Wo_{38-39}$  with analyses from NWA 8694. The  
433 heavily overlapping adjacent points in Fig. 5 are due to the most magnesian augite in five other nakhlites (Udry and  
434 Day, 2018); the minor element concentrations of these augites also overlap (Fig. 6). The minor elements in augite as  
435 a function of Ca also show a partial overlap between chassignites and augite cores in some other nakhlites (Udry and  
436 Day, 2018), as shown in Fig. 6. Major element compositions of NWA 8694 and Chassigny plagioclase and sanidine  
437 (Fig. 8a) are like those in nakhlite mesostases (Bunch and Reid, 1975; Jambon et al., 2016).

438  
439 However, most pyroxene rims in nakhlites are more ferroan; the more fractured nakhlites show a much  
440 wider range of minor element concentrations in pyroxene, off the scale of this figure for Al and Ti, and reaching  
441 much lower Cr values. The partial overlap in Fe/Mg in augite (Fig. 5) indicates very similar compositions for late  
442 interstitial melt in NWA 8694 and parental melt of the most primitive nakhlites. The partial overlap in minor  
443 elements (Fig. 6) for all chassignites and NWA 998 and Lafayette also indicate melt similarities at the stage of last  
444 and first augite crystallization, respectively, in their two hosts. The increases in the incompatible Al and Ti in most  
445 nakhlite augite, and the decrease in its compatible Cr show extensive fractional crystallization of a liquid like late  
446 chassignite interstitial liquid. Major element compositions of NWA 8694 and Chassigny mesostasis plagioclase and  
447 sanidine (Fig. 8a) are like those in nakhlite mesostases (Bunch and Reid, 1975; Jambon et al., 2016); The bulk  
448 composition of NWA 8694 mesostasis corresponds to basaltic trachyandesite to trachyte (Tables 7, S4), like the  
449 alkaline melt inclusions in the MIL 03346 nakhlite (Day et al., 2006). In addition, Chassigny, NWA 8694, and  
450 nakhlites have similar incompatible element concentrations in their mesostases (Fig. 13, 14).

451  
452 Chassignites and nakhlites have long been known to have similar ages and patterns of trace element  
453 distributions (e.g. Wadhwa and Crozaz, 1995; Beck et al., 2006). Here we have shown that mineral (other than  
454 cumulus olivine and chromite) and mesostasis compositions of NWA 8694 are similar to those of nakhlites. This  
455 confirms previous conclusions that chassignites and nakhlites are genetically related rocks derived from the same  
456 mantle source (Wadhwa and Crozaz, 1995; Beck et al., 2006; Udry and Day, 2018), and is consistent with the  
457 invasion of both chassignite intercumulus liquids and nakhlite parent magma with Cl-rich fluids (McCubbin et al.,  
458 2013). Thus the parent liquid of NWA 8694 must be closely related to nakhlite liquids. We explore below whether  
459 fractional crystallization of model parent liquids, magnesian or nakhlitic, can yield olivine and late liquid of the  
460 compositions seen in NWA 8694.

## 461 462 463 **4.2 Crystallization modeling**

### 464 465 *4.2.1 Magnesian parent Liquids*

466 Udry and Day (2018) showed that subtraction of 12-15% olivine and 2-5% pyroxene from a chassignite  
467 parent magma with 15 wt % MgO would produce a composition like that of the most primitive nakhlites. This  
468 magma would resemble a depleted basaltic komatiite, except in being more ferroan. The subtraction model suggests  
469 that fractional crystallization could produce the chassignites and the nakhlites from a single magma, which appears

470 to be consistent with trace element similarities. The complexities of modeling crystallization of martian liquid  
471 compositions are well known (e.g. Stockstill et al., 2005; Udry et al., 2014) and the three chassignites have an  
472 extensive range of olivine composition, from Fo<sub>79</sub> to Fo<sub>53</sub>. We have found that PETROLOG (Danyushevsky and  
473 Plechov, 2011) can explain the formation of shergottite NWA 10414 (Hewins et al., 2019). We use it here to see  
474 whether proposed chassignite parent melts could crystallize olivine and late liquid of the compositions found in  
475 NWA 8694.

476  
477 The PETROLOG program calculates pseudo-liquidus temperatures using mineral-melt equilibria models  
478 for all possible minerals. We used the optional models of Sack et al. (1980) for melt oxidation state and Ariskin et  
479 al. (1993) for silicate mineral-melt equilibria, with a variable K<sub>D</sub> for olivine/melt Fe/Mg partitioning, ranging  
480 between 0.32 and 0.35 during crystallization. Calculated pseudo-liquidus temperatures are compared to determine  
481 which phase(s) should crystallize.

482  
483 We first evaluated the reconstructed parental melt composition of melt inclusions in olivine in NWA 2737  
484 termed A# with 12.1% MgO (He et al., 2013) to see whether it could crystallize the olivine of all three chassignites.  
485 Fractional crystallization of NWA 2737 A# at 1 bar starts at 1335°C and produces 21% olivine Fo<sub>79-64</sub>, and at 5 kb  
486 11% olivine/ Fo<sub>79-73</sub>, with an oxygen fugacity relative to the fayalite-magnetite-quartz oxygen buffer of FMQ -1 log  
487 units. Augite appeared too early for the ferroan composition of NWA 8694 olivine to be achieved. Similar results  
488 were obtained with many other proposed parent liquids, e.g. for Chassigny parent A\* (Johnson et al., 1991) we  
489 found Fo<sub>68-61</sub> was crystallized, again falling well short of NWA 8694 olivine. Clearly a more complex process than  
490 fractionation of a single magma is needed to produce the range of chassignite olivine compositions stretching to Fo<sub>53</sub>  
491 and the even more ferroan olivine in nakhlites. Given the prevalence of multiple magma chambers and mush zones  
492 under large volcanoes, mixing of primitive and fractionated liquids is likely, as well as contamination by wall rocks.  
493 We therefore turned our attention to liquids with closer affinities to NWA 8694.

494  
495 *4.4.2 Nakhlitic parent liquids*  
496 We considered the NWA 8694 interstitial mesostasis analyses with added olivine as a possible parent melt,  
497 but this composition failed to produce sufficiently alkaline daughter liquids, probably because the mesostasis  
498 analyses are not representative of the liquid (Hewins et al., 2017). Bearing in mind the number of similarities  
499 between nakhlites and chassignites, as well as their alkaline nature (Prinz et al., 1974; Floran et al., 1978; Day et al.,  
500 2006; Nekvasil et., 2007; Udry and Day, 2012; Barrat and Bachèlery, 2019) we considered more alkaline parent  
501 liquids with nakhlite affinities.

502  
503 In Fig. 14, we show four bulk REE patterns for the three chassignites along with nakhlite bulk and  
504 mesostasis compositions (Jambon et al., 2016). Note that the four patterns for chassignites are nearly parallel, and  
505 reflect different quantities of trapped liquid. The chassignite patterns show a strong resemblance to those of nakhlite  
506 mesostases and bulk nakhlites. LREE contents of the NWA 8694 mesostasis liquids (as shown in Fig. 14) overlap  
507 with those of trace-element-rich nakhlites NWA817, MIL03346 and NWA5790 (Jambon et al., 2016), rather than  
508 those of trace-element-poor nakhlites (Udry and Day, 2018), though the HREE appear to be affected by  
509 undersampled carrier phases, as discussed above. In a search for a parent for NWA 8694, we selected a relatively  
510 Na- and K-rich nakhlite reheated melt inclusion composition with intermediate silica, NA01a of Stockstill et al.  
511 (2005). This composition (Table 7) did indeed produce relatively alkaline daughter liquids with PETROLOG (Fig.  
512 16) at FMQ-1, based on an estimate of FMQ-1.3 for Chassigny (Floran et al. (1978), and 1 bar, but was not olivine-  
513 saturated.

514  
515 We added Nakhla core olivine (Treiman, 2005) to the NA01a parent in different amounts, to construct a  
516 series of olivine-saturated liquid compositions. Modeling of these parent liquids gave olivine compositions  
517 overlapping that in NWA 8694 (Fig. 17) and alkaline daughter liquids (Fig. 16). These compositions were  
518 crystallized at 1 bar and at 5 kb. The 5 kb calculations deviated further from NWA 8694 interstitial liquid  
519 composition than the corresponding 1 bar calculations, and those runs are not illustrated in the figures. The silica  
520 enrichment trend caused by olivine crystallization was reversed when olivine gave way to pyroxene, but continued  
521 when pyroxene was joined by plagioclase. The pyroxene was augite, with no pigeonite. The daughter liquids also  
522 passed close to NWA mesostasis compositions (Fig. 16), with the composition with 10% added olivine producing a  
523 better match than that with 20% added olivine. Olivine Fo<sub>54-50</sub> formed in the 10% composition from 1144-1118°C at  
524 1 bar, when it was replaced by augite; augite was joined by plagioclase at 1085°C, and the two phases cocrystallized  
525 until the liquid was 80% solidified at 797°C. The latter calculated daughter liquids are virtually Mg-free, unlike the

526 analyses of trapped liquid in NWA 8694 (Fig. 16), because early magnesian crystals are removed in the calculation  
527 whereas they remain in the natural mesostasis (Fig. 2d). Trapped liquids in the cumulate pile would undergo Fe-Mg  
528 exchange with cumulate minerals (e.g., Coogan and O'Hara, 2015; Lissenberg and MacLeod, 2016) limiting the  
529 extent of the Fe-enrichment achieved compared with a fractional crystallization calculation.  
530

531 We have satisfied the minimum requirements of a parent magma for NWA 8694, to produce relatively  
532 ferroan olivine and alkaline mesostasis, but are far from having a unique solution and a rigorous history for the  
533 formation of NWA 8694. Nevertheless, we have identified a liquid composition capable of producing chassignite-  
534 like cumulates and nakhlite-like daughter liquids. The strong relationship between chassignites and nakhlites is  
535 supported, in particular in the similar alkaline nature of mesostases (Day et al., 2006).  
536

### 537 4.3 Trace Element Geochemistry

#### 538 4.3.1 REE of mesostasis and possible parental liquids

539 The close parallelism between incompatible trace element abundance patterns for bulk chassignites and  
540 mesostasis-rich nakhlites (Fig. 13) indicates a close genetic relationship, in which crystal fractionation must have  
541 played a role (this work, Beck et al., 2006, Jambon et al., 2016). The REE patterns for olivine indicate that small  
542 melt inclusions (enriched in LREE) are ubiquitous in the large (50-100  $\mu\text{m}$ ) spots used to analyze REE in the  
543 olivines in Chassigny, but are significantly less in olivine from NWA 8694.  
544

545 Mesostasis constitutes ~5% of the bulk rock, based on incompatible element ratios such as La/Yb and  
546 Gd/Yb. As we have ~4% modal feldspar, this indicates that most of the pyroxene (~9%) is accumulated in origin. The  
547 analyses of the interstitial material exhibit compositional heterogeneity that is more complex than could be produced  
548 solely by fractional crystallization. It was shown that the true composition of Chassigny interstitial material was  
549 difficult to determine owing to the impossibility of avoiding the surrounding mafic silicates, but it shows significant  
550 enrichment of lithophile incompatible elements, including REE. The NWA 8694 interstitial material shows less  
551 contamination by mafic silicates, reaching extremely low MgO contents (<1 wt. %), but some analyses exhibit  
552 strong plagioclase or phosphate signatures (Fig. 14b).  
553

554 Bulk REE concentrations result from the mixing of mafic silicates with average mesostasis, but mesostasis  
555 exhibits great variations in REE contents. The plagioclase-dominated patterns of NWA 8694 mesostasis are low in  
556 REE abundance and exhibit large positive Eu anomalies, with Eu/Eu\* of 40-100. Fig. 18 is a plot of the Eu anomaly  
557 against the CI-normalized La abundance ( $\text{La}_{\text{CI}}$ ) for the interstitial material and shows a mixing curve between  
558 phosphate-dominated mesostasis analyses at the high  $\text{La}_{\text{CI}}$  end with slightly negative Eu anomaly, and low  $\text{La}_{\text{CI}}$  with  
559 large positive Eu anomalies for the plagioclase-rich analyses. A few of the Chassigny interstitial material  
560 compositions plot along the correlation defined by the NWA 8694 mesostasis analyses, but most of the Chassigny  
561 analyses plot away from the mixing curve towards the bulk and olivine+pyroxene points at lowest  $\text{La}_{\text{CI}}$  with small  
562 negative Eu anomalies. Fig. 18 shows that most of the NWA 8694 mesostasis patches (black diamonds) are mixtures  
563 of plagioclase and phosphate, which probably crystallized from the interstitial liquid. The average REE pattern is  
564 matched by a mixture of 96% plagioclase and 4% apatite from NWA 2737 for La-Gd (Fig. S5), while HREE were  
565 below the detection limit in plagioclase (Beck et al., 2006). Measurements of the bulk NWA 8694 composition  
566 exhibit small negative Eu anomalies. We note that most Chassigny mesostasis points but only a few NWA 8694  
567 points plot close to the Nakhla parental magma composition (Treiman, 2005) in Fig. 18. The latter exhibits no Eu  
568 anomaly and has a  $(\text{La}/\text{Yb})_{\text{CI}}$  ratio of 6, similar to the  $(\text{La}/\text{Yb})_{\text{CI}}$  (5-7) of mesostasis compositions for nakhlites NWA  
569 5790, NWA 817, and MIL 03346 (Jambon et al., 2016). The dispersion of the NWA 8694 points in Fig. 15 is a  
570 challenge in searching both for chassignite relationships and for parent magma compositions.  
571

#### 572 4.3.2 Processes modifying trace element distributions

573 The LREE concentrations in mesostasis in NWA 8694 are similar to those of Chassigny and nakhlites  
574 (Treiman, 2015), consistent with a fractionation relationship, although the HREE are difficult to explain. Curiously,  
575 the interstitial material in both Chassigny and NWA 8694 has strongly sloping REE patterns (Fig. 14c) that exhibit a  
576 higher  $(\text{La}/\text{Yb})_{\text{CI}}$  ratio than that of nakhlites (8-17 in Chassigny interstitial material; 48-103 in NWA 8694 interstitial  
577 material; Fig. 18). Even the phosphate-dominated mesostasis analysis from NWA 8694 has a  $(\text{La}/\text{Yb})_{\text{CI}}$  of 74 and its  
578 REE pattern is parallel to those of the other NWA 8694 interstitial patches. Thus, fractional crystallization within the  
579 NWA 8694 mesostasis appears not to have changed the slope of the REE pattern. If these interstitial patches are the  
580

581 last dregs of the crystallizing magma, then interstitial material from Chassigny more closely resembles nakhlite  
582 mesostasis, and hence a nakhlite parental magma: the late liquid in NWA 8694 has a more strongly sloping REE  
583 pattern than probable nakhlite parental melt compositions by about an order of magnitude. Very few processes can  
584 fractionate heavy REE (HREE) during fractional crystallization. Neither pyroxene nor olivine removal could remove  
585 enough of the HREE to increase the slope of the REE pattern that significantly. A phase high in HREE relative to  
586 melt that possibly could be invoked is zircon, but removal of zircon would also lower the Zr-Hf abundances, which  
587 is not observed. Some HREE-rich mesostasis phases, baddeleyite and zirconolite, are attached to the surrounding  
588 olivine, and are therefore undersampled in the laser spot on plagioclase-rich mesostasis areas. This undersampling  
589 explains the steep REE pattern, as baddeleyite (1%)-mesostasis mixtures give less steep patterns resembling nakhlite  
590 mesostasis (Fig.S6).

591 With the discovery of the second chassignite, NWA 2737, olivine fractionation from parental melt(s)  
592 appeared to be the major process influencing chassignite compositions (Beck et al., 2006). Other igneous processes  
593 e.g. different degrees of melting of the same source seen for nakhlites and hotspot basalts (Goodrich et al., 2013;  
594 Vlastélic et al., 2018), trapping of different amounts of liquid (Barrat and Bartélery, 2019), and migration of  
595 mesostasis liquid (Treiman, 2005) could also have influenced melt compositions. In addition, a series of interactions  
596 with the exterior, e.g. assimilation (Humayun et al., 2020), fluid infiltration (McCubbin et al., 2013; Nagao et al.,  
597 2019) and outgassing (Yang et al., 2019) have been shown to modify chassignite compositions. Fig. 19 shows the  
598 incompatible element abundances for the interstitial material plotted on a Martian mantle-normalized plot (Yang et  
599 al., 2015) with elements organized according to decreasing incompatibility from left to right. Difficulties may arise  
600 from the heterogeneity and small size of mesostasis patches, and overlap on melt inclusions and other phases for  
601 olivine and pyroxene. For example, positive anomalies in Ba and Sr in the mesostasis patches are likely due to  
602 plagioclase oversampling (Fig. 19), while the steep slope of their REE (high La/Yb) seen in Figs. 14b and 19 may be  
603 due to undersampling of baddeleyite or oversampling of phosphate. However, other processes must be involved, as  
604 we see poor correlation between Cs (and Tl) and Rb (Table 7, S2) for the interstitial material with the highest Rb  
605 contents even though K, Rb, Tl and Cs are likely to be in the same phases. Here we discuss the roles of fractional  
606 crystallization versus other processes on trace element distribution during the formation of NWA 8694.

#### 607 608 *Fluids*

609 McCubbin et al. (2013) argued that chassignites and nakhlites were invaded by Cl-rich fluids after  
610 crystallization of the cumulus phases. Bellucci et al. (2016) showed that radiogenic Pb was introduced into  
611 Chassigny minerals by surface fluids entering fractures that were subsequently annealed. Hydrothermal fluids  
612 operated pervasively in Chassigny (Lorand et al., 2018) and in NWA 8694 as shown by magmatic sulfides that were  
613 converted to pyrite. We cannot demonstrate trace element modification by fluids, but Nagao et al. (2019) showed  
614 from noble gas data that NWA 8694, like the MIL nakhlites, had interacted with surface fluids.

#### 615 616 *Fractional crystallization*

617 The most highly incompatible elements (Cs-Nd) are concentrated by factors of 25 in NWA 8694 and  
618 Chassigny mesostasis (Fig. 19), as well as in nakhlite mesostasis, relative to the martian mantle. The bulk NWA  
619 8694 composition plots close to martian mantle abundances (Yang et al., 2015) for Cs-Nd, with the exception of  
620 excesses of Tl and U. The abundances of these two elements might be increased by terrestrial alteration in the desert  
621 (known for U), but five spot analyses of pyroxene from NWA 8694 also exhibit positive Tl and U anomalies (Fig.  
622 16) indicating that strong separation of U and Tl is a feature of pyroxene accumulation. Anomalies in Tl and U are  
623 not seen in the mesostasis, indicating that pyroxene fractionated from the parental melt but that mesostasis  
624 crystallization cannot account for their compositions.

625  
626 Thorium and U are highly incompatible elements, with U being slightly preferred over Th in the lattice of  
627 clinopyroxene (LaTourette and Burnett, 1995). The Th/U ratio is systematically low in olivines (<0.2) from both  
628 Chassigny and NWA 8694, implying that some U is present in the olivine lattice, while Th is near the detection limit  
629 (Table7 and S2). The Th/U ratio is ~2 in pyroxenes from Chassigny and even lower (<0.5) in pyroxenes from NWA  
630 8694, consistent with experimental constraints for Th-U partitioning in low-pressure pyroxenes (LaTourette and  
631 Burnett, 1995). The Th/U ratio is systematically higher in NWA 8694 mesostasis (5.1) than in Chassigny interstitial  
632 material (3.9). Nakhlites are known to exhibit a superchondritic Th/U ratio (~4), but NWA 8694 interstitial patches

633 are even higher in Th/U than any nakhlite. These observations suggest that nakhlitic liquid crystallized pyroxene in  
634 NWA 8694 and evolved to mesostasis composition.  
635

636 Bulk NWA 8694 and NWA 8694 interstitial material also exhibit a small deficiency of Nb-Ta and of Zr-Hf  
637 (Fig. 19). The Zr-Hf deficiency is also observed in Chassigny interstitial material to a lesser degree. These Nb-Ta-Zr-  
638 Hf deficiencies point to Fe-Ti oxide crystallization since pyroxene from NWA 8694 also exhibits the Zr-Hf  
639 deficiency. Ilmenite is an accessory phase in interstitial mesostasis, as are the undersampled baddeleyite and a few  
640 Nb- and Th-rich Ca-Ti-Zr microphases, notably zirconolite, that explain the slope of the REE pattern.  
641

#### 642 *Outgassing*

643 The concentrations of Ge and Zn in the olivine and pyroxene in chassignites and nakhlites appear to be  
644 controlled by fractional crystallization (Yang et al., 2019). However, olivine, pyroxene, and mesostasis in NWA  
645 8694 have lower Ge than expected from its incompatible nature (Table 7). The Ge/Si ratio is relatively constant in  
646 the martian mantle (Yang et al., 2015). The Ge contents (~2.5 ppm) and Ge/Si ratios of Chassigny interstitial  
647 material are similar to those of bulk chassignites, but the NWA 8694 interstitial material is depleted in Ge (~0.6-0.8  
648 ppm). Melting of a more garnet-rich source for NWA 8694 interstitial material could explain both the higher  
649 (La/Yb)<sub>CI</sub> and the lower Ge/Si ratios observed, but for the Ge/Si ratio this depletion is still larger than expected.  
650 Magmatic outgassing has been shown to lower Ge/Si ratios in shergottites (Yang et al., 2019) to values similar to  
651 that observed in NWA 8694 interstitial material. Thus, a late-stage outgassing of the melts from which NWA 8694  
652 mesostasis was trapped, or a distinct magmatic origin for the interstitial material, is indicated by the Ge-Si  
653 systematics. This evidence makes it hard to derive nakhlites by fractional crystallization from the same melt as  
654 NWA 8694, and implies that nakhlites and chassignites were derived from multiple magma bodies.  
655

## 656 **4.4 Terrestrial Analogues and Geological Setting**

### 657 *4.4.1 A single cumulate pile or separate flows*

658 In plutonic and most hypabyssal rocks pigeonite exsolves augite and inverts to orthopyroxene because of  
659 slow cooling (Hess, 1960; Robinson, 1980). The augite lamellae in pigeonite in NWA 8694 are ~2 μm in apparent  
660 width (Fig. 2b), comparable to or a little wider than those in Chassigny (Monkawa et al., 2004), suggesting a near-  
661 surface environment, such as a thick flow, or shallow reservoir, rather than plutonic cooling. The fine plagioclase  
662 laths in Nakhla mesostasis also indicate rapid cooling (Treiman, 1986). The reverse zoning of Ca in olivine  
663 indicating only partial loss of Ca (as in Chassigny), the failure of pigeonite to invert, and the fine grain size of the  
664 mesostasis, are also inconsistent with emplacement at significant depth. The adcumulate texture of chassignites  
665 does, however, indicate slower cooling than for nakhlites, raising the question of mode of emplacement.  
666  
667

668 Since nakhlites and chassignites have similar ages and trace element abundance patterns, these meteorites  
669 must be genetically related, although contextual details are lacking. Different chassignites and nakhlites may  
670 represent separate flows or shallow intrusions (Treiman, 1986; Treiman, 2005), but the idea of a single body for all  
671 nakhlites has been widely explored (Mikouchi et al., 2003; Day et al., 2006). The nakhlites and chassignites have  
672 been ordered in terms of Mg#, extent of zoning, mesostasis content, and cooling rate estimate, to give a sequence  
673 within a proposed flow unit or cumulate pile (Mikouchi et al., 2003; McCubbin et al., 2013). However, considering  
674 subtle differences between otherwise similar nakhlites, and the probability of a series of eruptions from a complex  
675 long-lived sub-volcanic zone, it is unlikely that all these rocks fit in a single flow unit. Several flows or flow lobes  
676 were proposed recently over a short time period (Jambon et al., 2016; Balta et al., 2017; Udry and Day, 2018; Cohen  
677 et al., 2017). The similarity of augite core compositions, feldspar compositions, and REE patterns in NWA 8694 and  
678 in nakhlites, suggest a close genetic relationship such as derivation from the same source. However, we have shown  
679 here from the Ge/Si ratios that they could not have formed from the same melts. They may differ in that nakhlites  
680 were emplaced at depth or extruded promptly (no degassing based on Ge/Si systematics) while NWA 8694  
681 accumulated from a melt that outgassed in the caldera of a volcano.  
682

### 683 *4.4.2 Archean komatiite-tholeiite association*

684 The associated chassignites and nakhlites have been compared to terrestrial volcanic rocks: they are  
685 reminiscent of the association of Archean komatiites and tholeiites (Arndt et al., 1977; Friedman-Lenz et al., 1999).  
686 Tholeiitic rocks in Munro Township include layered dunite-pyroxenite flows like Theo's Flow, where the augite  
687 cumulate layer is very similar to nakhlite (Friedman-Lentz et al., 1999). However, understanding of such flows is

688 complicated by the possibility of blanketing of hot flows by subsequent eruptions (Murri et al., 2019), and the  
689 underlying olivine layer has an orthocumulate texture (Arndt et al., 1977), not the adcumulate texture as in  
690 chassignites. In thin komatiite flows there is also only olivine orthocumulate, but thicker komatiite units (>150 m)  
691 have adcumulate lower dunite (B2) zones (Houlé et al., 2002). The proposed parent liquid A# of the most magnesian  
692 chassignite NWA 2737 contains 12.1% MgO (He et al., 2013) and a liquidus temperature of ~1335°C (this work).  
693 Such liquids would be effective at melting surface rocks, causing assimilation, and cutting a channel (Hill et al.,  
694 1995). High Sn/Sm contents in NWA 2737 are evidence of such contamination (Humayun et al., 2020). The  
695 adcumulate textures of chassignites are like those of layers of adcumulate dunite in thick komatiites that were  
696 interpreted as forming as channel fill (Hill et al., 1995; Houlé et al., 2002). Thus chassignites and nakhlites are in  
697 some ways analogous to Archean komatiites and tholeiites, though the latter, while spatially related, are not closely  
698 genetically related based on trace element data (Arndt, 1991; Rajamani et al., 1989). Moreover, the differences of  
699 both olivine compositions and textures make it difficult to place most chassignites and nakhlites in the same flow  
700 unit.

#### 701 702 4.4.3 Basaltic shield volcanoes

703 Major volcanic centers on Earth include plume-fed shield volcanoes, e.g. on Hawai'i, Ascension, and La  
704 Réunion. Dunites have been observed in association with the Piton de la Fournaise volcano on La Réunion. They  
705 occur within layered cumulates in low altitude surface exposures and in drill cores from at least 3 km depth, as well  
706 as occurring as xenoliths in basalts (Barrat and Bachèlery, 2019; Babkine et al., 1966). The xenoliths in particular  
707 have textures very similar to those of chassignites, and the same crystallization sequence (Udry and Day, 2017;  
708 Barrat and Bachèlery, 2019). Barrat and Bachèlery (2019) showed that Chassigny had similar relationships in  
709 incompatible element distributions between trapped melt inclusions and parent magmas as at Piton de la Fournaise,  
710 implying in both cases a close relationship. The feldspar in NWA 8694 and nakhlites has a similar range to those of  
711 alkaline and nephelinitic lavas from shield volcanoes on Maui (Keil et al., 1972), though lacking calcic phenocrysts.  
712 The alkaline nature of melt inclusions in Nakhla (Day et al., 2006) and Chassigny (Nekvasil et al., 2007) also makes  
713 an origin from shield volcanoes more likely than origin from a komatiite-tholeiite association.

714  
715 Magma is understood to crystallize within solidification fronts on magma chamber walls (Marsh, 1996),  
716 and in the case of Piton de la Fournaise dendritic olivine forms harrisitic mush zones on the cold walls (Welsch et al.,  
717 2013). Erupting liquid can tear olivine from the fragile mush zone giving olivine-rich lavas. As such picrite flows  
718 are found on the flanks of Piton de la Fournaise at low elevations, they must come from depth in the complex  
719 magma reservoir, while evolved liquids including trachyte erupt from the summit (Famin et al., 2009). Similar  
720 processes could occur in the case of chassignites, with a nakhlitic liquid rising through the olivine mush. Though  
721 dunites occur as cumulate layers and xenoliths in shield volcanoes, major flows could also conceivably develop  
722 adcumulate dunites, as in the komatiite case.

723  
724 Dating of six nakhlites using the  $^{40}\text{Ar}/^{39}\text{Ar}$  method defined at least four discrete events over a time period of  
725  $93 \pm 12$  Ma between 1416 and 1322 Ma consistent with a plume-fed volcano (Cohen et al. 2017). This duration is  
726 well over an order of magnitude longer than for shield volcanoes on Earth. The long history and the general large  
727 size of martian volcanoes give opportunities for processes such as crystal fractionation, assimilation, recharge and  
728 magma mixing to occur. Treiman and Irving (2008) argued that intercumulus magma moved through and was  
729 expelled from the augite cumulate of the nakhlite NWA 998. Goodrich et al. (2013) showed that two different  
730 liquids are trapped as melt inclusions in Nakhla, a Si-rich melt in augite representing the Nakhla parent magma;  
731 and a Si-poor more primitive liquid that crystallized the olivine. The two liquids could have resulted from  
732 different degrees of melting of the same source at different depths. Goodrich et al. (2013) concluded that the  
733

734 Nakhla parent liquid rose through the olivine cumulates formed from the earlier Si-poor magma,  
735 incorporating olivine crystals. The parent liquids proposed for NWA 2737 (He et al. 2013) and for Chassigny  
736 (Johnson et al., 1991) are such Si-poor liquids, while we have modified a Nakhla parent liquid (Stockstill et al.,  
737 2005) to yield a less Si-poor parent capable of yielding the olivine and alkaline mesostasis of NWA 8694. The  
738 similarities of augite, feldspar, and mesostasis compositions between NWA 8694 and nakhlites are consistent  
739 with chassignites and nakhlites originating in a shield volcano. Based on Ge degassing, NWA 8694 formed  
740 from magma that communicated with the surface, in contrast to other chassignites. Eruption from the summit is  
741 possible but unlikely from density considerations, and it could have solidified in the feeder pipe. Alternatively it  
742 could have formed in the lava pond of a satellitic shield or as cumulates in a thick flow. We illustrate the latter

743 possibilities in Fig. 20, which is based on the Piton de la Fournaise volcano (Famin et al., 2009; Welsch et al., 2013;  
744 Barrat and Bachèlery, 2019).

745

746

#### 4. CONCLUSIONS

747

748 NWA 8694, the third chassignite, has an olivine composition ( $Fe_{54}$ ) intermediate between those of the other  
749 chassignites and nakhlites, and has pigeonite as the dominant pyroxene. Cumulus chromite has a similar  
750 composition range to that in Chassigny but it extends to more Fe-Ti-rich compositions. The trachytic mesostasis has  
751 feldspar compositions ( $An_{27}-Or_{79}$ ) like those in both Chassigny and nakhlites. NWA 8694 augite is more ferroan  
752 than Chassigny augite, but has the same composition ( $En_{41-40}Wo_{38-39}$ ) as augite cores in the most primitive nakhlites,  
753 e.g. NWA 998. The igneous pyrrhotite is also slightly more ferroan ( $(Fe/Fe+Ni)_{at.} = 0.98$ ) compared to Chassigny  
754 pyrrhotite ( $(Fe/Fe+Ni)_{at.} = 0.97$ ). Mineralogically NWA 8694 constitutes a direct link between the chassignites and  
755 the nakhlites.

756

757 The bulk REE patterns of the three chassignites have the same shape as those of nakhlite mesostases, and  
758 like nakhlite mesostases, have Cs-Nd levels  $\sim 25x$  chondrites, suggesting a nakhlitic parent magma. However, the  
759 REE pattern of interstitial material in NWA 8694 is steeper than all other chassignite or nakhlite patterns, which can  
760 be explained by undersampling of baddeleyite and zirconolite that occur at olivine contacts with mesostasis. Positive  
761 Th and U anomalies in pyroxene indicate fractional crystallization of pyroxene in NWA 8694 from its parent  
762 magma, but mesostasis is unfractionated. Th/U ratios in mesostasis are highly enriched compared to nakhlites.

763

764 Major element compositions of chassignites and Ge contents of olivine and pyroxene are consistent with  
765 crystal fractionation of olivine, chromite and pyroxene from closely related magma compositions. However, Ge-Si  
766 systematics indicate a late-stage outgassing of the melts from which NWA 8694 mesostasis was trapped, or a  
767 distinct magmatic origin of the interstitial material.

768

769 Proposed parent melt compositions such as NWA 2737 A# with 12.1% MgO (He et al., 2013) cannot  
770 produce olivine as ferroan as in NWA8694 by fractional crystallization, showing a more complex process is  
771 required, e.g. different degrees of partial melting or magma mixing. Olivine and potassic late liquid of the  
772 compositions observed in NWA 8694 are produced by model crystallization of a nakhlite parent liquid NA01a  
773 (Stockstill et al., 2005) with 10% added Nakhla olivine.

774

775 As all chassignite olivine cannot be produced by fractionation of a single liquid, chassignites and nakhlites  
776 cannot be crystallized together in a closed system like a single thick lava flow. Chassignites and nakhlites formed as  
777 flows or hypabyssal intrusions with entrained olivine and augite crystals. They show textural and geochemical  
778 similarities to cumulates and basalts of the terrestrial shield volcano on La Réunion (Barrat and Bachèlery, 2019),  
779 where later eruptions appear to have removed crystals from the solidification fronts of earlier more magnesian  
780 magmas.

781

782

783 Acknowledgments—We are indebted to L. Labenne, for the sample; to M. Fialin and N. Rividi for help with the  
784 electron probe; and to M. J. Carr for IGPET and A. Danyushevsky for PETROLOG. We are particularly indebted  
785 to R. M. Hewins for drafting Fig. 20. We are grateful for funding from NASA Solar Systems Workings program  
786 grant NNX16AP98G (M. Humayun), ANR grant MARS-PRIME ANR-16-CE31-0012 (N. Mangold) and CNES  
787 INSU grant 2013-PNP (B. Zanda). The National High Magnetic Field Laboratory is supported by the National  
788 Science Foundation through NSF/DMR-1644779 and the state of Florida.



789  
790  
791  
792  
793  
794  
795  
796  
797  
798  
799  
800  
801  
802  
803  
804  
805  
806  
807  
808  
809  
810  
811  
812  
813  
814  
815  
816  
817  
818  
819  
820  
821  
822  
823  
824  
825  
826  
827  
828  
829  
830  
831  
832  
833  
834  
835  
836  
837  
838  
839  
840  
841  
842  
843

## REFERENCES

- Ali A., Jabeen I., Gregory D., Verish R. and Banerjee, N. R. (2016) New triple oxygen isotope data of bulk and separated fractions from SNC meteorites: Evidence for mantle homogeneity of Mars. *Meteorit. Planet. Sci.* **51**, 981-995.
- Ariskin A. A., Frenkel M. Ya., Barmina G. S. and Nielsen R. (1993) COMAGMAT: a FORTRAN program to model magma differentiation processes. *Comput. Geosci.* **19**, 1155-1170.
- Arndt N. T. (1991) High Ni in Archean tholeiites. *Tectonophysics* **187**, 411-419.
- Arndt N.T., Naldrett A.J. and Pyke D.R. (1977) Komatiitic and iron-rich tholeiitic lavas of Munro Township, northeast Ontario. *J. Petrol.* **18**, 319-369.
- Babkine J., Conquére F. and Vilminot J. C. (1966) Nodules de péridotite et cumulats d'olivine. *Bulletin de Minéralogie*, **89**, 262-268.
- Balta B., Sanborn M. E., Mayne R. G., Wadhwa M., McSween, H. Y. Jr and Crossley S. D. (2017) Northwest Africa 5790: A previously unsampled portion of the upper part of the nakhlite pile. *Meteor. Planet. Sci.* **52**, 36–59.
- Barrat J. A. and Bachèlery, P. (2019) La Réunion Island dunites as analogs of the Martian chassignites: Tracking trapped melts with incompatible trace elements. *Lithos* **344**, 452-463.
- Barrat J.-A., Zanda B., Moynier F., Bollinger C., Liorzou C. and Bayon G. (2012) Geochemistry of CI chondrites: major and trace elements, and Cu and Zn isotopes. *Geochim. Cosmochim. Acta* **83**, 79–92.
- Barrat J.A., Jambon A., Ferrière L., Bollinger C., Langlade J., Liorzou C., Boudouma O. and Fialin M. (2014) No martian soil component in shergottite meteorites. *Geochim. Cosmochim. Acta* **125**, 23-33.
- Barrat J.A., Dauphas N., Gillet P., Bollinger C., Etoubleau J., Bischoff A. and Yamaguchi A. (2016) Evidence from Tm anomalies for non-CI refractory lithophile element proportions in terrestrial planets and achondrites. *Geochim. Cosmochim. Acta* **176**, 1-17.
- Beck P., Barrat J. A., Gillet P., Wadhwa M., Franchi I. A., Greenwood R. C., Bohn M., Cotten J., de Moortele B. V. and Reynard B. (2006) Petrography and geochemistry of the chassignite Northwest Africa 2737 (NWA 2737). *Geochim. Cosmochim. Acta* **70**, 2127–2139.
- Bellucci J. J., Nemchin A. A., Whitehouse M. J., Snape J. F., Kielman R. B., Bland P. A. and Benedix, G. K. (2016). A Pb isotopic resolution to the Martian meteorite age paradox. *Earth Planet. Sci. Lett.* **433**, 241-248.
- Bunch T. E. and Keil K. (1971) Chromite and ilmenite in nonchondritic meteorites. *Amer. Mineral.* **56**, 146-157.
- Bunch T. E., and Reid A. M. (1975) The nakhlites Part I: Petrography and mineral chemistry. *Meteoritics* **10**, 303-315.
- Chevrier V., Lorand J.-P. and Sautter V. (2011). Sulfide petrology of four nakhlites (NWA817, NWA998, Nakhla, Governador Valadares). *Meteorit. Planet. Sci.* **46**, 769-784.
- Cohen B.E., Mark D.F., Cassata W.S., Lee M.R., Tomkinson T. and Smith C.L. (2017) Taking the pulse of Mars via dating of a plume-fed volcano. *Nature Communications* **8**, 640.
- Coogan L. A. and O'Hara M. J. (2015) MORB differentiation: In situ crystallization in replenished-tapped magma chambers. *Geochim. Cosmochim. Acta* **158**, 147-161.

844 Danyushevsky L. V. and Plechov P. (2011) Petrolog3: Integrated software for modeling crystallization processes,  
845 *Geochem. Geophys. Geosyst.* **12**, Q07021.  
846

847 Day J. M. D., Taylor L. A., Floss C. and McSween H. Y. (2006) Petrology and chemistry of MIL 03346 and its  
848 significance in understanding the petrogenesis of nakhlites on Mars. *Meteorit. Planet. Sci.* **41**, 581-606.  
849

850 Dymek R.F. (1983) Titanium, aluminum and interlayer cation substitutions in biotite from high-grade gneisses,  
851 West Greenland. *Amer. Mineral.* **68**, 880-899.  
852

853 Famin V., Welsch B., Okumura S., Bachèlery P. and Nakashima S. (2009) Three differentiation stages of a single  
854 magma at Piton de la Fournaise volcano (Reunion hot spot). *Geochemistry, Geophysics, Geosystems* **10**(1)  
855

856 Floran R. J., Prinz M., Hlava P. F., Keil K., Nehru C. E. and Hinthorne J. R. (1978). The Chassigny meteorites: A  
857 cumulate dunite with hydrous amphibole-bearing melt inclusions. *Geochim. Cosmochim. Acta* **42**, 1213–  
858 1229.  
859

860 Franchi I. A., Wright I. P., Sexton A. S. and Pillinger C. T. (1999) The oxygen-isotopic composition of Earth and  
861 Mars. *Meteorit. Planet. Sci.* **34**, 657–661.  
862

863 Franz H. B., Kim S. T., Farquhar J., Day J. M., Economos R. C., McKeegan K. D., ... and Dottin III, J. (2014)  
864 Isotopic links between atmospheric chemistry and the deep sulphur cycle on Mars. *Nature* **508**, 364-368.  
865

866 Friedman-Lentz R. C., Taylor G. J. and Treiman A. H. (1999) Formation of a martian pyroxenite: a comparative  
867 study of the nakhlite meteorites and Theo's Flow. *Meteorit. Planet. Sci.* **34**, 919–932.  
868

869 Gale N.H., Arden J.W. and Hutchison R. (1975) The chronology of the Nakhla achondrite meteorite. *Earth Planet.*  
870 *Sci. Lett.* **26**, 195–206.  
871

872 Gattacceca J., Hewins R. H., Lorand J.-P., Rochette P., Lagroix F., Cournède C., Uehara M., Pont S., Sautter V.,  
873 Scorzelli R. B., Hombourger C., Munayco P., Zanda B., Chennaoui H. and Ferrière L. (2013) Magnetism of a  
874 pristine sample from Mars: the Tissint Martian meteorite. *Meteorit. Planet. Sci.* **48**, 199-936.  
875

876 Giesting, P. A., Schwenzer, S. P., Filiberto, J., Starkey, N. A., Franchi, I. A., Treiman, A. H., ... and Grady, M. M.  
877 (2015). Igneous and shock processes affecting chassignite amphibole evaluated using chlorine/water  
878 partitioning and hydrogen isotopes. *Meteorit. Planet. Sci.* **50**, 433-460.  
879

880 Goodrich C. A., Treiman A. H., Filiberto J., Gross J. and Jercinovic M. (2013) K<sub>2</sub>O-rich trapped melt in olivine in  
881 the Nakhla meteorite: Implications for petrogenesis of nakhlites and evolution of the Martian mantle.  
882 *Meteorit. Planet. Sci.* **48**, 2371–2405.  
883

884 He Q., Xiao L., Hsu W., Balta J. B., McSween H. Y. and Liu Y. (2013). The water content and parental magma of  
885 the second chassignite NWA 2737: Clues from trapped melt inclusions in olivine. *Meteorit. Planet. Sci.* **48**,  
886 474–492.  
887

888 Hess H. H. (1960) Stillwater Igneous Complex, Montana, a quantitative mineralogical study. *Geological Society of*  
889 *America Memoir* **80**, 230 pp.  
890

891 Hewins R. H., Zanda B., Pont S., Humayun M., Assayag N. and Cartigny P. (2015) NWA 8694, a ferroan  
892 chassignite. *Lunar Planet Sci. XLVI*. Lunar Planet. Inst., Houston. #2249 (abstr.).  
893

894 Hewins R. H., J.-A. Barrat, M. Humayun, S. Pont and B. Zanda (2017) NWA 8694 and the chassignite parent liquid  
895 problem. *Lunar Planet Sci. XLVIII*. Lunar Planet. Inst., Houston. #2533 (abstr.).  
896

897 Hill R. E. T., Barnes S. J., Gole M. J. and Dowling, S. E. (1995) The volcanology of komatiites as deduced from  
898 field relationships in the Norseman-Wiluna greenstone belt, Western Australia. *Lithos* **34**, 159-188.  
899

- 900 Houlé M.G., Davis P.C., Leshner C.M. and Arndt N.T. (2002) Extrusive and intrusive komatiites, komatiitic basalt  
901 and peperite and ore genesis at the Dundonald Ni-Cu-(PGE) Deposit, Abitibi Greenstone Belt, Canada. *9th*  
902 *International Platinum Symposium Abstract Volume*, Billings, Montana, p. 181-184.  
903
- 904 Humayun M., Simon S. B. and Grossman L. (2007) Tungsten and hafnium distribution in calcium-aluminum  
905 inclusions CAIs from Allende and Efremovka. *Geochim. Cosmochim. Acta* **71**, 4609–4627.  
906
- 907 Humayun M., Davis F. A. and Hirschmann M. M. (2010) Major element analysis of natural silicates by laser  
908 ablation ICP-MS. *J. Anal. At. Spectrom.* **25**, 998–1005.  
909
- 910 Humayun M., Yang S., Righter K., Zanda B. and Hewins R. H. (2016) The germanium dichotomy in martian  
911 meteorites. *Lunar Planet. Sci. Conf. XLVII*. Lunar Planet. Inst., Houston. #2459 (abstr.).  
912
- 913 Humayun M., Yang S., Irving A. J. and Righter, K. (2019) Sulfide assimilation and mineralization in ancient (2.4  
914 Ga) shergottites. (abstract). *Meteorit. Planet. Sci.* 54 (Suppl.) #6380.pdf.  
915
- 916 Humayun M., Yang S., Irving A. J., Hewins R. H., Zanda B., Righter K. and Peslier A. H. (2020) Tin abundances  
917 require that chassignites originated from multiple magmatic bodies distinct from nakhlites. *Lunar Planet. Sci.*  
918 *Conf. 51<sup>st</sup>*. Lunar Planet. Inst., Houston. #1338 (abstr.)  
919
- 920 Jambon A., Sautter V., Barrat J. A., Gattacceca J., Rochette P., Boudouma O., Badia D. and Devouard B. (2016)  
921 Northwest Africa 5790: Revisiting nakhlite petrogenesis. *Geochim. Cosmochim. Acta* **190**, 191–212.  
922
- 923 Jochum K.-P., Weis U., Stoll B., Kuzmin D., Yang Q., Raczek I., Jacob D. E., Stracke A., Birbaum K., Frick D. A.,  
924 Günther D. and Enzweiler J. (2011) Determination of reference values for NIST SRM 610–617 glasses  
925 following ISO guidelines. *Geostand. Geoanal. Res.* **35**, 397-429.  
926
- 927 Johnson M. C., Rutherford M. J. and Hess P. C. (1991) Chassigny petrogenesis–melt compositions, intensive  
928 parameters, and water contents of Martian (?) magmas. *Geochim. Cosmochim. Acta* **55**, 349–366.  
929
- 930 Keil K., Fodor R. V., and Bunch, T. E. (1972) Contributions to the mineral chemistry of Hawaiian rocks II.  
931 Feldspars and interstitial material in rocks from Haleakala and West Maui volcanoes, Maui, Hawaii.  
932 *Contrib. to Mineral. Petrol.* **37**, 253-275.  
933
- 934 Langenhorst F. and Greshake A. (1999) A transmission electron microscope study of Chassigny: Evidence for  
935 strong shock metamorphism. *Meteorit. Planet. Sci.* **34**, 43-48.  
936
- 937 LaTourrette T. Z. and Burnett, D. S. (1992) Experimental determination of U and Th partitioning between  
938 clinopyroxene and natural and synthetic basaltic liquid. *Earth Planet. Sci. Lett.* **110**, 227-244.  
939
- 940 Lissenberg C. J. and MacLeod C. J. (2016) A reactive porous flow control on mid-ocean ridge magmatic evolution.  
941 *J. Petrol.* **57**, 2195-2220.  
942
- 943 Lorand J.-P., Barrat J.-A., Chevrier V., Sautter V. and Pont S. (2012) Metal-saturated sulfide assemblages in  
944 chassignite NWA 2737; evidence for impact-related sulfur devolatilisation. *Meteorit. Planet. Sci.* **47**, 1830-  
945 1841.  
946
- 947 Lorand J.-P., Hewins R.H., Pont S., Zanda B., Humayun M., Nemchin A., Grange M., Kennedy A. and Göpel C.  
948 (2015) Nickeliferous pyrite tracks late hydrothermalism in Martian regolith breccia NWA 7533. *Meteorit.*  
949 *Planet. Sci.*, **50**, 2099–2120.  
950
- 951 Lorand J.-P., Pont S., Chevrier V., Luguét A., Zanda B. and Hewins R. H. (2018) Petrogenesis of martian sulfides in  
952 the Chassigny meteorite. *Amer. Mineral.*, special issue “Planetary Sulfides” **103**, 872-885.  
953
- 954 Mari N., Riches A.J.V., Hallis L.J., Marrocchi Y., Villeneuve J., Gleissner P., Becker H. and Lee, M. (2019)  
955 Syneruptive incorporation of martian surface sulphur in the nakhlite lava flows revealed by S and Os

- 956 isotopes and highly siderophile elements : implication for mantle sources in Mars. *Geochim. Cosmochim.*  
957 *Acta* **266**, 416-43.
- 958
- 959 Marsh, B. D. (1996). Solidification fronts and magmatic evolution. *Mineral. Mag.* **60**, 5-40.
- 960
- 961 Mason B., Nelen J. A., Muir P. and Taylor S. R. (1976) The composition of the Chassigny meteorite. *Meteoritics* **11**,  
962 21-27.
- 963
- 964 McCubbin F. M., Smirnov A., Nekvasil H., Wang J., Hauri E. and Lindsley D. H. (2010) Hydrous magmatism on  
965 Mars: A source of water for the surface and subsurface during the Amazonian. *Earth Planet. Sci. Lett.* **292**,  
966 132-138.
- 967
- 968 McCubbin F. M., Elardo S. M., Shearer C. K., Smirnov A., Hauri E. H. and Draper D. S. (2013) A petrogenetic  
969 model for the comagmatic origin of chassignites and nakhlites: Inferences from chlorine-rich minerals,  
970 petrology, and geochemistry. *Meteorit. Planet. Sci.* **48**, 819–853.
- 971
- 972 Mikouchi T., Koizumi E., Monkawa A., Ueda Y. and Miyamoto M. (2003) Mineralogy and petrology of Yamato  
973 000593: Comparison with other Martian nakhlite meteorites. *Antarctic Meteorite Research* **16**, 34–57.
- 974
- 975 Mikouchi T., Monkawa A., Koizumi E., Chokai J. and Miyamoto M. (2005) MIL03346 Nakhlite and NWA2737"  
976 Diderot" Chassignite: Two New Martian Cumulate Rocks from Hot and Cold Deserts. *Lunar Planet. Sci.*  
977 *Conf. XXXVI*. Lunar Planet. Inst., Houston. #1944 (abstr.).
- 978
- 979 Mikouchi T., Miyamoto1, E. Koizumi M., Makishima J. and McKay G. (2006) Relative burial depths of nakhlites:  
980 an update. *Lunar Planet. Sci. Conf. XXXVII*. Lunar Planet. Inst., Houston. #1865 (abstr.).
- 981
- 982 Mikouchi T., Takenouchi A. and Zolensky M. E. (2017) Multiple igneous bodies for nakhlites and chassignites as  
983 inferred from olivine cooling rates using calcium zoning. *Meteorit. Planet. Sci.* **52** (Suppl.) #6177.pdf.
- 984
- 985 Murri M., Domeneghetti M. C., Fioretti A. M., Nestola F., Vetere F., Perugini D., .. Pisello A., Faccenda M., and  
986 Alvaro M. (2019) Cooling history and emplacement of a pyroxenitic lava as proxy for understanding Martian  
987 lava flows. *Scientific Reports* **9**, 1-7.
- 988
- 989 Nagao K., Park J., Choi J., Baek J. M., Haba M. K., Mikouchi T., Zolensky M. E., Herzog G. F., Park C., Lee J. I.  
990 and Lee M. J. (2019). Genetic Relationship Between Martian Chassignites and Nakhlites Revealed from  
991 Noble Gases. *Meteorit. Planet. Sci.* **54** (Suppl.) #6183.pdf.
- 992
- 993 Nekvasil H., Filiberto J., McCubbin F.M. and Lindsley, D.H. (2007) Alkalic parental magmas for the chassignites?  
994 *Meteorit. Planet. Sci.* **42**, 979-992.
- 995
- 996 Nyquist L. E., Bogard D. D., Shih C.-Y., Greshake A., Stöffler D. and Eugster O. (2001) Ages and geologic  
997 histories of martian meteorites. In *Chronology and Evolution of Mars*, Kallenbach, R., Geiss, J., Hartmann,  
998 W.K. (Eds.). Kluwer Academic Publishers, Dordrecht, pp. 105–164.
- 999
- 1000 Oulton J., Humayun M., Fedkin A. and Grossman L. (2016) Chemical evidence for differentiation, evaporation and  
1001 recondensation from silicate clasts in Gujba. *Geochim. Cosmochim. Acta* **177**, 254–274.
- 1002
- 1003 Prinz M., Hlava P. F. and Keil K. (1974) The Chassigny meteorite: a relatively iron-rich cumulate dunite.  
1004 *Meteoritics* **9**, 393-394.
- 1005
- 1006 Rajamani V., Shirey S. B. and Hanson G. N. (1989) Fe-rich Archean tholeiites derived from melt-enriched mantle  
1007 sources: evidence from the Kolar Schist Belt, South India. *J. Geol.* **97**, 487-501.
- 1008
- 1009 Reid A.M. and Bunch T.E. (1975) The nakhlites—II: where, when, and how. *Meteoritics* **10**, 317–324.
- 1010
- 1011 Richter F., Chaussidon M., Mendybaev R. and Kite E. (2016) Reassessing the cooling rate and geologic setting of

1012 Martian meteorites MIL 03346 and NWA 817. *Geochim. Cosmochim. Acta* **182**, 1-23.  
1013  
1014 Robinson P. (1980) The composition space of terrestrial pyroxenes; internal and external limits. *Rev. Mineral.*  
1015 *Geochem.* **7**, 419-494.  
1016  
1017 Rumble D., Farquhar J., Young E. D. and Christensen C. P. (1997) In situ oxygen isotope analysis with an excimer  
1018 laser using F2 and BrF5 reagents and O2 gas as analyte. *Geochim. Cosmochim. Acta* **61**, 4229–4234.  
1019  
1020 Sack R. O., Carmichael I. S. E., Rivers M. L. and Ghiorso M. S. (1980) Ferric-ferrous equilibria in natural silicate  
1021 liquids at 1 bar. *Contrib. Mineral. Petrol.* **75**, 369-376.  
1022  
1023 Sautter V., Barrat J. A., Jambon A., Lorand J. P., Gillet P., Javoy M., Joron J. L. and Lesourd M. (2002) A new  
1024 Martian meteorite from Morocco: The nakhlite Northwest Africa 817. *Earth Planet. Sci. Lett.* **195**, 223–238.  
1025  
1026 Stockstill, K. R., McSween H. Y. Jr. and Bodnar R. J. (2005) Melt inclusions in augite of the Nakhla martian  
1027 meteorite: Evidence for basaltic parental melt. *Meteorit. Planet. Sci.* **40**, 377–396.  
1028  
1029 Stolper E. M., McSween H. Y. Jr. and Hays J. F. (1979) A petrogenetic model of the relationships among achondrite  
1030 meteorites. *Geochim. Cosmochim. Acta* **43**, 589-602.  
1031  
1032 Treiman A. H. (1986) The parental magma of the Nakhla achondrite: Ultrabasic volcanism on the shergottite parent  
1033 body. *Geochim. Cosmochim. Acta* **50**, 1061-1070.  
1034  
1035 Treiman A. H. (2005) The nakhlite meteorites: Augite-rich igneous rocks from Mars. *Chem. Erde* **65**, 203–270.  
1036  
1037 Treiman A. H., Dyar M. D., McCanta M., Noble S. K. and Pieters C. M. (2007) Martian dunite NWA 2737:  
1038 Petrographic constraints on geological history, shock events, and olivine color. *J. Geophys. Res.-Planets* **112**,  
1039 1–20.  
1040  
1041 Treiman A. H. and Irving A. J. (2008) Petrology of the nakhlite (Martian) meteorite Northwest Africa (NWA) 998.  
1042 *Meteorit. Planet. Sci.* **43**, 829–854.  
1043  
1044 Udry A. and Day J.M. (2018) 1.34 billion-year-old magmatism on Mars evaluated from the co-genetic nakhlite and  
1045 chassignite meteorites. *Geochim. Cosmochim. Acta* **238**, 292-315.  
1046  
1047 Udry A., McSween H. Y. Jr., Lecumberri-Sanchez P. and Bodnar R. J. (2012) Paired nakhlites MIL 090030,  
1048 090032, 090136, and 03346: Insights into the Miller Range parent meteorite, *Meteorit. Planet. Sci.* **47**, 1575–  
1049 1589.  
1050  
1051 Udry A., Balta J. B. and McSween H. Y. Jr. (2014) Exploring fractionation models for Martian magmas. *J.*  
1052 *Geophys. Res. Planets* **119**, 1–18.  
1053  
1054 Valley J. W., Kitchen N. E., Kohn M. J., Niendorf C. R. and Spicuzza M. J. (1995) UWG-2, a garnet standard for  
1055 oxygen isotope ratios: Strategies for high precision and accuracy with laser heating. *Geochim. Cosmochim.*  
1056 *Acta* **59**, 5223–5231.  
1057  
1058 Vlastélic I., Di Muro A., Bachèlery P., Gurioli L., Auclair D. and Gannoun, A. (2018) Control of source fertility on  
1059 the eruptive activity of Piton de la Fournaise volcano, La Réunion. *Scientific Reports* **8**, 1-7.  
1060  
1061 Wadhwa M. and G. Crozaz (1995) Trace and minor elements in minerals of nakhlites and Chassigny: Clues to their  
1062 petrogenesis. *Geochim. Cosmochim. Acta* **59**, 3629–3645.  
1063  
1064 Wager L. R., Brown G. M. and W. J. Wadsworth, J. (1960) Types of Igneous Cumulates. *J. Petrol.* **1**, 73–85.  
1065  
1066 Watson L.L., Hutcheon I.D., Epstein S. and Stolper E.M. (1994) Water on Mars — clues from deuterium/hydrogen  
1067 and water contents of hydrous phases in SNC meteorites. *Science* **265**, 86–90.

1068  
 1069 Welsch, B., Faure, F., Famin, V. and Bachèlery, P. (2013) Dendritic crystallization: a single process for all the  
 1070 textures of olivine in basalts? *J. Petrol.* **54**, 539–574.  
 1071  
 1072 Yang S., Humayun M., Righter K., Jefferson G., Fields D. and Irving A. J. (2015) Siderophile and chalcophile  
 1073 element abundances in shergottites: implications for Martian core formation. *Meteorit. Planet. Sci.* **50**, 691–  
 1074 714.  
 1075  
 1076 Yang S., Humayun, M. Irving A. J., Righter K., Peslier A. H., Zanda B. and Hewins R. H. (2019) A two gigayear  
 1077 history of germanium outgassing from shergottites. A two gigayear history of germanium outgassing from  
 1078 shergottites. Lunar Planet. Sci. Conf. 50<sup>th</sup>. Lunar Planet. Inst., Houston #1908 (abstr.).  
 1079  
 1080 Zhang S.H., Zhao Y., Yang Z.Y., He Z.F. and Wu H. (2009) The 1.35 Ga diabase sills from the northern North  
 1081 China Craton: implications for breakup of the Columbia (Nuna) supercontinent. *Earth Planet. Sci. Lett.* **288**,  
 1082 588-600.  
 1083  
 1084  
 1085

1086  
 1087 APPENDIX A. SUPPLEMENTARY MATERIAL

1088 Research Data associated with this article are uploaded as a zip file and can be found, in the online version, at  
 1089 <https://doi.org/10.1016/j.gca>  
 1090 Gca.....

1091  
 1092 Table S1. All EMP analyses for NWA 8694, Chassigny and NWA 2737(Excel file).  
 1093

1094 Table S2. All LA-ICP-MS analyses of NWA 8694 and Chassigny (Excel file).  
 1095

1096  
 1097  
 1098 Fig. S1. Oxygen isotope composition of NWA 8694 with SNC data tabulated by Ali et al. (2016) that were used to  
 1099 calculate the Mars Fractionation Line (MFL) by regression .  
 1100

1101 Fig. S2. Full size BSE images of the three chassignites (a) NWA 8694 (b) Chassigny (c) NWA 3737. Fig. S3. BSE  
 1102 image. Olivine (off-white), pigeonite (medium grey), and augite (dark grey) in NWA 8694. The common orientation  
 1103 of pyroxene exsolution lamellae NW-SE indicates that pyroxene is poikilitic to olivine.  
 1104

1105 Fig. S3. BSE image. Olivine (off-white), pigeonite (medium grey), and augite (dark grey) in NWA 8694. The  
 1106 common orientation of pyroxene exsolution lamellae NW-SE indicates that pyroxene is poikilitic to olivine.  
 1107

1108 Fig. S4. Pyroxene quadrilaterals for NWA 8694 (a) interstitial-poikilitic (b) interstitial mesostasis and (c) melt  
 1109 inclusions.  
 1110

1111 Fig. S5. The calculated REE pattern of missing phase in NWA 8694 based on excess of bulk P and REE over  
 1112 concentrations calculated from major phases resembles apatite. The figure shows that an assemblage of 96%  
 1113 plagioclase and 4% apatite from NWA 2737 (Beck et al., 2006) matches the REE (La-Gd) of the average trapped  
 1114 liquid in NWA 8694.  
 1115

1116 Fig. S6. A mixture of 1% baddeleyite (Zhang et al., 2009) and 99% NWA 8694 mesostasis give an REE pattern  
 1117 close to that of nakhlite mesostases (Jambon et al., 2016).

Fig. 1 **Back scattered electron (BSE) maps of chassignites (a) NWA 8694 (b) Chassigny (c) NWA 2737. In each image the brightest phase is chromite, followed by olivine, then dark grey pyroxene and black feldspar and glass, but in (c) shocked olivine contains medium grey ribbons or patches.**

Fig. 2. NWA 8694 BSE images. (a) Melt inclusion in olivine surrounded by radial fractures: orthopyroxene (Opx); amphibole (Am); K-rich glass (K); and K-poor glass (Na). Note also tiny melt inclusions in the same olivine grain. (b) **Olivine and interstitial mesostasis: subophitic pyroxene (medium grey) with feldspar or maskelynite laths (black).**

Fig. 3 BSE images of sulfides in NWA 8694. (a) Ni-bearing pyrrhotite in melt inclusion in olivine, associated with apatite and alkali feldspathic glass. (b) Enclosed euhedral Ni-bearing Pyrrhotite crystal associated with fractured apatite inside alkali feldspathic glass. (c) Intercumulus pyrrhotite bleb (light grey) in contact with interstitial glass (dark grey) and olivine (medium grey). (d) Intercumulus pyrite showing fracture networks filled with Fe oxyhydroxides; this grain shares grain boundaries with olivine (light grey), pyroxene (medium grey) and interstitial glass (dark). (e) Baddeleyite and (f) zirconolite, both occurring in or near contacts between olivine and intercumulus material. PO pyrrhotite, PY pyrite, GL alkali feldspar glass, B baddeleyite, Z zirconolite.

Fig. 4. Olivine compositions. (Top) NWA 8694 is intermediate between the other chassignites and nakhlites in FeO content, with a typical martian FeO/MnO ratio. (Bottom) Though Fe and Mg are equilibrated Ca varies due to weak zoning. Nakhlite data are from Sautter et al. (2002), Treiman (2005), Udry et al. (2012), and **Udry and Day (2018).**

Fig. 5. **Comparison of compositions of NWA 8694, Chassigny and NWA 2737 pyroxene and olivine with those of nakhlites (Treiman, 2005; Treiman and Irving, 2008; Sautter et al., 2002; Jambon et al., 2016; Treiman et al., 2005; Udry et al., 2012; and Udry and Day, 2018), showing overlap for augite in NWA 998 and Lafayette at  $En_{41-40}Wo_{38-39}$ .**

Fig. 6. Pyroxene compositions (afu) showing Ca and (a) Cr, (b) Na, (c) Ti, and (d) Al. There is a partial overlap for augite in chassignites with augite in NWA 998 and cores in some other nakhlites (Udry and Day (2018) for incompatible minor elements. The other nakhlites show a much wider range of minor element concentrations in augite than the chassignites.

Fig. 7. Composition of chromite in chassignites projected from spinel s.s. **onto the chromite-ulvöspinel-magnetite plane. NWA 8694 lacks the Cr-rich chromite found in the other chassignites.**

Fig. 8. Compositions of (a) interstitial feldspar for NWA 8694, Chassigny (**this work, Floran et al., 1978**), NWA 2737, and nakhlites (**Bunch and Reid, 1975; Jambon, 2017**), and (b) NWA 8694 melt inclusion glass compositions projected onto the An-Ab-Or plane, and compared to those in the two other chassignites (Floran et al., 1978; Mason et al., 1976; Johnson, et al., 1991; Beck et al., 2006; Treiman et al., 2007; He et al., 2013).

Fig. 9. Compositions of interstitial feldspar (**FSP**), melt inclusion (MI) phases, and bulk interstitial material (the latter from LA-ICP-MS analyses) in NWA 8694 in afu on an eight oxygen basis. **Half the plagioclase join  $Ab_{100} - An_{50}$  to  $An_{50} - Ab_{100}$  is shown for reference.**

Fig. 10. Glass and feldspar compositions plotted in afu. The tieline shows the albite(orthoclase)-An<sub>50</sub> join. Some Al-rich glasses plot close to feldspar; other glasses are all Si-rich relative to feldspar, with Al-poor and K-rich points forming a cluster.

Fig. 11. Histograms of Ni content of pyrrhotite (po) and pyrite (py) in NWA 8694 and Chassigny **show a shift of Ni content towards lower values in NWA 8694.**

Fig. 12. Concentrations of F and Cl in biotite in wt% **for NWA 8694 interstitial mesostasis and melt inclusions**

Fig. 13. ICP-SFMS analyses for chassignites and mesostasis-rich nakhlites (this work, Beck et al., 2005, and Jambon et al., 2016) normalized to CI values (Barrat et al., 2012).

Fig. 14. REE data for NWA 8694 and Chassigny (this work); and NWA 2737 (Beck et al., 2006). (a) Olivine and pyroxene. (b) Mesostasis (interstitial trapped liquid). (c) Mesostasis and bulk compositions of chassignites compared to those of nakhlites (Jambon et al., 2016). The subsamples of NWA 8694 differ in trapped liquid content, with REE concentration pattern of that measured by LA-ICP-MS being close to that of NWA 2737, while the other is almost identical to Chassigny.

Fig. 15. Interstitial material in Chassigny (red diamonds) resembles nakhlite mesostasis, but in NWA 8694 (black diamonds) shows a mixing curve between phosphate-dominated analyses (high  $La_{CI}$ ) and plagioclase-rich analyses (strong positive Eu anomalies). Nakhlite data from Trieman (2005).

Fig. 16. Incompatible element abundances for NWA 8694 and Chassigny mesostases (top two curves) normalized to Martian mantle (Yang et al., 2015) with elements organized according to decreasing incompatibility from left to right. Chassigny mesostasis is very similar to nakhlite mesostases (Jambon et al., 2016), but that in NWA 8694 is depleted in Zr, Hf, HREE and Sc.

Fig. 17. TAS diagram for daughter liquids from nakhlite parent melt NA01a (Stockstill et al., 2005) with 0%, 10% and 20% added olivine. Crystallization of olivine, augite, and augite plus plagioclase at 1 bar and FMQ-1 produces a match for NWA 8694 mesostasis for the parent with 10% olivine added.

Fig. 18. AFM diagram for nakhlite parent NA01a (Stockstill et al. 2005) with 0%, 10% and 20% added olivine showing calculated olivine and daughter liquid compositions. Crystallization yields olivine matching olivine in NWA 8694, but the calculated liquid is displaced from the natural mesostasis, which retains Mg-bearing pyroxene.

Fig. 19. A cartoon of a zone in a magma chamber from which olivine undersaturated nakhlite magmas and nakhlite-contaminated chassignite magmas could be extracted to form NWA 998 and NWA 8694. Olivine mauve, pigeonite red, and augite yellow; plagioclase not shown.

Fig. S1. An assemblage of 96% plagioclase and 4% apatite from NWA 2737 (Beck et al., 2005) matches the REE (La-Gd) of the average trapped liquid in NWA 8694.

Fig. S2. A mixture of 1% baddeleyite (Zhang et al., 2009) and NWA 8694 mesostasis give a REE pattern close to that of nakhlite mesostases (Jambon et al., 2016).

Fig. S3. TAS diagram for selected parent liquids (Table 6).



Table 1 Chassignite modal abundances.

Table 2a. Selected analyses of olivine, chromite, biotite and amphibole.

Table 2b. Selected analyses of pyroxene.

Table 3. Selected analyses of feldspars.

Table 4. Selected analyses of glass, and average apatite in NWA 8694.

Table 5 Mean composition of NWA 8694 sulfides.

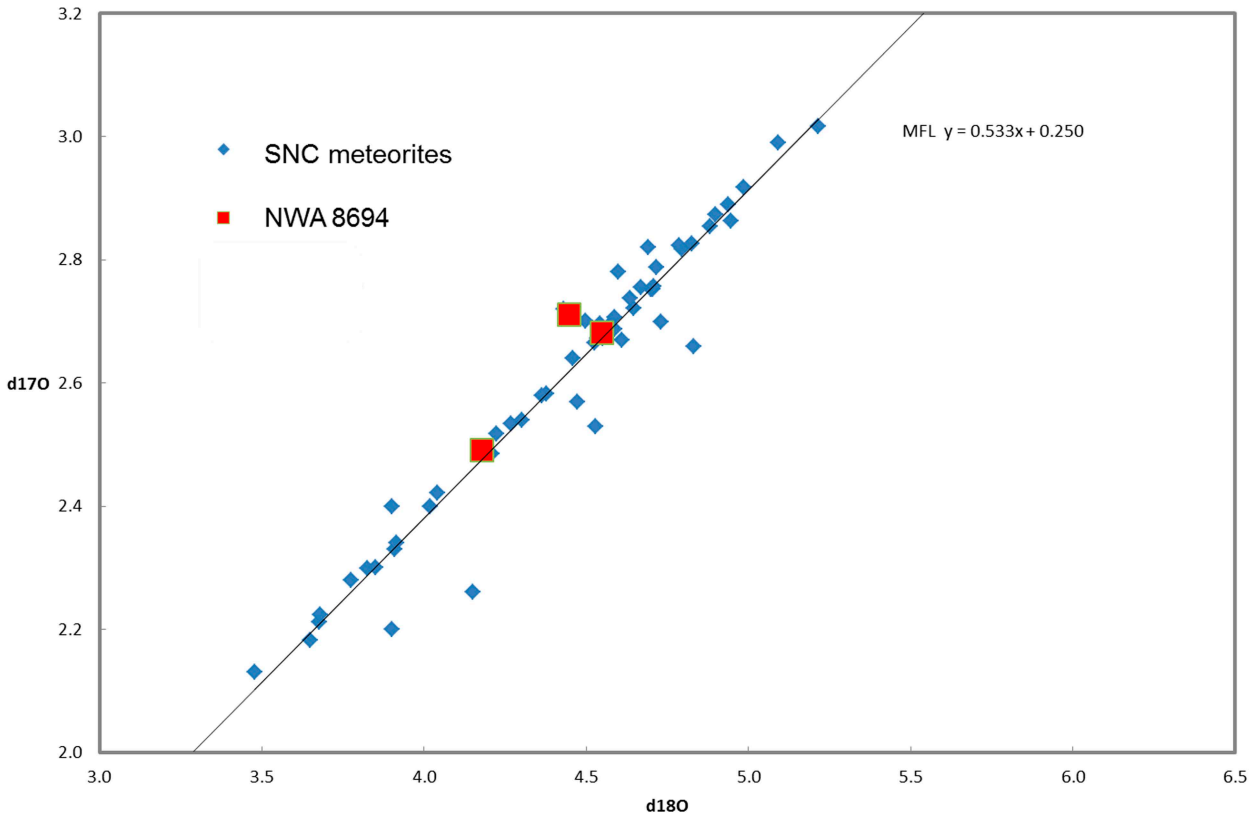
Table 6. Whole Rock analyses of three chassignites.

Table 7. LA-ICP-MS average analyses for NWA 8694 and Chassigny.

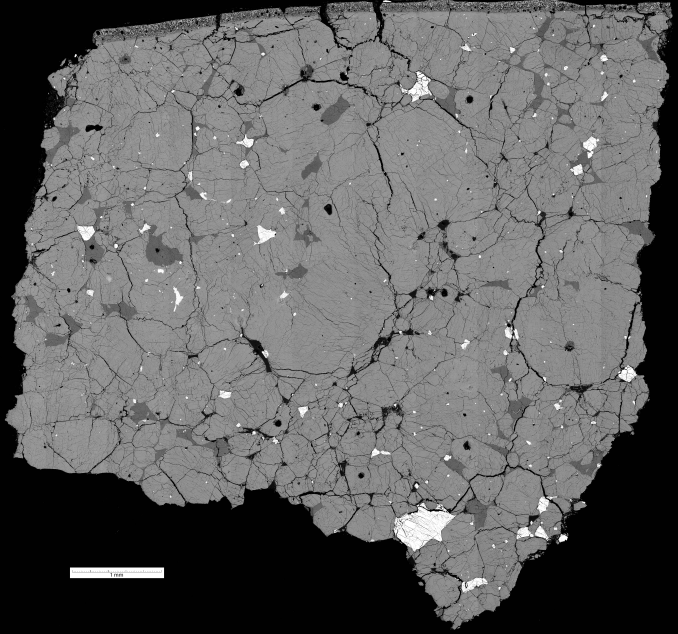
Table 7. Table 7. LA-ICP-MS average analyses (continued).

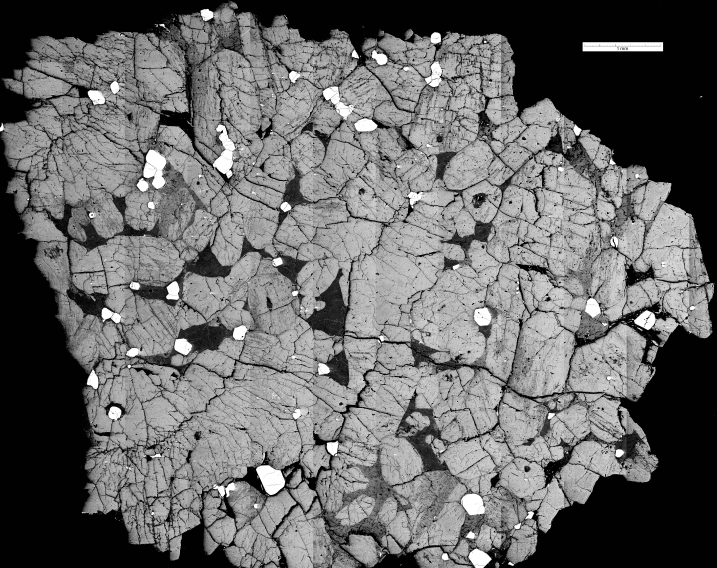
Table 8. Compositions of parent liquids used in PETROLOG calculations.

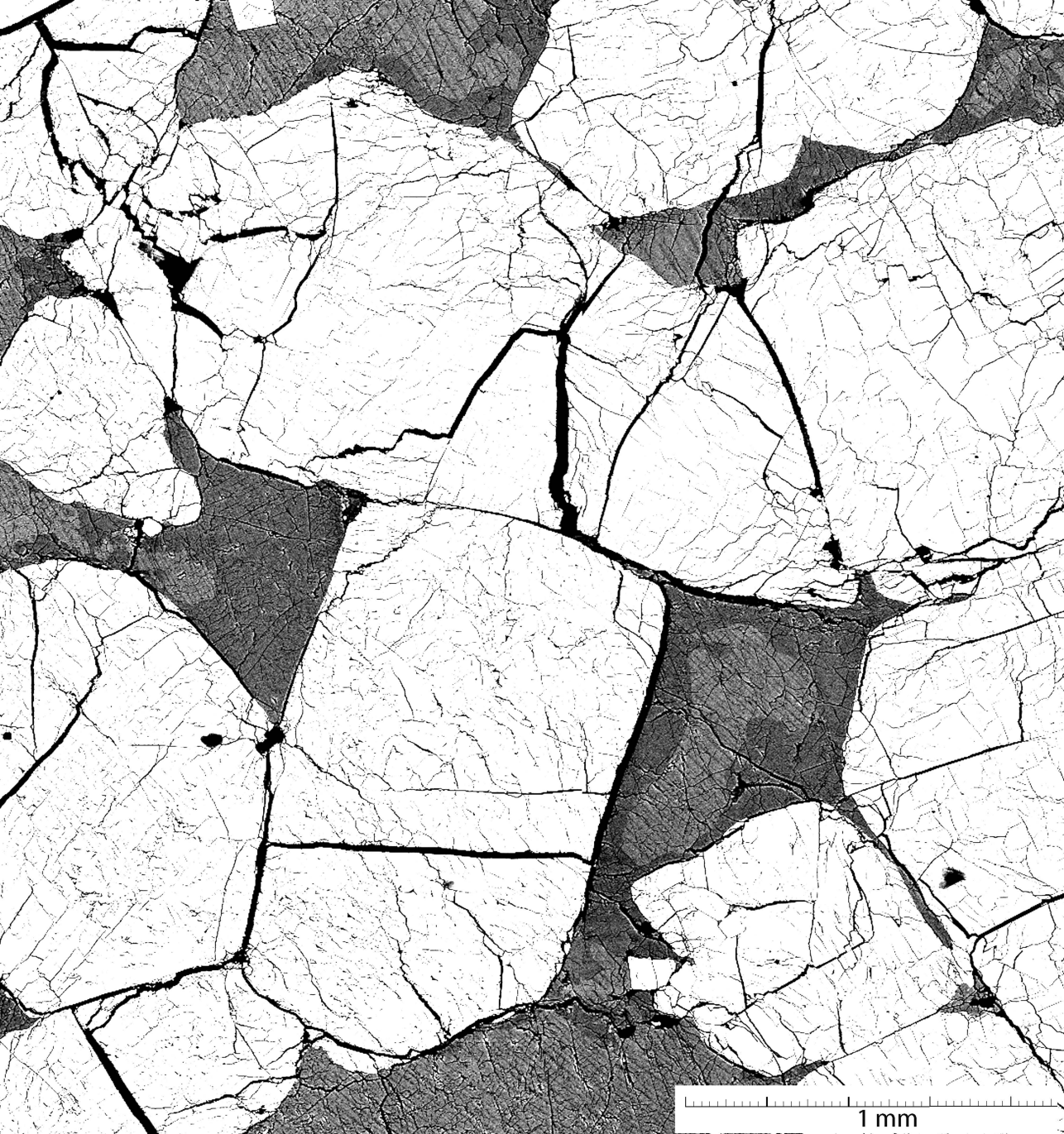
Table S1. All LA-ICP-MS analyses for NWA 8694 and Chassigny.









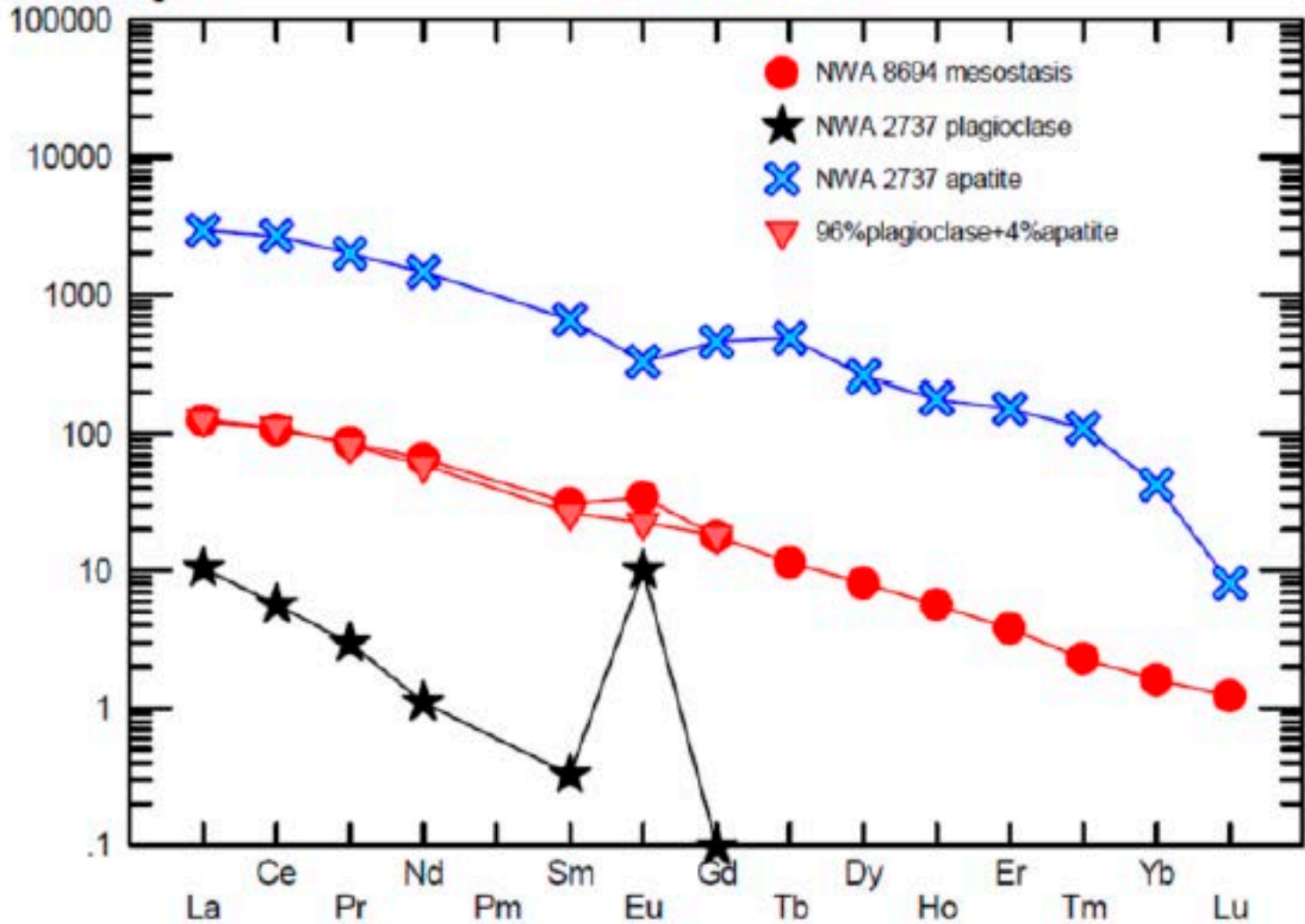


1 mm

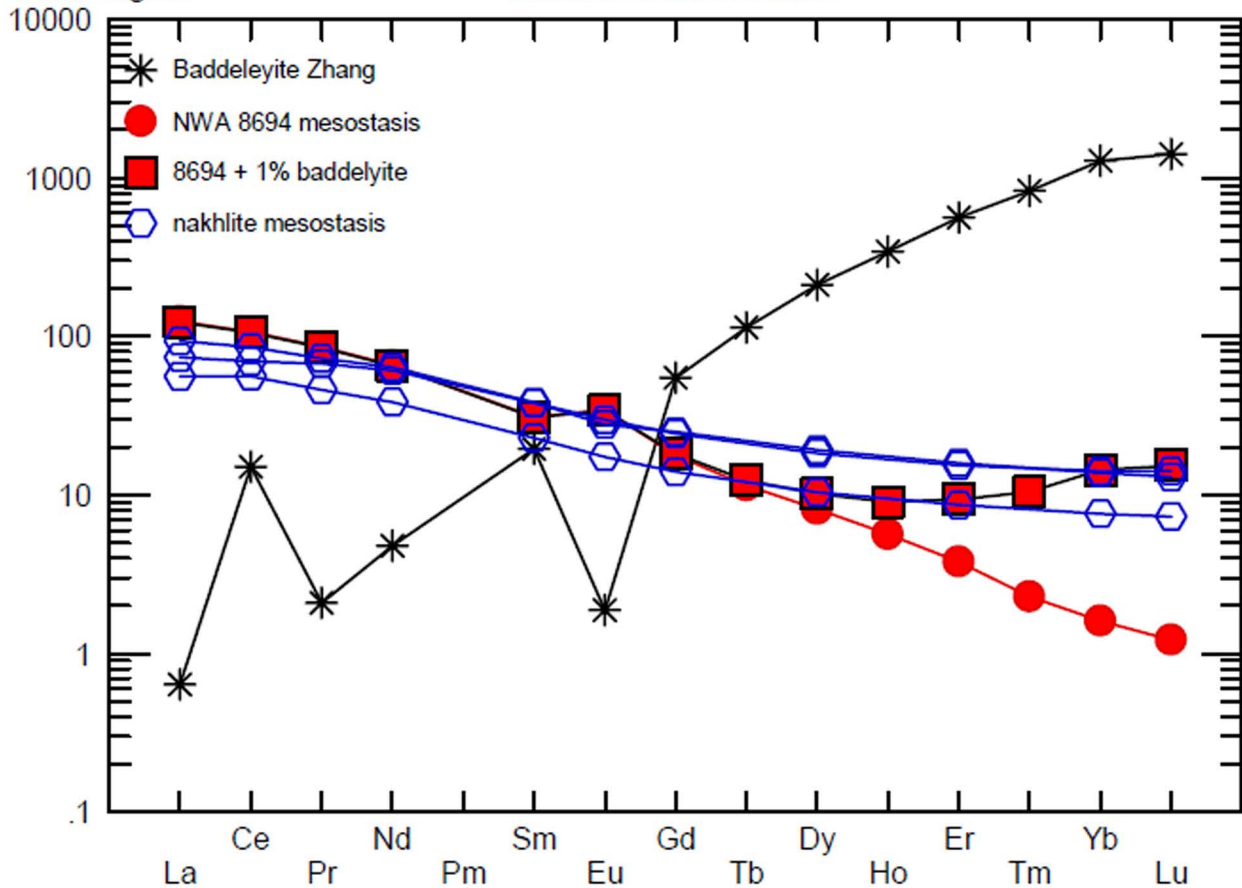


Rock/Orgueil

Barrat GCA 2012-REEs







Supplementary Table Olivine Analyses.

Point	Session	Fo	Fa	SiO <sub>2</sub>	Al <sub>2</sub> O <sub>3</sub>	TiO <sub>2</sub>	Cr <sub>2</sub> O <sub>3</sub>	FeO	MnO	MgO	CaO
<b>NWA 8694</b>											
1	121114	53,72	46,28	35,75	0,02	0,09	0,04	39,18	0,82	25,51	0,23
6	121114	53,61	46,39	35,87	0,02	bd	0,02	39,06	0,79	25,32	0,16
7	121114	53,17	46,83	35,31	0,04	bd	0,03	39,14	0,78	24,93	0,29
12	121114	52,48	47,52	35,53	0,03	0,04	0,04	39,45	0,76	24,44	0,18
20	121114	53,92	46,08	35,72	0,05	0,02	0,20	38,21	0,77	25,08	0,13
21	121114	53,24	46,76	35,89	bd	0,05	bd	39,05	0,79	24,95	0,19
22	121114	53,44	46,56	36,11	0,03	bd	0,05	38,54	0,81	24,81	0,17
23	121114	53,19	46,81	36,06	0,03	0,04	bd	39,44	0,82	25,14	0,22
34	121114	52,89	47,11	36,10	0,05	0,02	bd	39,07	0,78	24,60	0,13
52	121114	53,01	46,99	35,74	0,07	0,04	0,07	38,81	0,75	24,56	0,19
85	121114	53,32	46,68	36,38	0,01	0,03	0,04	39,26	0,83	25,15	0,18
87	121114	53,32	46,68	36,26	0,02	0,01	0,03	39,11	0,80	25,06	0,23
88	121114	53,29	46,71	35,75	bd	0,04	bd	39,02	0,80	24,98	0,18
91	121114	52,98	47,02	36,11	0,03	0,06	0,04	39,26	0,74	24,82	0,17
94	121114	53,42	46,58	35,74	0,01	0,06	0,06	38,81	0,76	24,97	0,28
95	121114	53,11	46,89	36,35	0,06	0,03	bd	39,06	0,78	24,82	0,23
97/62	121114	53,19	46,81	35,74	0,02	0,04	0,04	38,99	0,78	24,85	0,12
97/63	121114	53,09	46,91	35,19	0,02	0,05	bd	38,65	0,78	24,54	0,13
97/64	121114	53,15	46,85	35,49	0,02	0,04	0,03	38,61	0,80	24,57	0,12
97/65	121114	53,31	46,69	35,40	0,04	0,06	0,04	39,04	0,76	25,00	0,14
97/66	121114	53,00	47,00	35,43	0,04	bd	0,06	38,83	0,76	24,56	0,12
94	021214	53,63	46,37	36,03	0,05	bd	0,08	38,71	0,86	25,11	0,15
95	021214	53,55	46,45	35,69	0,06	0,06	0,06	38,45	0,81	24,87	0,16
96	021214	53,32	46,68	35,30	bd	0,04	bd	38,93	0,86	24,95	0,20
97	021214	54,22	45,78	35,64	0,02	0,01	0,02	38,12	0,88	25,32	0,19
98	021214	53,26	46,74	36,06	0,01	bd	0,03	39,23	0,91	25,07	0,21
99	021214	53,35	46,65	35,62	bd	0,09	bd	39,18	0,75	25,14	0,12
100	021214	53,30	46,70	35,93	0,04	bd	0,03	38,48	0,80	24,64	0,18
101	021214	53,04	46,96	35,46	0,01	0,06	0,01	39,15	0,77	24,81	0,17
102/1	021214	53,59	46,41	35,74	0,03	0,01	0,05	38,79	0,82	25,13	0,15
102/2	021214	53,65	46,35	35,35	0,02	bd	bd	38,57	0,77	25,05	0,16
102/3	021214	52,84	47,16	35,02	0,10	0,06	0,01	39,17	0,80	24,62	0,18
102/4	021214	52,94	47,06	35,24	0,08	bd	bd	38,50	0,88	24,30	0,20
102/6	021214	53,10	46,90	35,98	0,03	0,01	bd	38,93	0,87	24,73	0,19
102/7	021214	53,22	46,78	35,47	0,02	0,04	0,04	39,21	0,78	25,03	0,17
102/8	021214	53,53	46,47	35,12	bd	0,06	0,05	38,63	0,79	24,97	0,16
102/9	021214	53,29	46,71	35,26	0,04	bd	0,03	38,99	0,78	24,95	0,21
102/10	021214	52,97	47,03	34,65	0,10	0,02	0,03	39,03	0,82	24,66	0,21
102/12	021214	52,54	47,46	35,48	0,06	0,05	bd	39,68	0,76	24,64	0,16
102/13	021214	53,25	46,75	35,67	0,02	0,04	0,01	38,93	0,73	24,87	0,16
102/14	021214	53,42	46,58	35,39	0,01	0,06	0,01	38,93	0,88	25,04	0,16
102/15	021214	53,35	46,65	35,73	bd	bd	bd	39,37	0,81	25,26	0,16
102/16	021214	53,46	46,54	35,53	0,02	0,02	0,01	38,68	0,78	24,92	0,13
102/17	021214	53,15	46,85	35,90	0,05	0,07	0,01	38,90	0,80	24,75	0,12
102/18	021214	53,58	46,42	35,68	bd	bd	bd	38,86	0,88	25,16	0,04
102/19	021214	53,95	46,05	35,76	bd	0,04	0,03	38,11	0,93	25,05	0,14
102/20	021214	53,11	46,89	35,24	bd	0,02	bd	39,02	0,79	24,79	0,21
102/21	021214	52,74	47,26	35,27	0,03	0,09	bd	38,64	0,78	24,19	0,25
102/22	021214	53,40	46,60	35,19	bd	0,01	bd	38,96	0,92	25,05	0,18
102/23	021214	53,55	46,45	35,41	bd	bd	bd	38,66	0,85	25,00	0,16
102/24	021214	53,29	46,71	35,27	0,06	0,03	0,01	38,40	0,83	24,58	0,19
102/25	021214	53,22	46,78	35,48	0,04	bd	bd	38,84	0,75	24,79	0,16
102/26	021214	53,16	46,84	35,17	0,02	0,06	0,01	38,70	0,83	24,64	0,24
102/27	021214	52,81	47,19	35,95	bd	0,03	bd	39,24	0,77	24,63	0,18
102/28	021214	53,34	46,66	35,42	0,02	0,04	bd	38,94	0,75	24,97	0,14
102/29	021214	53,86	46,14	35,37	0,03	bd	0,01	38,23	0,78	25,03	0,14

102/30	021214	53,29	46,71	35,17	bd	0,04	0,02	38,57	0,84	24,69	0,21
102/31	021214	53,45	46,55	35,47	0,04	0,01	0,01	38,72	0,74	24,94	0,18
102/32	021214	53,65	46,35	35,46	bd	0,09	bd	38,64	0,91	25,09	0,13
102/33	021214	53,59	46,41	35,70	0,04	0,04	0,02	39,32	0,82	25,47	0,14
102/36	021214	52,85	47,15	35,94	0,07	0,05	0,07	39,19	0,81	24,65	0,15
102/37	021214	53,84	46,16	35,68	0,02	0,05	bd	38,48	0,84	25,18	0,14
102/38	021214	53,85	46,15	35,70	0,01	bd	0,02	38,92	0,82	25,48	0,11
102/39	021214	52,97	47,03	34,78	0,06	0,02	bd	38,48	0,80	24,31	0,13
102/40	021214	53,17	46,83	35,59	0,01	0,03	bd	38,50	0,80	24,52	0,12
102/41	021214	53,29	46,71	35,65	0,05	0,04	0,01	38,82	0,79	24,84	0,14
102/42	021214	53,43	46,57	35,74	0,06	0,03	0,01	38,67	0,84	24,89	0,15
102/43	021214	53,82	46,18	35,27	bd	bd	bd	38,02	0,88	24,86	0,13
102/44	021214	53,75	46,25	35,53	bd	0,03	bd	38,64	0,85	25,19	0,13
102/45	021214	53,53	46,47	35,53	0,02	0,03	bd	38,52	0,72	24,89	0,11
102/46	021214	53,31	46,69	36,00	0,02	0,05	bd	39,06	0,89	25,03	0,11
102/47	021214	53,25	46,75	35,79	0,05	0,09	0,05	39,01	0,84	24,92	0,12
102/48	021214	52,88	47,12	35,73	0,09	0,06	0,01	39,15	0,86	24,65	0,14
102/50	021214	53,04	46,96	36,00	0,17	0,02	bd	38,86	0,87	24,62	0,17
102/51	021214	53,70	46,30	35,68	bd	0,04	bd	38,26	0,77	24,89	0,10
102/52	021214	53,52	46,48	35,49	0,01	bd	bd	38,68	0,78	24,99	0,11
102/53	021214	53,80	46,20	35,44	0,02	0,03	0,04	38,20	0,82	24,96	0,12
102/54	021214	53,71	46,29	35,64	0,03	bd	bd	38,68	0,85	25,17	0,09
102/55	021214	53,78	46,22	35,79	0,01	0,04	0,07	38,46	0,89	25,10	0,12
102/56	021214	53,66	46,34	35,55	0,06	bd	bd	38,78	0,89	25,19	0,08
102/57	021214	53,91	46,09	36,13	0,01	0,01	0,04	38,36	0,86	25,17	0,09
102/58	021214	53,57	46,43	35,47	0,06	bd	0,04	38,83	0,82	25,13	0,11
102/59	021214	54,25	45,75	35,31	0,02	0,06	bd	38,71	0,80	25,75	0,09
102/60	021214	54,83	45,17	35,40	bd	0,03	0,06	37,11	0,83	25,27	0,08
1	121114	53,72	46,28	35,75	0,02	0,09	0,04	39,18	0,82	25,51	0,23
6	121114	53,61	46,39	35,87	0,02	bd	0,02	39,06	0,79	25,32	0,16
7	121114	53,17	46,83	35,31	0,04	bd	0,03	39,14	0,78	24,93	0,29
12	121114	52,48	47,52	35,53	0,03	0,04	0,04	39,45	0,76	24,44	0,18
20	121114	53,92	46,08	35,72	0,05	0,02	0,20	38,21	0,77	25,08	0,13
21	121114	53,24	46,76	35,89	bd	0,05	bd	39,05	0,79	24,95	0,19
22	121114	53,44	46,56	36,11	0,03	bd	0,05	38,54	0,81	24,81	0,17
23	121114	53,19	46,81	36,06	0,03	0,04	bd	39,44	0,82	25,14	0,22
34	121114	52,89	47,11	36,10	0,05	0,02	bd	39,07	0,78	24,60	0,13
52	121114	53,01	46,99	35,74	0,07	0,04	0,07	38,81	0,75	24,56	0,19
85	121114	53,32	46,68	36,38	0,01	0,03	0,04	39,26	0,83	25,15	0,18
87	121114	53,32	46,68	36,26	0,02	0,01	0,03	39,11	0,80	25,06	0,23
88	121114	53,29	46,71	35,75	bd	0,04	bd	39,02	0,80	24,98	0,18
91	121114	52,98	47,02	36,11	0,03	0,06	0,04	39,26	0,74	24,82	0,17
94	121114	53,42	46,58	35,74	0,01	0,06	0,06	38,81	0,76	24,97	0,28
95	121114	53,11	46,89	36,35	0,06	0,03	bd	39,06	0,78	24,82	0,23
97/62.	121114	53,19	46,81	35,74	0,02	0,04	0,04	38,99	0,78	24,85	0,12
97/63.	121114	53,09	46,91	35,19	0,02	0,05	bd	38,65	0,78	24,54	0,13
97/64.	121114	53,15	46,85	35,49	0,02	0,04	0,03	38,61	0,80	24,57	0,12
97/65.	121114	53,31	46,69	35,40	0,04	0,06	0,04	39,04	0,76	25,00	0,14
97/66.	121114	53,00	47,00	35,43	0,04	bd	0,06	38,83	0,76	24,56	0,12
26-LA-ICP-MS		67,86	32,14	35,30	0,02	0,02	0,02	38,02	0,84	25,50	0,24
27-LA-ICP-MS		54,45	45,55	35,07	0,02	0,02	0,02	38,44	0,82	25,35	0,21
28-LA-ICP-MS		54,03	45,97	35,07	0,05	0,04	0,19	38,38	0,84	25,36	0,21
29-LA-ICP-MS		54,08	45,92	35,41	0,02	0,03	0,02	38,24	0,83	25,22	0,20
30-LA-ICP-MS		54,03	45,97	35,18	0,02	0,02	0,02	38,24	0,84	25,42	0,24
<b>Chassigny</b>											
10	071211	68,12	32,28	37,51	0,03	0,03	0,02	28,69	0,55	33,77	0,15
11	071211	68,12	31,88	37,41	0,03	0,02	0,04	28,50	0,55	34,16	0,16
12	071211	67,69	31,88	37,84	0,03	0,02	0,12	28,38	0,48	34,03	0,12
5	200913	67,86	32,14	38,11	0,02	bd	0,02	28,61	0,55	33,89	0,15

8	200913	67,94	32,06	37,90	0,01	0,03	bd	28,27	0,54	33,62	0,16
11	200913	67,42	32,58	37,40	0,02	0,02	0,03	28,89	0,59	33,54	0,11
13	200913	67,32	32,68	37,06	0,03	bd	0,06	28,97	0,54	33,48	0,13
102	111213	67,42	32,58	35,67	bd	bd	0,02	28,84	0,63	33,48	0,13
22	111213	67,62	32,38	36,45	0,01	0,05	0,07	28,39	0,55	33,26	0,15
24	111213	68,54	31,46	35,73	0,03	0,09	0,09	27,79	0,44	33,95	0,14
26	111213	67,81	32,19	35,28	0,07	0,07	0,05	28,38	0,57	33,54	0,16
4	111213	67,86	32,14	36,87	0,02	0,01	bd	28,66	0,68	33,96	0,09
18	220318	68,31	31,69	37,65	0,01	0,02	0,02	28,24	0,58	34,16	0,14
19	220318	68,10	31,90	36,92	0,00	0,04	0,03	28,39	0,54	34,00	0,11
20	220318	67,96	32,04	37,37	0,03	0,01	0,05	28,56	0,51	33,98	0,13
21	220318	68,01	31,99	37,96	0,05	0,06	0,02	28,62	0,53	34,14	0,17
22	220318	68,18	31,82	37,37	0,04	0,04	0,03	27,91	0,53	33,54	0,14
23	220318	67,96	32,04	37,55	0,03	bd	0,02	28,56	0,54	33,98	0,21
24	220318	67,89	32,11	37,94	0,02	bd	0,03	28,67	0,56	34,00	0,27
25	220318	68,38	31,62	37,90	0,03	0,02	0,05	28,30	0,61	34,33	0,23
26	220318	68,40	31,60	38,14	0,03	0,03	0,04	28,04	0,53	34,05	0,13
27	220318	68,17	31,83	38,27	0,01	0,03	0,03	28,34	0,49	34,05	0,13
26-LA-ICP-MS		67,69	32,31	36,47	0,02	0,02	0,02	28,82	0,57	33,88	0,15
27-LA-ICP-MS		67,24	32,76	36,21	0,11	0,03	0,31	29,07	0,57	33,48	0,17
28-LA-ICP-MS		68,07	31,93	36,46	0,02	0,02	0,02	28,53	0,57	34,12	0,19
29-LA-ICP-MS		68,03	31,97	36,28	0,02	0,02	0,03	28,64	0,56	34,19	0,22
30-LA-ICP-MS		67,64	32,36	36,46	0,02	0,02	0,03	28,84	0,57	33,82	0,21
31-LA-ICP-MS		67,77	32,23	36,43	0,02	0,02	0,02	28,77	0,57	33,95	0,18
32-LA-ICP-MS		67,61	32,39	36,44	0,02	0,02	0,03	28,87	0,57	33,81	0,19

**NWA 2737**

50/1.	181217	77,86	22,14	39,10	0,01	0,04	0,03	20,78	0,37	40,97	0,11
54/1.	181217	78,13	21,87	39,97	0,02	bd	0,04	20,33	0,41	40,71	0,09
56/1.	181217	78,04	21,96	39,86	bd	bd	0,04	20,45	0,38	40,81	0,14
59/1.	181217	78,29	21,71	40,30	bd	0,04	0,07	20,17	0,44	40,82	0,13
61/1.	181217	78,30	21,70	39,19	0,20	bd	bd	19,89	0,40	40,25	0,18
64/1.	181217	78,04	21,96	39,13	0,04	0,04	0,06	20,36	0,42	40,61	0,11
66/1.	181217	78,01	21,99	39,43	0,07	0,02	0,05	20,47	0,44	40,74	0,25
68/1.	181217	78,45	21,55	39,24	0,02	bd	0,03	20,13	0,40	41,10	0,12
74/1.	181217	78,12	21,88	39,76	bd	bd	0,02	20,34	0,35	40,77	0,13
77/1.	181217	77,97	22,03	39,12	0,03	0,03	0,05	20,45	0,41	40,58	0,13
81/1.	181217	78,33	21,67	39,57	bd	bd	bd	20,01	0,31	40,58	0,12
81/2.	181217	77,81	22,19	39,14	bd	0,02	0,04	20,54	0,46	40,43	0,15
81/3.	181217	77,99	22,01	39,94	0,05	0,02	bd	20,42	0,44	40,57	0,11
81/4.	181217	77,79	22,21	39,35	0,10	bd	0,04	20,37	0,40	40,01	0,30
81/5.	181217	78,01	21,99	38,24	0,10	0,04	0,01	19,54	0,29	38,89	1,20
81/6.	181217	77,92	22,08	40,15	0,03	0,04	0,02	20,46	0,41	40,47	0,14
81/7.	181217	78,17	21,83	40,25	0,03	0,04	0,02	20,32	0,41	40,79	0,10
81/8.	181217	78,03	21,97	39,51	bd	bd	0,02	20,29	0,44	40,42	0,11
81/11.	181217	78,90	21,10	39,54	0,30	bd	0,03	19,32	0,45	40,54	0,15
81/12.	181217	78,12	21,88	39,21	0,44	0,05	0,02	19,80	0,42	39,61	0,18
81/15.	181217	78,70	21,30	40,09	0,06	0,03	0,02	19,65	0,43	40,73	0,16
81/16.	181217	78,77	21,23	39,69	0,23	0,03	bd	19,39	0,45	40,33	0,35
81/18.	181217	78,18	21,82	39,91	0,06	0,01	0,01	20,31	0,38	40,85	0,13
81/19.	181217	78,31	21,69	39,75	0,02	0,01	0,04	20,22	0,40	40,91	0,11
81/20.	181217	77,86	22,14	38,44	0,11	0,02	0,03	19,39	0,41	38,25	1,31
81/22.	181217	78,44	21,56	39,55	0,06	0,04	0,01	20,16	0,40	41,14	0,16
81/24.	181217	78,28	21,72	39,89	0,03	bd	0,06	20,12	0,44	40,70	0,11
81/25.	181217	78,01	21,99	39,91	bd	bd	0,05	20,39	0,33	40,57	0,16
81/26.	181217	78,27	21,73	39,81	bd	0,02	0,04	20,15	0,33	40,75	0,09
81/27.	181217	78,44	21,56	39,96	bd	0,05	0,02	19,96	0,46	40,71	0,07
81/28.	181217	78,37	21,63	39,09	0,20	0,02	bd	19,72	0,37	40,09	0,17
81/29.	181217	78,65	21,35	38,92	bd	0,05	0,03	19,60	0,36	40,52	0,13
81/30.	181217	78,27	21,73	39,82	0,02	0,03	bd	20,06	0,36	40,54	0,13

81/31.	181217	77,95	22,05	40,13	0,02	0,01	0,04	20,50	0,36	40,67	0,12
81/32.	181217	78,17	21,83	39,75	0,05	0,04	0,01	20,23	0,40	40,67	0,18
81/33.	181217	77,79	22,21	39,46	0,01	0,02	0,03	20,48	0,37	40,23	0,11
81/34.	181217	78,19	21,81	39,36	bd	bd	0,09	20,37	0,40	40,95	0,17
81/35.	181217	78,14	21,86	39,94	0,03	0,03	0,02	20,34	0,38	40,80	0,13
81/36.	181217	78,23	21,77	40,16	0,01	0,02	0,07	20,24	0,43	40,84	0,10
81/37.	181217	78,32	21,68	39,64	0,02	0,04	0,07	20,22	0,36	40,95	0,14
81/38.	181217	78,76	21,24	39,73	bd	0,02	0,10	19,68	0,47	40,93	0,14
81/60.	181217	78,56	21,44	39,21	0,03	0,03	0,16	19,85	0,31	40,80	0,16
81/61.	181217	78,42	21,58	39,82	0,01	0,03	0,06	20,08	0,43	40,95	0,05
81/62.	181217	78,50	21,50	39,54	bd	0,02	0,06	20,07	0,39	41,13	0,03
81/63.	181217	77,55	22,45	38,83	0,14	0,02	0,04	20,88	0,39	40,46	0,14
81/64.	181217	78,54	21,46	38,88	0,03	0,01	0,02	19,94	0,47	40,92	0,10
81/65.	181217	78,60	21,40	38,85	bd	0,05	0,04	19,99	0,41	41,19	0,13
81/66.	181217	78,74	21,26	39,09	0,02	0,05	0,02	19,79	0,40	41,12	0,11
81/67.	181217	78,14	21,86	38,96	0,02	0,04	0,03	20,37	0,40	40,87	0,11
81/69.	181217	78,37	21,63	38,55	bd	bd	bd	20,21	0,44	41,06	0,13
81/70.	181217	78,22	21,78	39,27	0,08	0,09	bd	20,39	0,43	41,11	0,03
81/71.	181217	77,88	22,12	39,40	bd	bd	0,01	20,52	0,43	40,52	0,14
81/72.	181217	78,06	21,94	39,34	bd	bd	0,01	20,37	0,35	40,64	0,11
81/80.	181217	78,32	21,68	39,54	0,03	0,06	0,06	20,16	0,45	40,85	0,10
81/81.	181217	78,22	21,78	39,68	0,01	0,03	0,01	20,27	0,40	40,89	0,11
81/82.	181217	77,97	22,03	39,47	0,04	0,01	0,05	20,57	0,39	40,87	0,11
81/83.	181217	78,59	21,41	39,47	bd	bd	0,01	19,97	0,44	41,11	0,15
81/84.	181217	78,84	21,16	39,16	0,02	bd	0,04	19,68	0,41	41,16	0,12
81/85.	181217	78,26	21,74	38,50	bd	0,04	0,01	20,09	0,46	40,56	0,14
81/86.	181217	77,81	22,19	39,37	bd	0,04	bd	20,71	0,45	40,74	0,14
81/87.	181217	79,14	20,86	37,92	bd	bd	0,02	19,13	0,41	40,70	0,12
81/88.	181217	78,01	21,99	39,19	0,04	0,03	0,04	20,43	0,44	40,68	0,14
81/89.	181217	77,88	22,12	39,14	0,02	0,03	bd	20,63	0,41	40,76	0,10
81/90.	181217	78,29	21,71	39,37	0,05	0,06	0,03	20,15	0,40	40,75	0,15
81/91.	181217	78,36	21,64	39,24	bd	bd	0,01	20,16	0,43	40,97	0,19
81/92.	181217	78,15	21,85	39,40	0,01	0,03	0,01	20,46	0,42	41,08	0,18
81/93.	181217	78,18	21,82	39,19	0,05	0,02	0,02	20,43	0,43	41,03	0,16
81/94.	181217	77,75	22,25	39,61	bd	0,02	0,02	20,78	0,41	40,75	0,17
81/95.	181217	77,81	22,19	39,29	bd	0,03	0,05	20,72	0,42	40,73	0,21
81/96.	181217	78,01	21,99	39,70	bd	0,02	0,08	20,38	0,39	40,58	0,16
81/97.	181217	78,62	21,38	39,43	0,02	0,02	0,17	19,88	0,35	41,04	0,17
81/100.	181217	77,97	22,03	39,01	bd	0,03	0,14	20,52	0,34	40,69	0,16
82/1.	181217	77,76	22,24	39,56	0,03	bd	0,02	20,66	0,40	40,53	0,16
82/2.	181217	78,24	21,76	39,54	bd	0,04	0,02	20,14	0,41	40,61	0,21
82/3.	181217	78,09	21,91	39,62	0,02	0,02	bd	20,29	0,42	40,55	0,22
82/4.	181217	77,63	22,37	39,69	0,05	0,04	0,06	20,93	0,39	40,77	0,13
82/5.	181217	78,07	21,93	39,33	0,09	0,03	0,04	20,29	0,42	40,49	0,19
82/6.	181217	78,12	21,88	39,45	0,05	0,01	0,03	20,31	0,38	40,72	0,17
82/7.	181217	77,87	22,13	39,11	0,11	bd	0,04	20,36	0,42	40,20	0,19
82/8.	181217	78,30	21,70	39,67	0,09	bd	0,03	19,94	0,44	40,37	0,15
82/9.	181217	78,09	21,91	39,49	0,05	0,01	0,06	20,21	0,42	40,43	0,44
82/10.	181217	78,17	21,83	39,57	0,05	0,03	0,01	20,08	0,41	40,31	0,57
82/11.	181217	77,62	22,38	39,58	0,03	0,03	0,02	20,94	0,36	40,75	0,25
82/12.	181217	78,03	21,97	40,05	0,02	0,01	0,03	20,45	0,45	40,72	0,18
82/13.	181217	77,91	22,09	39,58	0,07	0,02	0,07	20,34	0,41	40,26	0,16
82/14.	181217	78,15	21,85	39,15	0,06	bd	0,05	20,23	0,42	40,61	0,20
82/15.	181217	78,14	21,86	39,06	0,02	0,01	0,02	20,19	0,40	40,51	0,17
82/16.	181217	77,88	22,12	38,26	0,13	0,01	0,04	19,69	0,45	38,92	1,48
82/21.	181217	78,02	21,98	39,27	0,05	0,02	0,04	20,47	0,45	40,73	0,17
82/22.	181217	77,95	22,05	39,20	0,07	0,02	0,02	20,67	0,26	40,99	0,25
82/23.	181217	77,93	22,07	39,33	0,04	0,02	0,03	20,36	0,36	40,30	0,19
82/24.	181217	77,90	22,10	38,86	0,02	bd	0,04	20,57	0,41	40,67	0,14

82/25.	181217	78,19	21,81	39,15	0,03	bd	0,03	20,18	0,43	40,58	0,18
82/26.	181217	77,58	22,42	39,12	0,05	bd	0,02	20,73	0,52	40,22	0,14
82/27.	181217	78,01	21,99	38,79	0,02	bd	bd	20,38	0,38	40,57	0,24
82/28.	181217	77,94	22,06	39,57	bd	0,03	0,05	20,51	0,33	40,61	0,16
82/29.	181217	77,91	22,09	39,53	0,05	bd	0,05	20,51	0,39	40,54	0,18
82/30.	181217	77,95	22,05	39,28	0,02	0,02	0,04	20,37	0,33	40,42	0,19
82/31.	181217	77,75	22,25	39,45	bd	0,05	0,01	20,77	0,40	40,70	0,14
82/32.	181217	78,22	21,78	38,93	0,07	0,02	0,05	19,98	0,40	40,27	0,21
82/33.	181217	77,62	22,38	39,24	0,03	0,02	0,02	20,82	0,45	40,52	0,25
82/34.	181217	78,82	21,18	37,81	bd	bd	0,05	19,36	0,34	40,44	0,23
82/35.	181217	77,86	22,14	39,73	0,02	bd	0,02	20,59	0,39	40,60	0,20
82/36.	181217	78,07	21,93	39,18	0,01	0,01	0,04	20,43	0,42	40,78	0,19
82/37.	181217	78,24	21,76	38,42	0,04	0,01	0,02	20,08	0,42	40,50	0,14
82/38.	181217	78,05	21,95	39,21	0,05	0,01	0,06	20,46	0,48	40,78	0,10
82/39.	181217	77,62	22,38	39,36	0,02	0,03	0,01	20,79	0,41	40,47	0,15
82/40.	181217	77,76	22,24	39,38	0,04	0,01	bd	20,51	0,41	40,25	0,13
82/41.	181217	78,15	21,85	39,31	0,02	bd	0,01	20,25	0,39	40,67	0,10
82/42.	181217	78,25	21,75	39,11	bd	bd	0,03	20,08	0,45	40,51	0,18
82/43.	181217	78,02	21,98	38,99	0,01	bd	0,02	20,51	0,57	40,86	0,14
82/44.	181217	77,94	22,06	39,38	bd	bd	bd	20,66	0,41	40,96	0,13
82/45.	181217	78,08	21,92	39,83	0,05	bd	0,05	20,32	0,33	40,61	0,16
82/47.	181217	78,27	21,73	39,44	0,06	0,01	0,02	20,05	0,39	40,53	0,18
82/48.	181217	78,01	21,99	39,33	0,03	0,01	0,02	20,43	0,37	40,67	0,23
82/49.	181217	78,04	21,96	39,38	bd	0,05	0,04	20,50	0,54	40,87	0,11
82/50.	181217	77,81	22,19	39,54	0,04	0,02	0,02	20,68	0,42	40,67	0,21
82/51.	181217	78,16	21,84	39,23	0,11	bd	0,02	20,13	0,35	40,42	0,19
82/52.	181217	77,85	22,15	39,50	bd	0,02	0,02	20,62	0,44	40,65	0,17
82/53.	181217	78,04	21,96	38,83	0,05	0,01	0,07	20,37	0,47	40,59	0,22
82/56.	181217	78,12	21,88	39,34	bd	0,05	bd	20,33	0,44	40,72	0,18
82/57.	181217	78,09	21,91	39,31	bd	bd	0,02	20,19	0,48	40,40	0,19
82/58.	181217	78,20	21,80	39,40	0,01	0,02	0,06	20,11	0,37	40,47	0,21
82/59.	181217	77,88	22,12	39,41	0,09	0,03	0,07	20,62	0,40	40,71	0,14
82/60.	181217	77,88	22,12	39,50	0,03	0,02	0,03	20,46	0,41	40,39	0,20
82/61.	181217	77,79	22,21	39,70	bd	0,02	0,02	20,79	0,38	40,84	0,18
82/62.	181217	79,17	20,83	38,80	0,35	0,03	0,04	18,79	0,43	40,02	0,28
82/64.	181217	78,05	21,95	39,60	0,06	0,04	0,04	20,11	0,33	40,09	0,19
82/65.	181217	78,06	21,94	39,53	0,01	0,03	0,04	20,37	0,40	40,65	0,19
82/66.	181217	77,58	22,42	39,16	0,01	bd	0,05	20,88	0,37	40,51	0,19
82/67.	181217	77,76	22,24	39,72	0,02	bd	0,04	20,68	0,35	40,56	0,21
82/68.	181217	78,13	21,87	39,37	0,01	0,01	0,04	20,04	0,34	40,17	0,30
82/69.	181217	77,88	22,12	39,51	0,03	0,02	0,04	20,55	0,36	40,57	0,20
82/70.	181217	77,75	22,25	39,70	0,04	0,02	0,04	20,62	0,35	40,43	0,20
82/71.	181217	78,21	21,79	39,91	0,05	0,06	0,03	20,11	0,45	40,51	0,19
82/72.	181217	77,76	22,24	39,34	0,03	0,02	0,05	20,66	0,44	40,50	0,15
82/73.	181217	78,13	21,87	39,48	0,04	0,02	bd	20,18	0,44	40,49	0,16
82/75.	181217	78,11	21,89	38,10	0,23	0,02	bd	19,71	0,34	39,41	0,25
82/76.	181217	78,15	21,85	39,43	0,08	0,04	0,05	20,01	0,34	40,13	0,20
82/77.	181217	78,06	21,94	39,40	0,03	bd	0,05	20,45	0,41	40,84	0,18
82/78.	181217	78,08	21,92	39,11	0,05	0,04	0,08	20,36	0,45	40,73	0,16
82/79.	181217	78,28	21,72	39,24	0,04	0,01	0,04	20,08	0,55	40,56	0,15
82/80.	181217	78,30	21,70	39,18	0,04	0,03	0,01	19,59	0,34	39,68	0,20
82/81.	181217	77,87	22,13	39,97	bd	0,02	bd	20,70	0,33	40,89	0,14
82/82.	181217	77,87	22,13	39,44	0,01	0,01	bd	20,61	0,41	40,69	0,19
82/83.	181217	77,77	22,23	39,60	0,02	0,03	0,03	20,71	0,37	40,67	0,21
82/84.	181217	78,05	21,95	39,43	0,05	0,02	0,06	20,51	0,41	40,87	0,17
82/85.	181217	78,22	21,78	38,93	0,01	0,04	0,06	20,26	0,35	40,82	0,20
82/86.	181217	78,04	21,96	39,63	0,03	0,04	0,04	20,25	0,39	40,39	0,14
82/87.	181217	77,93	22,07	39,37	0,02	bd	0,04	20,53	0,43	40,67	0,17
82/88.	181217	78,40	21,60	39,39	0,01	0,01	0,03	20,09	0,42	40,93	0,20

82/89.	181217	78,53	21,47	39,09	0,06	0,02	0,02	19,94	0,36	40,92	0,14
82/91.	181217	78,19	21,81	39,53	0,07	0,02	0,01	20,25	0,35	40,75	0,14
82/92.	181217	78,02	21,98	39,36	0,03	0,04	0,07	20,50	0,45	40,79	0,16
82/93.	181217	77,85	22,15	39,41	bd	bd	0,02	20,74	0,42	40,86	0,17
82/94.	181217	78,15	21,85	39,51	0,02	0,03	0,03	20,32	0,35	40,80	0,12
82/95.	181217	77,89	22,11	39,30	0,04	0,03	0,09	20,60	0,41	40,71	0,17
82/96.	181217	78,14	21,86	39,55	0,02	0,05	0,03	20,40	0,34	40,88	0,18
82/97.	181217	78,09	21,91	39,05	0,01	0,02	0,03	20,25	0,46	40,45	0,13
82/98.	181217	78,30	21,70	39,68	bd	0,02	0,03	20,25	0,48	40,96	0,23
82/99.	181217	77,88	22,12	39,40	0,03	0,01	0,02	20,48	0,42	40,44	0,16
82/100.	181217	77,77	22,23	39,60	0,05	0,02	0,06	20,68	0,36	40,56	0,15
99/1.	181217	78,81	21,19	40,19	0,04	0,03	0,14	19,66	0,32	41,02	0,21
99/2.	181217	78,62	21,38	39,99	0,01	bd	0,07	19,67	0,36	40,58	0,19
99/3.	181217	78,45	21,55	39,69	0,03	0,01	0,15	19,71	0,46	40,26	0,24
99/4.	181217	78,49	21,51	40,03	0,03	0,04	0,14	20,09	0,41	41,13	0,13
99/5.	181217	78,84	21,16	39,73	0,02	bd	0,18	19,82	0,42	41,42	0,07
99/6.	181217	79,21	20,79	39,89	0,05	bd	0,26	19,39	0,33	41,40	0,07
99/7.	181217	79,72	20,28	39,70	bd	bd	0,29	18,88	0,36	41,61	0,17
99/8.	181217	79,67	20,33	39,87	0,05	bd	0,38	19,00	0,39	41,80	0,16
139/1.	181217	78,03	21,97	39,78	0,04	0,03	0,01	20,43	0,32	40,70	0,11
142/1.	181217	78,19	21,81	40,11	0,02	0,02	0,04	20,27	0,48	40,77	0,13
145/1.	181217	78,09	21,91	40,39	0,06	0,01	0,03	20,40	0,45	40,76	0,10
145/5.	181217	77,84	22,16	40,45	0,05	0,01	bd	20,69	0,47	40,80	0,10
145/6.	181217	77,89	22,11	40,24	bd	0,05	0,04	20,67	0,43	40,84	0,10
145/8.	181217	77,85	22,15	40,14	bd	0,04	0,05	20,50	0,41	40,41	0,25
145/9.	181217	78,18	21,82	40,13	0,05	0,03	0,05	20,32	0,42	40,82	0,13
145/11.	181217	78,33	21,67	40,30	0,02	0,04	0,03	20,10	0,42	40,74	0,11
145/12.	181217	78,32	21,68	39,83	0,06	0,03	0,03	20,05	0,42	40,64	0,15
145/13.	181217	77,91	22,09	40,00	0,04	bd	0,03	20,48	0,31	40,51	0,14
145/14.	181217	77,94	22,06	39,56	0,54	0,02	0,06	20,22	0,36	40,11	0,26
145/15.	181217	78,08	21,92	38,92	0,50	0,05	0,05	20,01	0,41	39,95	0,38
145/67.	181217	78,05	21,95	39,26	0,05	0,02	0,03	20,36	0,43	40,62	0,35
145/68.	181217	77,68	22,32	39,38	0,02	bd	0,03	20,81	0,41	40,64	0,15
145/70.	181217	78,23	21,77	39,78	0,01	0,04	0,04	20,07	0,41	40,49	0,15
145/71.	181217	78,14	21,86	39,91	bd	bd	0,03	20,22	0,32	40,56	0,18
148/1.	181217	78,24	21,76	39,49	0,03	0,03	0,05	20,18	0,35	40,73	0,19
148/2.	181217	78,34	21,66	39,74	0,13	0,03	bd	19,81	0,41	40,18	0,18
148/3.	181217	77,92	22,08	39,64	0,07	0,02	0,05	20,46	0,45	40,46	0,21
148/4.	181217	78,38	21,62	39,03	0,20	0,02	0,03	19,91	0,44	40,50	0,13
148/5.	181217	78,27	21,73	39,73	0,20	bd	0,06	19,87	0,40	40,18	0,13
148/6.	181217	78,26	21,74	39,99	0,06	0,07	0,02	20,20	0,49	40,78	0,09
148/7.	181217	78,38	21,62	39,59	0,07	0,03	bd	19,96	0,40	40,57	0,17
148/8.	181217	78,70	21,30	38,53	0,40	0,01	0,01	19,06	0,45	39,47	0,22
148/9.	181217	77,92	22,08	39,93	0,14	0,01	0,02	20,44	0,40	40,48	0,13
148/10.	181217	78,05	21,95	39,50	0,07	0,01	0,04	20,40	0,36	40,67	0,09
148/11.	181217	78,37	21,63	39,82	0,02	0,01	0,02	20,21	0,47	41,06	0,14
148/12.	181217	77,80	22,20	40,28	bd	0,04	0,01	20,70	0,42	40,71	0,13
148/13.	181217	77,80	22,20	40,34	0,02	bd	0,05	20,70	0,41	40,71	0,09
148/14.	181217	77,96	22,04	39,88	bd	bd	0,02	20,41	0,41	40,53	0,10
148/15.	181217	77,83	22,17	39,90	bd	0,04	0,04	20,70	0,40	40,77	0,13
148/16.	181217	77,77	22,23	39,84	0,06	0,04	0,01	20,70	0,41	40,63	0,13
148/17.	181217	77,83	22,17	39,68	0,04	0,01	bd	20,60	0,38	40,57	0,15
148/18.	181217	78,01	21,99	39,44	0,03	0,01	0,05	20,47	0,39	40,74	0,12
148/19.	181217	78,07	21,93	39,90	0,03	0,03	0,02	20,36	0,42	40,66	0,11
148/20.	181217	77,71	22,29	39,47	bd	0,02	0,04	20,71	0,46	40,54	0,12
148/21.	181217	78,35	21,65	39,31	0,02	0,02	0,02	19,92	0,48	40,48	0,14
148/22.	181217	77,80	22,20	39,86	0,03	bd	0,02	20,66	0,47	40,58	0,12
148/23.	181217	78,22	21,78	39,78	0,02	0,02	0,04	20,27	0,35	40,84	0,09
148/25.	181217	78,11	21,89	39,36	0,37	bd	0,06	20,07	0,44	40,21	0,18

148/26.	181217	77,73	22,27	39,99	0,04	0,03	0,03	20,75	0,40	40,62	0,17
148/27.	181217	77,85	22,15	39,87	0,02	bd	0,03	20,72	0,36	40,84	0,14
148/28.	181217	77,89	22,11	39,74	bd	bd	bd	20,50	0,46	40,53	0,20
148/29.	181217	77,98	22,02	39,79	0,01	0,05	0,03	20,46	0,35	40,65	0,09
148/30.	181217	77,57	22,43	39,61	0,06	0,04	0,05	21,08	0,43	40,93	0,12
148/31.	181217	77,63	22,37	40,12	0,02	0,01	0,05	20,82	0,33	40,49	0,16
148/32.	181217	78,19	21,81	39,88	0,40	bd	bd	19,89	0,44	40,04	0,12
148/33.	181217	78,34	21,66	39,42	0,65	bd	0,01	19,66	0,36	39,87	0,16
148/34.	181217	78,06	21,94	39,68	0,25	0,03	0,05	20,16	0,44	40,19	0,25
148/35.	181217	77,91	22,09	39,76	0,07	bd	bd	20,57	0,46	40,71	0,21
148/36.	181217	78,00	22,00	39,18	0,35	0,04	bd	20,04	0,50	39,88	0,26
148/38.	181217	77,87	22,13	38,68	0,73	bd	0,03	20,03	0,37	39,55	0,34
148/39.	181217	77,93	22,07	39,69	0,22	0,02	0,03	20,31	0,39	40,24	0,33
148/40.	181217	77,92	22,08	39,72	0,26	0,04	0,02	20,29	0,39	40,21	0,28
148/42.	181217	78,11	21,89	39,21	bd	bd	0,03	20,43	0,45	40,88	0,19
148/43.	181217	78,39	21,61	39,62	bd	bd	bd	19,96	0,49	40,65	0,18
148/44.	181217	78,38	21,62	40,15	bd	0,03	0,04	20,06	0,43	40,81	0,19
148/45.	181217	77,80	22,20	40,04	0,02	0,02	0,05	20,66	0,33	40,61	0,11
148/46.	181217	77,64	22,36	39,82	0,12	0,03	0,03	20,77	0,51	40,47	0,12
148/47.	181217	77,79	22,21	39,94	bd	0,02	0,02	20,52	0,44	40,29	0,12
148/49.	181217	78,04	21,96	39,72	0,05	0,02	0,02	20,27	0,42	40,38	0,21
148/53.	181217	79,50	20,50	38,02	0,03	0,03	bd	18,85	0,37	41,04	0,12
148/54.	181217	78,73	21,27	38,64	bd	bd	0,05	19,74	0,39	40,97	0,22
148/55.	181217	78,01	21,99	40,11	bd	0,04	0,07	20,44	0,43	40,71	0,14
148/56.	181217	78,29	21,71	39,53	0,02	bd	0,03	20,17	0,42	40,79	0,15
148/57.	181217	78,46	21,54	40,21	0,02	0,02	bd	19,98	0,43	40,85	0,17
148/58.	181217	78,05	21,95	39,46	0,14	0,02	bd	20,30	0,49	40,53	0,14
148/59.	181217	78,46	21,54	38,80	0,56	0,04	0,04	19,73	0,41	40,30	0,19
148/60.	181217	78,34	21,66	39,64	0,08	0,05	bd	19,89	0,32	40,35	0,21
148/61.	181217	78,77	21,23	39,52	0,08	0,04	0,03	19,74	0,36	41,09	0,13
148/62.	181217	78,01	21,99	39,79	0,01	0,01	0,03	20,51	0,41	40,81	0,17
148/63.	181217	78,00	22,00	39,96	0,07	0,02	0,02	20,46	0,32	40,70	0,11
148/64.	181217	78,48	21,52	39,75	0,26	0,02	0,03	19,67	0,37	40,20	0,17
148/65.	181217	77,89	22,11	39,26	0,06	0,03	0,02	20,55	0,37	40,58	0,16
148/66.	181217	78,48	21,52	39,75	0,05	0,07	0,04	20,11	0,34	41,12	0,10
148/67.	181217	78,33	21,67	39,26	0,37	bd	bd	19,91	0,34	40,32	0,17
148/68.	181217	78,22	21,78	39,68	0,34	bd	0,01	19,82	0,41	39,96	0,18
148/69.	181217	77,79	22,21	39,94	0,01	bd	0,03	20,76	0,44	40,78	0,18
148/70.	181217	78,39	21,61	39,93	bd	0,03	bd	20,08	0,41	40,90	0,14
148/71.	181217	78,10	21,90	39,90	bd	0,03	bd	20,35	0,46	40,72	0,13
148/72.	181217	78,25	21,75	39,60	bd	bd	0,01	20,25	0,50	40,87	0,19
148/74.	181217	78,03	21,97	39,78	0,01	0,02	0,01	20,49	0,40	40,83	0,08
148/75.	181217	78,13	21,87	40,01	0,04	0,03	bd	20,25	0,44	40,62	0,19
148/76.	181217	78,08	21,92	39,80	0,23	0,04	bd	20,35	0,47	40,66	0,15
148/77.	181217	77,98	22,02	39,65	0,11	bd	0,06	20,07	0,50	39,89	0,30
148/80.	181217	78,37	21,63	38,98	0,07	0,03	bd	19,56	0,42	39,77	0,74
148/81.	181217	78,39	21,61	39,69	bd	bd	0,03	19,96	0,41	40,63	0,09
148/82.	181217	77,49	22,51	39,04	0,49	0,03	bd	20,19	0,39	39,03	0,73
148/85.	181217	78,32	21,68	39,25	0,04	0,03	0,03	19,78	0,35	40,08	0,36
148/86.	181217	77,78	22,22	39,47	0,21	0,02	0,03	20,18	0,41	39,62	0,20
148/87.	181217	78,17	21,83	38,89	0,13	0,02	bd	20,06	0,43	40,33	0,25
148/88.	181217	77,88	22,12	39,99	0,05	0,01	0,03	20,56	0,41	40,62	0,16
148/89.	181217	77,83	22,17	39,63	0,01	0,02	0,01	20,66	0,41	40,65	0,15
148/90.	181217	77,98	22,02	39,91	0,01	bd	bd	20,52	0,45	40,81	0,20
148/91.	181217	77,91	22,09	39,85	bd	0,04	bd	20,51	0,39	40,61	0,18
148/92.	181217	77,94	22,06	40,23	0,03	0,07	0,05	20,44	0,36	40,51	0,16
148/94.	181217	78,10	21,90	39,78	bd	0,02	0,05	20,41	0,41	40,83	0,22
148/95.	181217	77,98	22,02	39,38	0,34	0,03	bd	20,15	0,45	40,01	0,21
148/96.	181217	77,86	22,14	39,87	bd	bd	0,01	20,51	0,45	40,48	0,23



148/97.	181217	78,37	21,63	39,75	0,17	0,03	0,02	19,78	0,46	40,17	0,24
148/98.	181217	78,06	21,94	39,32	0,47	0,01	0,05	20,00	0,39	39,92	0,27
148/99.	181217	78,55	21,45	39,51	0,18	bd	0,01	19,61	0,44	40,27	0,22
148/100.	181217	78,14	21,86	39,62	bd	bd	0,01	20,11	0,40	40,31	0,20
148/101.	181217	77,81	22,19	39,72	0,04	0,03	0,04	20,69	0,37	40,68	0,09
148/102.	181217	78,19	21,81	39,40	0,03	0,05	0,01	20,33	0,49	40,85	0,15
148/103.	181217	78,07	21,93	40,15	0,06	0,01	0,04	20,31	0,42	40,58	0,11
148/104.	181217	78,16	21,84	39,80	0,05	0,03	bd	20,18	0,35	40,49	0,14
148/105.	181217	78,05	21,95	39,83	0,01	0,03	bd	20,47	0,42	40,83	0,12
148/106.	181217	78,02	21,98	39,59	0,04	0,04	0,03	20,41	0,42	40,68	0,13

---

High Al points in shocked olivine that is dark or striped in BSE. 'bd' =below detection limit.

<b>Na<sub>2</sub>O</b>	<b>Total</b>
bd	101,64
bd	101,07
bd	100,53
0,02	100,46
bd	100,30
bd	100,86
bd	100,49
bd	101,76
0,01	100,67
bd	100,13
bd	101,94
0,02	101,48
0,01	100,77
bd	101,12
bd	100,72
0,02	101,39
0,02	100,61
bd	99,29
bd	99,72
bd	100,51
bd	99,72
bd	101,02
bd	100,33
bd	100,43
bd	100,18
bd	101,41
bd	100,85
bd	100,06
0,01	100,48
bd	100,94
0,03	100,06
0,03	100,01
bd	99,04
bd	100,83
bd	100,71
bd	99,83
0,03	100,46
0,02	99,59
bd	100,94
bd	100,57
0,02	100,55
0,02	101,28
bd	100,08
bd	100,71
0,01	100,78
0,02	100,04
bd	100,25
bd	99,21
0,03	100,39
0,02	100,16
0,01	99,62
0,01	100,21
0,01	99,68
bd	100,88
bd	100,30
0,02	99,68

bd	99,59
0,01	100,03
bd	100,33
0,02	101,69
bd	100,98
bd	100,36
0,04	101,00
0,01	98,39
bd	99,48
bd	100,38
0,01	100,40
bd	99,12
0,02	100,54
0,03	99,91
bd	101,13
bd	100,76
bd	100,65
0,02	100,72
bd	99,63
bd	99,90
bd	99,57
bd	100,28
bd	100,48
bd	100,45
bd	100,75
bd	100,48
0,01	100,63
bd	98,94
bd	101,64
bd	101,07
bd	100,53
0,02	100,46
bd	100,30
bd	100,86
bd	100,49
bd	101,76
0,01	100,67
bd	100,13
bd	101,94
0,02	101,48
0,01	100,77
bd	101,12
bd	100,72
0,02	101,39
0,02	100,61
bd	99,29
bd	99,72
bd	100,51
bd	99,72
0,01	99,96
0,02	99,95
0,02	99,97
0,02	99,98
0,02	99,97
bd	100,76
0,01	100,89
bd	101,01
bd	101,41

bd	100,61
bd	100,67
bd	100,33
bd	98,8
bd	98,98
bd	98,33
bd	98,19
bd	100,34
0,01	101,03
bd	100,09
0,01	101,06
bd	101,67
0,01	99,75
0,01	101,07
bd	101,62
0,01	101,61
bd	101,08
bd	101,41
0,01	99,96
0,02	99,97
0,02	99,95
0,02	99,98
0,01	99,98
0,02	99,98
0,02	99,97
0,04	101,65
bd	101,58
0,03	101,72
0,01	101,98
0,04	100,14
bd	100,75
0,03	101,51
0,03	101,07
0,05	101,44
0,03	100,83
bd	100,60
0,05	100,83
0,03	101,59
0,08	100,65
0,06	98,40
0,02	101,75
0,02	102,02
0,03	100,85
0,05	100,37
0,10	99,82
0,05	101,23
0,06	100,55
0,05	101,71
bd	101,47
0,04	98,00
0,04	101,56
0,02	101,37
bd	101,40
0,04	101,23
0,01	101,25
0,12	99,80
0,09	99,70
0,03	101,00

0,03	101,89
bd	101,35
0,03	100,75
0,04	101,38
bd	101,71
bd	101,89
0,05	101,49
0,02	101,11
0,06	100,61
0,02	101,46
0,06	101,31
0,05	100,95
0,04	100,41
0,07	100,72
bd	100,61
0,04	100,83
0,03	100,42
0,02	101,41
0,05	101,07
0,03	100,87
0,01	101,27
0,03	101,43
0,02	101,54
0,05	101,19
0,05	100,65
0,05	99,86
0,04	101,51
0,08	98,39
0,02	101,02
0,02	101,11
0,02	100,99
bd	101,02
0,01	101,61
0,03	101,36
0,03	101,79
0,03	101,49
0,03	101,34
0,05	101,13
0,02	100,89
0,02	101,38
0,03	101,00
0,01	101,15
0,04	102,12
0,05	100,93
0,01	101,16
0,05	100,48
0,05	100,78
0,05	101,17
0,03	101,06
0,04	102,01
0,02	101,93
0,08	101,02
0,04	100,78
0,01	100,40
0,05	99,06
0,05	101,27
0,01	101,53
0,05	100,67
0,04	100,76

0,03	100,61
0,02	100,83
0,04	100,45
0,02	101,28
0,03	101,29
0,04	100,71
0,04	101,57
0,01	99,94
0,06	101,41
0,07	98,31
0,02	101,58
0,02	101,08
0,04	99,67
0,04	101,19
0,04	101,30
0,03	100,78
0,05	100,84
0,02	100,40
0,03	101,14
bd	101,54
0,05	101,44
0,02	100,72
0,01	101,14
0,04	101,53
0,03	101,63
0,04	100,54
0,03	101,46
0,06	100,66
0,02	101,08
bd	100,60
0,02	100,68
0,04	101,53
bd	101,09
0,05	101,99
0,02	98,76
0,02	100,47
0,03	101,26
0,03	101,19
0,01	101,59
0,06	100,35
0,04	101,32
0,05	101,46
0,01	101,34
0,12	101,33
bd	100,85
0,08	98,16
0,04	100,32
0,04	101,44
0,03	101,02
0,01	100,68
0,38	99,48
0,06	102,12
0,02	101,40
0,01	101,65
0,03	101,56
0,05	100,73
0,03	100,98
0,06	101,30
0,01	101,09

0,05	100,60
0,01	101,14
0,02	101,42
0,02	101,69
bd	101,20
0,03	101,38
0,19	101,66
0,03	100,44
0,04	101,71
0,05	101,02
0,03	101,50
0,01	101,64
0,03	100,91
0,01	100,56
0,03	102,02
bd	101,68
0,02	101,41
0,04	101,07
0,03	101,68
0,01	101,45
0,01	102,10
0,01	102,21
bd	102,58
0,04	102,42
0,05	101,89
bd	101,99
0,04	101,81
bd	101,21
0,03	101,55
0,04	101,19
0,10	100,38
0,01	101,14
0,03	101,48
0,04	101,03
0,02	101,24
0,02	101,06
0,03	100,52
0,01	101,36
0,05	100,31
0,01	100,58
0,06	101,74
0,01	100,82
0,03	98,19
0,02	101,58
0,02	101,16
0,04	101,79
0,03	102,31
bd	102,31
0,01	101,39
0,02	102,00
0,02	101,84
0,01	101,45
0,02	101,26
0,01	101,55
0,02	101,39
0,03	100,41
0,01	101,76
0,03	101,45
0,08	100,78

0,02	102,05
0,01	101,98
0,05	101,50
0,07	101,48
bd	102,31
0,03	102,04
0,03	100,84
0,01	100,16
0,01	101,06
0,03	101,83
0,06	100,32
0,03	99,79
0,05	101,30
bd	101,23
0,03	101,24
0,03	100,94
0,03	101,72
0,01	101,85
0,04	101,92
0,05	101,40
0,06	101,16
0,04	98,53
0,01	100,03
0,03	101,98
0,02	101,12
0,02	101,72
0,03	101,12
0,05	100,11
0,04	100,61
0,04	101,08
0,05	101,80
0,01	101,68
bd	100,49
0,02	101,04
0,06	101,65
bd	100,36
0,05	100,46
0,02	102,19
0,01	101,53
bd	101,61
0,02	101,43
0,03	101,64
0,05	101,64
0,02	101,72
bd	100,62
0,06	99,66
0,02	100,85
0,10	100,00
0,04	99,96
0,04	100,18
0,12	100,24
0,04	101,88
0,03	101,57
0,04	101,94
0,01	101,59
0,01	101,86
0,05	101,77
0,02	100,61
0,05	101,60



0,06	100,67
0,03	100,46
0,03	100,28
0,03	100,68
0,04	101,71
0,02	101,33
0,02	101,70
0,04	101,11
0,01	101,74
<u>0,02</u>	<u>101,36</u>

**Supplementary Table Pyroxene Analyses.**

Point	Session	En	Fs	Wo	SiO <sub>2</sub>	Al <sub>2</sub> O <sub>3</sub>	TiO <sub>2</sub>	Cr <sub>2</sub> O <sub>3</sub>	FeO	MnO	MgO	CaO	Na <sub>2</sub> O	Total
<b>NWA 8694 Melt Inclusion</b>														
10	121114	59,13	38,74	2,13	52,49	0,78	0,12	0,18	23,95	0,81	20,50	1,03	0,06	99,95
11	121114	59,50	39,14	1,36	53,38	1,72	-0,05	0,08	23,95	0,73	20,43	0,65	0,01	100,94
72	100215	59,49	38,22	2,28	53,16	1,14	0,20	0,10	23,43	0,75	20,46	1,09	0,08	100,40
74	121114	56,45	40,42	3,14	50,22	3,63	0,39	0,09	24,16	0,72	18,93	1,46	0,05	99,58
74	100215	64,17	34,77	1,07	52,93	0,90	0,08	0,04	21,47	0,64	22,22	0,51	0,05	98,82
76	121114	56,10	41,14	2,77	50,00	4,56	0,49	0,06	24,34	0,68	18,62	1,28	0,03	100,05
77	121114	56,45	41,07	2,48	51,48	3,81	0,39	0,18	24,48	0,70	18,88	1,15	0,03	101,22
81	100215	28,95	25,21	45,83	51,48	2,81	0,84	0,04	14,47	0,30	9,32	20,53	0,80	100,71
104	100215	59,10	38,64	2,25	53,78	0,72	0,16	0,14	24,38	0,74	20,92	1,11	0,04	102,02
107	100215	59,51	37,77	2,73	52,49	0,63	0,17	0,02	23,42	0,81	20,71	1,32	0,06	99,57
108	100215	61,46	37,37	1,18	52,73	0,46	0,11	0,00	23,51	0,67	21,69	0,58	0,14	99,88
<b>NWA 8694 Mesostasis</b>														
122	100215	63,06	36,50	0,44	53,98	0,22	-0,01	0,04	23,22	0,83	22,51	0,22	-0,02	100,98
125	100215	58,57	40,09	1,34	51,23	1,19	0,06	0,02	25,08	0,78	20,55	0,66	0,04	99,59
50	121114	59,85	38,67	1,48	54,16	0,14	-0,01	0,03	24,04	0,89	20,87	0,72	-0,02	100,88
56	121114	60,28	37,04	2,68	54,18	0,33	0,18	0,12	23,28	0,75	21,25	1,32	0,02	101,39
51	121114	59,52	37,46	3,02	52,92	0,80	0,20	0,22	22,93	0,70	20,44	1,44	0,01	99,72
80	121114	59,88	36,39	3,73	54,28	0,38	0,36	0,14	22,59	0,69	20,85	1,81	0,02	101,19
43	121114	59,26	36,93	3,81	54,09	0,28	0,15	0,15	22,92	0,82	20,63	1,84	0,02	100,84
83	121114	59,74	36,13	4,13	53,96	0,49	0,21	0,23	22,57	0,73	20,93	2,01	0,03	101,23
67	100215	56,64	38,93	4,43	53,32	0,35	0,28	0,16	24,02	0,81	19,60	2,13	0,04	100,62
119	100215	58,93	36,55	4,52	53,75	0,42	0,22	0,16	23,10	0,87	20,89	2,23	0,06	101,72
99	100215	58,07	37,18	4,76	53,42	0,40	0,17	0,42	23,02	0,92	20,17	2,30	0,06	100,85
68	100215	58,86	36,34	4,80	53,87	0,32	0,27	0,13	22,74	0,78	20,66	2,35	0,02	101,24
70	100215	57,78	37,14	5,08	52,57	0,40	0,23	0,15	22,94	0,78	20,02	2,45	0,04	99,60
44	121114	56,48	37,53	5,99	53,51	0,39	0,47	0,13	23,15	0,86	19,54	2,88	0,09	100,97
112	100215	55,95	35,28	8,77	51,70	0,49	0,28	0,22	21,77	0,78	19,37	4,22	0,09	98,91
113	100215	55,29	35,12	9,60	52,74	0,45	0,31	0,16	21,63	0,79	19,10	4,61	0,07	99,96
101	100215	43,97	22,60	33,43	51,59	1,22	0,25	0,57	13,75	0,46	15,00	15,87	0,33	99,05
116	100215	41,42	20,66	37,92	50,76	1,44	0,34	0,75	12,32	0,50	13,85	17,64	0,31	97,98
71	100215	41,86	17,13	41,01	52,74	0,46	0,33	0,31	10,51	0,44	14,41	19,64	0,28	99,05
82	121114	42,24	16,49	41,26	54,29	0,60	0,15	0,28	10,35	0,42	14,88	20,22	0,27	101,46
42	121114	40,43	16,83	42,74	54,47	0,77	0,24	0,50	10,41	0,43	14,03	20,64	0,35	101,87
53	121114	40,76	15,80	43,43	53,41	0,65	0,22	0,37	9,78	0,32	14,15	20,97	0,31	100,21
<b>NWA 8694 Poikilitic</b>														
66	121114	57,23	39,33	3,44	52,95	0,74	0,20	0,35	24,20	0,81	19,75	1,65	0,00	100,61
68	121114	58,45	37,85	3,69	53,76	0,64	0,13	0,32	23,35	0,79	20,23	1,78	0,05	101,01
27	121114	56,15	39,07	4,78	53,52	0,53	0,20	0,31	24,34	0,82	19,63	2,33	0,05	101,70
35	121114	55,94	39,14	4,92	53,77	0,52	0,12	0,23	24,62	0,80	19,73	2,41	0,04	102,28
29	121114	55,81	38,71	5,48	53,55	0,54	0,17	0,30	23,97	0,74	19,39	2,65	0,05	101,33
25	121114	55,65	38,03	6,32	53,48	0,52	0,12	0,30	23,83	0,78	19,56	3,09	0,06	101,75
27	121114	55,95	37,66	6,39	53,66	0,58	0,13	0,29	23,44	0,77	19,54	3,10	0,05	101,54
26	121114	54,69	36,93	8,39	53,36	0,56	0,21	0,35	23,22	0,69	19,29	4,12	0,06	101,84
15	121114	54,71	35,29	10,01	52,89	0,69	0,19	0,39	21,86	0,69	19,01	4,84	0,09	100,68
24	121114	47,42	25,91	26,66	53,87	1,09	0,24	0,73	15,85	0,52	16,27	12,73	0,29	101,55
92	121114	43,89	24,52	31,59	53,11	1,13	0,29	0,58	15,00	0,53	15,06	15,08	0,29	101,00
93	121114	43,69	24,19	32,11	53,28	1,05	0,26	0,67	14,78	0,55	14,98	15,31	0,30	101,13
30	121114	43,00	22,26	34,74	53,56	1,02	0,22	0,61	13,43	0,51	14,56	16,36	0,25	100,56
69	121114	41,46	22,04	36,50	52,37	1,31	0,31	0,75	13,33	0,47	14,07	17,23	0,31	100,37
36	121114	41,24	21,23	37,53	52,85	1,87	0,40	0,68	12,83	0,51	13,99	17,71	0,33	101,20
67	121114	40,67	15,74	43,59	53,83	1,01	0,23	0,40	9,74	0,36	14,11	21,05	0,34	101,06
97/7	121114	56,50	37,41	6,09	53,29	0,41	0,24	0,15	22,86	0,82	19,37	2,90	0,08	100,11
97/8	121114	57,16	37,33	5,50	53,63	0,38	0,29	0,13	22,65	0,86	19,46	2,61	0,06	100,09
97/9	121114	56,41	35,69	7,90	53,61	0,85	0,23	0,15	21,45	0,76	19,02	3,71	0,23	99,97
97/10	121114	54,49	36,14	9,37	52,71	4,43	0,21	0,13	19,17	0,63	16,21	3,88	1,34	98,90
97/36	121114	56,09	38,79	5,12	52,07	0,41	0,35	0,17	22,82	0,83	18,52	2,35	0,04	97,67
97/37	121114	55,49	38,61	5,90	52,50	0,43	0,34	0,17	22,74	0,80	18,34	2,72	0,06	98,14
97/38	121114	55,74	37,07	7,19	52,17	0,42	0,23	0,16	22,14	0,74	18,68	3,35	0,05	97,97
97/39	121114	56,03	36,91	7,05	52,91	0,35	0,37	0,11	22,27	0,78	18,97	3,32	0,07	99,24
97/40	121114	56,20	36,99	6,81	53,07	0,40	0,33	0,16	22,51	0,78	19,19	3,23	0,07	99,73

97/41	121114	56,82	37,51	5,67	53,03	0,43	0,42	0,13	22,66	0,80	19,26	2,67	0,07	99,46
97/42	121114	56,06	37,45	6,49	52,88	0,41	0,41	0,20	22,85	0,85	19,18	3,09	0,06	99,92
97/43	121114	55,78	37,08	7,13	53,04	0,42	0,41	0,20	22,83	0,81	19,26	3,43	0,07	100,47
97/45	121114	55,36	37,27	7,36	51,79	0,44	0,33	0,19	22,29	0,81	18,57	3,44	0,07	98,03
97/46	121114	54,53	37,72	7,75	52,45	0,43	0,31	0,21	22,16	0,77	17,97	3,56	0,10	98,20
97/55	121114	57,16	37,16	5,68	52,65	0,51	0,39	0,17	23,33	0,89	20,13	2,78	0,04	100,84
97/58	121114	54,48	39,65	5,86	52,13	0,72	0,29	0,19	22,59	0,79	17,41	2,61	0,17	97,02
97/59	121114	56,17	37,52	6,31	53,01	0,39	0,21	0,20	22,74	0,81	19,09	2,99	0,08	99,54

**Chassigny Interstitial-poikilitic**

60	191018	67,47	27,90	4,63	55,23	0,29	0,13	0,27	17,72	0,57	24,03	2,29	0,02	100,58
61	191018	67,16	27,95	4,89	55,23	0,45	0,16	0,32	17,83	0,58	24,04	2,44	0,08	101,13
63	191018	66,71	28,44	4,85	55,08	0,47	0,13	0,27	18,27	0,61	24,04	2,43	0,04	101,36
65	191018	66,95	28,08	4,97	55,06	0,43	0,14	0,24	17,85	0,57	23,88	2,47	0,05	100,70
66	191018	66,69	28,49	4,82	55,02	0,40	0,13	0,26	17,99	0,60	23,62	2,38	0,08	100,47
67	191018	66,76	28,40	4,84	55,10	0,38	0,12	0,22	18,03	0,59	23,77	2,40	0,05	100,66
48	191018	62,44	23,80	13,76	55,08	0,70	0,14	0,42	15,14	0,48	22,28	6,83	0,14	101,21
50	191018	63,08	24,44	12,49	55,26	0,71	0,20	0,48	15,52	0,55	22,47	6,19	0,15	101,52
57	191018	60,56	24,02	15,42	55,11	0,78	0,20	0,53	15,28	0,49	21,62	7,66	0,18	101,85
68	191018	60,22	21,84	17,94	54,27	0,97	0,21	0,54	13,77	0,46	21,31	8,83	0,28	100,65
52	191018	47,13	15,17	37,70	53,13	1,13	0,29	0,76	9,47	0,33	16,50	18,37	0,32	100,31
53	191018	47,44	15,25	37,31	53,47	1,09	0,26	0,78	9,40	0,28	16,42	17,96	0,24	99,91
54	191018	47,16	14,98	37,86	53,98	1,07	0,28	0,81	9,40	0,29	16,61	18,55	0,25	101,25
55	191018	46,25	14,21	39,54	54,00	1,45	0,40	0,84	8,82	0,28	16,11	19,16	0,32	101,39
56	191018	46,39	14,66	38,95	53,43	1,50	0,39	0,84	9,13	0,32	16,21	18,93	0,31	101,07
59/1	191018	46,69	14,67	38,64	53,69	1,31	0,31	0,83	9,09	0,32	16,23	18,69	0,34	100,80
59/2	191018	46,76	14,92	38,32	54,00	1,26	0,36	0,78	9,28	0,32	16,31	18,60	0,31	101,23
59/3	191018	46,38	14,70	38,92	54,83	1,24	0,32	0,83	9,25	0,29	16,37	19,12	0,31	102,57
59/5	191018	45,70	15,65	38,65	54,50	1,41	0,33	0,82	9,89	0,29	16,20	19,06	0,30	102,80
59/6	191018	46,45	14,93	38,62	54,21	1,30	0,30	0,79	9,26	0,30	16,16	18,69	0,28	101,29
59/7	191018	45,94	15,55	38,51	53,41	1,19	0,38	0,79	9,74	0,28	16,15	18,83	0,27	101,07
59/8	191018	46,72	15,20	38,09	53,70	1,28	0,33	0,80	9,50	0,32	16,38	18,58	0,31	101,18
59/9	191018	46,31	14,88	38,81	54,20	1,33	0,30	0,78	9,32	0,35	16,27	18,97	0,32	101,85
59/10	191018	46,06	14,98	38,96	53,52	1,29	0,33	0,80	9,42	0,32	16,24	19,11	0,29	101,32
59/11	191018	46,38	14,85	38,78	54,14	1,26	0,31	0,81	9,29	0,33	16,29	18,95	0,33	101,70
59/12	191018	46,91	14,66	38,42	53,77	1,25	0,30	0,78	9,21	0,36	16,52	18,83	0,27	101,28
59/13	191018	46,59	14,94	38,47	54,87	1,32	0,30	0,82	9,33	0,31	16,33	18,76	0,31	102,37
59/14	191018	47,12	14,73	38,15	53,47	1,33	0,33	0,79	9,17	0,30	16,46	18,54	0,34	100,73
59/16	191018	47,43	14,87	37,70	53,06	1,24	0,30	0,73	9,40	0,31	16,82	18,60	0,27	100,76
59/19	191018	46,34	15,54	38,12	53,92	1,19	0,34	0,79	9,81	0,32	16,41	18,78	0,31	101,90
59/20	191018	47,53	15,21	37,26	53,86	1,23	0,34	0,80	9,47	0,33	16,60	18,11	0,34	101,07
59/21	191018	47,10	15,45	37,44	54,13	1,27	0,32	0,73	9,64	0,30	16,49	18,24	0,28	101,42
59/22	191018	46,73	15,15	38,12	52,95	1,27	0,33	0,79	9,44	0,33	16,35	18,55	0,27	100,29
59/23	191018	47,13	15,13	37,74	53,97	1,22	0,28	0,79	9,48	0,33	16,56	18,45	0,33	101,41
59/24	191018	47,23	15,19	37,58	54,10	1,26	0,32	0,81	9,46	0,34	16,50	18,26	0,28	101,36
59/25	191018	47,06	15,86	37,07	53,79	1,25	0,30	0,72	9,96	0,32	16,58	18,17	0,28	101,39
59/26	191018	46,97	15,14	37,89	53,87	1,21	0,38	0,83	9,55	0,33	16,62	18,65	0,31	101,76
59/27	191018	46,39	15,45	38,16	53,89	1,29	0,29	0,79	9,62	0,33	16,20	18,54	0,30	101,26
59/28	191018	47,20	14,93	37,87	53,11	1,26	0,31	0,77	9,28	0,34	16,45	18,37	0,32	100,21
59/29	191018	46,71	15,54	37,75	53,95	1,24	0,29	0,82	9,73	0,31	16,41	18,46	0,26	101,48
59/30	191018	46,70	15,36	37,95	53,61	1,39	0,35	0,79	9,56	0,33	16,31	18,44	0,29	101,10
59/31	191018	46,11	15,60	38,29	52,65	1,35	0,34	0,78	9,45	0,34	15,68	18,12	0,34	99,06
59/32	191018	46,81	14,98	38,21	53,66	1,32	0,39	0,76	9,27	0,32	16,26	18,46	0,33	100,79
59/33	191018	47,15	15,23	37,63	52,94	1,45	0,31	0,84	9,52	0,31	16,54	18,37	0,33	100,62
59/34	191018	46,54	15,75	37,71	53,37	1,37	0,36	0,79	9,67	0,31	16,03	18,07	0,34	100,33

**NWA 2737 interstitial-poikilitic**

137	181217	77,66	19,57	2,77	56,22	0,64	0,47	0,25	12,95	0,33	28,85	1,44	0,09	101,26
141	181217	78,40	18,62	2,98	56,43	0,38	0,40	0,19	12,29	0,42	29,01	1,53	0,04	100,82
51	181217	71,16	17,82	11,02	55,82	0,51	0,15	0,47	11,63	0,39	26,05	5,60	0,18	101,03
55	181217	72,94	18,77	8,30	55,76	0,47	0,11	0,34	12,52	0,41	27,31	4,31	0,15	101,38
58	181217	70,01	17,02	12,97	55,86	0,60	0,11	0,68	11,01	0,41	25,38	6,53	0,25	100,84
60	181217	75,37	18,06	6,57	56,70	0,38	0,10	0,36	11,96	0,45	27,98	3,39	0,13	101,44
63	181217	74,73	19,14	6,13	56,19	0,62	0,08	0,36	12,71	0,46	27,81	3,17	0,07	101,51
79	181217	74,00	19,54	6,46	55,24	0,45	0,14	0,35	12,94	0,41	27,53	3,34	0,11	100,59

80	181217	74,10	19,80	6,11	55,16	0,43	0,10	0,33	12,98	0,54	27,26	3,13	0,13	100,29
81/59	181217	75,18	19,63	5,18	54,79	1,41	0,16	0,46	12,39	0,35	26,64	2,56	0,15	98,92
99/46	181217	76,75	17,31	5,94	55,67	0,41	0,14	0,77	11,49	0,35	28,60	3,09	0,09	100,61
99/47	181217	76,60	18,01	5,39	54,55	0,78	0,18	0,69	11,79	0,40	28,09	2,75	0,11	99,36
99/48	181217	71,79	16,80	11,41	55,18	0,54	0,16	0,65	11,07	0,42	26,50	5,84	0,20	100,57
99/49	181217	75,27	18,72	6,02	55,40	0,50	0,12	0,55	12,45	0,41	28,07	3,12	0,10	100,72
99/50	181217	75,15	18,19	6,66	55,34	0,44	0,13	0,54	11,96	0,37	27,73	3,41	0,10	100,02
99/51	181217	75,66	18,74	5,60	54,43	1,16	0,10	0,47	12,23	0,38	27,70	2,86	0,04	99,40
75	181217	50,92	10,74	38,34	53,75	1,01	0,21	0,84	6,86	0,26	18,26	19,14	0,35	100,69
76	181217	51,17	11,17	37,66	54,36	1,01	0,35	0,91	7,13	0,31	18,29	18,73	0,35	101,45
145/19	181217	51,13	11,05	37,82	54,61	1,00	0,31	0,90	6,97	0,26	18,10	18,64	0,38	101,17
145/20	181217	52,38	12,11	35,51	54,80	1,08	0,21	0,85	7,71	0,30	18,66	17,61	0,33	101,55
145/21	181217	50,79	11,29	37,92	54,65	1,05	0,23	0,93	7,08	0,25	17,90	18,59	0,33	101,03
145/23	181217	49,22	10,16	40,62	52,56	1,04	0,25	0,89	6,27	0,27	17,08	19,61	0,34	98,30
145/25	181217	50,73	10,70	38,58	54,49	1,03	0,30	1,00	6,83	0,21	18,18	19,24	0,33	101,63
145/26	181217	51,36	10,25	38,39	54,19	0,99	0,23	0,98	6,42	0,20	18,04	18,77	0,31	100,17
145/28	181217	53,13	11,77	35,10	54,75	0,98	0,28	0,90	7,48	0,22	18,99	17,45	0,32	101,37
145/29	181217	50,41	10,68	38,90	54,33	0,98	0,26	0,97	6,80	0,30	18,00	19,32	0,29	101,26
145/30	181217	55,60	12,82	31,58	54,96	0,98	0,28	0,76	8,16	0,23	19,85	15,70	0,27	101,19
145/31	181217	50,10	10,47	39,42	54,63	0,98	0,31	0,95	6,61	0,20	17,74	19,41	0,35	101,21
145/32	181217	49,58	10,52	39,90	54,70	0,96	0,25	1,01	6,66	0,36	17,57	19,68	0,29	101,48
145/33	181217	50,81	10,55	38,64	54,20	0,97	0,28	0,96	6,63	0,30	17,92	18,97	0,28	100,55
145/34	181217	55,96	13,32	30,72	54,98	0,97	0,27	0,83	8,46	0,29	19,91	15,21	0,19	101,10
145/35	181217	52,91	12,11	34,98	53,80	1,16	0,24	0,80	7,65	0,40	18,72	17,22	0,27	100,30
145/36	181217	51,29	10,45	38,26	54,46	1,40	0,26	0,95	6,54	0,27	18,02	18,69	0,34	100,97
145/41	181217	53,00	11,89	35,11	54,51	1,00	0,32	0,88	7,65	0,25	19,10	17,61	0,35	101,67
145/42	181217	49,55	9,93	40,52	54,70	1,04	0,29	0,96	6,18	0,25	17,33	19,72	0,36	100,82
145/43	181217	50,55	9,65	39,80	54,35	1,05	0,30	1,02	6,04	0,24	17,78	19,48	0,34	100,60
145/44	181217	50,34	10,88	38,79	54,35	1,11	0,28	0,96	6,97	0,18	18,07	19,37	0,35	101,63
145/45	181217	52,07	11,04	36,89	54,25	0,92	0,26	0,90	6,90	0,27	18,27	18,02	0,32	100,11
145/46	181217	51,90	10,95	37,14	54,58	1,03	0,29	0,97	6,96	0,26	18,47	18,40	0,32	101,30
145/47	181217	49,63	10,03	40,33	54,30	1,11	0,34	1,01	6,34	0,28	17,60	19,91	0,36	101,25
145/48	181217	51,64	10,90	37,45	54,45	1,02	0,29	0,96	6,88	0,23	18,31	18,48	0,29	100,90
145/49	181217	49,50	10,07	40,43	53,82	1,04	0,30	0,98	6,32	0,20	17,40	19,77	0,37	100,23
145/51	181217	50,31	9,99	39,70	54,38	1,04	0,31	0,94	6,34	0,27	17,91	19,68	0,31	101,17
145/52	181217	52,43	11,46	36,11	54,56	0,95	0,27	0,89	7,23	0,26	18,52	17,74	0,32	100,77
145/53	181217	51,52	10,53	37,95	53,88	1,03	0,31	0,92	6,74	0,25	18,44	18,91	0,39	100,87
145/55	181217	50,60	10,39	39,01	54,21	1,03	0,29	0,96	6,60	0,21	18,01	19,33	0,32	100,97
145/56	181217	51,65	11,07	37,28	54,25	0,95	0,26	0,91	7,05	0,24	18,51	18,59	0,32	101,09
145/57	181217	50,65	9,93	39,41	54,24	1,11	0,26	0,90	6,23	0,21	17,86	19,34	0,36	100,51
145/58	181217	52,32	11,78	35,90	54,38	1,06	0,28	0,88	7,46	0,33	18,61	17,78	0,33	101,14
145/59	181217	50,94	10,02	39,03	53,36	1,58	0,26	0,89	6,20	0,26	17,71	18,90	0,30	99,45
145/60	181217	52,95	11,63	35,42	53,81	1,31	0,28	0,91	7,33	0,30	18,69	17,38	0,34	100,37
145/62	181217	50,94	10,48	38,58	53,88	1,47	0,30	0,94	6,64	0,29	18,09	19,08	0,38	101,12

**Supplementary Table Chromite Analyses**

Point	Sesssion	Spin	Chrom	Usp	Mgt	SiO2	Al2O3	TiO2
<b>NWA 8694</b>								
18	121114	12,46	75,33	4,52	7,26	0,12	5,82	1,65
19	121114	11,96	75,94	4,54	7,32	0,07	5,59	1,66
16	161219	13,00	72,93	5,41	8,19	0,13	6,12	1,99
17	161219	13,16	73,43	5,70	7,44	0,08	6,17	2,09
25	161219	14,55	72,72	5,82	6,62	0,08	6,91	2,16
24	161219	14,50	70,78	7,30	7,19	0,06	6,92	2,73
46	161219	15,14	68,62	7,91	8,55	-0,06	7,16	2,93
23	161219	14,75	69,65	8,26	6,84	0,14	7,14	3,13
28	161219	15,07	67,06	8,52	8,94	0,11	7,19	3,18
26	161219	17,22	65,01	8,78	9,00	0,00	8,20	3,28
17	121114	14,69	67,88	8,94	8,21	0,08	6,91	3,29
45	161219	18,08	63,66	9,33	8,36	0,16	8,57	3,47
100	110215	16,39	63,87	10,12	9,31	0,09	7,74	3,75
40	161219	16,25	64,20	10,41	8,51	0,17	7,66	3,84
43	161219	17,66	61,27	10,69	10,30	0,02	8,47	4,02
41	161219	16,55	60,20	11,03	10,28	0,54	7,87	4,11
28	121114	20,75	58,16	11,52	9,06	0,14	9,83	4,28
42	161219	16,96	61,88	11,88	8,81	0,13	8,08	4,43
27	161219	14,77	63,73	12,10	8,98	0,11	7,00	4,50
86	121114	16,80	59,72	12,46	10,82	0,06	7,85	4,56
19	161219	17,47	61,05	12,48	8,77	0,07	8,39	4,70
37	161219	18,52	59,25	12,74	9,26	0,07	8,86	4,77
22	161219	15,29	60,74	12,95	10,55	0,13	7,20	4,78
38	161219	15,66	60,67	13,17	10,18	0,09	7,37	4,85
21	161219	16,32	59,17	13,20	11,12	0,06	7,80	4,94
44	161219	16,71	58,02	13,86	11,33	0,02	7,93	5,15
20	161219	15,80	59,59	14,37	10,02	0,06	7,56	5,39
29	161219	13,86	58,40	16,71	11,26	bd	6,47	6,12
30	161219	12,53	57,27	18,35	11,74	bd	5,85	6,71
39	161219	11,08	58,41	19,54	11,06	bd	5,12	7,08
<b>Chassigny</b>								
12	200913	17,11	71,77	5,75	5,21	0,04	8,14	2,14
9	200913	19,22	67,65	6,74	6,24	0,05	9,29	2,55
7	200913	21,02	63,40	9,22	6,19	0,05	10,16	3,49
10	200913	20,17	67,23	6,84	5,56	0,06	9,74	2,59
6	200913	12,74	77,48	3,53	5,98	0,08	6,10	1,32
23	111213	12,75	77,48	3,71	5,48	0,16	6,02	1,37
<b>NWA 2737</b>								
52	2737	15,01	74,83	4,17	5,44	0,09	7,44	1,61
53	2737	13,16	78,80	3,13	4,07	0,11	6,49	1,21
57	2737	14,57	75,09	3,88	6,05	0,05	7,17	1,48
62	2737	12,97	78,63	3,13	4,85	0,07	6,39	1,20
65	2737	20,73	69,72	3,54	5,45	0,07	10,27	1,38
70	2737	13,15	79,09	3,06	4,57	0,03	6,45	1,18
71	2737	15,41	62,01	13,67	8,64	0,04	7,40	5,14
73	2737	16,32	74,28	4,48	4,91	0,46	8,03	1,73

78	2737	20,29	69,46	4,17	5,66	0,05	9,87	1,58
81/41	2737	19,04	68,79	5,00	6,89	0,05	9,49	1,95
81/42	2737	17,53	71,53	4,58	6,09	0,04	8,70	1,79
81/43	2737	16,02	74,10	4,10	5,50	0,05	7,91	1,59
81/44	2737	14,95	76,34	3,82	4,75	0,01	7,30	1,46
81/45	2737	14,79	77,07	3,55	4,59	0,01	7,20	1,36
81/46	2737	14,30	77,64	3,83	3,95	0,04	7,00	1,46
81/47	2737	13,99	77,05	3,61	5,07	0,04	6,90	1,38
81/48	2737	13,59	78,22	3,41	4,37	0,05	6,63	1,30
81/49	2737	13,25	77,86	3,40	5,48	-0,01	6,52	1,30
81/50	2737	13,57	78,06	3,34	4,62	0,06	6,62	1,29
81/51	2737	13,57	77,76	3,40	5,26	0,01	6,65	1,31
81/52	2737	13,48	77,99	3,54	4,98	-0,01	6,63	1,36
81/53	2737	13,88	78,15	3,34	4,49	0,01	6,76	1,27
81/54	2737	13,88	77,45	3,48	4,49	0,10	6,83	1,35
81/55	2737	14,35	76,82	3,75	4,52	0,07	7,01	1,44
81/56	2737	15,21	74,41	4,10	6,01	0,03	7,51	1,59
81/57	2737	16,26	72,24	4,51	6,44	0,08	8,03	1,73
81/98	2737	21,08	67,99	5,14	5,52	0,04	10,30	1,98
81/99	2737	20,95	67,70	4,72	5,79	0,12	10,32	1,83
98/1	2737	23,66	62,20	6,23	7,77	0,01	11,82	2,44
99/11	2737	18,13	70,27	3,88	7,16	0,09	8,93	1,51
99/12	2737	17,46	71,86	4,24	5,75	0,10	8,58	1,62
99/13	2737	16,72	72,57	4,09	6,34	0,04	8,28	1,57
99/14	2737	16,16	73,01	4,09	6,46	0,04	8,01	1,58
99/15	2737	16,23	73,40	4,09	6,14	0,02	8,01	1,58
99/16	2737	15,73	74,48	3,89	5,49	0,05	7,68	1,49
99/17	2737	15,67	74,13	4,10	5,82	0,05	7,70	1,58
99/18	2737	15,34	73,66	3,68	6,34	0,15	7,40	1,40
99/19	2737	17,35	70,72	3,53	0,05	1,15	8,10	1,29
99/20	2737	15,28	75,42	3,75	5,27	0,04	7,53	1,46
99/21	2737	14,93	75,68	3,68	5,29	0,05	7,37	1,42
99/22	2737	14,52	76,04	3,61	5,82	0,01	7,17	1,41
99/23	2737	14,06	75,99	3,75	5,92	0,04	6,90	1,43
99/24	2737	14,65	76,25	3,68	5,28	0,03	7,20	1,41
99/25	2737	14,41	76,09	3,68	5,67	0,01	7,13	1,42
99/26	2737	14,11	76,60	3,75	5,54	0,00	6,89	1,44
99/27	2737	14,43	76,72	3,48	5,10	0,04	7,09	1,34
99/28	2737	14,02	76,37	3,54	5,65	0,05	6,92	1,36
99/29	2737	13,95	76,44	3,40	6,07	0,01	6,89	1,30
99/30	2737	14,13	77,00	3,62	4,70	0,08	7,02	1,42
99/31	2737	13,57	77,17	3,47	5,37	0,05	6,63	1,32
99/32	2737	14,00	76,74	3,54	5,44	0,05	6,91	1,38
99/33	2737	13,74	76,65	3,40	5,79	0,06	6,75	1,31
99/34	2737	13,54	76,48	3,61	5,81	0,07	6,66	1,38
99/35	2737	14,19	76,06	3,48	6,27	0,18	6,96	1,34
99/36	2737	14,16	76,15	3,47	6,09	0,02	6,97	1,34
99/37	2737	13,75	76,48	3,61	5,88	0,05	6,73	1,37
99/38	2737	14,06	75,92	3,47	6,13	0,07	6,89	1,34
99/39	2737	13,72	76,04	3,81	6,43	-0,01	6,74	1,46

99/40	2737	14,64	75,10	3,75	6,51	0,00	7,25	1,45
99/41	2737	14,50	75,68	3,96	5,59	0,04	7,13	1,52
99/42	2737	14,98	74,12	4,02	6,60	0,03	7,40	1,57
99/43	2737	15,36	73,01	4,02	7,47	0,02	7,60	1,56
99/44	2737	15,08	72,92	4,23	7,49	0,05	7,34	1,61
144	2737	20,81	68,00	5,39	5,66	0,01	10,44	2,12
146	2737	16,24	75,75	4,39	3,06	0,07	8,01	1,69
147	2737	15,52	76,24	3,97	4,14	0,03	7,73	1,56

Cr2O3	FeO	Fe2O3	MnO	MgO	Total
52,46	35,19	1,07	nd	2,33	98,63
52,93	34,98	1,06	nd	2,45	98,74
51,14	30,00	6,04	0,42	2,62	98,45
51,31	30,15	5,46	0,37	2,51	98,14
51,46	31,00	4,92	0,36	2,32	99,21
50,37	31,65	5,38	0,44	2,28	99,84
48,33	31,46	6,33	0,26	2,32	98,72
50,27	32,77	5,19	0,44	2,18	101,27
47,68	32,55	6,68	0,36	2,07	99,82
46,15	32,20	6,72	0,36	2,21	99,11
47,59	37,09	1,12	nd	2,55	98,63
44,98	31,92	6,21	0,42	2,44	98,17
44,98	38,57	1,16	nd	2,47	98,75
45,10	32,75	6,28	0,39	2,09	98,29
43,80	32,35	7,73	0,45	2,59	99,43
42,66	33,16	7,65	0,40	2,40	98,79
41,06	40,42	1,21	nd	1,69	98,62
43,94	33,51	6,58	0,47	2,10	99,23
45,02	33,23	6,67	0,42	2,20	99,15
41,62	41,04	1,25	nd	1,80	98,18
43,74	33,21	6,60	0,46	2,52	99,70
42,23	33,12	6,94	0,21	2,65	98,85
42,67	33,63	7,79	0,35	2,07	98,63
42,55	33,26	7,51	0,48	2,17	98,29
42,16	33,91	8,32	0,43	2,16	99,78
41,03	33,67	8,42	0,41	2,25	98,87
42,52	33,72	7,51	0,44	2,51	99,72
40,67	34,45	8,24	0,39	1,97	98,25
39,85	35,28	8,58	0,49	1,79	98,59
40,25	35,91	8,01	0,37	1,47	98,19
50,88	32,47	0,97	nd	3,65	98,31
48,75	34,18	1,00	nd	3,64	99,46
45,70	35,17	1,03	nd	3,54	99,15
48,43	34,01	1,00	nd	3,49	99,32
55,31	31,77	0,94	nd	4,09	99,62
54,48	31,27	0,94	nd	3,95	98,19
55,30	29,22	0,84	nd	6,38	100,88
57,87	28,55	0,82	nd	5,99	101,04
55,03	30,24	0,87	nd	5,74	100,58
57,71	29,19	0,84	nd	5,73	101,13
51,54	31,32	0,90	nd	5,07	100,55
57,85	28,73	0,83	nd	5,70	100,77
44,46	34,92	1,03	nd	5,43	98,42
54,50	29,53	0,85	nd	5,67	100,77



50,34	31,52	0,92	nd	4,67	98,95
51,10	30,99	0,88	nd	6,13	100,59
52,89	30,24	0,86	nd	6,04	100,56
54,49	29,87	0,86	nd	5,80	100,57
55,58	28,95	0,84	nd	5,71	99,85
55,97	28,27	0,82	nd	5,84	99,47
56,64	28,60	0,83	nd	5,68	100,25
56,65	29,30	0,84	nd	5,85	100,96
56,87	28,51	0,83	nd	5,79	99,98
57,04	29,19	0,84	nd	5,84	100,72
56,84	28,45	0,83	nd	5,93	100,02
56,86	28,97	0,84	nd	5,84	100,48
57,12	28,74	0,83	nd	5,92	100,59
56,78	28,49	0,83	nd	5,71	99,85
56,78	29,06	0,84	nd	5,83	100,79
55,94	28,78	0,84	nd	5,85	99,93
54,82	29,77	0,85	nd	6,09	100,66
53,18	30,41	0,87	nd	6,06	100,36
49,51	31,60	0,92	nd	4,82	99,17
49,76	31,81	0,92	nd	5,15	99,91
46,31	33,87	0,96	nd	5,10	100,51
51,56	31,23	0,90	nd	5,69	99,91
52,66	30,80	0,89	nd	5,49	100,14
53,54	30,59	0,88	nd	5,78	100,68
53,96	30,93	0,89	nd	5,70	101,11
53,95	30,50	0,88	nd	5,62	100,56
54,28	29,57	0,86	nd	5,77	99,70
54,33	30,21	0,87	nd	5,65	100,39
52,99	28,10	0,83	nd	6,80	97,67
49,24	27,32	0,83	nd	6,89	94,82
55,39	30,01	0,86	nd	5,54	100,83
55,73	29,69	0,85	nd	5,82	100,93
55,95	29,78	0,86	nd	5,79	100,97
55,58	29,93	0,87	nd	5,74	100,49
55,88	29,56	0,85	nd	5,67	100,60
56,11	30,03	0,86	nd	5,71	101,27
55,69	29,42	0,86	nd	5,62	99,92
56,19	29,46	0,85	nd	5,66	100,63
56,14	29,75	0,86	nd	5,86	100,94
56,28	30,14	0,87	nd	5,70	101,19
56,96	29,86	0,85	nd	5,63	101,82
56,21	29,35	0,85	nd	5,75	100,16
56,46	29,77	0,86	nd	5,73	101,16
56,12	29,99	0,87	nd	5,68	100,78
56,10	30,22	0,87	nd	5,67	100,97
55,55	30,06	0,87	nd	5,60	100,56
55,90	29,84	0,86	nd	5,83	100,76
55,79	29,98	0,87	nd	5,60	100,39
55,48	30,04	0,87	nd	5,74	100,43
55,70	30,09	0,87	nd	5,78	100,63

55,34	30,28	0,87	nd	5,84	101,03
55,50	29,54	0,85	nd	5,92	100,50
54,62	30,43	0,87	nd	5,95	100,87
53,86	30,80	0,88	nd	6,04	100,76
52,96	30,68	0,89	nd	5,85	99,38
50,82	31,52	0,89	nd	5,51	101,31
55,70	28,84	0,83	nd	5,59	100,73
56,60	28,65	0,82	nd	6,08	101,47

Supplementary Table Feldspar Analyses.

S#	Type	An	Ab	Or	SiO2	Al2O3	TiO2	FeO	MgO	CaO	Na2O	K2O
<b>NWA 8694</b>												
13	180417	27,27	66,80	5,93	60,39	23,38	0,10	0,53	0,01	5,56	7,51	1,02
18	180417	27,03	65,88	7,09	60,01	23,06	0,04	0,37	bd	5,47	7,36	1,20
24	180417	26,85	65,89	7,26	59,27	22,96	bd	0,73	0,05	5,46	7,41	1,25
30	130417	26,51	64,30	9,19	60,98	23,38	0,01	0,39	0,06	5,45	7,30	1,59
67	180417	26,20	66,41	7,39	61,37	24,12	0,07	0,53	0,03	5,52	7,72	1,30
69	180417	25,26	69,24	5,50	61,89	24,23	0,08	0,86	0,03	5,32	8,07	0,98
56	180417	25,07	66,67	8,27	61,86	25,22	0,09	0,83	0,02	5,33	7,83	1,48
23	130417	25,06	70,28	4,65	61,66	24,75	0,07	0,57	bd	5,38	8,31	0,84
57	180417	25,00	66,18	8,82	61,04	23,70	0,06	0,70	0,29	5,06	7,38	1,50
45	180417	24,44	69,65	5,91	62,08	23,94	0,11	0,49	0,04	5,14	8,08	1,04
19	180417	24,44	67,20	8,37	61,08	22,69	0,08	0,70	0,03	4,91	7,48	1,42
22	130417	24,41	70,34	5,25	61,36	24,27	0,01	0,73	bd	5,07	8,09	0,91
29	130417	24,37	67,95	7,68	60,55	23,58	0,08	0,62	0,12	4,95	7,61	1,30
25	130417	24,29	71,51	4,21	62,11	24,13	0,03	0,68	bd	4,92	7,98	0,70
55	180417	23,48	70,32	6,19	62,44	24,35	0,08	0,91	0,05	5,03	8,35	1,11
68	180417	23,18	66,02	10,81	62,34	23,71	0,09	0,83	0,02	4,89	7,71	1,93
42	180417	22,05	71,65	6,30	63,10	23,35	0,05	0,57	0,01	4,63	8,30	1,10
46	180417	21,62	71,88	6,50	62,08	23,48	bd	0,69	0,02	4,45	8,20	1,14
65	180417	20,86	68,58	10,56	63,35	23,82	0,09	0,60	0,03	4,34	7,88	1,85
53	180417	18,93	75,33	5,73	63,42	23,04	0,13	0,34	0,06	3,90	8,58	1,00
50	180417	17,17	73,05	9,78	64,40	22,67	bd	0,89	bd	3,59	8,46	1,71
43	180417	15,97	73,15	10,87	64,95	22,42	0,05	0,36	bd	3,29	8,31	1,88
59	180417	14,29	75,13	10,58	65,35	22,59	0,08	0,49	bd	3,02	8,76	1,86
64	180417	14,78	67,68	17,55	64,02	21,74	bd	0,86	bd	3,07	7,74	3,04
60	180417	13,36	58,07	28,57	63,76	21,54	0,07	0,37	0,09	2,75	6,59	4,93
58	180417	7,37	45,00	47,63	65,15	20,77	0,11	0,48	0,07	1,52	5,15	8,28
52	180417	2,89	29,83	67,28	65,88	18,69	0,11	0,85	0,02	0,60	3,36	11,53
44	180417	2,27	27,01	70,72	65,81	19,61	0,14	0,53	bd	0,45	3,01	11,97
51	180417	0,53	24,47	75,00	65,57	19,23	0,12	0,67	bd	0,10	2,74	12,76
47	180417	1,15	20,08	78,77	64,67	19,16	0,02	0,47	0,01	0,23	2,30	13,73
63	180417	0,53	98,55	0,92	66,79	22,29	0,05	0,93	0,04	0,12	11,67	0,16
<b>Chassigny</b>												
55	190618	20,08	66,73	13,19	64,28	22,91	0,17	0,47	0,04	3,58	6,58	1,98
47	190618	19,86	64,76	15,38	63,75	22,72	0,11	0,97	0,03	3,40	6,14	2,21
67	190618	18,10	68,41	13,49	62,03	22,08	0,15	0,47	0,01	3,50	7,32	2,19
50	190618	17,58	68,68	13,74	64,25	23,29	0,10	0,50	0,02	3,18	6,87	2,09
49	190618	17,57	69,36	13,07	63,77	23,11	0,10	0,44	0,02	3,13	6,83	1,95
68	190618	17,37	68,37	14,26	62,72	22,33	0,11	0,57	0,04	3,43	7,46	2,37
60	190618	16,90	71,92	11,18	63,92	22,11	0,11	0,42	0,02	3,57	8,41	1,99
58	190618	15,82	70,89	13,29	62,53	21,42	0,11	0,49	0,12	3,21	7,94	2,26
57	190618	15,71	73,54	10,74	63,71	21,43	0,15	0,53	0,03	3,07	7,94	1,76
56	190618	15,37	65,90	18,72	64,70	21,72	0,08	0,56	0,04	2,75	6,51	2,81
64	190618	14,94	71,08	13,98	63,86	21,73	0,10	0,42	0,02	2,94	7,74	2,31
61	190618	14,89	71,52	13,59	62,49	21,79	0,14	0,35	0,01	3,08	8,17	2,36
53	190618	14,49	76,92	8,59	63,37	21,51	0,10	0,40	0,02	2,98	8,73	1,48
63	190618	14,40	69,89	15,71	63,21	21,64	0,07	0,47	bd	2,93	7,85	2,68
66	190618	14,31	72,31	13,38	63,39	21,42	0,11	0,42	0,05	2,84	7,92	2,23

59	190618	14,20	67,46	18,34	63,38	21,57	0,14	0,71	0,02	2,80	7,35	3,04
48	190618	14,14	73,71	12,16	63,37	22,04	0,16	0,39	0,03	2,77	7,99	2,00
65	190618	11,51	64,79	23,70	63,63	20,72	0,09	0,50	0,02	2,36	7,35	4,09
62	190618	11,40	59,57	29,03	63,15	21,05	0,17	0,35	0,03	2,31	6,68	4,95
54	190618	9,45	65,07	25,48	63,52	20,16	0,12	0,48	0,04	1,93	7,35	4,37

**NWA 2737**

138	181217	12,37	70,88	16,76	66,03	21,87	0,15	0,38	0,01	2,59	8,22	2,95
143	181217	9,72	73,53	16,75	64,30	21,75	0,10	0,68	0,21	2,08	8,75	3,03
140	181217	8,56	73,37	18,07	66,78	21,31	0,14	0,60	0,03	1,75	8,32	3,10
94	181217	6,09	75,93	17,98	66,09	21,06	0,16	0,62	0,06	1,21	8,36	3,02
93	181217	6,05	74,82	19,13	68,17	20,56	0,14	0,43	0,02	1,21	8,22	3,19
91	181217	5,80	75,17	19,03	66,97	20,54	0,16	0,42	0,01	1,21	8,56	3,29
95	181217	5,68	75,78	18,54	67,43	20,49	0,19	0,55	0,03	1,17	8,61	3,20
89	181217	5,44	74,90	19,65	66,73	20,83	0,18	0,41	0,02	1,15	8,65	3,45
96	181217	5,05	74,73	20,22	67,11	20,05	0,21	0,60	0,06	1,01	8,34	3,44
92	181217	5,03	74,44	20,53	67,72	19,85	0,15	0,25	0,01	0,98	8,11	3,41
49	181217	4,82	75,36	19,82	65,40	20,96	0,21	0,34	bd	1,01	8,75	3,49
87	181217	4,75	76,26	19,00	67,01	21,02	0,18	0,43	0,02	0,97	8,63	3,27
86	181217	4,74	76,32	18,95	67,04	20,86	0,17	0,29	0,01	0,99	8,90	3,36
47	181217	4,71	75,04	20,26	67,05	22,68	0,17	0,34	0,02	0,93	8,18	3,35
84	181217	4,58	75,28	20,14	68,29	20,42	0,12	0,40	0,02	0,91	8,40	3,42
85	181217	4,54	76,39	19,07	66,33	20,81	0,17	0,29	0,02	0,98	9,01	3,41
90	181217	4,51	76,33	19,15	66,98	20,47	0,16	0,48	0,01	0,92	8,51	3,26
88	181217	4,04	76,85	19,11	68,11	20,05	0,11	0,43	bd	0,84	8,77	3,32

---

---

**Total**

---

---

98,57  
97,56  
97,21  
99,24  
100,65  
101,64  
102,71  
101,66  
99,74  
101,36  
98,49  
100,46  
98,83  
100,61  
102,31  
101,54  
101,23  
100,37  
102,14  
100,57  
101,74  
101,26  
102,23  
100,56  
100,32  
101,54  
101,11  
101,52  
101,22  
100,65  
102,12  
  
100,00  
99,33  
97,74  
100,30  
99,43  
99,02  
100,57  
98,11  
98,66  
99,20  
99,13  
98,39  
98,59  
98,89  
98,40

99,04  
98,79  
98,83  
98,70  
98,02

102,29  
101,06  
102,08  
100,61  
102,05  
101,15  
101,62  
101,44  
100,84  
100,47  
100,19  
101,51  
101,56  
102,72  
102,03  
101,07  
100,77  
101,64

Supplementary Table Analyses of Glass in Melt Inclusions.

M.I.	Kcode	SiO2	Al2O3	FeO	MgO	CaO	Na2O	K2O	Cl	Total
<b>Al-poor</b>										
3	130417	67,23	21,17	1,39	0,32	0,42	10,10	0,03	nd	100,65
28	180417	72,51	16,53	0,72	0,02	0,10	9,10	0,06	0,06	99,41
39	180417	71,87	15,42	1,69	0,05	0,17	8,09	0,44	bd	97,81
40	180417	73,07	15,58	0,99	bd	0,20	7,26	0,54	0,02	97,82
<b>Al-rich</b>										
7	130417	64,28	20,93	1,19	bd	0,23	10,91	0,39	nd	98,02
26	180417	64,08	20,96	1,44	0,06	0,15	11,50	0,18	0,02	98,40
27	180417	64,74	21,45	1,19	0,15	0,89	11,10	0,08	0,02	99,68
32	130417	63,6	21,71	1,33	0,20	0,16	8,49	0,86	nd	96,64
33	130417	64,01	21,43	0,91	bd	0,28	9,40	0,29	nd	96,67
62	180417	67,49	21,88	0,91	bd	0,15	12,24	0,09	0,25	103,06
<b>K-rich</b>										
21	180417	71,02	14,30	1,04	bd	1,06	5,69	3,44	1,15	97,94
29	180417	68,92	15,38	0,90	0,02	2,24	5,14	3,96	1,29	98,23
30	180417	70,33	15,62	0,89	0,06	1,81	5,95	3,03	0,90	98,88
73	121114	71,95	16,79	0,50	bd	4,01	1,47	4,21	nd	99,01
78	100215	71,35	15,44	1,03	bd	1,31	4,27	4,81	1,18	99,47
80	100215	76,35	15,48	1,15	0,02	2,42	3,78	3,38	1,28	103,89
109	100215	70,24	16,43	0,88	0,02	2,58	3,78	5,20	1,38	100,53
<b>Cat-poor</b>										
8	130417	74,21	21,52	0,98	0,04	0,23	1,56	0,05	nd	98,94
45	121114	79,44	17,31	0,93	0,01	0,00	0,48	1,34	nd	99,53
46	121114	75,38	17,89	0,98	bd	1,69	0,54	1,50	nd	99,16
76	100215	72,82	23,05	1,09	bd	0,05	3,07	0,10	nd	100,25
79	100215	77,44	16,64	1,03	0,01	0,00	3,91	0,27	nd	99,42
105	100215	71,56	22,53	1,02	0,01	0,27	2,69	0,08	nd	98,48
110	100215	76,41	17,38	0,73	bd	0,03	3,88	0,31	nd	98,92

Table S2. All LA-ICP-MS analyses for NWA 8694 and Chassigny.

	olivine	olivine	olivine	olivine	olivine	pyroxene	pyroxene
	26-NWA8694	27-NWA8694	28-NWA8694	29-NWA8694	30-NWA8694	31-NWA8694	32-NWA8694
<b>Major elements (wt. %)</b>							
SiO <sub>2</sub>	35,3	35,1	35,1	35,4	35,2	52,2	52,6
Al <sub>2</sub> O <sub>3</sub>	0,02	0,02	0,05	0,02	0,02	0,74	0,66
TiO <sub>2</sub>	0,022	0,024	0,035	0,030	0,018	0,180	0,157
Cr <sub>2</sub> O <sub>3</sub>	0,018	0,017	0,186	0,020	0,019	0,853	0,408
FeOT	38,02	38,44	38,38	38,24	38,24	21,97	22,00
MnO	0,839	0,824	0,839	0,834	0,843	0,768	0,755
MgO	25,50	25,35	25,36	25,22	25,42	18,82	18,83
CaO	0,24	0,21	0,21	0,20	0,24	5,18	4,85
Na <sub>2</sub> O	0,01	0,02	0,02	0,02	0,02	0,13	0,14
K <sub>2</sub> O	0,003	0,004	0,007	0,006	0,006	0,012	0,011
P <sub>2</sub> O <sub>5</sub>	0,03	0,05	0,02	0,01	0,02	0,00	0,01
<b>Trace elements (ppm)</b>							
Li	3,7	5,0	5,2	3,9	4,7	4,1	3,8
Be	0,01	0,01	0,01	0,01	0,01	0,11	0,08
B	1,0	0,9	1,3	0,8	0,9	3,4	3,1
S	0,01	0,01	0,01	0,01	0,01	0,01	0,01
Sc	7,1	6,7	6,8	6,6	6,7	25,9	26,9
V	6	6	21	7	7	142	116
Cr	127	115	1274	134	132	5835	2793
Co	124	122	125	125	124	55	56
Ni	346	338	352	344	346	110	114
Cu	2	1	5	1	1	4	4
Zn	108	107	106	114	111	94	81
Ga	0,2	0,1	0,3	0,2	0,1	2,0	1,4
Ge	1,4	1,2	1,3	1,2	1,3	2,2	2,2
As	0,1	0,0	0,0	0,0	0,1	0,0	0,0
Se	0,1	0,1	0,0	0,1	0,0	0,0	0,0
Rb	0,1	0,1	0,2	0,2	0,2	0,4	0,3
Sr	3	3	4	3	2	10	9
Y	0,56	0,45	0,42	0,49	0,43	2,96	2,58
Zr	0,16	0,42	0,21	0,67	0,17	1,94	1,14
Nb	0,00	0,01	0,01	0,01	0,00	0,24	0,12
Mo	0,083	0,079	0,095	0,087	0,102	0,103	0,087
Ru							
Rh							
Pd							
Ag	0,001	0,001	0,002	0,001	0,001	0,002	0,002
Cd	0,111	0,071	0,082	0,170	0,214	0,105	0,089
In	0,004	0,003	0,004	0,005	0,005	0,009	0,008
Sn	0,024	0,019	0,017	0,019	0,022	0,036	0,028
Sb	0,00	0,00	0,00	0,01	0,02	0,00	0,00
Te	0,1	0,0	0,0	0,1	0,0	0,1	0,2
Cs	0,0	0,0	0,1	0,1	0,1	0,1	0,1



<b>Ba</b>	1	1	1	1	1	1	1
<b>La</b>	0,005	0,009	0,006	0,006	0,001	0,103	0,171
<b>Ce</b>	0,006	0,012	0,005	0,006	0,002	0,452	0,547
<b>Pr</b>	0,001	0,002	0,001	0,001	0,000	0,103	0,102
<b>Nd</b>	0,007	0,010	0,008	0,004	0,003	0,670	0,601
<b>Sm</b>	0,003	0,004	0,004	0,004	0,002	0,286	0,229
<b>Eu</b>	0,001	0,001	0,001	0,001	0,001	0,063	0,057
<b>Gd</b>	0,023	0,018	0,012	0,014	0,017	0,391	0,344
<b>Tb</b>	0,006	0,004	0,004	0,005	0,005	0,079	0,063
<b>Dy</b>	0,070	0,055	0,048	0,053	0,050	0,537	0,450
<b>Ho</b>	0,023	0,017	0,013	0,018	0,017	0,115	0,101
<b>Er</b>	0,082	0,065	0,065	0,077	0,064	0,343	0,292
<b>Tm</b>	0,015	0,013	0,011	0,013	0,012	0,045	0,043
<b>Yb</b>	0,101	0,098	0,087	0,097	0,079	0,291	0,263
<b>Lu</b>	0,019	0,017	0,018	0,018	0,016	0,045	0,044
<b>Hf</b>	0,004	0,011	0,007	0,014	0,005	0,065	0,048
<b>Ta</b>	0,000	0,000	0,001	0,001	0,000	0,007	0,003
<b>W</b>	0,005	0,003	0,008	0,003	0,003	0,019	0,029
Re							
Os							
Ir							
Pt							
Au							
<b>Tl</b>	0,001	0,001	0,002	0,001	0,001	0,003	0,003
<b>Pb</b>	0,303	0,093	0,219	0,110	0,055	0,223	0,192
<b>Bi</b>	0,003	0,002	0,002	0,004	0,005	0,003	0,001
<b>Th</b>	0,000	0,001	0,001	0,001	0,000	0,017	0,018
<b>U</b>	0,035	0,024	0,046	0,021	0,024	0,109	0,103

---

pyroxene pyroxene pyroxene mesostasis mesostasis mesostasis mesostasis mesostasis  
33-NWA869 34-NWA869 35-NWA869 36-NWA869 37-NWA869 38-NWA869 39-NWA869 40-NWA869

51,1	52,7	52,6	42,5	57,9	58,1	59,6	60,5
0,64	0,65	0,64	5,74	21,72	19,84	23,84	23,77
0,146	0,150	0,155	0,072	0,073	0,055	0,078	0,076
0,373	0,338	0,411	0,009	0,003	0,002	0,001	0,001
22,69	22,87	21,85	27,34	4,40	2,65	0,55	0,24
0,765	0,792	0,771	0,598	0,063	0,050	0,009	0,006
19,14	19,18	18,88	18,14	1,77	1,25	0,35	0,28
5,33	3,51	4,96	2,17	4,50	5,44	4,89	4,62
0,16	0,12	0,13	2,21	7,46	7,18	9,04	8,42
0,020	0,024	0,019	0,441	1,82	3,35	1,50	2,04
0,01	0,01	0,01	0,82	0,34	2,04	0,12	0,11
3,6	3,8	3,8	15,0	34,4	35,4	119,8	105,2
0,13	0,08	0,07	0,40	1,10	1,06	1,17	1,14
3,3	4,1	2,9	5,0	8,1	7,8	3,1	4,9
0,01	0,01	0,01	0,03	0,92	0,02	0,00	-0,01
25,7	23,4	27,1	6,0	4,5	4,6	8,8	5,6
109	94	119	3	1	1	1	1
2552	2315	2810	63	18	11	7	7
59	56	54	85	156	16	1	0
126	113	108	261	100	42	67	56
5	8	3	16	22	8	4	4
78	88	81	88	15	12	4	3
1,4	1,5	1,3	4,8	15,3	15,9	16,7	17,2
2,1	2,2	2,4	1,3	0,9	0,6	-0,4	-0,3
0,0	0,0	0,0	0,0	-0,1	-0,2	-0,1	-0,8
0,0	0,0	0,0	0,0	2,4	0,2	-1,3	-0,2
0,8	1,0	0,9	8,1	42,5	73,7	24,4	33,6
12	12	9	196	601	681	761	765
3,46	2,44	2,48	4,19	2,23	11,01	0,21	0,48
3,83	2,94	1,64	2,13	13,58	2,86	0,30	14,11
0,46	0,53	0,18	5,53	2,06	0,36	0,09	2,79
0,089	0,118	0,085	0,204	0,423	0,367	1,256	0,973
0,031	0,002	0,003	0,011	0,032	0,057	-0,011	0,065
0,099	0,115	0,077	0,044	0,101	0,040	0,250	0,246
0,040	0,007	0,008	0,010	0,013	0,012	0,123	0,035
0,052	0,047	0,037	0,179	0,198	0,565	0,186	0,218
0,00	0,00	0,00	0,00	-0,04	-0,04	-0,27	-0,17
0,1	0,1	0,1	0,6	0,5	0,2	-0,1	0,0
0,1	0,1	0,1	0,7	2,3	2,5	6,0	4,9

1	3	1	106	350	538	442	559
0,393	0,198	0,071	11,98	9,89	38,03	3,39	3,84
1,362	0,529	0,289	23,60	17,40	81,14	4,94	5,65
0,250	0,098	0,073	3,06	2,01	10,57	0,43	0,71
1,425	0,530	0,471	12,93	8,12	41,78	1,50	2,55
0,435	0,195	0,211	2,12	1,34	6,74	0,16	0,29
0,084	0,043	0,052	0,63	1,63	2,18	1,89	2,02
0,542	0,290	0,313	1,72	0,96	5,29	0,12	0,33
0,097	0,057	0,059	0,202	0,125	0,598	0,016	0,034
0,654	0,419	0,429	1,001	0,607	2,852	0,024	0,335
0,133	0,097	0,097	0,167	0,072	0,437	0,009	0,028
0,376	0,287	0,289	0,362	0,152	0,845	0,003	0,069
0,052	0,037	0,040	0,035	0,025	0,082	0,001	0,005
0,295	0,256	0,260	0,174	0,069	0,264	0,006	0,023
0,045	0,042	0,041	0,027	0,011	0,034	0,023	-0,004
0,113	0,074	0,052	0,051	0,417	0,071	0,011	0,386
0,015	0,029	0,013	0,280	0,191	0,043	0,005	0,144
0,043	0,083	0,032	0,569	0,150	1,392	0,011	0,555

0,004	0,004	0,003	0,012	0,032	0,030	0,008	-0,008
0,365	0,281	0,119	2,528	6,667	9,217	4,639	6,806
0,002	0,001	0,002	0,001	0,002	0,005	-0,001	0,009
0,046	0,050	0,027	1,378	0,996	3,137	0,043	0,434
0,098	0,111	0,091	0,264	0,183	0,655	0,019	0,082

---

mesostasis mesostasis mesostasis mesostasis mesostasis mesostasis mesos (phos) track  
 41-NWA869 42-NWA869 43-NWA869 44-NWA869 45-NWA869 46-NWA869 47-NWA869 48-NWA869

59,2	58,3	61,7	52,7	58,6	59,5	47,5	33,2
22,96	19,92	18,97	15,17	23,78	24,04	15,91	12,82
0,086	0,046	0,093	0,087	0,046	0,071	0,030	1,281
0,001	0,003	0,001	0,052	0,002	0,000	0,000	0,308
1,36	3,42	2,99	11,19	2,42	0,22	1,93	23,18
0,027	0,067	0,061	0,278	0,035	0,004	0,044	0,527
0,79	1,76	1,79	7,65	0,94	0,14	0,26	13,71
5,14	4,86	1,47	5,79	5,21	5,58	15,07	11,21
7,86	6,86	6,05	5,14	8,04	8,09	4,93	2,71
1,95	3,18	6,52	0,87	0,89	1,82	4,15	0,56
0,63	1,50	0,32	1,10	0,04	0,56	10,09	0,78

31,5	28,4	21,4	24,9	24,5	34,3	19,5	2,5
0,92	1,35	0,91	0,93	1,29	1,22	0,45	0,33
11,2	12,6	16,3	5,2	6,6	6,9	16,3	5,4
0,01	0,05	0,01	0,04	0,02	0,01	0,10	0,08
3,4	3,3	3,3	6,6	2,7	3,4	4,3	28,6
1	1	1	18	2	1	1	79
4	18	10	358	14	0	3	2107
4	10	11	31	1	0	1	70
32	50	42	100	24	23	23	613
3	9	3	15	9	6	39	13
9	12	11	39	3	5	8	55
16,2	15,1	13,5	12,8	15,5	16,1	21,5	21,8
0,6	0,5	0,6	0,8	0,6	0,5	-0,1	2,5
-0,2	-0,1	-0,2	0,0	-0,1	-0,2	-0,4	0,2
0,5	-0,7	-0,2	-0,4	0,3	0,2	-0,5	0,3
20,6	41,9	89,1	7,1	6,5	17,6	91	22
843	676	380	733	904	870	794	284
3,88	8,35	2,01	7,51	0,19	2,60	56	85
41,8	2,99	106	8,25	0,33	40,0	1458	392
6,45	0,39	37,99	0,84	0,09	4,61	15,49	22,19
0,279	0,307	0,336	0,392	0,176	0,480	0,295	0,190

0,030	0,033	0,021	0,006	0,002	0,094	0,243	0,035
0,119	0,094	0,115	0,048	0,049	0,195	0,238	0,292
0,024	0,018	0,012	0,010	0,022	0,024	0,019	0,198
0,142	0,170	0,251	0,088	0,059	0,181	0,273	1,671
-0,05	-0,05	-0,06	-0,04	-0,07	-0,03	-0,03	0,01
0,1	0,8	0,3	0,7	0,2	-0,1	0,6	0,6
2,0	1,8	2,0	1,3	1,2	1,7	2,0	0,5

552	602	901	317	413	619	761	169
15,17	30,48	9,66	23,16	4,12	12,19	189	27
29,90	65,61	37,29	52,03	5,63	22,94	422	51
4,23	8,35	2,23	6,50	0,49	2,93	52	8
14,95	33,49	8,09	26,70	2,00	12,06	202	41
2,20	5,45	1,26	3,93	0,16	1,70	32	12
2,22	2,05	1,43	1,97	1,90	2,23	4,09	3,39
1,83	4,30	0,95	3,45	0,17	1,48	23,5	18,0
0,211	0,466	0,108	0,395	0,021	0,145	2,80	2,91
1,000	2,211	0,499	1,910	0,053	0,694	13,62	18,92
0,165	0,359	0,080	0,301	0,010	0,096	2,13	3,97
0,256	0,630	0,204	0,607	0,009	0,186	4,23	11,25
0,035	0,052	0,022	0,058	0,002	0,020	0,36	1,48
0,177	0,233	0,096	0,315	0,013	0,082	1,76	8,81
0,015	0,029	0,007	0,030	0,002	0,012	0,17	1,41
1,089	0,090	2,344	0,294	0,034	1,464	33,76	13,95
0,514	0,031	1,726	0,073	0,008	0,593	3,511	2,208
0,202	0,565	0,130	0,152	0,282	0,870	0,763	2,716

0,026	0,035	0,044	0,039	0,016	0,015	0,175	0,122
4,304	4,634	5,915	3,170	3,953	4,283	7,090	13,110
0,001	0,000	0,003	-0,001	0,002	0,006	0,009	0,038
1,617	2,510	5,199	1,321	0,035	1,153	16,709	5,279
0,303	0,523	0,917	0,321	0,152	0,224	2,814	1,008

---

bulk raster bulk raster bulk raster bulk raster bulk raster bulk raster bulk raster bulk raster  
 25-NWA869 26-NWA869 27-NWA869 28-NWA869 29-NWA869 30-NWA869 31-NWA869 32-NWA869

35,4	34,3	33,8	33,6	33,6	33,3	34,0	33,6
0,28	0,31	0,36	0,36	0,12	0,20	0,84	0,49
0,041	0,058	0,086	0,046	0,036	0,051	0,083	0,059
0,172	0,352	0,667	0,268	0,167	0,299	0,359	0,249
38,31	39,24	39,49	39,97	40,12	40,46	39,25	39,96
0,838	0,838	0,842	0,845	0,852	0,862	0,828	0,844
23,61	23,65	23,80	24,12	24,30	24,23	23,55	23,81
1,05	1,04	0,73	0,50	0,71	0,45	0,62	0,60
0,10	0,10	0,10	0,11	0,04	0,06	0,28	0,16
0,047	0,039	0,057	0,055	0,039	0,033	0,076	0,062
0,18	0,04	0,06	0,09	0,04	0,09	0,11	0,13
3,0	3,1	3,0	3,3	3,8	3,6	3,7	3,7
0,03	0,04	0,04	0,03	0,02	0,02	0,05	0,03
1,6	1,6	1,8	1,3	1,4	1,6	1,4	1,7
0,01	0,02	0,01	0,01	0,00	0,01	0,01	0,01
7,7	7,7	7,2	6,5	7,3	6,2	6,9	7,2
26	40	62	27	22	27	38	27
1174	2409	4566	1831	1140	2045	2456	1704
110	114	114	114	114	116	111	112
308	322	318	318	316	320	308	310
3,4	7,8	4,3	2,9	3,9	3,3	3,1	4,0
110	114	120	113	112	116	115	113
0,61	0,75	1,10	0,64	0,46	0,63	1,10	0,78
1,2	1,2	1,1	1,1	1,2	1,1	1,1	1,1
0,1	0,0	0,0	0,0	0,0	0,0	0,0	0,0
0,2	0,2	0,1	0,1	0,1	0,0	0,0	0,1
1,02	1,19	2,21	0,98	0,89	1,11	0,87	0,92
14	15	12	19	8	13	40	25
1,30	0,99	0,92	0,92	0,95	0,96	0,98	1,25
1,19	2,36	5,33	1,85	2,02	3,03	3,42	4,15
0,14	0,40	1,00	0,25	0,14	0,47	0,62	0,55
0,015	0,016	0,010	0,010	0,017	0,012	0,009	0,023
0,007	0,013	0,015	0,015	0,018	0,007	0,004	0,003
0,001	0,002	0,002	0,002	0,002	0,001	0,000	0,000
0,009	0,011	0,018	0,007	0,010	0,015	0,015	0,011
0,006	0,019	0,008	0,005	0,004	0,005	0,004	0,005
0,029	0,027	0,022	0,020	0,025	0,023	0,020	0,019
0,004	0,022	0,007	0,003	0,004	0,003	0,004	0,003
0,095	0,155	0,107	0,031	0,166	0,079	0,106	0,066
0,00	0,01	0,06	0,00	0,00	0,00	0,00	0,01
0,2	0,4	0,4	0,2	0,2	0,2	0,2	0,2
0,1	0,2	0,4	0,2	0,1	0,1	0,1	0,1

6	5	6	12	4	4	25	15
1,71	0,29	0,39	1,10	0,24	1,14	1,32	1,68
4,64	0,94	1,17	2,73	0,77	2,79	3,22	4,20
0,60	0,14	0,16	0,34	0,11	0,34	0,40	0,52
2,23	0,64	0,67	1,24	0,51	1,24	1,54	1,97
0,41	0,16	0,15	0,21	0,13	0,20	0,26	0,33
0,05	0,04	0,03	0,05	0,02	0,03	0,10	0,07
0,38	0,19	0,17	0,22	0,15	0,21	0,27	0,33
0,05	0,03	0,03	0,03	0,03	0,03	0,03	0,04
0,28	0,19	0,17	0,18	0,17	0,18	0,19	0,25
0,05	0,04	0,04	0,04	0,04	0,04	0,04	0,05
0,15	0,12	0,12	0,11	0,12	0,12	0,12	0,15
0,02	0,02	0,02	0,02	0,02	0,02	0,02	0,02
0,12	0,11	0,11	0,11	0,11	0,11	0,12	0,13
0,02	0,02	0,02	0,02	0,02	0,02	0,02	0,02
0,037	0,067	0,132	0,056	0,071	0,087	0,125	0,139
0,007	0,022	0,053	0,013	0,009	0,028	0,045	0,048
0,045	0,059	0,076	0,051	0,042	0,053	0,065	0,104
0,001	0,001	0,001	0,001	0,001	0,001	0,001	0,003
0,002	0,003	0,002	0,003	0,003	0,002	0,002	0,002
0,002	0,003	0,003	0,003	0,003	0,001	0,001	0,003
0,000	0,004	0,001	0,003	0,006	0,003	0,000	0,001
0,021	0,001	0,001	0,001	0,065	0,003	0,005	0,040
0,008	0,020	0,010	0,008	0,028	0,007	0,010	0,016
0,368	0,595	0,375	0,389	0,282	0,318	0,493	0,611
0,001	0,010	0,002	0,001	0,080	0,001	0,001	0,012
0,080	0,049	0,116	0,085	0,059	0,124	0,130	0,160
0,066	0,083	0,057	0,052	0,474	0,077	0,063	0,095

bulk raster		olivine	olivine	olivine	olivine	olivine	olivine
33-NWA8694		26-Chassigny	27-Chassigny	28-Chassigny	29-Chassigny	30-Chassigny	31-Chassigny
<b>Major Elements (wt. %)</b>							
34,7	<b>SiO<sub>2</sub></b>	36,5	36,2	36,5	36,3	36,5	36,4
0,19	<b>Al<sub>2</sub>O<sub>3</sub></b>	0,02	0,11	0,02	0,02	0,02	0,02
0,064	<b>TiO<sub>2</sub></b>	0,021	0,035	0,017	0,017	0,018	0,020
0,296	<b>Cr<sub>2</sub>O<sub>3</sub></b>	0,022	0,312	0,023	0,028	0,026	0,025
38,60	<b>FeOT</b>	28,82	29,07	28,53	28,64	28,84	28,77
0,839	<b>MnO</b>	0,571	0,574	0,566	0,564	0,568	0,572
23,48	<b>MgO</b>	33,88	33,48	34,12	34,19	33,82	33,95
1,73	<b>CaO</b>	0,15	0,17	0,19	0,22	0,21	0,18
0,05	<b>Na<sub>2</sub>O</b>	0,01	0,02	0,02	0,02	0,01	0,02
0,025	<b>K<sub>2</sub>O</b>	0,003	0,004	0,003	0,004	0,004	0,004
0,05	<b>P<sub>2</sub>O<sub>5</sub></b>	0,02	0,02	0,07	0,02	0,02	0,01
<b>Trace elements (ppm)</b>							
3,8	<b>Li</b>	3,5	3,6	5,2	4,3	4,2	4,2
0,03	<b>Be</b>	0,02	0,01	0,01	0,01	0,02	0,01
1,2	<b>B</b>	0,5	0,6	0,9	0,6	0,6	0,7
0,00	<b>S</b>	0,03	0,01	0,01	0,01	0,01	0,01
9,7	<b>Sc</b>	6,0	6,1	6,7	6,2	6,4	6,1
43	<b>V</b>	5	23	5	5	6	6
2024	<b>Cr</b>	151	2133	155	189	175	168
108	<b>Co</b>	132	134	132	131	133	133
299	<b>Ni</b>	509	505	494	490	499	501
2,9	<b>Cu</b>	1,0	1,0	0,8	0,4	0,4	0,5
110	<b>Zn</b>	69	71	68	69	71	70
0,64	<b>Ga</b>	0,13	0,42	0,11	0,12	0,11	0,12
1,3	<b>Ge</b>	1,0	1,1	1,3	1,3	1,3	1,1
0,0	<b>As</b>	0,1	0,0	0,0	0,0	0,0	0,1
0,0	<b>Se</b>	0,1	0,1	0,0	0,0	0,0	0,0
0,79	<b>Rb</b>	0,1	0,1	0,1	0,1	0,1	0,1
8	<b>Sr</b>	0,0	0,2	0,0	0,2	0,0	0,1
1,61	<b>Y</b>	0,3	0,4	0,3	0,3	0,3	0,3
3,25	<b>Zr</b>	0,5	0,2	0,1	0,1	0,1	0,1
0,29	<b>Nb</b>	0,0	0,0	0,0	0,0	0,0	0,0
0,007	<b>Mo</b>	0,054	0,057	0,068	0,086	0,069	0,071
0,004	<b>Ru</b>	0,005	0,003	0,005	0,010	0,007	0,008
0,000	<b>Rh</b>	0,001	0,000	0,001	0,000	0,000	0,000
0,009	<b>Pd</b>	0,007	0,004	0,005	0,005	0,003	0,005
0,003	<b>Ag</b>	0,006	0,028	0,003	0,002	0,001	0,005
0,028	<b>Cd</b>	0,089	0,077	0,067	0,075	0,090	0,090
0,004	<b>In</b>	0,006	0,005	0,005	0,006	0,008	0,007
0,212	<b>Sn</b>	0,035	0,031	0,025	0,018	0,026	0,027
0,00	<b>Sb</b>	0,02	0,01	0,02	0,01	0,01	0,02
0,1	<b>Te</b>	0,04	0,01	0,01	0,01	0,00	0,00
0,1	<b>Cs</b>	0,04	0,03	0,03	0,03	0,04	0,05



1	<b>Ba</b>	0	0	0	0	0	0
0,46	<b>La</b>	0,007	0,027	0,028	0,030	0,009	0,057
1,47	<b>Ce</b>	0,009	0,072	0,082	0,045	0,048	0,039
0,24	<b>Pr</b>	0,001	0,008	0,006	0,014	0,002	0,005
1,06	<b>Nd</b>	0,006	0,027	0,019	0,042	0,006	0,021
0,28	<b>Sm</b>	0,002	0,004	0,002	0,006	0,006	0,002
0,05	<b>Eu</b>	0,002	0,001	0,001	0,002	0,001	0,000
0,31	<b>Gd</b>	0,008	0,015	0,010	0,012	0,012	0,010
0,05	<b>Tb</b>	0,003	0,004	0,004	0,004	0,004	0,003
0,33	<b>Dy</b>	0,038	0,051	0,033	0,043	0,040	0,033
0,07	<b>Ho</b>	0,012	0,014	0,013	0,013	0,013	0,012
0,20	<b>Er</b>	0,052	0,058	0,050	0,048	0,047	0,048
0,03	<b>Tm</b>	0,009	0,019	0,009	0,008	0,009	0,009
0,16	<b>Yb</b>	0,068	0,076	0,075	0,071	0,066	0,076
0,03	<b>Lu</b>	0,014	0,013	0,014	0,013	0,015	0,014
0,099	<b>Hf</b>	0,019	0,007	0,004	0,003	0,002	0,004
0,024	<b>Ta</b>	0,001	0,001	0,000	0,001	0,000	0,000
0,040	<b>W</b>	0,009	0,035	0,007	0,008	0,012	0,009
0,001	<b>Re</b>	0,000	0,000	0,000	0,001	0,000	0,000
0,001	<b>Os</b>	0,000	0,000	0,000	0,001	0,000	0,000
0,001	<b>Ir</b>	0,000	0,000	0,000	0,000	0,000	0,000
0,002	<b>Pt</b>	-0,001	0,001	0,001	0,000	0,000	0,000
0,001	<b>Au</b>	0,001	0,002	0,001	0,001	0,000	0,001
0,005	<b>Tl</b>	0,001	0,000	0,001	0,001	0,000	0,000
0,207	<b>Pb</b>	0,71	0,12	0,10	0,07	0,06	0,09
0,001	<b>Bi</b>	0,003	0,002	0,003	0,002	0,002	0,002
0,054	<b>Th</b>	0,001	0,002	0,000	0,000	0,000	0,000
0,049	<b>U</b>	0,004	0,002	0,003	0,002	0,001	0,002

olivine	pyroxene	pyroxene	pyroxene	pyroxene	pyroxene	pyroxene	pyroxene
32-Chassigny	33-Chassigny	34-Chassigny	35-Chassigny	36-Chassigny	37-Chassigny	38-Chassigny	39-Chassigny
36,4	41,6	39,2	52,0	48,1	47,5	53,1	40,6
0,02	0,33	0,80	1,28	1,58	9,31	0,83	2,22
0,017	0,082	0,202	0,306	0,323	0,130	0,182	0,597
0,028	0,401	2,384	0,760	0,638	0,204	0,343	12,9
28,87	24,11	23,78	9,30	11,40	12,91	15,42	19,48
0,573	0,567	0,511	0,358	0,371	0,434	0,481	0,537
33,81	30,61	28,55	17,25	19,00	22,55	23,12	19,02
0,19	2,14	4,43	18,41	17,05	4,36	6,35	4,44
0,02	0,08	0,12	0,36	0,43	1,97	0,17	0,14
0,004	0,008	0,010	0,005	0,020	0,623	0,029	0,015
0,02	0,03	0,04	0,01	1,12	0,01	0,00	0,01
5,1	4,5	5,1	4,9	4,3	315,9	2,6	2,7
0,01	0,05	0,08	0,04	0,14	0,96	0,17	0,10
0,8	1,4	1,6	1,1	1,3	9,6	4,0	1,6
0,01	0,02	0,04	0,01	0,02	0,06	1,13	0,03
6,0	12,4	15,9	52,5	53,5	26,8	29,3	20,1
6	49	171	196	179	56	108	621
190	2742	16313	5198	4363	1398	2347	88296
134	110	109	32	44	44	49	77
502	364	386	102	150	221	140	133
0,3	12,8	5,1	2,6	16,4	8,4	31,5	8,0
72	64	108	20	26	87	44	178
0,11	0,76	3,42	2,51	3,31	4,86	1,87	9,75
1,1	1,4	1,6	1,9	1,7	0,6	1,7	1,5
0,0	0,1	0,2	0,0	0,0	0,3	0,1	0,0
0,0	0,0	0,0	-0,1	0,0	1,7	0,7	0,0
0,2	0,2	0,4	0,2	0,4	30,0	1,6	0,6
0,0	4,0	8,2	50,3	104,7	3,0	6,4	6,0
0,3	1,7	2,3	11,0	17,6	4,5	5,7	2,5
0,2	1,4	2,0	7,5	16,9	14,0	12,1	2,0
0,0	0,1	0,4	0,1	0,3	0,4	1,0	0,3
0,098	0,081	0,078	0,063	0,056	3,031	0,065	0,085
0,005	0,005	0,008	0,005	0,006	0,310	0,007	0,019
0,001	0,001	0,001	0,000	0,001	0,071	0,002	0,001
0,007	0,015	0,011	0,021	0,026	0,249	0,020	0,012
0,007	0,243	0,066	0,015	0,010	0,167	0,081	0,029
0,118	0,272	0,081	0,088	0,083	0,899	0,115	0,145
0,006	0,011	0,007	0,016	0,016	0,140	0,011	0,010
0,033	1,543	0,111	0,030	0,045	0,139	0,088	0,482
0,01	0,04	0,14	0,02	0,02	-0,10	0,01	0,02
0,01	0,01	0,09	0,03	0,04	0,48	8,41	0,06
0,04	0,06	0,10	0,08	0,11	11,18	0,22	0,16

0	0	0	0	7	1	1	1
0,012	0,233	0,295	1,451	15,209	1,001	0,955	0,428
0,058	0,910	1,219	6,393	38,202	3,142	3,626	1,425
0,010	0,169	0,235	1,414	5,744	0,550	0,686	0,249
0,027	0,961	1,289	8,408	26,417	2,304	3,540	1,312
0,000	0,282	0,398	2,524	5,664	1,024	0,978	0,378
0,001	0,072	0,101	0,596	1,129	0,165	0,202	0,101
0,012	0,320	0,458	2,799	5,395	0,919	1,132	0,439
0,003	0,052	0,075	0,436	0,769	0,105	0,182	0,074
0,037	0,347	0,472	2,496	4,209	0,977	1,157	0,496
0,012	0,072	0,092	0,456	0,737	0,203	0,217	0,099
0,048	0,203	0,245	1,116	1,713	0,606	0,583	0,295
0,009	0,026	0,033	0,127	0,183	0,085	0,073	0,036
0,064	0,159	0,188	0,676	0,926	0,338	0,398	0,224
0,013	0,025	0,029	0,088	0,113	0,034	0,055	0,036
0,005	0,050	0,074	0,390	0,826	0,446	0,365	0,075
0,000	0,004	0,015	0,004	0,022	0,036	0,076	0,012
0,009	0,018	0,042	0,008	0,029	0,083	0,070	0,058
0,000	0,000	0,001	0,000	0,000	-0,009	0,000	0,001
0,000	0,001	0,001	0,000	0,001	0,071	0,000	0,000
0,000	0,000	0,001	0,000	0,000	-0,001	0,001	0,000
0,001	-0,001	0,000	0,001	0,000	-0,025	0,001	0,002
0,000	0,002	0,007	0,001	0,001	0,217	0,003	0,003
0,001	0,002	0,002	0,000	0,001	0,008	0,082	0,004
0,08	4,40	24,47	0,24	0,59	5,59	12,80	0,53
0,003	0,004	0,008	0,002	0,002	0,078	0,012	0,002
0,000	0,012	0,030	0,008	0,695	0,082	0,106	0,018
0,002	0,008	0,013	0,005	0,161	0,010	0,019	0,009

pyroxene?	melt/plag	mesostasis	mesostasis	olivine?	olivine?	olivine?	chromite
40-Chassigny	41-Chassigny	42-Chassigny	43-Chassigny	44-Chassigny	45-Chassigny	46-Chassigny	47-Chassigny
41,6	46,1	53,6	58,1	36,6	37,2	37,3	0,1
0,21	29,25	16,15	11,50	0,36	0,17	0,03	8,64
0,061	0,044	0,360	0,538	0,024	0,020	0,016	1,975
0,092	0,007	0,035	0,059	0,021	0,021	0,028	50,3
25,22	3,86	6,24	5,32	27,82	27,99	27,84	33,60
0,561	0,084	0,186	0,186	0,563	0,565	0,558	0,504
31,65	4,02	8,19	8,60	33,97	33,43	33,66	4,11
0,59	14,21	9,61	9,00	0,28	0,25	0,25	0,14
0,03	2,03	4,25	5,70	0,30	0,25	0,24	0,48
0,009	0,333	0,319	0,240	0,078	0,064	0,074	0,154
0,01	0,07	1,05	0,74	0,03	0,02	0,03	0,01
4,1	71,9	57,1	43,4	38,0	35,2	40,6	71,9
0,07	1,41	2,42	2,89	0,11	0,15	0,22	0,24
0,9	2,5	10,2	14,7	1,6	1,5	0,9	2,1
0,02	0,01	0,06	0,06	0,02	0,01	0,01	0,01
9,1	3,4	11,4	17,7	6,1	5,7	6,2	4,6
23	2	16	28	5	5	6	2066
629	46	243	404	146	143	189	343976
110	16	22	17	132	127	127	183
394	89	99	76	490	588	503	179
0,6	3,6	6,6	7,5	20,0	2,6	0,8	9,9
66	16	24	18	88	82	81	1274
0,51	16,45	10,12	7,69	0,37	0,31	0,20	38,72
1,2	1,3	2,3	2,5	0,9	1,1	1,1	0,9
0,0	-0,1	0,1	0,0	0,1	0,1	0,0	0,0
0,0	-0,2	-0,3	-0,5	-0,1	0,1	-0,2	-0,3
0,4	10,7	7,4	6,6	3,8	3,1	3,7	8,1
0,1	1592,8	751,5	182,5	9,9	6,9	0,1	0,3
0,8	1,0	21,4	24,9	0,3	0,3	0,2	0,0
1,0	1,5	56,4	103,8	0,7	0,4	0,1	3,2
0,1	0,2	5,5	7,7	0,1	0,0	0,0	1,0
0,089	0,608	0,434	0,315	0,353	0,329	0,397	0,685
0,005	0,051	0,053	0,035	0,043	0,059	0,041	0,263
0,001	0,014	0,005	0,011	0,008	0,001	-0,001	0,006
0,007	0,053	0,132	0,157	0,020	0,021	0,023	0,042
0,009	0,094	0,414	0,106	1,852	0,088	0,010	0,062
0,104	0,170	0,200	0,154	0,450	0,080	0,179	0,227
0,009	0,023	0,058	0,051	0,060	0,057	0,049	0,105
0,028	0,055	0,155	0,171	2,716	0,068	0,052	0,102
0,02	0,00	0,10	0,14	0,02	0,00	-0,01	0,00
0,01	0,18	0,15	0,11	0,11	0,35	-0,01	0,23
0,17	3,12	2,46	1,85	1,41	1,16	1,39	3,08

0	99	254	42	1	1	0	0
0,080	6,736	22,565	14,492	0,261	0,149	0,032	0,071
0,100	11,705	49,118	36,955	0,768	0,419	0,185	0,198
0,026	1,221	7,237	6,010	0,100	0,045	0,009	0,013
0,107	4,403	28,304	26,060	0,327	0,170	0,056	0,075
0,039	0,607	6,147	6,074	0,048	0,027	0,008	-0,006
0,012	3,197	2,253	1,391	0,027	0,026	0,008	0,011
0,069	0,562	5,889	6,318	0,065	0,038	0,008	0,024
0,015	0,071	0,896	1,016	0,010	0,007	0,000	0,005
0,143	0,275	4,988	5,635	0,038	0,061	0,013	0,004
0,032	0,056	0,839	1,055	0,017	0,011	0,014	-0,001
0,111	0,089	1,887	2,413	0,029	0,031	0,039	0,002
0,018	0,007	0,203	0,261	0,007	0,005	0,006	0,003
0,121	0,062	0,900	1,210	0,063	0,067	0,064	-0,007
0,019	0,009	0,108	0,158	0,015	0,014	0,015	0,002
0,034	0,033	1,578	2,948	0,030	0,010	0,003	0,122
0,002	0,017	0,443	0,534	0,006	0,004	0,000	0,037
0,027	0,051	0,723	0,962	0,028	0,025	0,006	0,044
0,000	-0,003	0,001	-0,002	0,005	-0,001	0,000	0,005
0,000	-0,004	0,005	0,001	-0,002	-0,004	0,007	-0,008
0,000	0,003	0,000	0,000	0,001	0,000	0,000	0,000
0,000	-0,008	0,002	0,006	-0,005	-0,001	0,002	-0,012
0,000	0,007	0,013	0,007	0,006	-0,001	-0,001	-0,006
0,001	0,012	0,017	0,036	0,003	0,001	0,000	0,003
0,15	1,89	2,27	2,10	0,55	0,26	0,03	1,30
0,002	0,006	0,020	0,003	0,015	0,004	0,001	0,001
0,013	0,050	1,460	1,535	0,018	0,007	0,000	0,004
0,003	0,035	0,367	0,355	0,007	0,005	0,000	0,005

? mesostasis mesostasis chromite mesostasis  
 48-Chassigny 49-Chassigny 50-Chassigny 51-Chassigny 52-Chassigny

33,0	53,8	50,4	3,3	55,8
12,65	12,11	7,26	7,74	19,72
1,276	0,718	0,845	1,765	0,047
0,297	0,124	0,135	47,5	0,021
23,45	11,88	14,85	32,29	5,81
0,525	0,209	0,353	0,509	0,114
13,67	11,19	19,01	6,33	6,88
11,10	2,43	3,25	0,06	4,04
2,72	6,33	2,44	0,36	6,57
0,556	0,741	1,261	0,118	1,032
0,78	0,46	0,17	0,01	0,02
2,1	35,1	5,4	46,5	14,4
0,34	3,76	1,81	0,33	0,55
5,4	20,2	8,5	1,3	2,2
0,09	2,71	0,22	0,01	0,02
28,1	11,8	14,7	5,4	2,9
80	49	54	1971	2
2035	849	926	325231	144
67	112	64	177	27
568	1358	299	200	114
10,8	559,1	30,0	2,7	3,5
56	37	44	885	21
20,55	5,04	4,45	30,07	10,70
2,3	1,9	2,7	0,8	0,7
0,2	0,1	0,1	0,0	0,1
0,4	6,9	0,5	-0,3	0,1
22,3	21,4	28,4	6,5	10,7
282,8	360,9	246,0	0,6	776,4
84,5	13,5	11,7	0,1	0,1
389,4	62,1	45,2	2,7	0,3
22,1	33,9	23,8	0,7	0,1
0,194	0,968	0,200	0,726	0,144
0,034	0,228	0,033	0,247	0,035
0,010	0,071	0,007	0,003	0,005
0,173	0,171	0,072	0,022	0,016
0,035	0,712	0,089	0,067	0,153
0,314	0,193	0,116	0,161	0,238
0,198	0,042	0,017	0,041	0,020
1,828	0,681	0,478	0,071	0,152
0,01	0,02	0,05	0,04	0,04
0,63	0,20	0,05	0,28	0,05
0,45	4,42	1,75	2,32	0,75

170	403	203	2	478
26,696	10,729	3,596	0,051	3,615
51,142	26,480	11,201	0,493	4,674
7,977	3,716	1,721	0,060	0,397
40,694	16,124	8,273	0,012	0,991
12,095	3,868	2,442	0,013	0,078
3,397	1,149	0,808	0,016	1,639
18,020	3,728	2,680	0,018	0,043
2,911	0,558	0,441	0,001	0,005
18,924	3,065	2,563	-0,001	0,010
3,971	0,511	0,451	0,001	0,004
11,226	1,149	1,116	0,021	0,012
1,479	0,124	0,122	0,001	0,001
8,827	0,623	0,658	0,007	0,013
1,413	0,073	0,075	0,000	0,003
13,981	1,513	1,372	0,082	0,009
2,177	1,543	1,012	0,021	0,009
3,653	1,411	0,745	0,015	0,022
0,002	0,009	0,001	0,011	0,000
0,037	0,003	0,000	0,003	0,002
0,039	0,000	0,000	0,003	0,000
0,033	0,207	0,033	0,001	-0,004
0,012	0,017	0,003	-0,007	0,605
0,119	0,031	0,027	0,007	0,009
13,45	5,05	5,02	3,52	4,92
0,038	0,011	0,005	0,003	0,031
5,289	1,269	0,577	0,004	0,009
1,030	0,337	0,163	0,009	0,009

Modal %	NWA2737	Chassigny	NWA8694
Olivine	87,9	89,6	85,3
Chromite	3,5	4,6	0,8
Pyroxene	6,7	4,1	11,6
Glass/Fsp	3,2	1,6	2,4
Phosphate	0,2	0,2	0,14
Carbonate	0,9	-	-



Table 1 Chassignite modal abundances

Modal %	NWA 2737 <sup>a</sup>	Chassigny <sup>b</sup>	NWA 8694
Olivine	87.9	89.6	85.3
Chromite	3.5	4.6	0.8
Pyroxenes	6.7	4.1	11.6
Glass/Fsp	3.2	1.6	2.4
Phosphate	0.2	0.2	*0.14
Carbonate	0.9	-	-

<sup>a</sup>Average in Treiman et al. (2007). <sup>b</sup>Floran et al. (1978).

\*Calculated from P abundance.

Table 2a. Selected analyses of olivine, chromite, biotite and amphibole.

	SiO <sub>2</sub>	Al <sub>2</sub> O <sub>3</sub>	TiO <sub>2</sub>	Cr <sub>2</sub> O <sub>3</sub>	FeO	MnO	MgO	CaO	Na <sub>2</sub> O	Total	Fo	Fa	
<b>NWA 8694</b>													
107/59	35.31	0.02	0.06	bd	38.71	0.80	25.75	0.09	0.01	100.63	54.25	45.75	
94	35.74	0.01	0.06	0.06	38.81	0.76	24.97	0.28	bd	100.72	53.42	46.58	
97/62	35.74	0.02	0.04	0.04	38.99	0.78	24.85	0.12	0.02	100.61	53.19	46.81	
88/14	35.08	0.01	0.03	0.06	38.89	0.76	24.59	0.13	bd	99.66	52.99	47.01	
LA mean	35.21	0.02	0.03	0.05	38.26	0.84	25.37	0.22	0.02	100.06	54.09	45.91	
<b>Chassigny</b>													
26	38.14	0.03	0.03	0.04	28.04	0.53	34.05	0.13	0.00	101.08	68.40	31.60	
22	37.37	0.04	0.04	0.03	27.91	0.53	33.54	0.14	0.01	99.75	68.18	31.82	
23	37.55	0.03	0.00	0.02	28.56	0.54	33.98	0.21	0.01	101.07	67.96	32.04	
03	37.62	0.02	0.01	0.03	28.69	0.56	33.63	0.14	bd	100.76	67.64	32.36	
LA mean	36.39	0.03	0.02	0.07	28.79	0.57	33.89	0.19	0.02	99.97	67.72	32.28	
<b>NWA 2737</b>													
8184	39.16	0.02	0.00	0.04	19.68	0.41	41.16	0.12	bd	100.65	78.84	21.16	
8279	39.24	0.04	0.01	0.04	20.08	0.55	40.56	0.15	bd	100.68	78.28	21.72	
771	39.12	0.03	0.03	0.05	20.45	0.41	40.58	0.13	bd	100.83	77.97	22.03	
8226	39.12	0.05	0.02	0.02	20.73	0.52	40.22	0.14	bd	100.83	77.58	22.42	
<b>NWA 8694 chromite</b>													
15	0.07	5.59	1.66	52.93	34.98	bd	2.45	bd	bd	97.67			
15nuit	0.06	8.65	2.95	49.05	33.39	bd	0.82	bd	bd	96.28			
100	0.09	7.74	3.75	44.98	38.57	bd	2.47	bd	bd	98.84			
28	0.14	9.83	4.28	41.06	40.42	bd	1.69	bd	bd	97.40			
<b>Chassigny chromite</b>													
6	0.08	6.10	1.32	55.31	31.77	0.00	4.09	bd	bd	99.06			
12	0.04	8.14	2.14	50.88	32.47	0.00	3.65	bd	bd	97.66			
7	0.05	10.16	3.49	45.70	35.17	0.00	3.54	bd	bd	98.58			
<b>NWA 2737</b>													
70	0.03	6.45	1.18	57.85	28.73	bd	5.70	bd	bd	99.99			
9936	0.02	6.97	1.34	55.90	29.84	bd	5.83	bd	bd	99.94			
9943	0.02	7.60	1.56	53.86	30.80	bd	6.04	bd	bd	100.04			
65	0.07	10.27	1.38	51.54	31.32	bd	5.07	bd	bd	99.70			
98	0.01	11.82	2.44	46.31	33.87	bd	5.10	bd	bd	99.61			
<b>NWA 8694</b>													
	SiO <sub>2</sub>	Al <sub>2</sub> O <sub>3</sub>	TiO <sub>2</sub>	Cr <sub>2</sub> O <sub>3</sub>	FeO	MnO	MgO	CaO	Na <sub>2</sub> O	K <sub>2</sub> O	F	Cl	Total*
inst biotite	40.11	12.12	0.77	0.26	11.21	0.09	20.33	0.13	0.16	8.70	0.99	0.82	95.75
M.I. biotite	39.59	13.25	0.16	0.02	11.54	0.12	20.02	0.09	0.45	8.50	0.26	0.17	94.27
M.I. amphibole	40.07	15.63	3.12	0.09	13.40	0.28	10.35	11.35	2.91	0.23	0.66	0.42	98.54

\*Corrected for O=F,Cl: 95.15, 94.12, & 98.17. LA = LA-ICP-MS, inst = interstitial and M.I. = melt inclusion.

Table 2b. Selected analyses of interstitial and melt-inclusion pyroxene.

	SiO2	Al2O3	TiO2	Cr2O3	FeO	MnO	MgO	CaO	Na2O	Total	En	Fs	Wo
<b>NWA 8694</b>													
51	52.92	0.80	0.20	0.22	22.93	0.70	20.44	1.44	0.01	99.72	59.52	37.46	3.02
112	52.74	0.45	0.31	0.16	21.63	0.79	19.10	4.61	0.07	99.96	55.29	35.12	9.60
36	52.85	1.87	0.40	0.68	12.83	0.51	13.99	17.71	0.33	101.20	41.24	21.23	37.53
71	52.74	0.46	0.33	0.31	10.51	0.44	14.41	19.64	0.28	99.05	41.86	17.13	41.01
LA mean	52.52	0.67	0.16	0.50	22.17	0.77	18.93	4.63	0.13	100.50	54.55	35.86	9.58
77 M.I.	51.48	3.81	0.39	0.18	24.48	0.70	18.88	1.15	0.03	101.22	56.45	41.07	2.48
81 M.I.	51.48	2.81	0.84	0.04	14.47	0.30	9.32	20.53	0.80	100.71	28.95	25.21	45.83
<b>Chassigny</b>													
60	55.23	0.29	0.13	0.27	17.72	0.57	24.03	2.29	0.02	100.58	67.47	27.90	4.63
51	55.26	0.71	0.20	0.48	15.52	0.55	22.47	6.19	0.15	101.52	63.08	24.44	12.49
LA 38Ch	53.07	0.83	0.18	0.34	15.42	0.48	23.12	6.35	0.17	100.0	63.63	23.81	12.56
53	53.47	1.09	0.26	0.78	9.40	0.28	16.42	17.96	0.24	99.91	47.44	15.25	37.31
55	54.00	1.45	0.40	0.84	8.82	0.28	16.11	19.16	0.32	101.39	46.25	14.21	39.54
LA 35Ch	51.96	1.28	0.31	0.76	9.30	0.36	17.25	18.41	0.36	100.0	48.32	14.61	37.07
<b>NWA 2737</b>													
141	56.43	0.38	0.40	0.19	12.29	0.42	29.01	1.53	0.04	100.82	78.40	18.62	2.98
99/51	54.43	1.16	0.10	0.47	12.23	0.38	27.70	2.86	0.04	99.40	75.66	18.74	5.60
58	55.86	0.60	0.11	0.68	11.01	0.41	25.38	6.53	0.25	100.84	70.01	17.02	12.97
145/45	54.25	0.92	0.26	0.90	6.90	0.27	18.27	18.02	0.32	100.11	52.07	11.04	36.89
145/49	53.82	1.04	0.30	0.98	6.32	0.20	17.40	19.77	0.37	100.23	49.50	10.07	40.43

LA = LA-ICP-MS; M.I. =melt inclusion.

Table 3. Selected analyses of feldspars.

	NWA 8694				Chassigny				NWA 2737		
SiO <sub>2</sub>	60.39	63.42	63.76	64.67	62.72	63.92	63.37	63.15	66.09	65.40	68.11
Al <sub>2</sub> O <sub>3</sub>	23.38	23.04	21.54	19.16	22.33	22.11	21.51	21.05	21.06	20.96	20.05
FeO	0.53	0.34	0.37	0.47	0.57	0.42	0.40	0.35	0.16	0.21	0.11
MgO	0.01	0.06	0.09	0.01	0.04	0.02	0.02	0.03	0.06	bd	bd
CaO	5.56	3.90	2.75	0.23	3.43	3.57	2.98	2.31	1.21	1.01	0.84
Na <sub>2</sub> O	7.51	8.58	6.59	2.30	7.46	8.41	8.73	6.68	8.36	8.75	8.77
K <sub>2</sub> O	1.02	1.00	4.93	13.73	2.37	1.99	1.48	4.95	3.02	3.49	3.32
Total	98.57	100.57	100.32	100.65	99.02	100.57	98.59	98.70	99.96	99.82	101.20
An	27.27	18.56	13.27	0.99	17.37	16.90	14.49	11.40	6.09	4.82	4.04
Ab	66.67	75.26	58.16	19.80	68.37	71.92	76.92	59.57	75.93	75.36	76.85
Or	6.06	6.19	28.57	79.21	14.26	11.18	8.59	29.03	17.98	19.82	19.11

Table 4. Selected analyses of glass, and average apatite in NWA 8694.

	Al-rich GL 27	Al-rich GL 3	K-rich GL 109	K-rich GL 78	Al-poor GL 28	Cat-poor GL 45	Fluorapatite ave
SiO <sub>2</sub>	64.74	67.23	70.24	71.35	72.51	79.44	0.48
Al <sub>2</sub> O <sub>3</sub>	21.45	21.17	16.43	15.44	16.53	17.31	0.06
FeO	1.19	1.39	0.88	1.03	0.72	0.93	0.70
MgO	0.15	0.32	0.02	b.d.	0.02	0.01	0.15
CaO	0.89	0.42	2.58	1.31	0.10	b.d.	53.48
Na <sub>2</sub> O	11.10	10.10	3.78	4.27	9.10	0.48	0.09
K <sub>2</sub> O	0.08	0.03	5.20	4.81	0.06	1.34	0.09
P <sub>2</sub> O <sub>5</sub>	b.d.	b.d.	b.d.	b.d.	b.d.	0.02	42.00
F	b.d.	b.d.	b.d.	b.d.	0.22	n.d.	2.34
Cl	0.02	n.d.	1.38	1.18	0.06	n.d.	2.20
Total	99.68	100.65	100.53	99.47	99.41	99.53	101.68
-O = F			0.01		0.09		0.99
-O = Cl			0.31	0.27	0.01		0.49
Total			100.21	99.21	99.30		100.20
Ca	4.00	2.18	16.55	8.81	0.00	0.00	
Na	95.00	97.71	43.74	52.41	100.00	36.36	
K	1.00	0.11	39.70	38.78	0.00	63.64	

Table 5. Mean composition of NWA 8694 sulfides

---

wt. %	enclosed pyrrhotite (n = 16)
Fe	58.1 (0.7)
Ni	1.3 (0.5)
S	39.7 (0.7)
Total	99.1
Fe+Ni/S (at.%)	0.87

---

n = number of analyses

Table 7. LA-ICP-MS average analyses (continued).

n	bulk rock	olivine	pigeonite	mesostasis	olivine	augite	pigeonite38	mesostasis
	NWA 8694	NWA8693	NWA8694	NWA8694	Chassigny	Chassigny	Chassigny	Chassigny
	8	5	5	11	7	2	1	6
La	0.830	0.005	0.188	30.790	0.024	8.330	0.955	10.289
Ce	3.442	0.006	0.636	67.687	0.051	22.297	3.626	23.355
Pr	0.280	0.001	0.125	8.256	0.007	3.579	0.686	3.384
Nd	1.117	0.006	0.739	32.125	0.021	17.412	3.540	14.026
Sm	0.226	0.003	0.271	4.990	0.003	4.094	0.978	3.203
Eu	0.067	0.001	0.060	2.146	0.001	0.862	0.202	1.740
Gd	0.225	0.017	0.376	3.856	0.011	4.097	1.132	3.203
Tb	0.034	0.005	0.071	0.447	0.004	0.602	0.182	0.498
Dy	0.209	0.055	0.498	2.164	0.039	3.353	1.157	2.756
Ho	0.043	0.018	0.108	0.335	0.013	0.596	0.217	0.486
Er	0.125	0.071	0.317	0.653	0.050	1.414	0.583	1.111
Tm	0.018	0.013	0.044	0.060	0.010	0.155	0.073	0.119
Yb	0.117	0.092	0.273	0.276	0.071	0.801	0.398	0.578
Lu	0.020	0.018	0.043	0.030	0.014	0.101	0.055	0.071
Hf	0.255	0.008	0.071	3.633	0.006	0.608	0.365	1.242
Ta	0.039	0.000	0.013	0.622	0.000	0.013	0.076	0.593
W	0.094	0.004	0.041	0.461	0.013	0.019	0.070	0.652
Re	0.0009				0.0002	-0.0001	0.0000	0.0007
Os	0.0008				0.0001	0.0002	0.0004	0.0009
Ir	0.0008				0.0001	0.0001	0.0010	0.0005
Pt	0.2336				0.0003	0.0006	0.0014	0.0393
Au	0.0006				0.0009	0.0007	0.0028	0.1086
Tl	0.007	0.001	0.003		0.001	0.001	0.082	0.022
Pb	0.545	0.156	0.236	5.516	0.177	0.418	12.803	3.542
Bi	0.005	0.003	0.002	0.003	0.003	0.002	0.012	0.013
Th	0.092	0.001	0.032	3.014	0.001	0.351	0.106	0.817
U	0.082	0.030	0.102	0.563	0.002	0.083	0.019	0.211

Table 7. LA-ICP-MS average analyses for NWA 8694 and Chassigny.

	bulk rock	olivine	pigeonite	mesostasis	olivine	augite	pigeonite38	mesostasis
	NWA 8694	NWA8693	NWA8694	NWA8694	Chassigny	Chassigny	Chassigny	Chassigny
n	8	5	5	10	7	2	1	6
SiO <sub>2</sub>	(EMP) 37,41	35,21	52,24	57,597	36,39	50,01	53,1	52,97
Al <sub>2</sub> O <sub>3</sub>	0,50	0,02	0,67	20,900	0,03	1,43	0,83	16,00
TiO <sub>2</sub>	0,06	0,03	0,16	0,067	0,02	0,31	0,182	0,43
Cr <sub>2</sub> O <sub>3</sub>	0,49	0,05	0,48	0,006	0,10	1,02	0,50	0,09
FeOT	36,16	38,26	22,28	2,852	28,79	10,35	15,42	7,99
MnO	0,81	0,84	0,77	0,059	0,57	0,36	0,481	0,19
MgO	23,46	25,37	18,97	1,543	33,89	18,13	23,12	9,64
CaO	0,82	0,22	4,77	5,687	0,19	17,73	6,35	7,09
Na <sub>2</sub> O	0,17	0,02	0,13	7,190	0,02	0,39	0,17	4,55
K <sub>2</sub> O	0,06	0,01	0,02	2,553	0,00	0,01	0,029	0,65
P <sub>2</sub> O <sub>5</sub>	0,05	0,03	0,01	1,531	0,03	0,57	0,00	0,42
Li	3,43	4,49	3,82	43,576	4,29	4,58	2,58	37,89
Be	0,04	0,01	0,09	1,048	0,01	0,09	0,17	2,14
B	1,09	1,00	3,35	8,999	0,67	1,20	4,0	9,73
S	0,01	0,01	0,01	0,104	0,01	0,02	1,13	0,51
Sc	7,62	6,77	25,82	4,581	6,21	52,99	29,3	10,31
V	38,04	9,37	115,87	2,727	8,01	187,69	108	24,98
Cr	0,34	356,33	3261,44	40,902	0,07	0,70	0,343	0,06
Co	101,89	124,04	56,17	20,972	132,72	38,27	49	43,07
Ni	258,72	345,13	114,08	51,030	500,06	126,18	140	338,98
Cu	5,94	2,21	4,73	11,083	0,65	9,49	31	101,72
Zn	95,87	109,16	84,45	10,979	70,01	22,91	44	26,44
Ga	0,84	0,19	1,51	15,969	0,16	2,91	1,9	9,08
Ge	0,84	1,28	2,23	0,554	1,19	1,83	1,73	1,91
As	0,03	0,05	0,03	0,000	0,05	0,04	0,06	0,04
Se	0,05	0,05	0,02	0,706	0,03	0,00	0,7	1,07
Rb	1,53	0,17	0,67	40,765	0,13	0,29	1,6	14,20
Sr	25,06	3,13	10,52	727,899	0,09	77,51	6,4	651,69
Y	1,07	0,47	2,79	8,563	0,33	14,27	5,7	12,10
Zr	9,64	0,33	2,30	153,441	0,18	12,23	12,1	44,90
Nb	0,58	0,01	0,31	6,469	0,01	0,17	1,0	11,87
Mo	0,11	0,09	0,10	0,480	0,07	0,06	0,065	0,44
Ru	0,006				0,006	0,005	0,007	0,072
Rh	0,001				0,000	0,001	0,002	0,019
Pd	0,016				0,005	0,023	0,020	0,100
Ag	0,022	0,001	0,008	0,058	0,007	0,013	0,081	0,261
Cd	0,049	0,129	0,097	0,136	0,087	0,085	0,115	0,178
In	0,053	0,004	0,014	0,028	0,006	0,016	0,011	0,035
Sn	0,468	0,020	0,040	0,212	0,028	0,037	0,088	0,282
Sb	0,030	0,008	0,002	0,000	0,014	0,022	0,015	0,059
Te	0,152	0,055	0,135	0,377	0,012	0,034	8,411	0,122
Cs	0,155	0,042	0,112	2,514	0,038	0,099	0,223	2,393
Ba	12,69	0,84	1,37	550,342	0,05	3,34	0,762	246,71

Table 7. LA-ICP-MS average analyses (continued).

	bulk rock	olivine	pigeonite	mesostasis	olivine	augite	pigeonite38	mesostasis
	NWA 8694	NWA8693	NWA8694	NWA8694	Chassigny	Chassigny	Chassigny	Chassigny
n	8	5	5	10	7	2	1	6
La	0,830	0,005	0,188	30,790	0,024	8,330	0,955	10,289
Ce	3,442	0,006	0,636	67,687	0,051	22,297	3,626	23,355
Pr	0,280	0,001	0,125	8,256	0,007	3,579	0,686	3,384
Nd	1,117	0,006	0,739	32,125	0,021	17,412	3,540	14,026
Sm	0,226	0,003	0,271	4,990	0,003	4,094	0,978	3,203
Eu	0,067	0,001	0,060	2,146	0,001	0,862	0,202	1,740
Gd	0,225	0,017	0,376	3,856	0,011	4,097	1,132	3,203
Tb	0,034	0,005	0,071	0,447	0,004	0,602	0,182	0,498
Dy	0,209	0,055	0,498	2,164	0,039	3,353	1,157	2,756
Ho	0,043	0,018	0,108	0,335	0,013	0,596	0,217	0,486
Er	0,125	0,071	0,317	0,653	0,050	1,414	0,583	1,111
Tm	0,018	0,013	0,044	0,060	0,010	0,155	0,073	0,119
Yb	0,117	0,092	0,273	0,276	0,071	0,801	0,398	0,578
Lu	0,020	0,018	0,043	0,033	0,014	0,101	0,055	0,071



Hf	0,255	0,008	0,071	3,633	0,006	0,608	0,365	1,242
Ta	0,039	0,000	0,013	0,622	0,000	0,013	0,076	0,593
W	0,094	0,004	0,041	0,461	0,013	0,019	0,070	0,652
Re	0,0009				0,0002	0,0000	0,0000	0,0007
Os	0,0008				0,0001	0,0002	0,0004	0,0009
Ir	0,0008				0,0001	0,0001	0,0010	0,0005
Pt	0,2336				0,0003	0,0006	0,0014	0,0393
Au	0,0006				0,0009	0,0007	0,0028	0,1086
Tl	0,007	0,001	0,003	0,042	0,001	0,001	0,082	0,022
Pb	0,545	0,156	0,236	5,516	0,177	0,418	12,803	3,542
Bi	0,005	0,003	0,002	0,004	0,003	0,002	0,012	0,013
Th	0,092	0,001	0,032	3,014	0,001	0,351	0,106	0,817
U	0,082	0,030	0,102	0,563	0,002	0,083	0,019	0,211

---

Table 7. LA-ICP-MS average analyses (continued).

	bulk rock	olivine	pigeonite	mesostasis	olivine	augite	pigeonite38	mesostasis
	NWA 8694	NWA8693	NWA8694	NWA8694	Chassigny	Chassigny	Chassigny	Chassigny
n	8	5	5	10	7	2	1	6
La	0,830	0,005	0,188	30,790	0,024	8,330	0,955	10,289
Ce	3,442	0,006	0,636	67,687	0,051	22,297	3,626	23,355
Pr	0,280	0,001	0,125	8,256	0,007	3,579	0,686	3,384
Nd	1,117	0,006	0,739	32,125	0,021	17,412	3,540	14,026
Sm	0,226	0,003	0,271	4,990	0,003	4,094	0,978	3,203
Eu	0,067	0,001	0,060	2,146	0,001	0,862	0,202	1,740
Gd	0,225	0,017	0,376	3,856	0,011	4,097	1,132	3,203
Tb	0,034	0,005	0,071	0,447	0,004	0,602	0,182	0,498
Dy	0,209	0,055	0,498	2,164	0,039	3,353	1,157	2,756
Ho	0,043	0,018	0,108	0,335	0,013	0,596	0,217	0,486
Er	0,125	0,071	0,317	0,653	0,050	1,414	0,583	1,111
Tm	0,018	0,013	0,044	0,060	0,010	0,155	0,073	0,119
Yb	0,117	0,092	0,273	0,276	0,071	0,801	0,398	0,578
Lu	0,020	0,018	0,043	0,033	0,014	0,101	0,055	0,071
Hf	0,255	0,008	0,071	3,633	0,006	0,608	0,365	1,242
Ta	0,039	0,000	0,013	0,622	0,000	0,013	0,076	0,593
W	0,094	0,004	0,041	0,461	0,013	0,019	0,070	0,652
Re	0,0009				0,0002	0,0000	0,0000	0,0007
Os	0,0008				0,0001	0,0002	0,0004	0,0009
Ir	0,0008				0,0001	0,0001	0,0010	0,0005
Pt	0,2336				0,0003	0,0006	0,0014	0,0393
Au	0,0006				0,0009	0,0007	0,0028	0,1086
Tl	0,007	0,001	0,003	0,042	0,001	0,001	0,082	0,022
Pb	0,545	0,156	0,236	5,516	0,177	0,418	12,803	3,542
Bi	0,005	0,003	0,002	0,004	0,003	0,002	0,012	0,013
Th	0,092	0,001	0,032	3,014	0,001	0,351	0,106	0,817
U	0,082	0,030	0,102	0,563	0,002	0,083	0,019	0,211

Table 7. LA-ICP-MS average analyses for NWA 8694 and Chassigny.

n	bulk rock	olivine	pigeonite	mesostasis	olivine	augite	pigeonite38	mesostasis
	NWA 8694	NWA8693	NWA8694	NWA8694	Chassigny	Chassigny	Chassigny	Chassigny
	8	5	5	11	7	2	1	6
SiO2	EMP 37.41	35.21	52.24	57.60	36.39	50.01	53.1	52.97
Al2O3	0.50	0.02	0.67	20.90	0.03	1.43	0.83	16.00
TiO2	0.06	0.03	0.16	0.07	0.02	0.31	0.182	0.43
Cr2O3	0.49	0.05	0.48	0.01	0.10	1.02	0.50	0.09
FeOT	36.16	38.26	22.28	2.85	28.79	10.35	15.42	7.99
MnO	0.81	0.84	0.77	0.06	0.57	0.36	0.481	0.19
MgO	23.46	25.37	18.97	1.54	33.89	18.13	23.12	9.64
CaO	0.82	0.22	4.77	5.69	0.19	17.73	6.35	7.09
Na2O	0.17	0.02	0.13	7.19	0.02	0.39	0.17	4.55
K2O	0.06	0.01	0.02	2.55	0.00	0.01	0.029	0.65
P2O5	0.05	0.03	0.01	1.53	0.03	0.57	0.00	0.42
Li	3.43	4.49	3.82	43.58	4.29	4.58	2.58	37.89
Be	0.04	0.01	0.09	1.05	0.01	0.09	0.17	2.14
B	1.09	1.00	3.35	9.00	0.67	1.20	4.0	9.73
S	0.01	0.01	0.01	0.10	0.01	0.02	1.13	0.51
Cl	269.00	385.31	388.60	363.28	372.72	642.33	367	497.14
Sc	7.62	6.77	25.82	4.58	6.21	52.99	29.3	10.31
V	38.04	9.37	115.87	2.73	8.01	187.69	108	24.98
Cr	0.34	356.33	3261.44	39.22	0.07	0.70	0.343	0.06
Co	101.89	124.04	56.17	20.97	132.72	38.27	49	43.07
Ni	258.72	345.13	114.08	51.03	500.06	126.18	140	338.98
Cu	5.94	2.21	4.73	11.08	0.65	9.49	31	101.72
Zn	95.87	109.16	84.45	10.98	70.01	22.91	44	26.44
Ga	0.84	0.19	1.51	15.97	0.16	2.91	1.9	9.08
Ge	0.84	1.28	2.23	0.38	1.19	1.83	1.73	1.91
As	0.03	0.05	0.03	-0.21	0.05	0.04	0.06	0.04
Se	0.05	0.05	0.02	0.02	0.03	-0.07	0.7	1.07
Rb	1.53	0.17	0.67	40.76	0.13	0.29	1.6	14.20
Sr	25.06	3.13	10.52	727.90	0.09	77.51	6.4	651.69
Y	1.07	0.47	2.79	8.56	0.33	14.27	5.7	12.10
Zr	9.64	0.33	2.30	153.44	0.18	12.23	12.1	44.90
Nb	0.58	0.01	0.31	6.47	0.01	0.17	1.0	11.87
Mo	0.11	0.09	0.10	0.48	0.07	0.06	0.065	0.44
	0.01				0.01	0.01	0.007	0.07
	0.00				0.00	0.00	0.002	0.02
	0.02				0.01	0.02	0.020	0.10
Ag	0.02	0.00	0.01	0.05	0.01	0.01	0.081	0.26
Cd	0.05	0.13	0.10	0.14	0.09	0.09	0.115	0.18
In	0.05	0.00	0.01	0.03	0.01	0.02	0.011	0.04
Sn	0.47	0.02	0.04	0.21	0.03	0.04	0.088	0.28
Sb	0.03	0.01	0.00	-0.08	0.01	0.02	0.015	0.06
Te	0.15	0.06	0.14	0.30	0.01	0.03	8.4	0.12
Cs	0.15	0.04	0.11	2.51	0.04	0.10	0.2	2.39
Ba	12.69	0.84	1.37	550.34	0.05	3.34	1	246.71

Table 8. Compositions of parent liquids and olivine used in PETROLOG calculations.

Parent Liquid	SiO <sub>2</sub>	TiO <sub>2</sub>	Al <sub>2</sub> O <sub>3</sub>	Cr <sub>2</sub> O <sub>3</sub>	FeO	MnO	MgO	CaO	Na <sub>2</sub> O	K <sub>2</sub> O	P <sub>2</sub> O <sub>5</sub>	Total
NWA 2737 A# (He)	49.37	1.98	8.44	0.26	19.00	0.22	12.11	6.06	1.58	0.61	0.16	99.70
Parent 1-3KD	50.92	0.09	8.00	0.39	26.00	0.58	6.50	3.45	2.70	1.44	0.41	100.48
Parent 2-1KD	51.93	0.12	6.36	0.59	26.14	0.58	6.54	3.96	2.66	0.92	0.58	100.38
Parent 2-5KD	48.07	0.09	4.78	0.46	32.40	0.72	8.1	3.1	1.59	0.84	0.25	100.40
Nakhla ol core (Treiman)	33.60	0.05	0.08	0.03	48.60	0.96	17.50	0.29	0.05	0.00	0.00	100.70
NA01a (Stockstill)	56.00	1.30	10.70	0.02	14.50	0.39	2.10	8.20	3.40	2.00	0.65	99.20
NA01a &10ol	53.76	1.18	9.64	0.02	17.91	0.45	3.64	7.41	3.07	1.80	0.59	99.35
NA01a &20ol	51.52	1.05	8.58	0.02	21.32	0.50	5.18	6.62	2.73	1.60	0.52	99.50

Table S1. All LA-ICP-MS analyses for NWA 8694 and Chassigny.

	olivine 26-NWA	olivine 27-NWA	olivine 28-NWA	olivine 29-NWA	olivine 30-NWA	pyroxene 31-NWA	pyroxene 32-NWA	pyroxene 33-NWA
<b>SiO2</b>	35,3	35,1	35,1	35,4	35,2	52,2	52,6	51,1
<b>Al2O3</b>	0,02	0,02	0,05	0,02	0,02	0,74	0,66	0,64
<b>TiO2</b>	0,022	0,024	0,035	0,030	0,018	0,180	0,157	0,146
<b>Cr2O3</b>	0,02	0,02	0,19	0,02	0,02	0,85	0,41	0,37
<b>FeOT</b>	38,02	38,44	38,38	38,24	38,24	21,97	22,00	22,69
<b>MnO</b>	0,839	0,824	0,839	0,834	0,843	0,768	0,755	0,765
<b>MgO</b>	25,50	25,35	25,36	25,22	25,42	18,82	18,83	19,14
<b>CaO</b>	0,24	0,21	0,21	0,20	0,24	5,18	4,85	5,33
<b>Na2O</b>	0,01	0,02	0,02	0,02	0,02	0,13	0,14	0,16
<b>K2O</b>	0,003	0,004	0,007	0,006	0,006	0,012	0,011	0,020
<b>P2O5</b>	0,03	0,05	0,02	0,01	0,02	0,00	0,01	0,01
<b>Li</b>	3,70	4,99	5,16	3,94	4,65	4,13	3,79	3,58
<b>Be</b>	0,01	0,01	0,01	0,01	0,01	0,11	0,08	0,13
<b>B</b>	1,03	0,91	1,35	0,84	0,87	3,35	3,13	3,27
<b>S</b>	0,01	0,01	0,01	0,01	0,01	0,01	0,01	0,01
<b>Cl</b>	414,38	399,34	374,20	380,21	358,39	435,03	364,58	407,57
<b>Sc</b>	7,13	6,68	6,77	6,58	6,69	25,95	26,95	25,71
<b>V</b>	6,46	6,07	21,04	6,60	6,66	142,05	116,12	108,68
<b>Cr</b>	126,52	114,87	1274,46	133,55	132,26	5835,79	2793,37	2552,16
<b>Co</b>	124,11	122,18	125,05	124,70	124,17	55,49	55,83	58,80
<b>Ni</b>	345,91	337,60	352,26	343,64	346,26	109,55	113,85	126,11
<b>Cu</b>	2,21	1,22	4,98	1,22	1,41	4,29	4,12	4,64
<b>Zn</b>	108	107	106	114	111	94	81	78
<b>Ga</b>	0,2	0,1	0,3	0,2	0,1	2,0	1,4	1,4
<b>Ge</b>	1,39	1,21	1,29	1,17	1,33	2,24	2,25	2,08
<b>As</b>	0,06	0,04	0,05	0,04	0,06	0,04	0,03	0,03
<b>Se</b>	0,05	0,08	0,01	0,06	0,04	0,05	0,01	0,01
<b>Rb</b>	0,06	0,15	0,21	0,20	0,22	0,39	0,34	0,76
<b>Sr</b>	2,88	2,93	4,41	2,94	2,49	9,65	9,31	12,16
<b>Y</b>	0,56	0,45	0,42	0,49	0,43	2,96	2,58	3,46
<b>Zr</b>	0,16	0,42	0,21	0,67	0,17	1,94	1,14	3,83
<b>Nb</b>	0,00	0,01	0,01	0,01	0,00	0,24	0,12	0,46
<b>Mo</b>	0,083	0,079	0,095	0,087	0,102	0,103	0,087	0,089
<b>Ru</b>								
<b>Rh</b>								
<b>Pd</b>								
<b>Ag</b>	0,001	0,001	0,002	0,001	0,001	0,002	0,002	0,031
<b>Cd</b>	0,111	0,071	0,082	0,170	0,214	0,105	0,089	0,099
<b>In</b>	0,004	0,003	0,004	0,005	0,005	0,009	0,008	0,040
<b>Sn</b>	0,024	0,019	0,017	0,019	0,022	0,036	0,028	0,052
<b>Sb</b>	0,005	0,002	0,003	0,010	0,017	0,002	0,002	0,002
<b>Te</b>	0,092	0,042	0,036	0,067	0,039	0,146	0,178	0,128
<b>Cs</b>	0,004	0,037	0,051	0,056	0,064	0,088	0,083	0,119
<b>Ba</b>	0,753	0,679	1,055	0,796	0,902	1,037	0,969	1,392
<b>La</b>	0,005	0,009	0,006	0,006	0,001	0,103	0,171	0,393

<b>Ce</b>	0,006	0,012	0,005	0,006	0,002	0,452	0,547	1,362
<b>Pr</b>	0,001	0,002	0,001	0,001	0,000	0,103	0,102	0,250
<b>Nd</b>	0,007	0,010	0,008	0,004	0,003	0,670	0,601	1,425
<b>Sm</b>	0,003	0,004	0,004	0,004	0,002	0,286	0,229	0,435
<b>Eu</b>	0,001	0,001	0,001	0,001	0,001	0,063	0,057	0,084
<b>Gd</b>	0,023	0,018	0,012	0,014	0,017	0,391	0,344	0,542
<b>Tb</b>	0,006	0,004	0,004	0,005	0,005	0,079	0,063	0,097
<b>Dy</b>	0,070	0,055	0,048	0,053	0,050	0,537	0,450	0,654
<b>Ho</b>	0,023	0,017	0,013	0,018	0,017	0,115	0,101	0,133
<b>Er</b>	0,082	0,065	0,065	0,077	0,064	0,343	0,292	0,376
<b>Tm</b>	0,015	0,013	0,011	0,013	0,012	0,045	0,043	0,052
<b>Yb</b>	0,101	0,098	0,087	0,097	0,079	0,291	0,263	0,295
<b>Lu</b>	0,019	0,017	0,018	0,018	0,016	0,045	0,044	0,045
<b>Hf</b>	0,004	0,011	0,007	0,014	0,005	0,065	0,048	0,113
<b>Ta</b>	0,000	0,000	0,001	0,001	0,000	0,007	0,003	0,015
<b>W</b>	0,005	0,003	0,008	0,003	0,003	0,019	0,029	0,043
<b>Re</b>								
<b>Os</b>								
<b>Ir</b>								
<b>Pt</b>								
<b>Au</b>								
<b>Tl</b>	0,001	0,001	0,002	0,001	0,001	0,003	0,003	0,004
<b>Pb</b>	0,303	0,093	0,219	0,110	0,055	0,223	0,192	0,365
<b>Bi</b>	0,003	0,002	0,002	0,004	0,005	0,003	0,001	0,002
<b>Th</b>	0,000	0,001	0,001	0,001	0,000	0,017	0,018	0,046
<b>U</b>	0,035	0,024	0,046	0,021	0,024	0,109	0,103	0,098

pyroxene	pyroxene	mesostasis	mesostasis	mesostasis	mesostasis	mesostasis
34-NWA8694	35-NWA8694	36-NWA8694	37-NWA8694	38-NWA8694	39-NWA8694	40-NWA8694
52,7	52,6	42,5	57,9	58,1	59,6	60,5
0,65	0,64	5,74	21,72	19,84	23,84	23,77
0,150	0,155	0,072	0,073	0,055	0,078	0,076
0,34	0,41	0,01	0,00	0,00	0,00	0,00
22,87	21,85	27,34	4,40	2,65	0,55	0,24
0,792	0,771	0,598	0,063	0,050	0,009	0,006
19,18	18,88	18,14	1,77	1,25	0,35	0,28
3,51	4,96	2,17	4,50	5,44	4,89	4,62
0,12	0,13	2,21	7,46	7,18	9,04	8,42
0,024	0,019	0,441	1,816	3,352	1,503	2,039
0,01	0,01	0,82	0,34	2,04	0,12	0,11
3,85	3,77	15,01	34,39	35,38	119,82	105,20
0,08	0,07	0,40	1,10	1,06	1,17	1,14
4,06	2,94	5,02	8,14	7,83	3,05	4,93
0,01	0,01	0,03	0,92	0,02	0,00	-0,01
373,14	362,68	1209,72	224,42	1121,37	-1853,00	-1581,53
23,36	27,11	5,98	4,48	4,65	8,75	5,56
93,93	118,54	3,40	1,45	1,08	0,98	0,93
2315,43	2810,46	62,79	18,08	10,54	-2,25	-2,57
56,26	54,50	85,25	156,33	15,51	1,03	-0,33
113,24	107,67	260,71	100,28	41,93	67,45	56,32
7,50	3,07	15,57	22,30	7,61	4,01	4,03
88	81	88	15	12	4	3
1,5	1,3	4,8	15,3	15,9	16,7	17,2
2,22	2,35	1,31	0,86	0,63	-0,45	-0,34
0,03	0,02	0,05	-0,08	-0,16	-0,10	-0,78
0,00	0,04	0,01	2,39	0,18	-1,26	-0,21
0,98	0,87	8,10	42,49	73,67	24,40	33,59
12,37	9,10	195,53	601,21	681,29	760,75	765,33
2,44	2,48	4,19	2,23	11,01	0,21	0,48
2,94	1,64	2,13	13,58	2,86	0,30	14,11
0,53	0,18	5,53	2,06	0,36	0,09	2,79
0,118	0,085	0,204	0,423	0,367	1,256	0,973
0,002	0,003	0,011	0,032	0,057	-0,011	0,065
0,115	0,077	0,044	0,101	0,040	0,250	0,246
0,007	0,008	0,010	0,013	0,012	0,123	0,035
0,047	0,037	0,179	0,198	0,565	0,186	0,218
0,002	0,002	0,002	-0,037	-0,042	-0,269	-0,170
0,146	0,078	0,613	0,529	0,158	-0,073	0,014
0,144	0,124	0,743	2,254	2,456	5,985	4,872
2,514	0,962	106	350	538	442	559
0,198	0,071	11,985	9,891	38,034	3,393	3,842

0,529	0,289	23,597	17,398	81,142	4,939	5,650
0,098	0,073	3,055	2,010	10,568	0,432	0,707
0,530	0,471	12,934	8,125	41,784	1,499	2,545
0,195	0,211	2,122	1,341	6,745	0,158	0,287
0,043	0,052	0,629	1,634	2,177	1,885	2,018
0,290	0,313	1,721	0,964	5,292	0,124	0,329
0,057	0,059	0,202	0,125	0,598	0,016	0,034
0,419	0,429	1,001	0,607	2,852	0,024	0,335
0,097	0,097	0,167	0,072	0,437	0,009	0,028
0,287	0,289	0,362	0,152	0,845	0,003	0,069
0,037	0,040	0,035	0,025	0,082	0,001	0,005
0,256	0,260	0,174	0,069	0,264	0,006	0,023
0,042	0,041	0,027	0,011	0,034	0,023	-0,004
0,074	0,052	0,051	0,417	0,071	0,011	0,386
0,029	0,013	0,280	0,191	0,043	0,005	0,144
0,083	0,032	0,569	0,150	1,392	0,011	0,555

0,004	0,003	0,012	0,032	0,030	0,008	-0,008
0,281	0,119	2,528	6,667	9,217	4,639	6,806
0,001	0,002	0,001	0,002	0,005	-0,001	0,009
0,050	0,027	1,378	0,996	3,137	0,043	0,434
0,111	0,091	0,264	0,183	0,655	0,019	0,082



mesostasis 41-NWA8694	mesostasis 42-NWA8694	mesostasis* 43-NWA8694	mesostasis 44-NWA8694	mesostasis 45-NWA8694	mesostasis 46-NWA8694	mesostasis (pH) 47-NWA8694
59,2	58,3	61,7	52,7	58,6	59,5	47,5
22,96	19,92	18,97	15,17	23,78	24,04	15,91
0,086	0,046	0,093	0,087	0,046	0,071	0,030
0,00	0,00	0,00	0,05	0,00	0,00	0,00
1,36	3,42	2,99	11,19	2,42	0,22	1,93
0,027	0,067	0,061	0,278	0,035	0,004	0,044
0,79	1,76	1,79	7,65	0,94	0,14	0,26
5,14	4,86	1,47	5,79	5,21	5,58	15,07
7,86	6,86	6,05	5,14	8,04	8,09	4,93
1,954	3,180	6,519	0,869	0,891	1,820	4,145
0,63	1,50	0,32	1,10	0,04	0,56	10,09
31,45	28,44	21,43	24,89	24,55	34,29	19,50
0,92	1,35	0,91	0,93	1,29	1,22	0,45
11,16	12,63	16,27	5,22	6,56	6,87	16,32
0,01	0,05	0,01	0,04	0,02	0,01	0,10
318,88	692,30	269,00	549,96	-125,90	470,59	3910,02
3,40	3,25	3,31	6,58	2,68	3,37	4,34
1,13	1,06	0,97	18,36	1,61	0,96	1,46
4,31	17,93	9,78	358,48	13,64	0,40	3,11
4,35	9,94	10,94	30,59	1,08	0,17	1,07
32,28	50,30	42,42	99,98	23,85	23,45	23,06
3,23	8,66	3,45	14,81	8,75	5,58	39,48
9	12	11	39	3	5	8
16,2	15,1	13,5	12,8	15,5	16,1	21,5
0,64	0,50	0,58	0,75	0,61	0,53	-0,12
-0,18	-0,10	-0,16	-0,03	-0,10	-0,20	-0,41
0,47	-0,70	-0,21	-0,42	0,30	0,19	-0,55
20,57	41,94	89,10	7,13	6,54	17,65	91,33
842,57	675,95	379,71	732,51	903,56	870,11	793,89
3,88	8,35	2,01	7,51	0,19	2,60	55,73
41,83	2,99	106,00	8,25	0,33	39,98	1457,61
6,45	0,39	37,99	0,84	0,09	4,61	15,49
0,279	0,307	0,336	0,392	0,176	0,480	0,295
0,030	0,033	0,021	0,006	0,002	0,094	0,243
0,119	0,094	0,115	0,048	0,049	0,195	0,238
0,024	0,018	0,012	0,010	0,022	0,024	0,019
0,142	0,170	0,251	0,088	0,059	0,181	0,273
-0,054	-0,048	-0,057	-0,042	-0,073	-0,033	-0,027
0,097	0,813	0,263	0,723	0,211	-0,061	0,584
2,002	1,837	2,024	1,319	1,179	1,733	1,994
552	602	901	317	413	619,1	760,9
15,174	30,476	9,660	23,157	4,123	12,185	188,750

29,899	65,611	37,286	52,027	5,628	22,944	422,032
4,230	8,347	2,227	6,503	0,489	2,929	52,367
14,949	33,489	8,095	26,695	1,998	12,062	202,130
2,204	5,447	1,263	3,926	0,158	1,697	31,669
2,222	2,049	1,432	1,969	1,899	2,229	4,087
1,833	4,302	0,947	3,446	0,165	1,475	23,544
0,211	0,466	0,108	0,395	0,021	0,145	2,798
1,000	2,211	0,499	1,910	0,053	0,694	13,619
0,165	0,359	0,080	0,301	0,010	0,096	2,130
0,256	0,630	0,204	0,607	0,009	0,186	4,228
0,035	0,052	0,022	0,058	0,002	0,020	0,363
0,177	0,233	0,096	0,315	0,013	0,082	1,757
0,015	0,029	0,007	0,030	0,002	0,012	0,171
1,089	0,090	2,344	0,294	0,034	1,464	33,761
0,514	0,031	1,726	0,073	0,008	0,593	3,511
0,202	0,565	0,130	0,152	0,282	0,870	0,763
0,026	0,035	0,044	0,039	0,016	0,015	0,175
4,304	4,634	5,915	3,170	3,953	4,283	7,090
0,001	0,000	0,003	-0,001	0,002	0,006	0,009
1,617	2,510	5,199	1,321	0,035	1,153	16,709
0,303	0,523	0,917	0,321	0,152	0,224	2,814

track		olivine	olivine	olivine	olivine	olivine
48-NWA8694		26-Chassigny	27-Chassigny	28-Chassigny	29-Chassigny	30-Chassigny
33,2	SiO2	36,5	36,2	36,5	36,3	36,5
12,82	Al2O3	0,02	0,11	0,02	0,02	0,02
1,281	TiO2	0,021	0,035	0,017	0,017	0,018
0,31	Cr2O3	e+A1	0,46	0,03	0,04	0,04
23,18	FeO(t)	28,82	29,07	28,53	28,64	28,84
0,527	MnO	0,571	0,574	0,566	0,564	0,568
13,71	MgO	33,88	33,48	34,12	34,19	33,82
11,21	CaO	0,15	0,17	0,19	0,22	0,21
2,71	Na2O	0,01	0,02	0,02	0,02	0,01
0,557	K2O	0,003	0,004	0,003	0,004	0,004
0,78	P2O5	0,02	0,02	0,07	0,02	0,02
2,46	Li	3,47	3,56	5,25	4,31	4,20
0,33	Be	0,02	0,01	0,01	0,01	0,02
5,39	B	0,52	0,62	0,85	0,55	0,58
0,08	S	0,03	0,01	0,01	0,01	0,01
538,40	Cl	388,72	378,24	387,75	346,26	379,90
28,60	Sc	6,00	6,06	6,69	6,22	6,41
79,33	V	5,14	23,25	5,26	5,42	5,62
2107,22	Cr	0,02	0,31	0,02	0,03	0,03
70,23	Co	132,49	134,32	131,53	131,21	133,19
613,09	Ni	509,00	505,32	494,34	489,57	498,85
13,11	Cu	0,98	1,02	0,83	0,42	0,43
55	Zn	69	71	68	69	71
21,8	Ga	0,1	0,4	0,1	0,1	0,1
2,55	Ge	1,03	1,14	1,34	1,33	1,25
0,25	As	0,08	0,04	0,04	0,05	0,03
0,28	Se	0,06	0,05	-0,02	0,02	0,05
22,22	Rb	0,11	0,13	0,10	0,13	0,13
284,50	Sr	0,05	0,25	0,04	0,15	0,03
85,15	Y	0,33	0,40	0,31	0,33	0,35
392,31	Zr	0,55	0,17	0,11	0,09	0,07
22,19	Nb	0,00	0,01	0,00	0,00	0,02
0,190	Mo	0,054	0,057	0,068	0,086	0,069
	Ru	0,005	0,003	0,005	0,010	0,007
	Rh	0,001	0,000	0,001	0,000	0,000
	Pd	0,007	0,004	0,005	0,005	0,003
0,035	Ag	0,006	0,028	0,003	0,002	0,001
0,292	Cd	0,089	0,077	0,067	0,075	0,090
0,198	In	0,006	0,005	0,005	0,006	0,008
1,671	Sn	0,035	0,031	0,025	0,018	0,026
0,010	Sb	0,022	0,013	0,018	0,014	0,006
0,603	Te	0,035	0,014	0,014	0,009	0,003
0,464	Cs	0,042	0,032	0,030	0,032	0,041
169,5	Ba	0,046	0,173	0,017	0,061	0,011
26,786	La	0,007	0,027	0,028	0,030	0,009

50,934	Ce	0,009	0,072	0,082	0,045	0,048
7,950	Pr	0,001	0,008	0,006	0,014	0,002
40,921	Nd	0,006	0,027	0,019	0,042	0,006
12,098	Sm	0,002	0,004	0,002	0,006	0,006
3,387	Eu	0,002	0,001	0,001	0,002	0,001
17,992	Gd	0,008	0,015	0,010	0,012	0,012
2,906	Tb	0,003	0,004	0,004	0,004	0,004
18,921	Dy	0,038	0,051	0,033	0,043	0,040
3,969	Ho	0,012	0,014	0,013	0,013	0,013
11,247	Er	0,052	0,058	0,050	0,048	0,047
1,483	Tm	0,009	0,019	0,009	0,008	0,009
8,815	Yb	0,068	0,076	0,075	0,071	0,066
1,408	Lu	0,014	0,013	0,014	0,013	0,015
13,947	Hf	0,019	0,007	0,004	0,003	0,002
2,208	Ta	0,001	0,001	0,000	0,001	0,000
2,716	W	0,009	0,035	0,007	0,008	0,012
	Re	0,000	0,000	0,000	0,001	0,000
	Os	0,000	0,000	0,000	0,001	0,000
	Ir	0,000	0,000	0,000	0,000	0,000
	Pt	-0,001	0,001	0,001	0,000	0,000
	Au	0,001	0,002	0,001	0,001	0,000
0,122	Tl	0,001	0,000	0,001	0,001	0,000
13,110	Pb	0,714	0,122	0,099	0,073	0,060
0,038	Bi	0,003	0,002	0,003	0,002	0,002
5,279	Th	0,001	0,002	0,000	0,000	0,000
1,008	U	0,004	0,002	0,003	0,002	0,001

olivine 31-Chassigny	olivine 32-Chassigny	pyroxene 33-Chassigny	pyroxene 34-Chassigny	pyroxene 35-Chassigny	pyroxene 36-Chassigny	pyroxene 37-Chassigny
36,4	36,4	41,6	39,2	52,0	48,1	47,5
0,02	0,02	0,33	0,80	1,28	1,58	9,31
0,020	0,017	0,082	0,202	0,306	0,323	0,130
0,04	0,04	0,59	3,48	1,11	0,93	0,30
28,77	28,87	24,11	23,78	9,30	11,40	12,91
0,572	0,573	0,567	0,511	0,358	0,371	0,434
33,95	33,81	30,61	28,55	17,25	19,00	22,55
0,18	0,19	2,14	4,43	18,41	17,05	4,36
0,02	0,02	0,08	0,12	0,36	0,43	1,97
0,004	0,004	0,008	0,010	0,005	0,020	0,623
0,01	0,02	0,03	0,04	0,01	1,12	0,01
4,19	5,06	4,48	5,14	4,89	4,27	315,95
0,01	0,01	0,05	0,08	0,04	0,14	0,96
0,74	0,81	1,43	1,59	1,13	1,27	9,61
0,01	0,01	0,02	0,04	0,01	0,02	0,06
372,89	355,32	427,58	353,27	317,76	966,91	453,90
6,06	6,02	12,45	15,88	52,53	53,45	26,81
5,62	5,76	48,74	171,19	196,04	179,34	56,47
0,02	0,03	0,40	2,38	0,76	0,64	0,20
132,56	133,73	110,30	108,55	32,29	44,25	43,78
501,02	502,33	364,22	385,70	102,21	150,14	220,70
0,54	0,34	12,84	5,12	2,60	16,39	8,35
70	72	64	108	20	26	87
0,1	0,1	0,8	3,4	2,5	3,3	4,9
1,11	1,15	1,43	1,63	1,94	1,72	0,60
0,05	0,04	0,15	0,23	0,04	0,04	0,34
0,02	0,00	0,01	0,02	-0,12	-0,02	1,72
0,15	0,16	0,22	0,36	0,22	0,36	29,97
0,06	0,04	4,00	8,18	50,32	104,71	2,99
0,31	0,32	1,74	2,28	10,98	17,57	4,52
0,11	0,16	1,42	1,98	7,54	16,92	13,97
0,00	0,00	0,07	0,38	0,05	0,28	0,43
0,071	0,098	0,081	0,078	0,063	0,056	3,031
0,008	0,005	0,005	0,008	0,005	0,006	0,310
0,000	0,001	0,001	0,001	0,000	0,001	0,071
0,005	0,007	0,015	0,011	0,021	0,026	0,249
0,005	0,007	0,243	0,066	0,015	0,010	0,167
0,090	0,118	0,272	0,081	0,088	0,083	0,899
0,007	0,006	0,011	0,007	0,016	0,016	0,140
0,027	0,033	1,543	0,111	0,030	0,045	0,139
0,015	0,011	0,042	0,136	0,021	0,023	-0,100
0,004	0,006	0,010	0,091	0,027	0,040	0,483
0,047	0,042	0,055	0,103	0,083	0,115	11,177
0,034	0,025	0,324	0,421	0,111	7	1
0,057	0,012	0,233	0,295	1,451	15,209	1,001

0,039	0,058	0,910	1,219	6,393	38,202	3,142
0,005	0,010	0,169	0,235	1,414	5,744	0,550
0,021	0,027	0,961	1,289	8,408	26,417	2,304
0,002	0,000	0,282	0,398	2,524	5,664	1,024
0,000	0,001	0,072	0,101	0,596	1,129	0,165
0,010	0,012	0,320	0,458	2,799	5,395	0,919
0,003	0,003	0,052	0,075	0,436	0,769	0,105
0,033	0,037	0,347	0,472	2,496	4,209	0,977
0,012	0,012	0,072	0,092	0,456	0,737	0,203
0,048	0,048	0,203	0,245	1,116	1,713	0,606
0,009	0,009	0,026	0,033	0,127	0,183	0,085
0,076	0,064	0,159	0,188	0,676	0,926	0,338
0,014	0,013	0,025	0,029	0,088	0,113	0,034
0,004	0,005	0,050	0,074	0,390	0,826	0,446
0,000	0,000	0,004	0,015	0,004	0,022	0,036
0,009	0,009	0,018	0,042	0,008	0,029	0,083
0,000	0,000	0,000	0,001	0,000	0,000	-0,009
0,000	0,000	0,001	0,001	0,000	0,001	0,071
0,000	0,000	0,000	0,001	0,000	0,000	-0,001
0,000	0,001	-0,001	0,000	0,001	0,000	-0,025
0,001	0,000	0,002	0,007	0,001	0,001	0,217
0,000	0,001	0,002	0,002	0,000	0,001	0,008
0,091	0,079	4,399	24,466	0,244	0,592	5,590
0,002	0,003	0,004	0,008	0,002	0,002	0,078
0,000	0,000	0,012	0,030	0,008	0,695	0,082
0,002	0,002	0,008	0,013	0,005	0,161	0,010

pyroxene 38-Chassigny	pyroxene 39-Chassigny	pyroxene? 40-Chassigny	melt? Plag 41-Chassigny	melt? 42-Chassigny	melt? 43-Chassigny	melt? 44-Chassigny
53,1	40,6	41,6	46,1	53,6	58,1	36,6
0,83	2,22	0,21	29,25	16,15	11,50	0,36
0,182	0,597	0,061	0,044	0,360	0,538	0,024
0,50	18,86	0,13	0,01	0,05	0,09	0,03
15,42	19,48	25,22	3,86	6,24	5,32	27,82
0,481	0,537	0,561	0,084	0,186	0,186	0,563
23,12	19,02	31,65	4,02	8,19	8,60	33,97
6,35	4,44	0,59	14,21	9,61	9,00	0,28
0,17	0,14	0,03	2,03	4,25	5,70	0,30
0,029	0,015	0,009	0,333	0,319	0,240	0,078
0,00	0,01	0,01	0,07	1,05	0,74	0,03
2,58	2,71	4,06	71,91	57,09	43,44	37,99
0,17	0,10	0,07	1,41	2,42	2,89	0,11
3,97	1,58	0,90	2,49	10,24	14,72	1,61
1,13	0,03	0,02	0,01	0,06	0,06	0,02
366,53	337,46	358,90	118,25	441,53	642,40	484,75
29,31	20,09	9,13	3,43	11,38	17,65	6,15
107,80	620,51	22,53	1,91	15,52	27,89	5,10
0,34	12,91	0,09	0,01	0,04	0,06	0,02
48,94	76,79	110,17	16,23	21,82	17,37	132,16
139,51	132,73	393,88	88,53	98,81	75,93	490,37
31,47	8,05	0,64	3,63	6,59	7,52	20,01
44	178	66	16	24	18	88
1,9	9,7	0,5	16,4	10,1	7,7	0,4
1,73	1,51	1,25	1,29	2,34	2,54	0,94
0,06	0,05	0,04	-0,10	0,11	0,00	0,09
0,75	-0,02	0,03	-0,24	-0,30	-0,52	-0,06
1,64	0,58	0,45	10,73	7,36	6,58	3,85
6,43	5,97	0,11	1592,84	751,50	182,48	9,91
5,68	2,48	0,84	0,95	21,36	24,94	0,29
12,05	1,97	1,04	1,45	56,45	103,77	0,75
1,01	0,33	0,06	0,25	5,52	7,68	0,13
0,065	0,085	0,089	0,608	0,434	0,315	0,353
0,007	0,019	0,005	0,051	0,053	0,035	0,043
0,002	0,001	0,001	0,014	0,005	0,011	0,008
0,020	0,012	0,007	0,053	0,132	0,157	0,020
0,081	0,029	0,009	0,094	0,414	0,106	1,852
0,115	0,145	0,104	0,170	0,200	0,154	0,450
0,011	0,010	0,009	0,023	0,058	0,051	0,060
0,088	0,482	0,028	0,055	0,155	0,171	2,716
0,015	0,020	0,017	0,000	0,097	0,139	0,023
8,411	0,064	0,008	0,182	0,149	0,109	0,108
0,223	0,161	0,169	3,120	2,464	1,853	1,414
1	1	0	99	254	42	1
1,0	0,4	0,1	6,7	22,6	14,5	0,3

3,6	1,4	0,1	11,7	49,1	37,0	0,8
0,7	0,2	0,0	1,2	7,2	6,0	0,1
3,5	1,3	0,1	4,4	28,3	26,1	0,3
1,0	0,4	0,0	0,6	6,1	6,1	0,0
0,2	0,1	0,0	3,2	2,3	1,4	0,0
1,1	0,4	0,1	0,6	5,9	6,3	0,1
0,2	0,1	0,0	0,1	0,9	1,0	0,0
1,2	0,5	0,1	0,3	5,0	5,6	0,0
0,2	0,1	0,0	0,1	0,8	1,1	0,0
0,6	0,3	0,1	0,1	1,9	2,4	0,0
0,1	0,0	0,0	0,0	0,2	0,3	0,0
0,4	0,2	0,1	0,1	0,9	1,2	0,1
0,1	0,0	0,0	0,0	0,1	0,2	0,0
0,365	0,075	0,034	0,033	1,578	2,948	0,030
0,076	0,012	0,002	0,017	0,443	0,534	0,006
0,070	0,058	0,027	0,051	0,723	0,962	0,028
0,000	0,001	0,000	-0,003	0,001	-0,002	0,005
0,000	0,000	0,000	-0,004	0,005	0,001	-0,002
0,001	0,000	0,000	0,003	0,000	0,000	0,001
0,001	0,002	0,000	-0,008	0,002	0,006	-0,005
0,003	0,003	0,000	0,007	0,013	0,007	0,006
0,082	0,004	0,001	0,012	0,017	0,036	0,003
12,803	0,534	0,155	1,891	2,273	2,101	0,549
0,012	0,002	0,002	0,006	0,020	0,003	0,015
0,106	0,018	0,013	0,050	1,460	1,535	0,018
0,019	0,009	0,003	0,035	0,367	0,355	0,007



melt? 45-Chassigny	melt? 46-Chassigny	chromite 47-Chassigny	opaque? 48-Chassigny	melt? 49-Chassigny	melt? 50-Chassigny	chromite 51-Chassigny
37,2	37,3	0,1	33,0	53,8	50,4	3,3
0,17	0,03	8,64	12,65	12,11	7,26	7,74
0,020	0,016	1,975	1,276	0,718	0,845	1,765
0,03	0,04	73,48	0,43	0,18	0,20	69,48
27,99	27,84	33,60	23,45	11,88	14,85	32,29
0,565	0,558	0,504	0,525	0,209	0,353	0,509
33,43	33,66	4,11	13,67	11,19	19,01	6,33
0,25	0,25	0,14	11,10	2,43	3,25	0,06
0,25	0,24	0,48	2,72	6,33	2,44	0,36
0,064	0,074	0,154	0,556	0,741	1,261	0,118
0,02	0,03	0,01	0,78	0,46	0,17	0,01
35,21	40,64	71,87	2,11	35,15	5,36	46,48
0,15	0,22	0,24	0,34	3,76	1,81	0,33
1,46	0,90	2,13	5,42	20,15	8,51	1,33
0,01	0,01	0,01	0,09	2,71	0,22	0,01
377,19	389,20	328,95	630,73	785,56	638,51	228,37
5,72	6,18	4,63	28,06	11,80	14,71	5,36
4,76	5,54	2066,33	79,86	48,63	53,53	1970,61
0,02	0,03	50,28	0,30	0,12	0,14	47,54
127,46	127,00	183,47	67,46	112,06	64,22	176,60
588,48	503,48	179,36	568,00	1358,25	298,79	200,28
2,63	0,83	9,88	10,84	559,05	30,04	2,74
82	81	1274	56	37	44	885
0,3	0,2	38,7	20,5	5,0	4,5	30,1
1,11	1,11	0,90	2,35	1,93	2,65	0,84
0,06	-0,03	-0,02	0,24	0,05	0,09	-0,03
0,13	-0,19	-0,27	0,35	6,90	0,48	-0,28
3,09	3,72	8,13	22,30	21,39	28,41	6,52
6,94	0,06	0,29	282,76	360,85	246,03	0,62
0,27	0,22	0,03	84,53	13,53	11,74	0,08
0,43	0,08	3,19	389,40	62,15	45,22	2,67
0,05	0,01	0,98	22,12	33,86	23,85	0,75
0,329	0,397	0,685	0,194	0,968	0,200	0,726
0,059	0,041	0,263	0,034	0,228	0,033	0,247
0,001	-0,001	0,006	0,010	0,071	0,007	0,003
0,021	0,023	0,042	0,173	0,171	0,072	0,022
0,088	0,010	0,062	0,035	0,712	0,089	0,067
0,080	0,179	0,227	0,314	0,193	0,116	0,161
0,057	0,049	0,105	0,198	0,042	0,017	0,041
0,068	0,052	0,102	1,828	0,681	0,478	0,071
0,001	-0,015	-0,002	0,014	0,024	0,051	0,043
0,346	-0,013	0,231	0,628	0,198	0,048	0,275
1,157	1,385	3,085	0,451	4,422	1,747	2,323
1	0,0	0,1	169,6	403,4	203,3	2,1
0,1	0,0	0,1	26,7	10,7	3,6	0,1

0,4	0,2	0,2	51,1	26,5	11,2	0,5
0,0	0,0	0,0	8,0	3,7	1,7	0,1
0,2	0,1	0,1	40,7	16,1	8,3	0,0
0,0	0,0	0,0	12,1	3,9	2,4	0,0
0,0	0,0	0,0	3,4	1,1	0,8	0,0
0,0	0,0	0,0	18,0	3,7	2,7	0,0
0,0	0,0	0,0	2,9	0,6	0,4	0,0
0,1	0,0	0,0	18,9	3,1	2,6	0,0
0,0	0,0	0,0	4,0	0,5	0,5	0,0
0,0	0,0	0,0	11,2	1,1	1,1	0,0
0,0	0,0	0,0	1,5	0,1	0,1	0,0
0,1	0,1	0,0	8,8	0,6	0,7	0,0
0,0	0,0	0,0	1,4	0,1	0,1	0,0
0,010	0,003	0,122	13,981	1,513	1,372	0,082
0,004	0,000	0,037	2,177	1,543	1,012	0,021
0,025	0,006	0,044	3,653	1,411	0,745	0,015
-0,001	0,000	0,005	0,002	0,009	0,001	0,011
-0,004	0,007	-0,008	0,037	0,003	0,000	0,003
0,000	0,000	0,000	0,039	0,000	0,000	0,003
-0,001	0,002	-0,012	0,033	0,207	0,033	0,001
-0,001	-0,001	-0,006	0,012	0,017	0,003	-0,007
0,001	0,000	0,003	0,119	0,031	0,027	0,007
0,258	0,035	1,305	13,454	5,046	5,024	3,525
0,004	0,001	0,001	0,038	0,011	0,005	0,003
0,007	0,000	0,004	5,289	1,269	0,577	0,004
0,005	0,000	0,005	1,030	0,337	0,163	0,009

melt? Plag

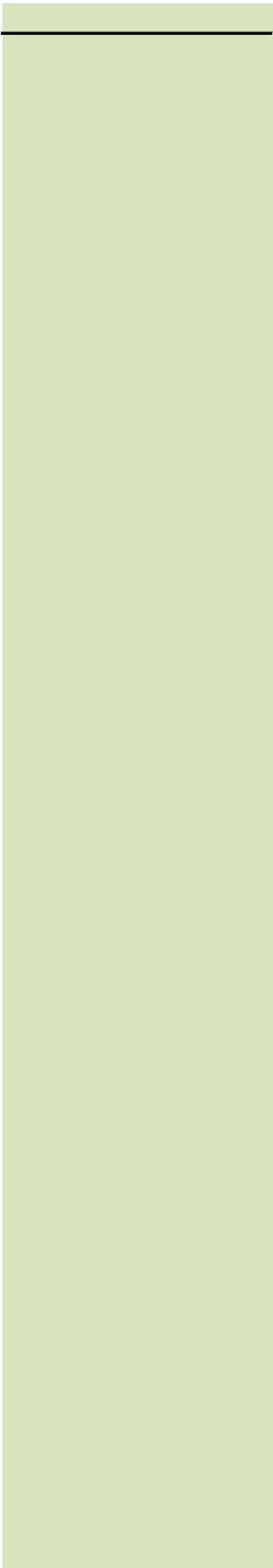
52-Chassigny	56-NWA8694	57-NWA8694	58-NWA8694	59-NWA8694	60-NWA8694
55,8 SiO2	32,1	31,2	31,2	32,2	31,4
19,72 Al2O3	0,63	0,41	0,42	0,81	0,58
0,047 TiO2	0,058	0,048	0,080	0,076	0,081
0,03 Cr2O3	0,39	0,26	0,78	0,52	0,72
5,81 FeOT	39,3	40,4	40,1	39,0	39,8
0,114 MnO	0,881	0,895	0,893	0,873	0,890
6,88 MgO	25,6	26,2	25,9	25,3	25,6
4,04 CaO	0,86	0,47	0,69	1,04	0,78
6,57 Na2O	0,22	0,15	0,13	0,26	0,19
1,032 K2O	0,063	0,069	0,052	0,086	0,057
0,02 P2O5	0,071	0,059	0,039	0,080	0,056
14,42 Li	3,56	3,83	3,79	3,86	3,72
0,55 Be	0,05	0,04	0,03	0,05	0,04
2,24 B	1,24	1,17	1,14	1,53	1,10
0,02 S	0,02	0,01	0,01	0,02	0,01
356,62 Cl	291,09	281,00	255,20	271,32	245,53
2,86 Sc	7,60	6,95	7,97	8,47	7,96
2,42 V	31,89	21,13	52,56	42,45	49,72
0,02 Cr	0,27	0,18	0,53	0,35	0,49
26,72 Co	112,99	115,20	114,14	109,96	111,57
113,59 Ni	285,53	296,49	290,61	287,48	281,65
3,50 Cu	4,39	5,50	6,02	11,59	6,94
21 Zn	102	101	106	105	107
10,7 Ga	0,9	0,6	1,0	1,1	1,0
0,73 Ge	0,88	0,88	0,90	0,92	0,91
0,07 As	0,01	0,01	0,03	0,04	0,06
0,08 Se	0,05	0,04	0,04	0,06	0,06
10,70	1,15	2,06	1,45	2,22	1,26
776,42 Rb	35,53	21,70	20,22	39,70	29,76
0,09 Sr	1,18	0,88	0,95	1,42	1,06
0,33 Y	10,07	7,84	10,73	10,45	9,85
0,09 Zr	0,55	1,41	0,64	0,61	0,45
0,144 Nb	0,097	0,102	0,124	0,119	0,119
0,035 Mo	0,005	0,007	0,008	0,014	0,006
0,005	0,001	0,001	0,001	0,003	0,001
0,016 Ag	0,017	0,014	0,018	0,018	0,016
0,153 Cd	0,023	0,017	0,024	0,023	0,025
0,238 In	0,044	0,031	0,161	0,034	0,032
0,020 Sn	0,007	0,007	0,390	0,012	0,012
0,152 Sb	0,234	0,385	0,530	0,697	0,672
0,042 Te	0,019	0,015	0,069	0,021	0,027
0,045	0,136	0,123	0,130	0,351	0,163
0,753 Cs	0,070	0,148	0,218	0,183	0,189
478,4 Ba	18,2	12,2	9,3	20,0	14,7
3,6 La	1,17	0,87	0,48	1,51	0,81

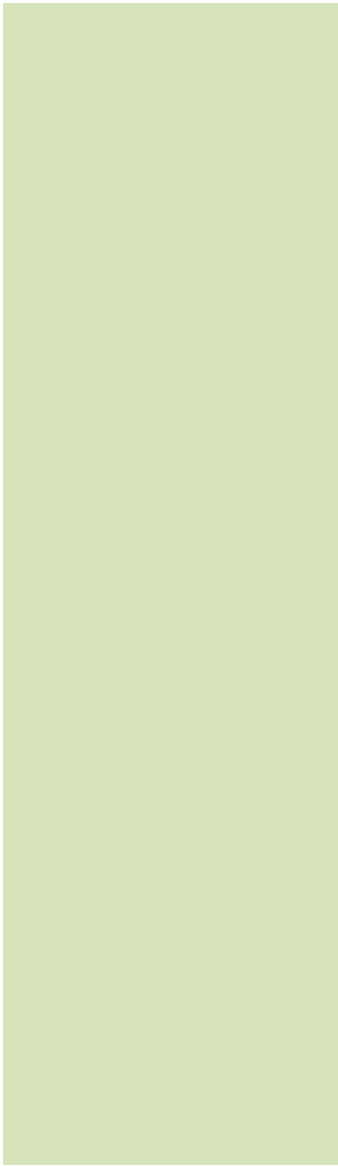
4,7 Ce	4,16	2,96	2,97	5,03	3,49
0,4 Pr	0,38	0,26	0,20	0,48	0,27
1,0 Nd	1,49	1,01	0,71	1,93	1,09
0,1 Sm	0,28	0,18	0,16	0,37	0,22
1,6 Eu	0,09	0,05	0,05	0,11	0,07
0,0 Gd	0,26	0,17	0,16	0,35	0,22
0,0 Tb	0,04	0,02	0,03	0,05	0,03
0,0 Dy	0,23	0,16	0,17	0,30	0,20
0,0 Ho	0,05	0,03	0,04	0,06	0,04
0,0 Er	0,13	0,11	0,12	0,16	0,13
0,0 Tm	0,02	0,02	0,02	0,02	0,02
0,0 Yb	0,12	0,11	0,12	0,13	0,12
0,0 Lu	0,02	0,02	0,02	0,02	0,02
0,009 Hf	0,261	0,203	0,262	0,284	0,260
0,009 Ta	0,045	0,068	0,043	0,051	0,032
0,022 W	0,091	0,111	0,092	0,111	0,106
0,000 Tl	0,000	0,000	0,004	0,000	0,002
0,002 Pb	0,001	0,000	0,001	0,003	0,001
0,000 Bi	0,001	0,001	0,001	0,003	0,001
-0,004 Th	1,895	0,066	0,005	0,002	0,002
0,605 U	0,001	0,001	0,001	0,001	0,001
0,009 Th/U	0,006	0,006	0,008	0,011	0,007
4,916	0,688	0,458	0,558	0,895	0,549
0,031 Cl-normalized F	0,005	0,003	0,012	0,004	0,008
0,009	0,123	0,123	0,078	0,135	0,076
0,009 La	0,071	0,069	0,068	0,088	0,226

61-NWA8694 62-NWA8694 63-NWA8694

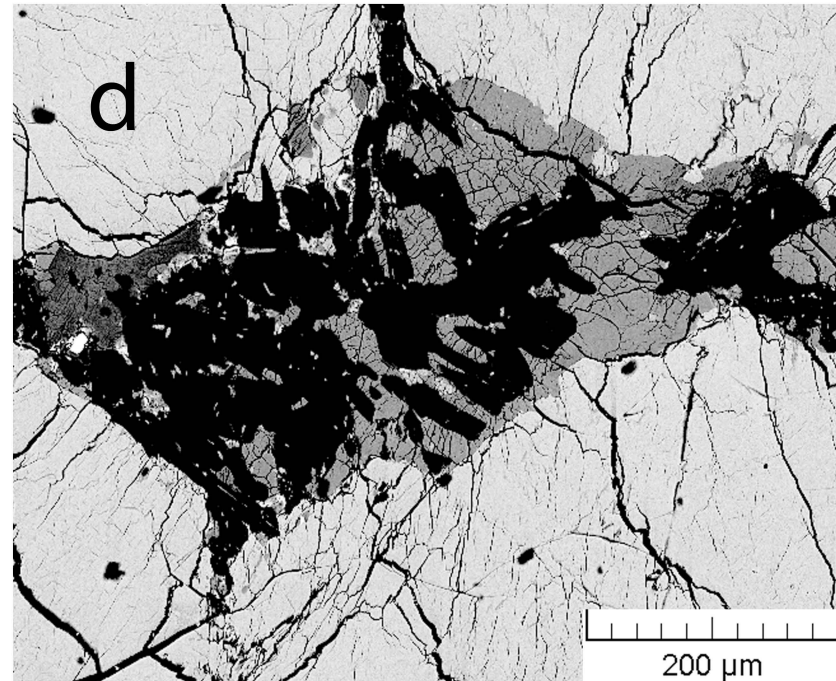
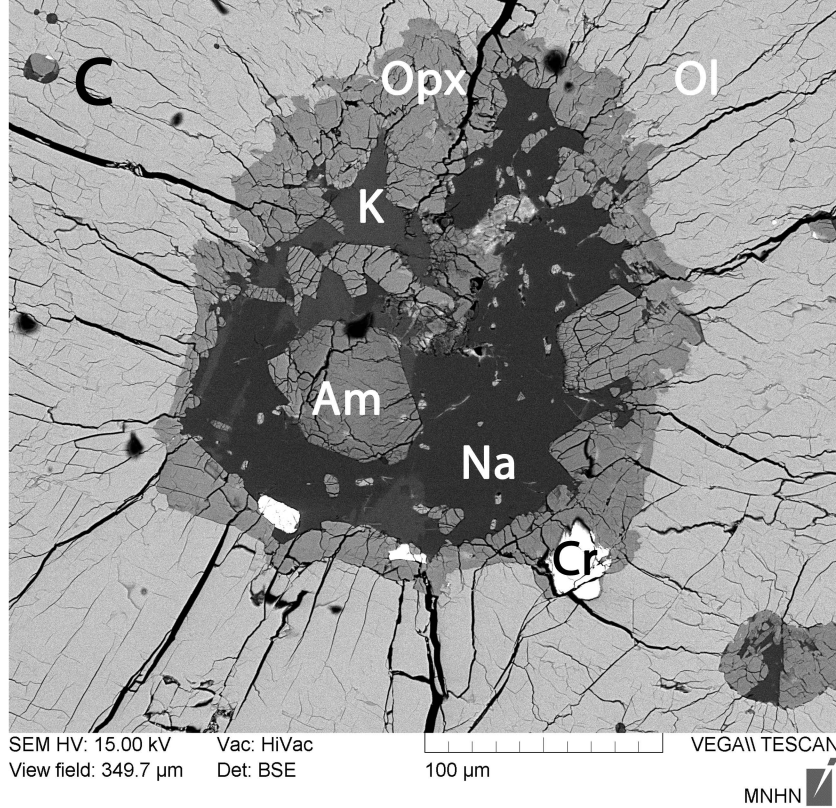
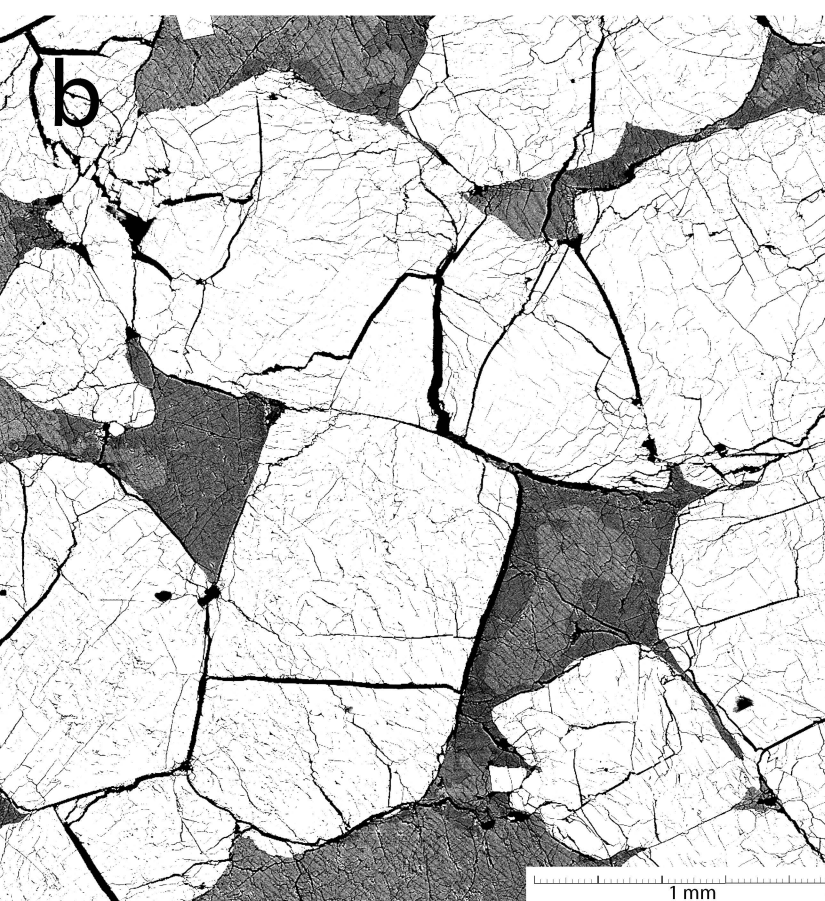
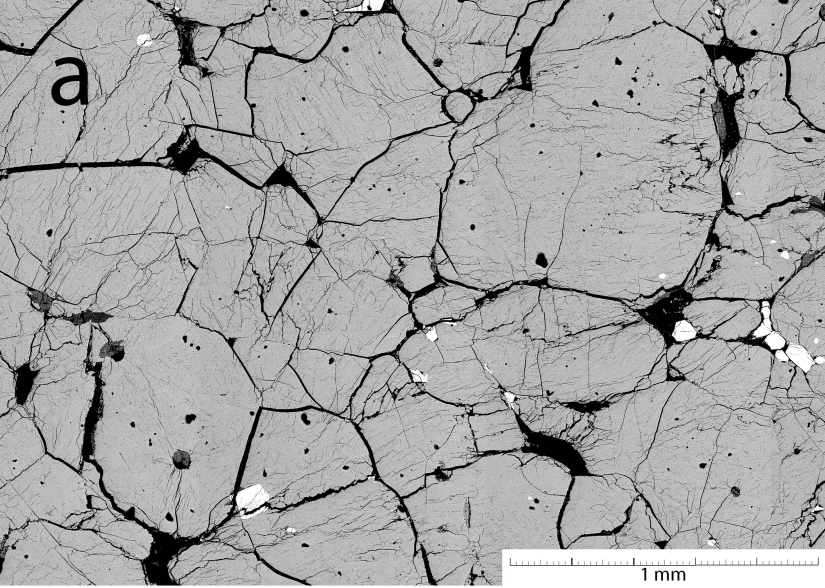
32,0	32,4	32,4
0,44	0,59	0,50
0,077	0,077	0,063
0,69	0,60	0,32
39,3	38,9	39,0
0,891	0,885	0,881
25,6	25,3	25,4
0,99	1,13	1,19
0,14	0,20	0,18
0,047	0,066	0,068
0,048	0,061	0,052
3,63	3,66	3,89
0,03	0,04	0,05
1,02	1,13	1,15
0,01	0,01	0,01
258,44	415,73	329,62
9,00	9,25	9,29
52,11	48,23	33,94
0,47	0,41	0,22
109,19	108,13	108,15
273,36	271,29	271,88
5,15	6,54	5,70
106	107	103
0,9	1,0	0,8
0,95	0,95	0,95
0,01	0,01	0,09
0,02	0,09	0,05
1,47	1,73	2,00
20,43	27,64	23,78
1,16	1,31	1,35
7,56	12,71	14,92
0,40	0,51	0,54
0,139	0,116	0,126
0,004	0,005	0,005
0,000	0,001	0,001
0,013	0,019	0,022
0,019	0,035	0,022
0,033	0,056	0,034
0,007	0,018	0,007
0,391	0,693	0,484
0,042	0,036	0,035
0,107	0,212	0,109
0,183	0,164	0,196
9,3	14,8	12,3
0,60	0,97	0,83

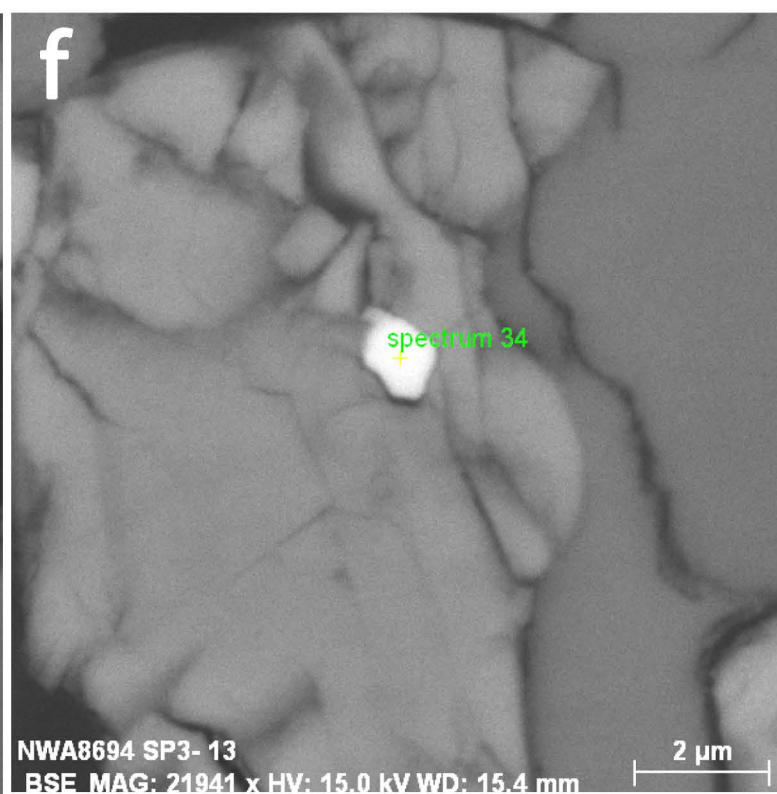
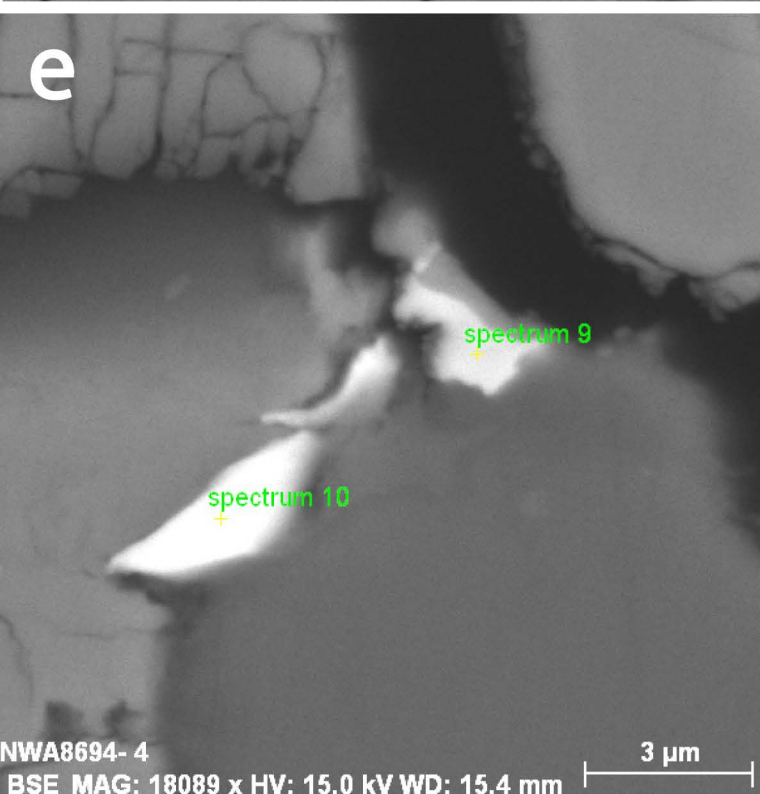
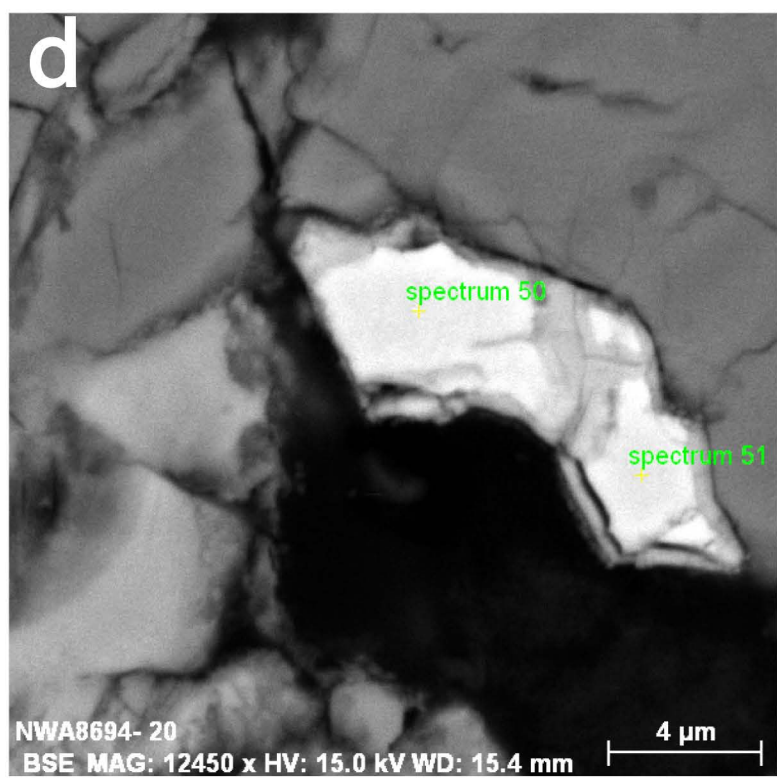
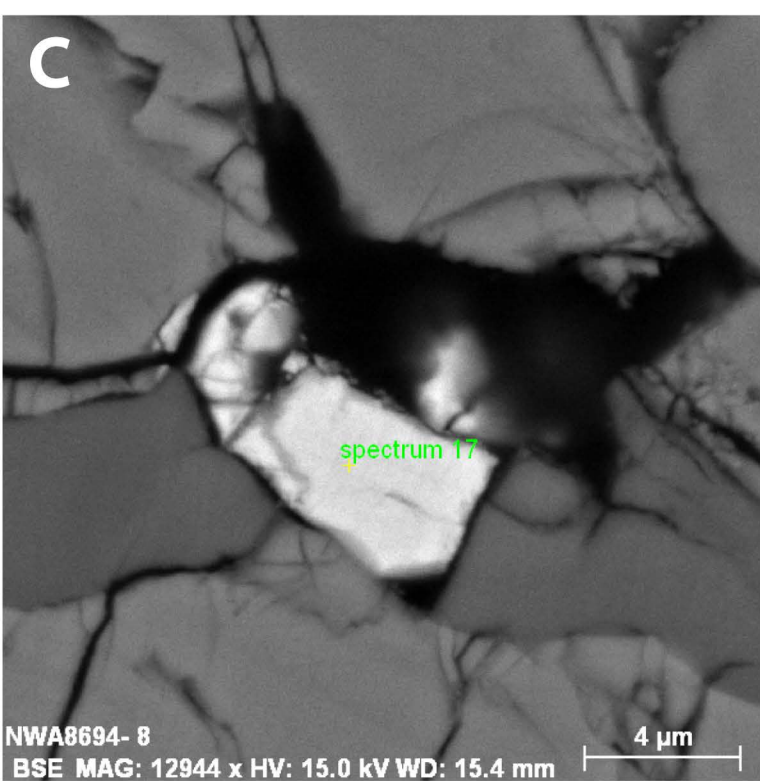
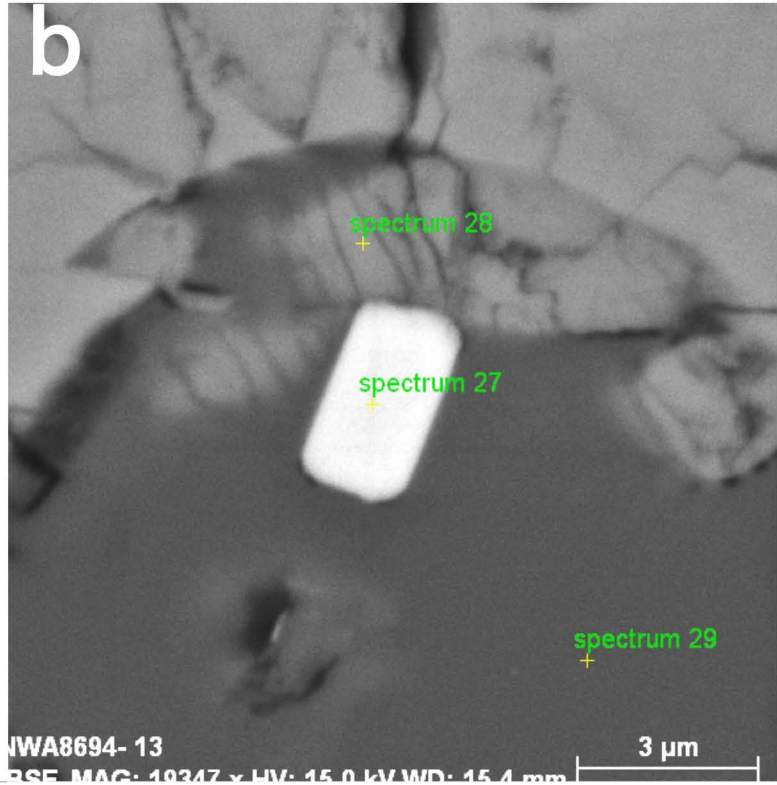
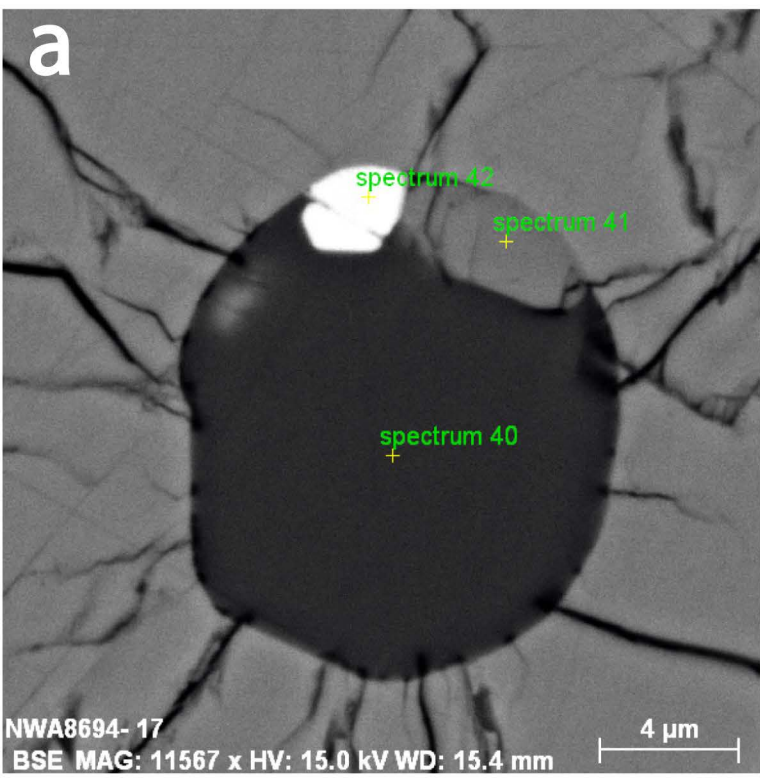
2,60	4,36	4,48
0,23	0,32	0,30
0,96	1,32	1,26
0,21	0,27	0,28
0,06	0,08	0,07
0,23	0,28	0,29
0,03	0,04	0,04
0,23	0,26	0,28
0,05	0,06	0,06
0,14	0,16	0,16
0,02	0,02	0,02
0,13	0,14	0,14
0,02	0,02	0,02
0,213	0,336	0,407
0,026	0,036	0,040
0,076	0,108	0,124
0,000	0,001	0,000
0,000	0,000	0,000
0,000	0,001	0,000
0,001	0,065	0,002
0,001	0,001	0,001
0,007	0,006	0,007
0,485	0,593	0,534
0,004	0,006	0,004
0,066	0,107	0,097
0,057	0,071	0,067

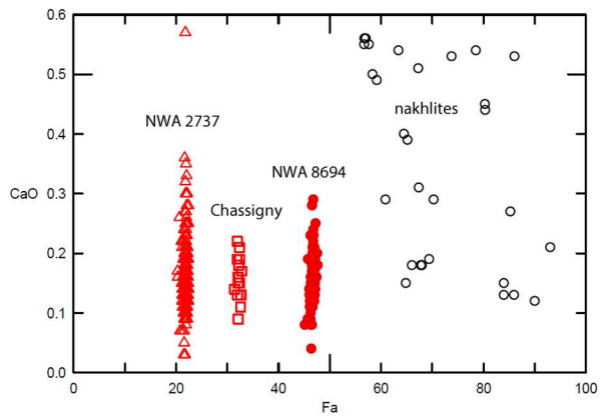
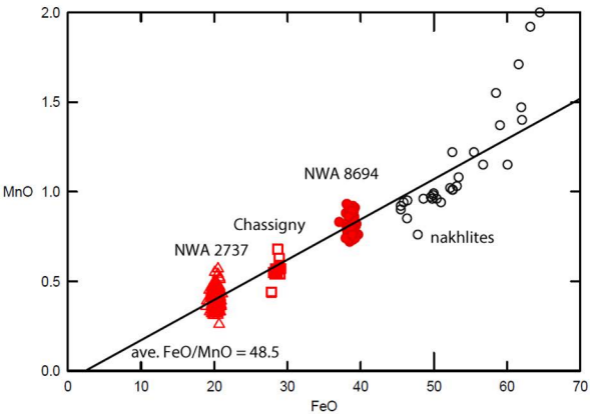


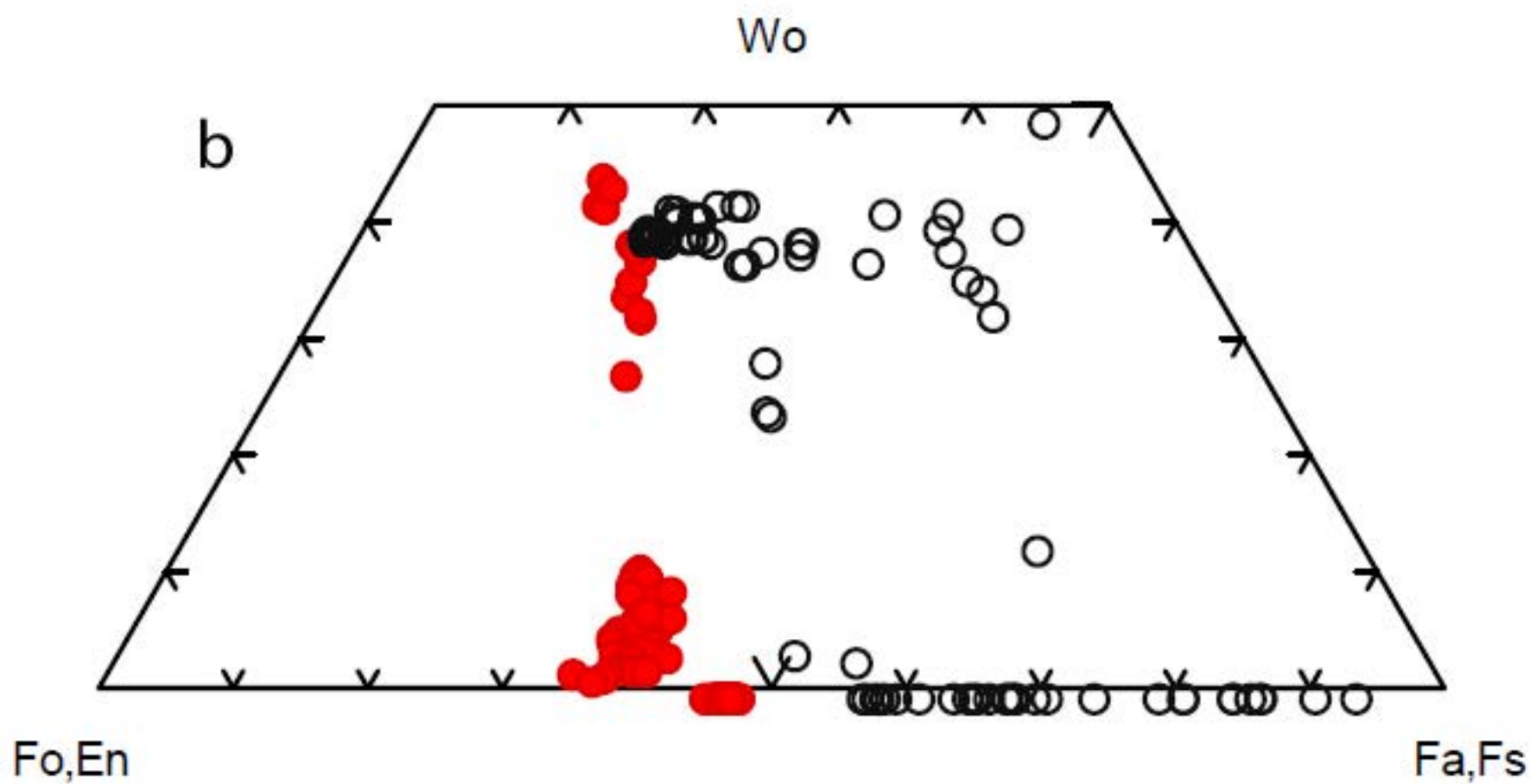
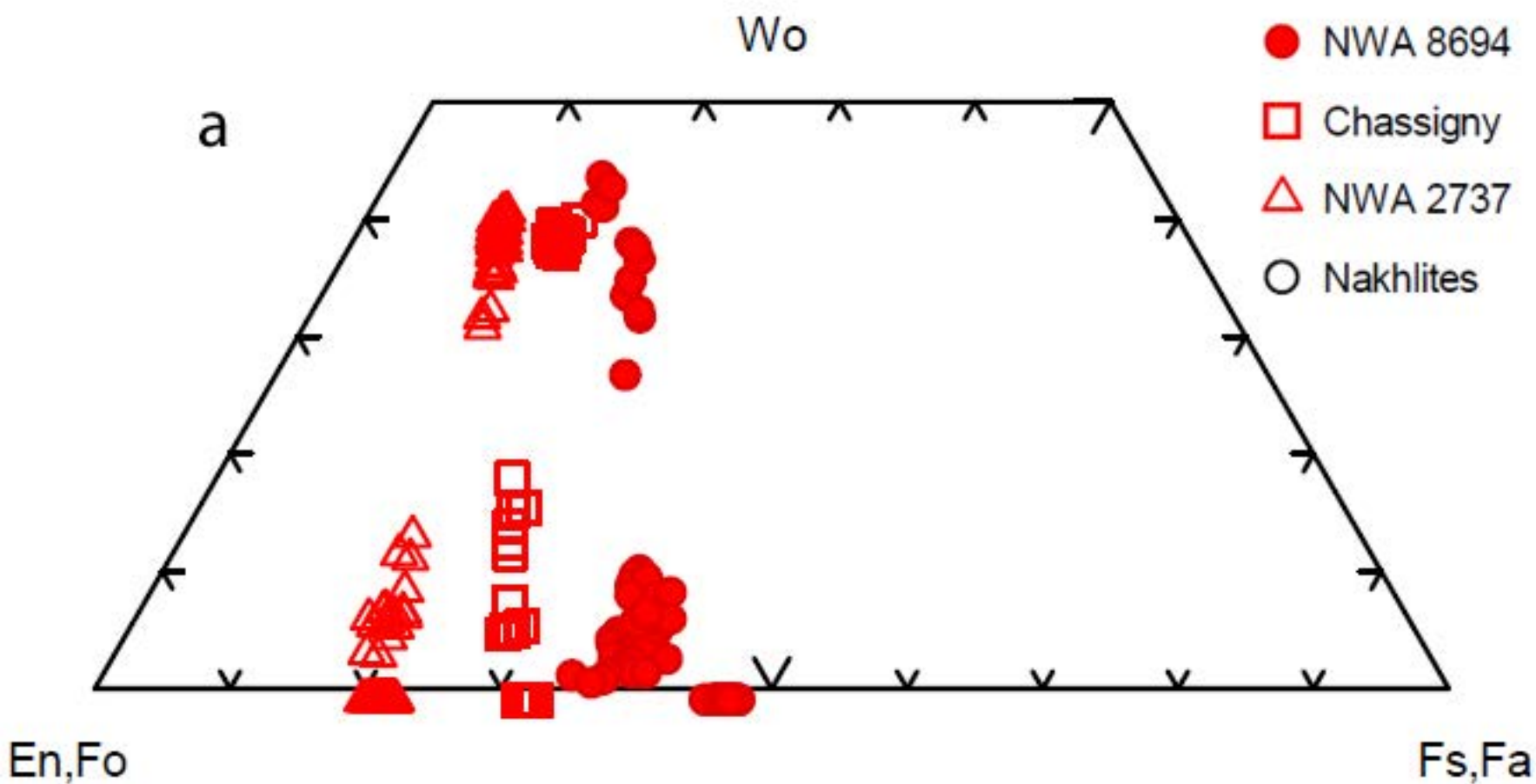


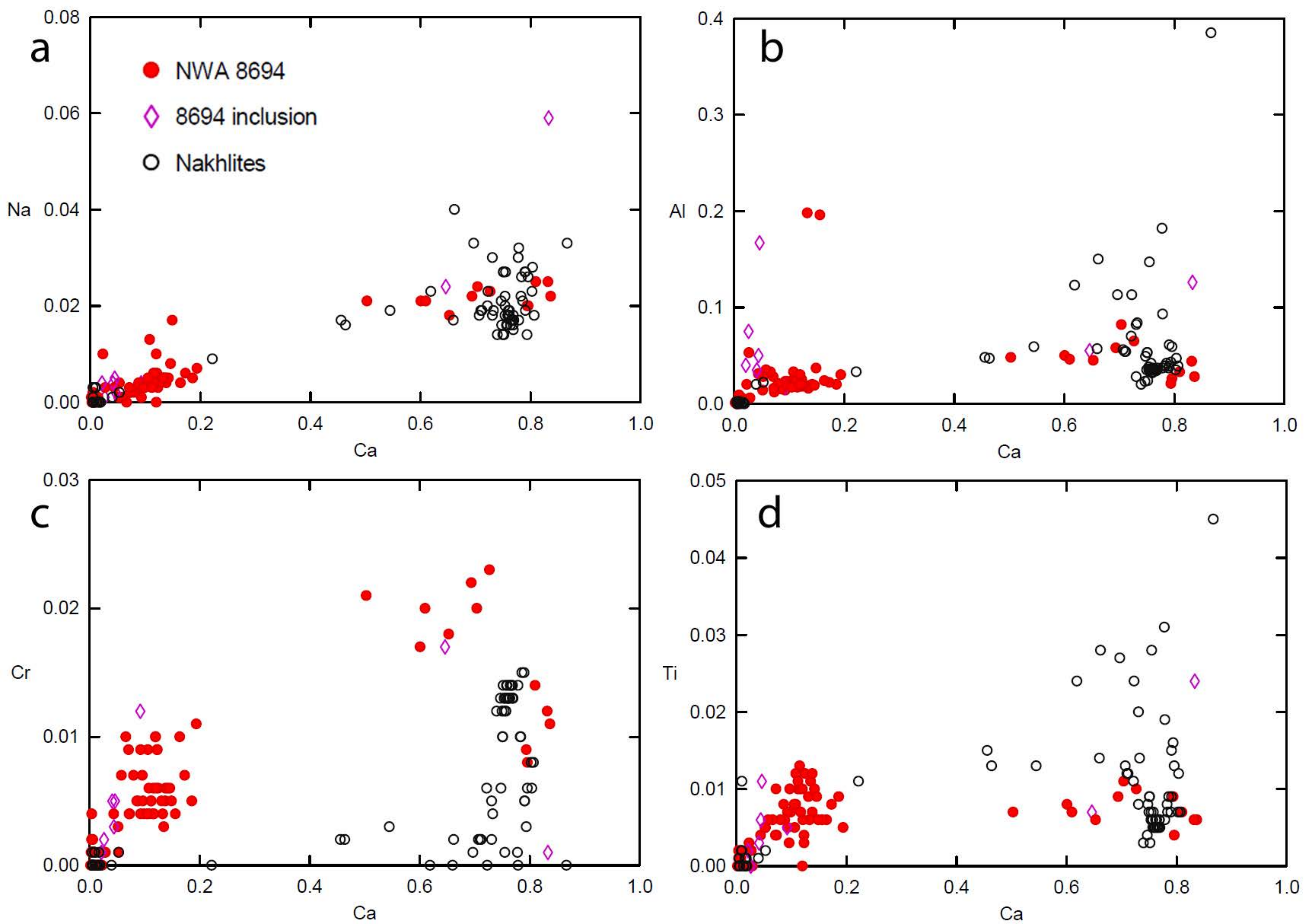






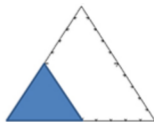






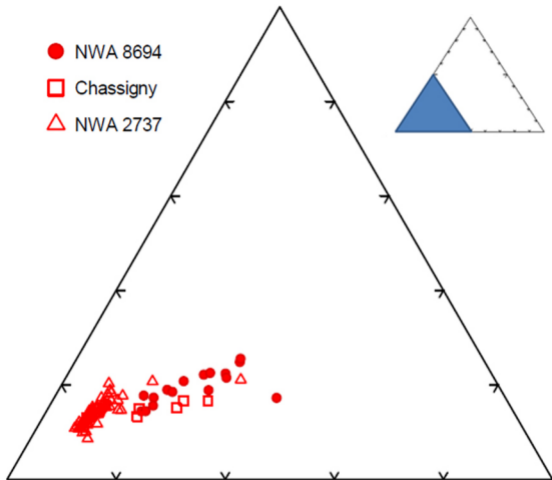
Mag50

- NWA 8694
- Chassigny
- △ NWA 2737



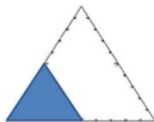
Chr100

Usp50



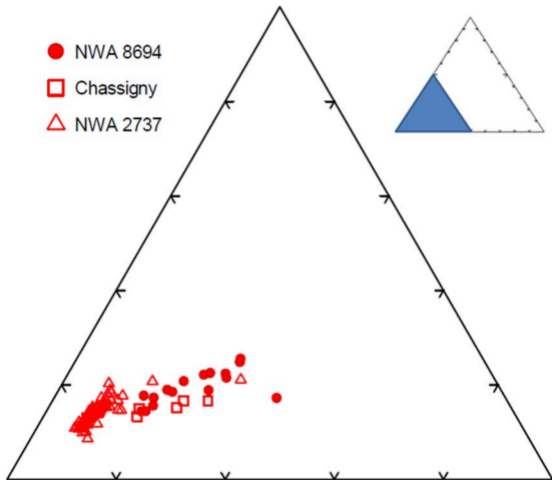
Mag50

- NWA 8694
- Chassigny
- △ NWA 2737



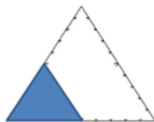
Chr100

Usp50



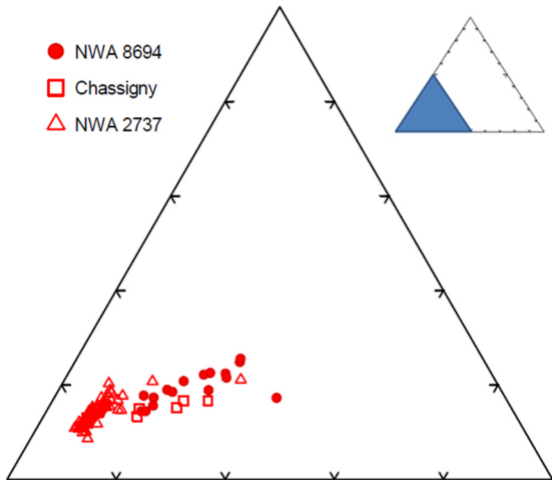
Mag50

- NWA 8694
- Chassigny
- △ NWA 2737

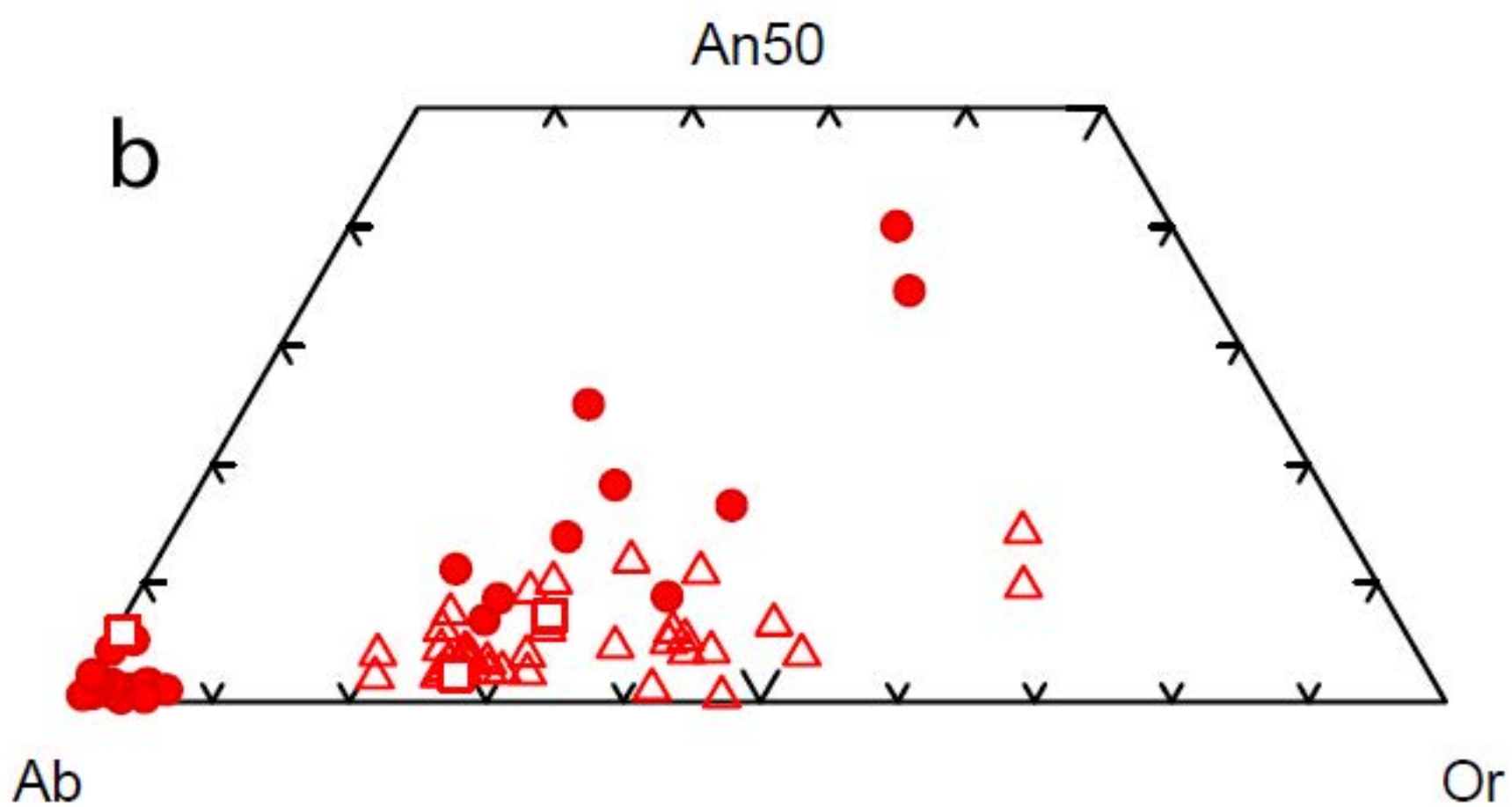
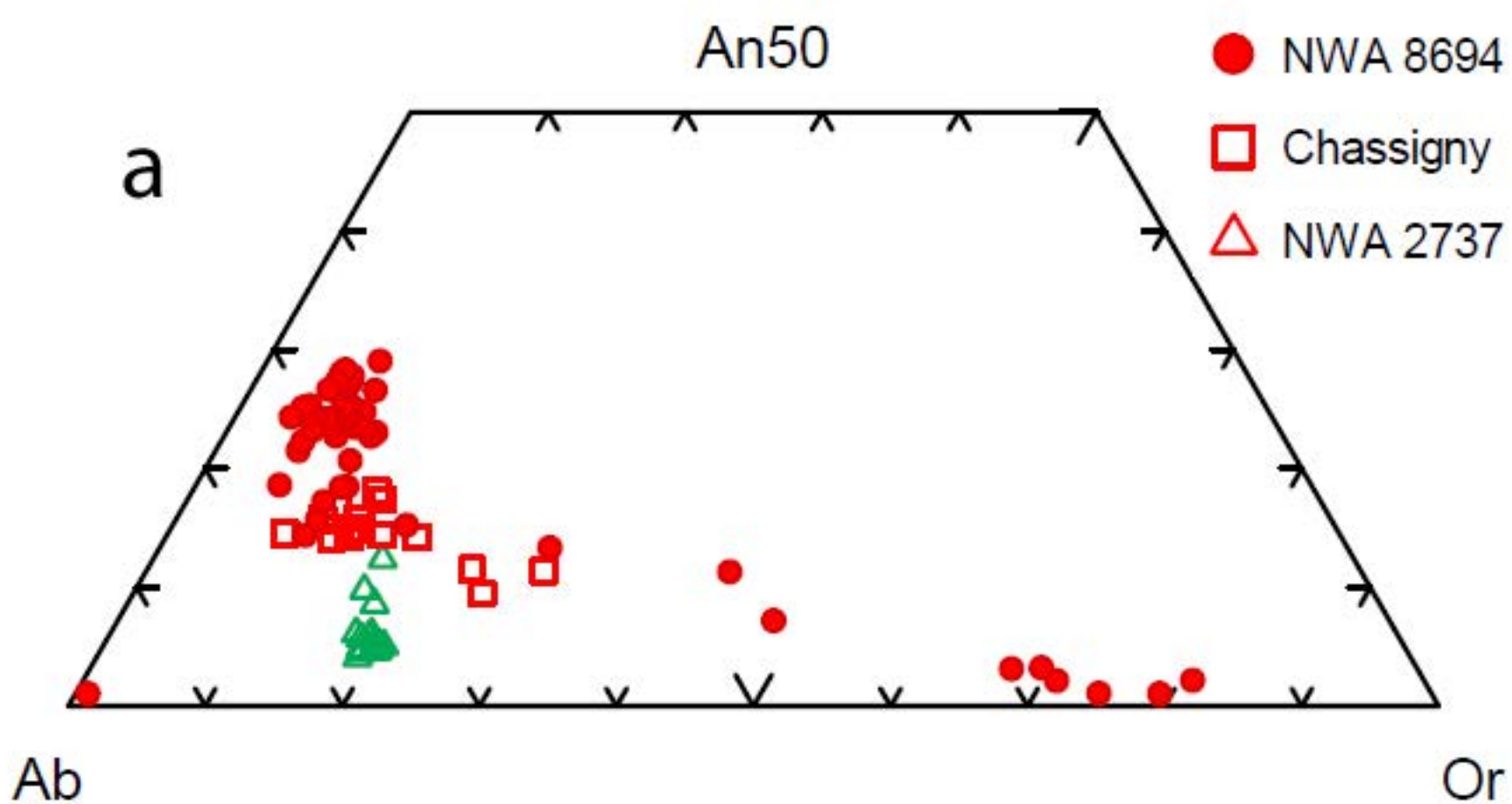


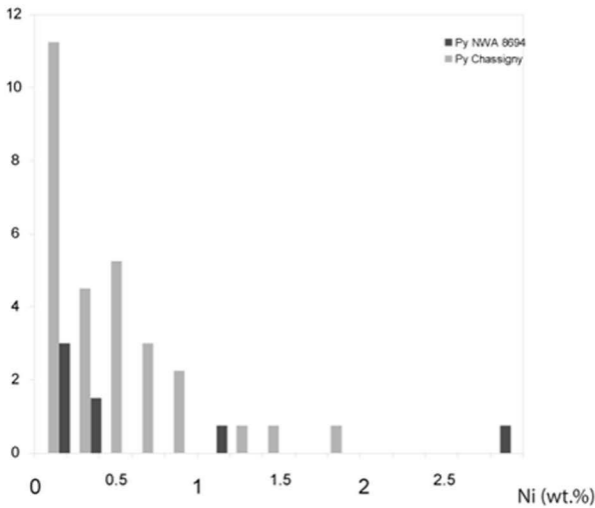
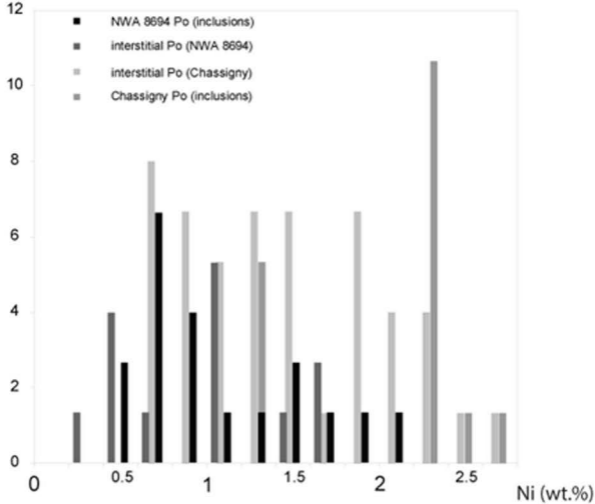
Chr100

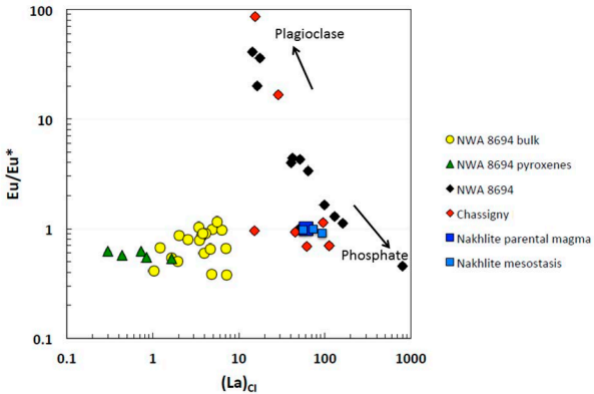
Usp50

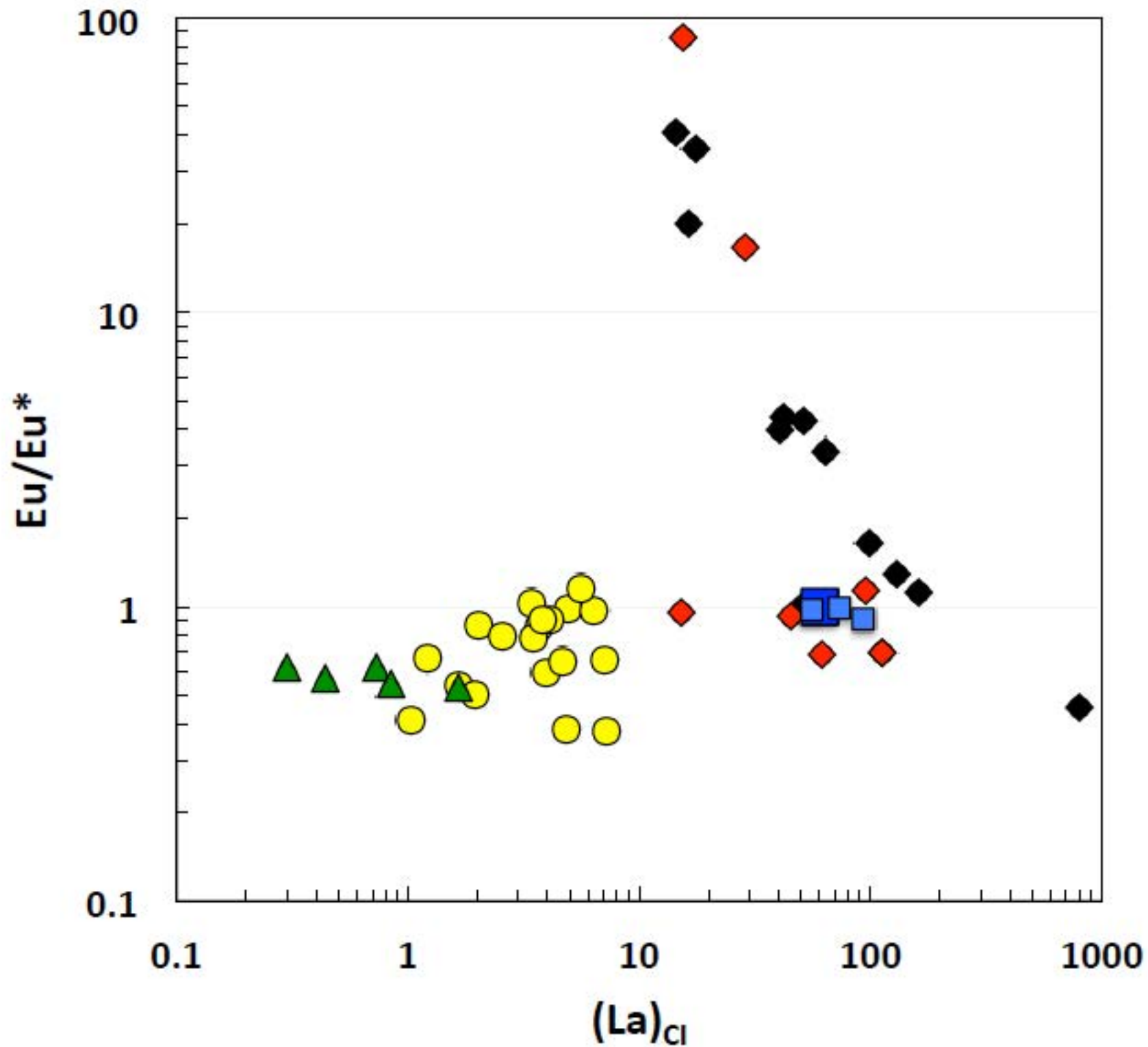


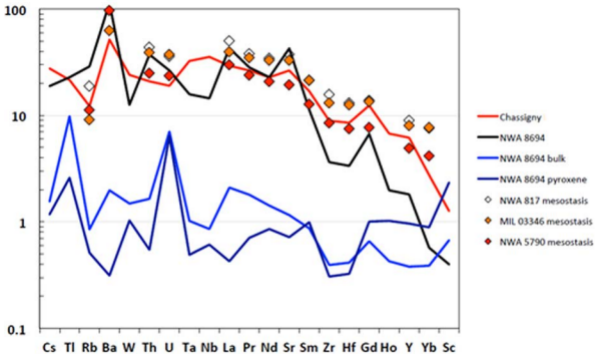


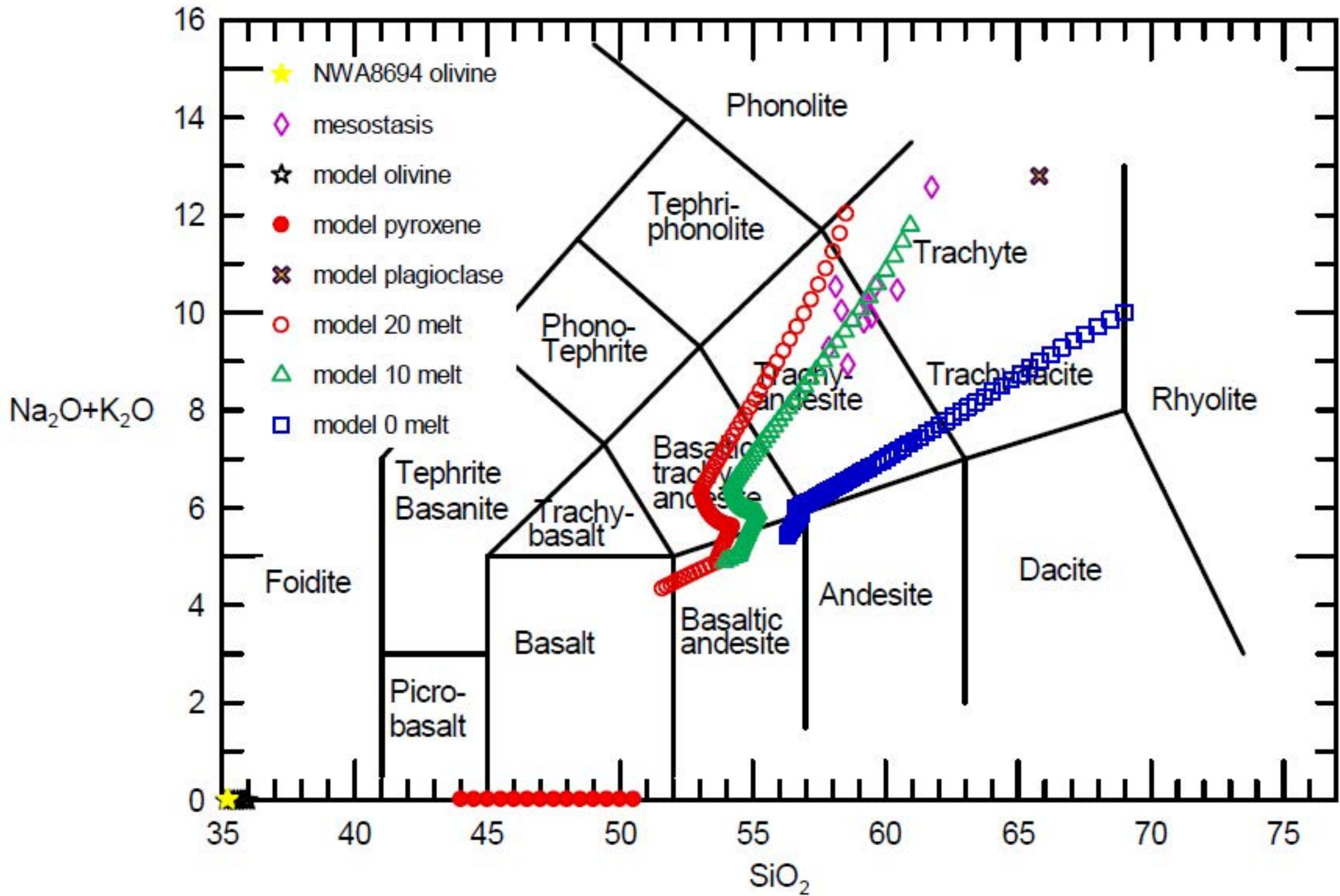


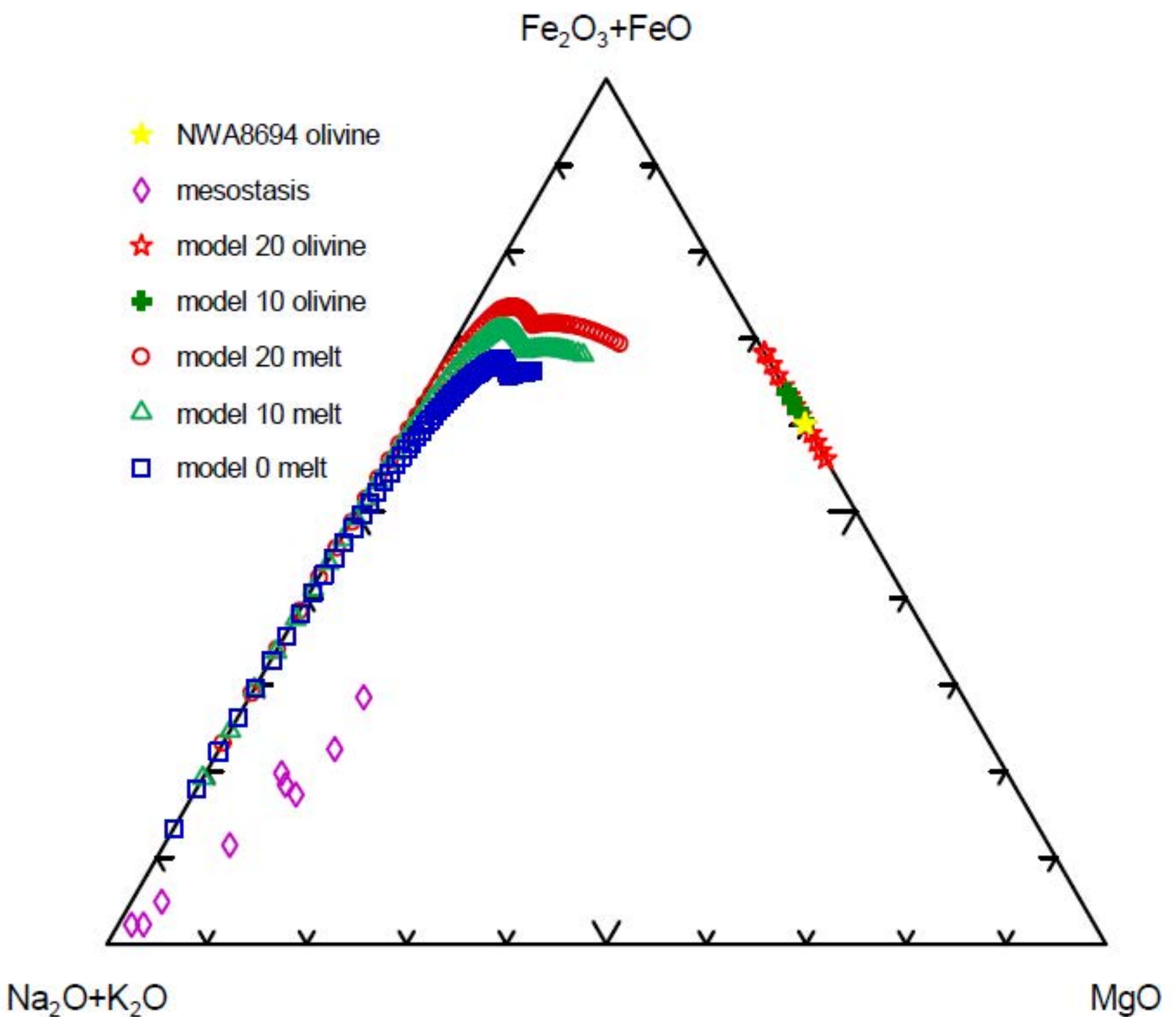






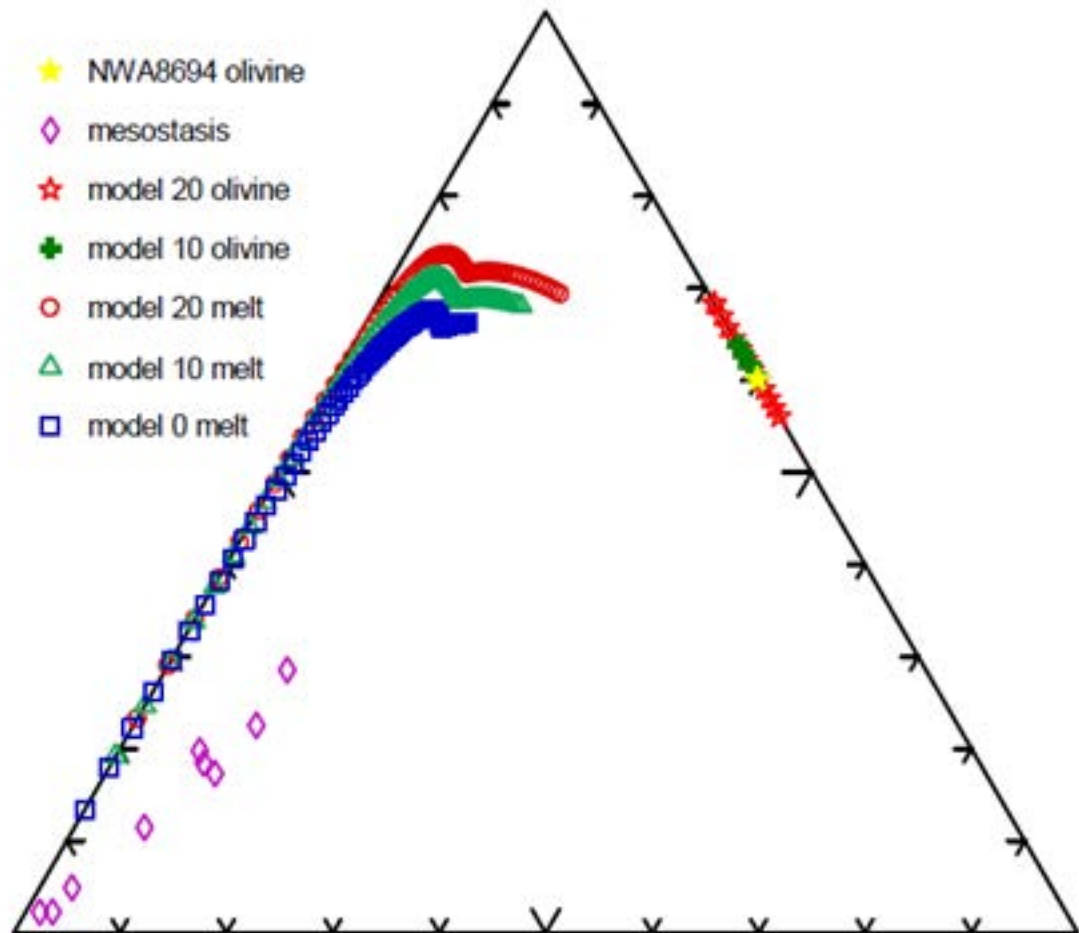






$\text{Fe}_2\text{O}_3+\text{FeO}$

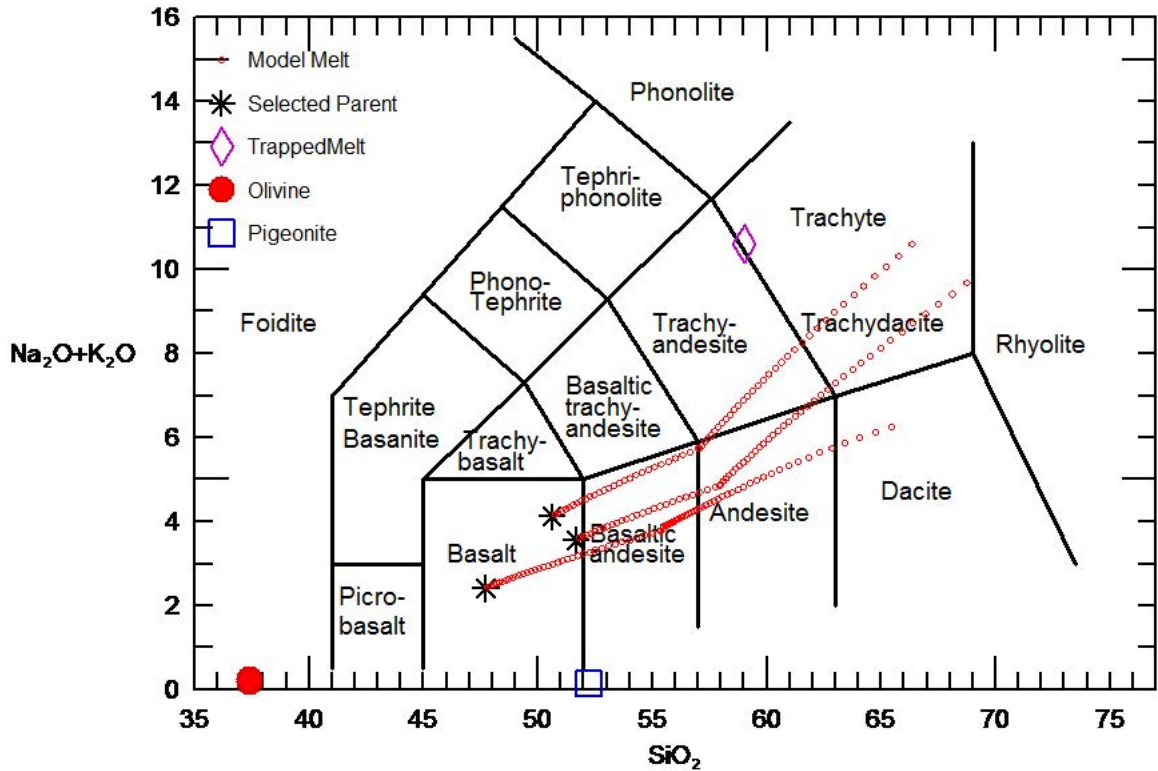
- ★ NWA8694 olivine
- ◇ mesostasis
- ★ model 20 olivine
- ✚ model 10 olivine
- model 20 melt
- △ model 10 melt
- model 0 melt

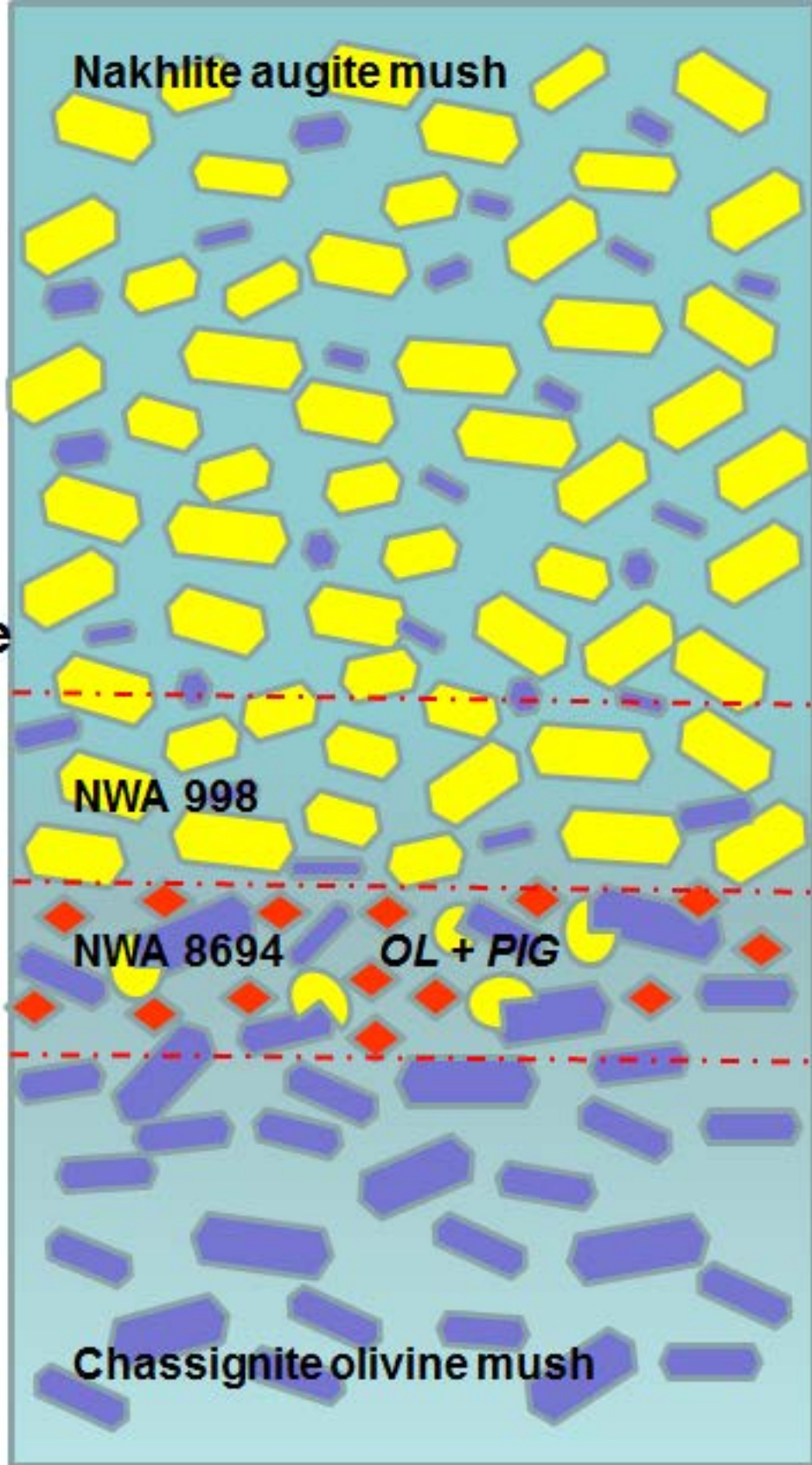


$\text{Na}_2\text{O}+\text{K}_2\text{O}$

$\text{MgO}$







Nakhlite augite mush

Nakhlite  
Liquid

NWA 998

NWA 8694

OL + PIG

Chassignite olivine mush

